DOCTOR OF PHILOSOPHY

Systemic Cytokine Expression and Endothelial Dysfunction
Insights from Innate Immune Models of Protein Phosphorylation

Akbar, Naveed

Award date:
2014

Systemic Cytokine Expression and Endothelial Dysfunction:

Insights from Innate Immune Models of Protein Phosphorylation

Naveed Akbar

A dissertation submitted in fulfilment of the requirements for the degree of Doctor of Philosophy

Division of Cardiovascular and Diabetes Medicine

Medical Research Institute

August 2014

Table of Contents

Appendix

(i) Longitudinal assessment of endothelial function in the microvasculature of mice *in-vivo*.

Acknowledgements

I would like to start by thanking my supervisors Dr Faisel Khan and Professor Jill Belch for giving me the opportunity to undertake my doctoral studies at the University of Dundee. You have equipped me with excellent guidance, training and advice that I will reflect on throughout my career. The department of vascular and inflammatory diseases allowed me to interact with both clinical and pre-clinical researchers, providing me with a complete, realistic view of how work within this thesis might lead to an improvement in health.

I would additionally like thank the labs of Dr Simon Arthur and Professor Philip Cohen for their support, especially Dr. Sambit Nanda and Mrs Julia Carr for their continued help; the facility managers Don Tennant and John Macleod; and finally the Division of Cardiovascular and Diabetes Medicine, the lab of Dr Will Fuller, particularly Dr Jacqueline Howie for answering my many, many questions.

List of Abbreviations

25(OH)D	25-hydroxy vitamin D
ABINS	The A20-binding inhibitors of NF-κB
ACh	Acetylcholine
ANP	Atrial natriuretic factor peptide
ApoE	Apolipoprotein E
ARE	Adenosine and uridine rich elements
AU	Arbitrary units
BH_4	Tetra-hydro-biopterin
BMI	Body mass index
BNP	Brain natriuretic peptide
BPM	Beats per minute
C57BL/6	C57Black/6
Ca^{2+}	Calcium
Calcitriol	1, 25hydroxy vitamin D
cGMP	Cyclic guanosine monophosphate
CHD	Coronary heart disease
CRP	C-reactive protein
CVD	Cardiovascular disease
DAMPS	Danger associated molecular patterns
DD	Death domain
DUSP-1	Dual specificity phosphatase-1
EC	Endothelial cell
EDTA	Ethylene diamine tetra acetic acid
eNOS	Endothelial nitric oxide synthase
ERK	Extracellular signal-regulated kinases
ET-1	Endothelin-1
EU	European Union
FMD	Flow-mediated vasodilatation
GM-CSF	Granulocyte macrophage – colony stimulating factor
HeNE	Helium neon
HFD	High fat diet
hs-CRP	High sensitive C-reactive protein
ICAM-1	Intracellular cell adhesion molecule-1
IFN-γ	Interferon-γ
IκB	Inhibitors of kB
IL-1ra	IL-1 receptor antagonist
IL-6	Interleukin-6
iNOS	Inducible nitric oxide synthase
IRAK	Intracellular receptor associated kinase
JNK	c-Jun-N terminal kinases
K^+	Potassium
KO	Knock-out
LBD	Ligand-binding domain

LDF	Laser Doppler flowmetry
LDI	Laser Doppler Imaging
LDL	Low density lipoproteins
LDLr	Low density lipoprotein receptor
L-NAME	N_{ω}-Nitro-L-arginine methyl ester hydrochloride
LPS	Lipopolysaccharide
LRR	Leucine rich repeat
MAP	Mean arterial blood pressure
MAPK	Mitogen-activated protein kinase
MAPKAP 2/3	Mitogen activated protein kinase activated-protein 2/ 3
MC	Myeloid cell
MCP-1	Macrophage chemoattractant protein-1
MI	Myocardial infarction
MMP	Matrix metalloproteinase
MSK1/ 2	Mitogen and stress activated-kinase 1 and 2
MSRU	Medical school resource unit
MyD88	Myeloid primary response gene 88
NADP	Nicotinamide adenine dinucleotide phosphatase
NEMO	NF-κB essential modulator
NF-κB	Nuclear factor kappa B
NLS	Nuclear localisation signal
NO	Nitric oxide
O-cuff	Occlusion cuff
oxLDL	Oxidised-low density lipoproteins
PAMPS	Pathogen associated molecular patterns
PBS	Phosphate-buffered saline
PE	Phenylephrine
RA	Rheumatoid arthritis
RBCs	Red blood cells
RHD	Rel-homology-domain
ROS	Reactive oxygen species
RPM	Rounds per minute
sICAM-1	Soluble intracellular adhesions molecule-1
SLE	Systemic lupus erythematosus
SNP	Sodium nitroprusside
STAT3	Signal transducer and activator of transcription 3
sVCAM-1	Soluble vascular cell adhesion molecule-1
TAB	TAK-1-binding proteins
TAK-1	Transforming growth factor-β-activated kinase-1
TIR	Toll\IL-1 receptor
TIRAP	MyD88-like adaptor (Mal)/TIR domain containing adaptor protein
TLRs	Toll-like receptors
TNF	Tumour necrosis factor
TNIP1	TNFAIP3-interacting protein-1
TRAF	Tumour necrosis factor receptor associated factor

TRAM	TRIF-related adaptor molecule
TRIF	TIR domain-containing adaptor inducing interferon (IFN-β)
TTP	Tristetraprolin
UV-B	Ultraviolet-B
VCAM-1	Vascular cell adhesion molecule-1
VDD	Vitamin D deficiency
VDRs	Vitamin D receptors
Vitamin D_2	Ergocalciferol
VPR	Volume pressure recording
VSMCs	Vascular smooth muscle cells
WT	Wild- type

List of Figures

Declaration

I, Naveed Akbar am the sole author of this thesis. The work of which is a record was carried out by myself unless otherwise stated and all references cited have been consulted. None of the work contained within this thesis has been previously accepted for a higher degree.

Signature of candidate

Naveed Akbar

Supervisors Statement

I certify that Naveed Akbar has fulfilled the conditions of ordinance and of the relevant regulations, such that he is qualified to submit this thesis in application for the higher degree of Doctor of Philosophy.

Signatures of supervisors

Dr Faisel Khan

Professor Jill J F Belch

‘All we know is still infinitely less than all that remains unknown’

William Harvey

Summary

Cardiovascular diseases (CVD) are united in pathology by atherosclerosis; signal transduction is essential in this process for the expression of cell adhesion molecules early in the disease, capturing, tethering and transmigrating monocytes into the sub-endothelial space. The local recruitment of inflammatory cells and release of pro-inflammatory mediators induces endothelial dysfunction, an early functional abnormality in CVD.

Plasma cytokines have been used to stratify CVD risk in humans. Studies have shown associations between pro-inflammatory tumour necrosis factor (TNF) and interleukin-6 (IL-6) and adverse cardiovascular events. However, the early pathophysiological signalling responsible for the expression of inflammatory molecules in vascular dysfunction remains poorly defined with limited *in vivo* studies.

The ability to quantify endothelial dysfunction in animal models is limited by the need to cull animals in order to obtain vascular tissue, prohibiting longitudinal studies. The development of an *in vivo* non-invasive technique in this thesis has allowed the longitudinal assessment of microvascular responses in mouse models of inflammation.

Candidate kinases in innate inflammatory signalling were assessed *in vivo* to better understand their role in endothelial dysfunction. These proteins are either essential in inflammatory homeostasis (A20 binding inhibitor of NF-κB-1 and mitogen and stress activated kinase 1/ 2) through negative regulation of inflammation or are fundamental in the cascade for cytokines synthesis (myeloid differentiation primary response gene 88, mitogen activated protein kinase activated-protein kinase 2/ 3). Through genetic alteration these models

produced a hyper-inflammatory CVD prone phenotype or one that is cardiovascular protective, respectively. Endothelium-dependent vasodilatation was attenuated in the presence of dyslipidaemia through reduced of nitric oxide (NO), cholesterol feeding induced increased expression of IL-6, IL-1α and TNF-α. Importantly, through abrogation of cytokine signalling, NO was preserved in the presence of dyslipidaemia through reduced cytokine release of IL-6 and IL-1α.

This data provides a novel insight into the cellular signalling in inflammation and subsequent cardiovascular health, with a translational potential to effectively enhance the understanding of clinical pathology and inflammatory risk. These pathways offer unique therapeutic avenues for pharmacological intervention to potentially limit CVD in the human population.

Chapter 1

Introduction

Preface

CVD remains a leading cause of death, it is estimated that 17.3 million people died in 2008 from all cause CVD, representing 30% of all global deaths (World Health Organisation). CVD is mostly preventable, but the significant increase in morbidity and death are often associated with western civilisation, attributing disease prevalence to a sedentary lifestyle, a diet high in cholesterol and smoking, thus these factors are associated with CVD risk. The biological basis for CVD remains poorly defined and the pathological basis for the significant heterogeneity in CVD risk remains an unanswered question (Libby *et al*., 2011). Inflammation is regarded as an underlying cause for CVD, contributing significantly to functional and structural changes throughout the cardiovascular system. The aim of this thesis is to contribute to the knowledge of inflammation induced CVD. The effects are measured by the release of cytokines into the systemic circulation of mice that have undergone genetic and diet alterations to study the effects of particular proteins of interest.

The thesis is structured, providing an introduction to CVD where the role of early endothelial dysfunction in atherosclerotic plaque formation is described, emphasis is placed on animal models and techniques used for the assessment of CVD, this is followed by the project aims and hypothesis. Subsequently, detailed descriptions of the experimental methods used to address the project objectives and meet the thesis aims are defined. Following chapters are organised into detailed studies and are summarised sequentially, discussing the significance of key findings relevant to the role of inflammation in the pathogenesis in CVD. A final discussion links together the relevance of the work contained within this thesis and draws on the major conclusions and contributions made to the field of cardiovascular medicine.

Background

CVD accounts for significant morbidity and mortality worldwide, accounting for 17.3 million deaths in 2008 (World Health Organisation). Within the European Union (EU) CVD causes 47% of all death; totalling 1.9 million individual cases and costs €196 billion per annum. Luengo-fernandez *et al* (2004) has previously reported a total cost of £29.1 billion to the United Kingdom economy, 23% of all expenditure is associated with a loss of productivity due to death and morbidity (Luengo-Fernandez *et al*., 2006). It was previously thought that males have a greater prevalent risk for CVD (Weidner and Cain, 2003) but recent statistics show women are more likely to suffer an adverse cardiovascular event in all countries within EU when compared to men (British Heart Foundation, 2012).

CVD broadly refers to a pathological state of dysfunction encompassing both the myocardium and the circulatory system. Albeit in the later stages of CVD other tissues may become severely affected in a process termed end organ damage. In this advanced stage the renal and/or retinal vascular system may become impaired leading to renal dysfunction or blindness respectively (London *et al*., 2003).

CVDs are plentiful and are named after the region of the body they affect, major CVDs include: myocardial infarction (MI), coronary heart disease (CHD), ischaemic stroke (of the cortex), aortic aneurysm and atherosclerosis. Patients are likely to display significant dysfunction in more than one vascular bed at any given time (van Kuijk *et al*., 2010). Nonetheless, CHD remains the number one cause of death in the EU followed closely by stroke (British Heart Foundation, 2012).

The progression and development of CVD is attributed to numerous lifestyle risk factors such as smoking, the intake of high dietary cholesterol, salt, alcohol as well as physical inactivity and obesity. Thus the dogma clinically encouraged for a healthy cardiovascular system is a diet that is low in salt, which maintains a significant reduction in dietary cholesterol, abstinence from smoking and moderate levels of exercise.

Traditional risk factors such as a diet high in cholesterol, obesity (body mass index (BMI) >30) and smoking may further exacerbate CVD risk in individuals that possess genetic polymorphisms, a genetic variation in genes associated with an increased risk of CVD. The exact dysfunction may vary from individual to individual, however the body's inability to metabolise cholesterol successfully has been studied and gene variations associated with irregularities in cholesterol efflux results in lipid accumulation in the plasma, an established factor for CVD (Eichner *et al*., 2002).

In addition to the aforementioned modifiable risk factors and inheritable genetic predispositions, other pathologies, so called co-morbidities such as diabetes type II (Grundy *et al*., 1999), rheumatic diseases including rheumatoid arthritis (RA) and systemic lupus erythematosus (SLE) are associated with elevated CVD risk (Turesson *et al*., 2008, Turesson and Matteson, 2013). Treatment or management of each factor (lifestyle, genetic or co-pathology) alone or in synergy have shown to reduce CVD. CVD risk is often calculated by measurements of plasma cholesterol, blood glucose, BMI and blood pressure. These parameters have been used widely in clinical trials and are routinely assessed in the clinic. On the contrary, early detection of CVD continues to be a clinical challenge. The above guidelines are therefore determined on the

treatment of risk factors and focus on those individuals who are regarded as '*at risk*' i.e. diabetic patients, overweight persons and those who display an elevated blood pressure or have a family history for CVD.

One way in which the risk is calculated is based on the Framingham Risk Score, a population based study that examined the onset on of arterial fibrillation, congestive heart failure, CHD, diabetes, hypertension, intermittent claudication (angina) and stroke (Dawber *et al*., 1951). The Framingham Heart Study (1948) was initially set up to identify the factors that cause CVD. The study was strengthened by the participation of individuals who had not developed CVD or suffered a MI, allowing researchers to monitor change over time. The repeated testing nature of the Framingham study allowed physical and lifestyle factors to be tracked and related them to mortality, in doing so identifying elevated blood pressure, cholesterol, obesity, smoking, physical inactivity and co-morbidities such as diabetes as major risk factors in the pathogenesis of CVD. Further factors including age, socioeconomic status and gender have provided insight into the aetiology of CVD. Limitations within the Framingham risk study are widely accepted, study participants were not randomly selected, were Caucasian and may have been healthier than the general population. Nonetheless the major factors identified as detailed above have been applied to different ethnic groups and similar trends have been identified, although the pattern of distribution various considerably. For example individuals of south Asian descent (Afghanistan, India, Pakistan, Maldives and Bangladesh) are at greater risk of adverse cardiovascular events and are more likely to experience these at an earlier age when compared to equivalent Caucasian individuals (Hussain *et al*., 2013). Body fat composition and body fat distribution is believed to be a factor responsible for this accelerated risk. South

Asian men are more likely to hold 6% greater abdominal body fat when compared to Caucasian men, a result of enlarged abdominal adipocytes, a risk factor for diabetes and insulin resistance, which are in turn CVD risk factors. Importantly the distribution of body fat has important pathophysiological implications, visceral adiposity is independently associated with increased CVD risk (Britton *et al*., 2013). Although risk factors are routinely used to assess CVD risk in individuals, the ability to identify disease early remains a clinical challenge. Patients are often treated for CVD after a major event such as MI or stroke, thus the ability to hinder early pathophysiological events that cause progressive diseases such as atherosclerotic plaque formation is limited. Importantly studies have identified the onset of early CVD in patients with known risk factors such as diabetes (Khan *et al*., 2000), therefore the ability to detect early disease manifestation holds great therapeutic promise. A potential avenue to retard pathophysiological disease processes before the onset of overt clinical disease.

The role of risk factors, genetic predisposition and co-morbidities in the aetiology of CVD share common physiological responses of inflammation. Inflammation specifically refers to the local recruitment of leucocytes from the plasma to tissues. Leucocyte recruitment and the sustained release of pro-inflammatory cytokines have been correlated with a wide range of clinical conditions including: hyperglycaemia, obesity, hypertension, hyperlipidaemia, periodontal disease and in particular diseases of the vascular system including atherosclerosis, CHD and endothelial dysfunction (Ait-Oufella *et al*., 2011, Mallat *et al*., 1999, Mallat and Tedgui, 2007, Tedgui and Mallat, 2006, Borel *et al*., 2009, Minet *et al*., 2012, Piconi *et al*., 2009, Rueda-Clausen *et al*., 2009).

Cardiovascular Disease and Inflammation

The role of inflammation in CVD development is complex. Patients displaying traditional risk factors (Herrera *et al*., 2010, Kathiresan *et al*., 2006, Roifman *et al*., 2011, Singhal, 2005) and those suffering from chronic inflammatory disease conditions such as RA (Galarraga *et al*., 2008) and SLE (Barbulescu *et al*., 2012) display elevated levels of circulating pro-inflammatory cytokines such as TNF-α and have an elevated risk for CVD. Plasma cytokines including TNF-α, IL-6 and C-reactive protein (CRP) have been used as prognostic markers for future adverse cardiovascular events in patient trials (Barbulescu *et al*., 2012, Clapp *et al*., 2005, Fernandez-Real *et al*., 2001, Fichtlscherer *et al*., 2004, Galarraga *et al*., 2008, Liu *et al*., Lu *et al*., 2007, Naya *et al*., 2007, Pradhan *et al*., 2001), in combination with the traditional risk factors such as BMI and plasma cholesterol. The efficacy of these plasma molecules as prognostic markers for future adverse cardiovascular events such as MI or stroke remains contentious, with some studies showing good, little or no predictive value.

Inflammatory molecules can be synthesised from a number of cell types including specialised leucocytes in response to both endogenous and noxious stimuli. In particular, the macrophage is regarded as the predominant inflammatory cell in the pathogenesis of CVD. Macrophage infiltration into the vascular lumen is regarded as an early event in CVD development and macrophages are readily detected in damaged and diseased tissues. Macrophages are recruited to the damaged myocardium following infarction where they propagate damage and mediate repair (Swirski *et al*., 2009, Nahrendorf *et al*., 2007). Macrophage depletion or abrogation of macrophage recruitment has shown cardio-protection (Leuschner *et al*., 2010b, Swirski *et al*., 2009). The infiltration of macrophages into damaged tissues remains

multifaceted. There are numerous signalling cascades that capture these highly specialised cells and induce transmigration deep into tissues, a prerequisite for atherosclerotic plaque formation. It has previously been established that macrophages are sensitive to activation. Inflammatory molecules such as Interferon-γ (IFN-γ) and TNF-α through receptor stimulation can activate macrophages and induce the production of reactive radicals, such as the reactive oxygen species (ROS) NO, through up regulation of inducible nitric oxide synthase (iNOS). Classically (M1) activated macrophages are associated with increased phagocytic behaviour and secrete high levels of pro-inflammatory molecules IL-1, IL-6 and IL-12 (Mosser, 2003). Conversely, molecules such as IL-4 can alternatively activate macrophage and induce an M2 or an anti-inflammatory phenotype. The induction of an M2 phenotype is associated with reduced phagocytic behaviour, silenced iNOS induction and a high production of anti-inflammatory IL-10 and IL-1 receptor antagonist (IL-1ra). Although the phenotype of macrophages appears to be definitive, numerous sub-subdivisions exist and have been associated with various physiological roles (Zawada *et al*., 2012).

Vascular lesions affect the arterial system and contrary to what was previously thought atherogenic lesions are multifaceted and not just the quiescent accumulation of lipids at arterials bends and bifurcations. The macrophage contributes to lesion development and progression through foam cell formation. Atherosclerotic plaques are the outcome of prolonged inflammatory signalling that results in the continual recruitment of lymphocytes, increased oxidative stress and the synthesis of collagen, forming a cell dense lesion that which reduces lumen diameter (Zhao and Qin, 2011, Libby *et al*., 2009).

Leucocyte extravasation is a specialised process and subsequent transmigration into the sub-endothelial space is achieved though activation of receptor-mediated pathways. Damaged or stimulated cells can express pro-inflammatory cytokines, inducing the expression of cell adhesion molecules such as vascular cell adhesion molecule-1 (VCAM-1), intracellular cell adhesion molecule-1 (ICAM-1), E-selectin, P-selectin and in combination with chemokines such as macrophage chemoattractant protein-1 (MCP-1) recruit macrophages to the area of tissue injury.

Macrophages captured from the circulating blood are adhered to the vascular endothelium and a process of transmigration through endothelial cell gap junctions (**Figure 1.1**) results in leucocyte recruitment. Infiltrated macrophages can occupy the sub-endothelial space; over time these cells encounter numerous physiological stimuli that induce the expression of pro-inflammatory genes. Oxidised lipids such as low density lipoproteins (LDL) are associated with adverse CVD events and can stimulate macrophage to release pro-inflammatory molecules. Infiltrated leucocytes are able to release a number of mediators into their surroundings including ROS and proteolytic enzymes. The release of cytokines is important in the removal of infections agents such as bacteria from tissues and the elimination of apoptotic cells; however extended or inappropriate activation of these pathways can be deleterious leading to profound injury to the vascular bed and more importantly the endothelial lining.

Elevated level of ROS can oxidise lipids such as LDL forming oxidised-LDL (oxLDL) in the blood. The oxLDL is recognised by the macrophage and ingested for removal, oxLDL accumulates within the growing macrophage to form a characteristic atherosclerotic foam cell (**Figure 1.2**). Progressively large

numbers of macrophages accumulate within the vessel wall. Sequentially these cells promote vascular inflammation through the release of pro-inflammatory cytokines and promote further cell recruitment. Atherosclerotic foam cells accumulate in such numbers that vascular remodelling is required to support the advancing cell mass, through the synthesis of collagen atherosclerotic plaque is formed.

Over time (decades in humans and months in genetically altered mice) these foam cells die and form a central highly noxious necrotic core. The growing vascular lesion, through increased cell recruitment and apoptotic mass extends towards the vascular lumen, reducing lumen diameter. Obstructed vessels are associated with the onset of ischaemia, end organ damage and even organ failure. Although numerous pathways have now been identified that contribute to atherosclerotic lesion formation there remains limited pharmacologically active drugs for the treatment of patients. Thus the ability to hinder these processes early before the onset of overt disease is of key clinical significance. The process of atherosclerosis begins with early endothelial dysfunction, a termed given to an imbalance in endogenous vasodilators and vasoconstrictors, VCAM-1 expression and the activation of platelets. Therapeutic strategies to limit the activation of the vascular endothelium through attenuation of inflammatory mediators offers a novel approach to retard pathophysiology early in the human population.

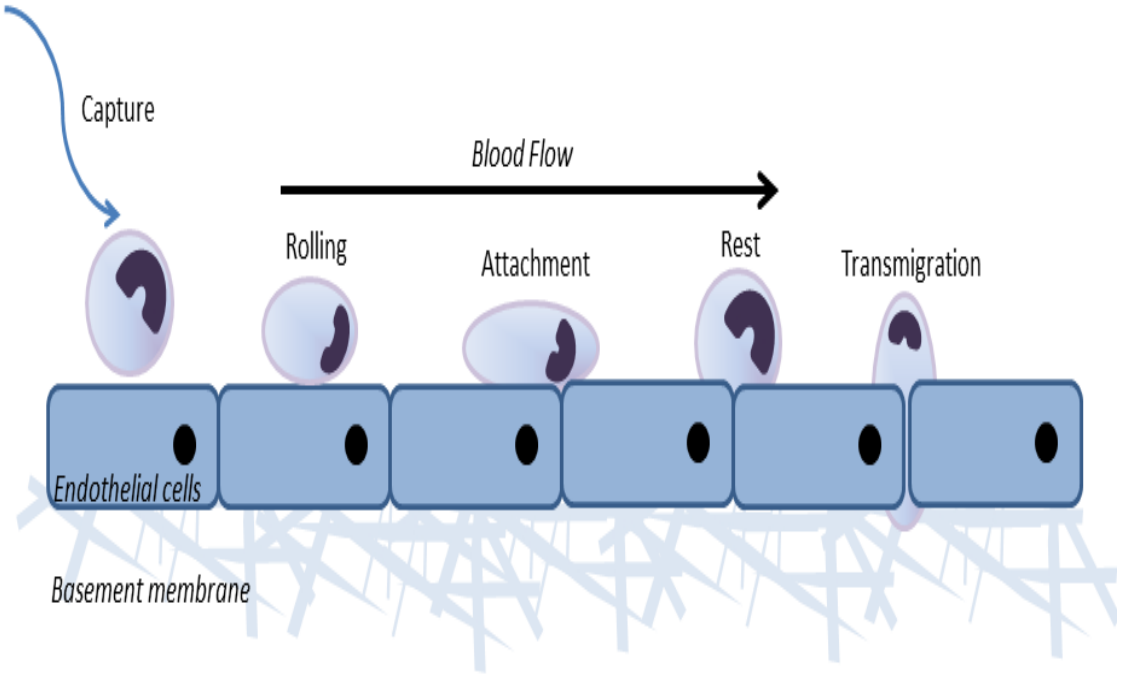

Figure 1.1. Leucocyte extravasation: Leucocyte adherence, tethering, attachment to the vascular endothelium and transmigration through endothelial cell gap junctions. Adapted from (Ley *et al*., 2007).

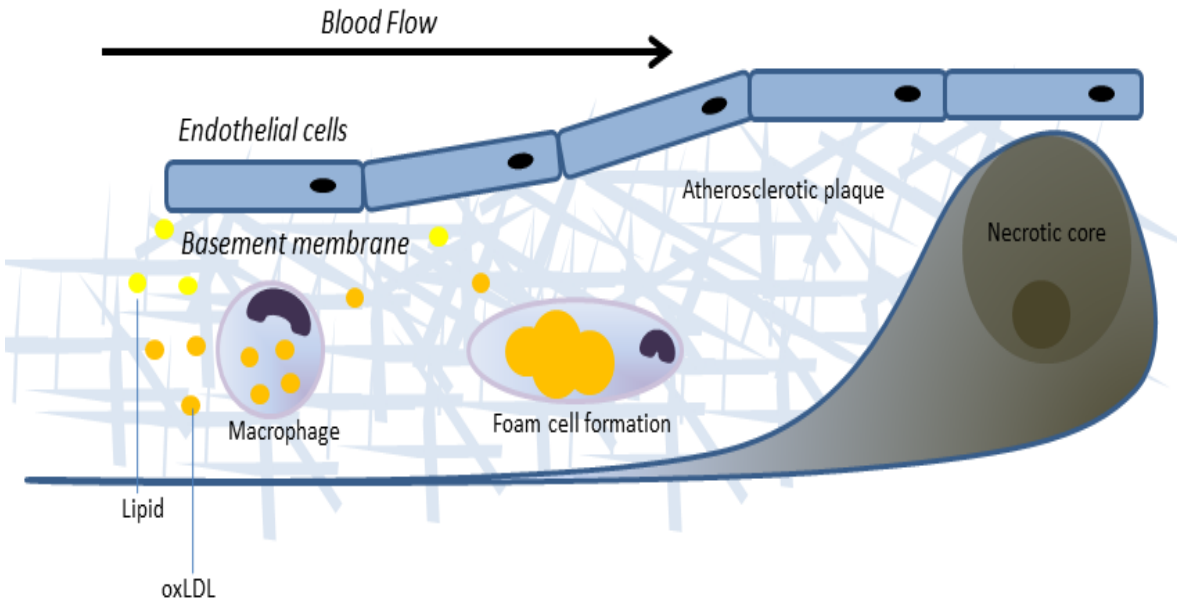

Figure 1.2. Atherosclerotic plaque formation: Oxidised lipids are recognised and engulfed by vascular macrophages. This cycle perpetuates and forms characteristic atherosclerotic foam cells, developing into a dense, toxic necrotic core that obstructs the vascular lumen.

Vascular Endothelium

The vascular endothelium has a number of specialised features that are accompanied by specific metabolic and synthetic functions. Molecules secreted from endothelial cells are able to significantly affect the behaviour of underlying vascular smooth muscle cells (VSMCs) and circulating white blood cells (Walker *et al*., 2010). Endothelial cells form one of the most important structures within the vascular tree and in turn pathogenesis (Cherry *et al*., 1982, Furchgott, 1984, Furchgott, 1983, Furchgott and Zawadzki, 1980). The mass endothelial cell weight in an adult human is approximately 1kg, equating to a total surface area of 1.7m^2 (Cines *et al*., 1998). Endothelial cells have a flattened structure and vary between 10-20μm in diameter. Overlaps between adjacent cells form tight junctions; in combination with their semi-permeable nature, the movement of molecules is strictly regulated. The squamous cells are composed around a central nucleus with organelles concentrated in the perinuclear area. Endothelial cells form a physical barrier between blood, bodily tissues and also serve as a functional component important in vessel integrity with a role in angiogenesis (Lamalice *et al*., 2007).

The vascular endothelium interfaces between circulating blood and the vessel wall to maintain an anti-inflammatory, anti-thrombotic phenotype. Endothelial cells are responsible for numerous biological processes, most importantly maintaining vascular basal tone (modulation of lumen diameter) and the adequate perfusion of tissues. Endothelial cells are able to regulate their environment locally through the release of biologically active mediators such as histamine as well as NO. Both molecules are essential factors in oedema formation and leucocyte recruitment (Leach *et al*., 1995, Duran *et al*., 2010)

Endothelial cells produce NO as a bi-product of the amino acid L-arginine oxidation to L-citrulline by enzymatic action of endothelial cell specific nitric oxide synthase (eNOS) (**Figure 3**). eNOS is highly expressed in endothelial cells within the vasculature and for this reason primarily contributes to vascular tone under basal conditions through generation of NO.

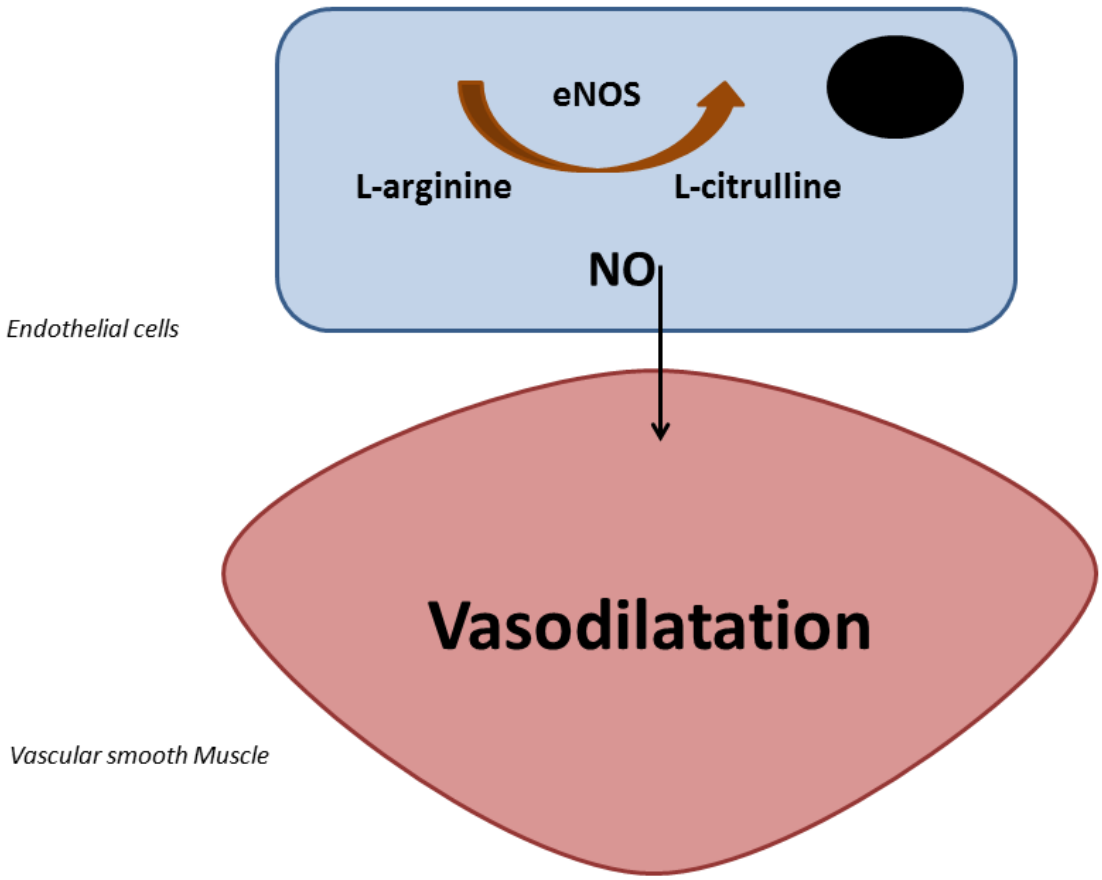

Figure 1.3. Bioavailability of nitric oxide: Enzymatic oxidation of L-arginine to L-citrulline through endothelial nitric oxide synthase (eNOS) produces nitric oxide (NO).

eNOS can be activated in response to changes in shear stress (Corson *et al*., 1996, Gallis *et al*., 1999) or by appropriate receptor stimulation from a range of agonist drugs including acetylcholine (ACh) and bradykinin (Cherry *et al*., 1982, Furchgott and Zawadzki, 1980).

eNOS activity requires oxygen, nicotinamide adenine dinucleotide phosphatase (NADP), tetra-hydro-biopterin (BH_4) and other cofactors including cysteine. NO is able to bind to the haem of guanylyl-cyclase found on VSMCs, converting GTP to cyclic GMP (cGMP), an important second messenger in VSMC relaxation. cGMP activates both potassium (K^+) and calcium (Ca^{2+}) channels and induces cell hyperpolarisation and cytoskeleton relaxation. cGMP inhibits cellular Ca^{2+} entry and further depletes intracellular sub-sarcolemmal storage sites causing VSMC fibre relaxation by activating an enzyme to dephosphorylate myosin light chains (Esper *et al*., 2006, Palmer *et al*., 1988). NO plays a further role in hemodynamic and platelet: adhesion, activation, secretion, aggregation and disaggregation, VSMC migration and proliferation (Inglessis *et al*., 2004, Semigran *et al*., 1994, Riddell and Owen, 1999).

NO is a heterodiatomic molecule, its low molecular weight and lipophilic properties allow passive diffusion through biological systems making it an important signalling molecule (Lamattina *et al*., 2003). The loss of NO bioavailability is thus associated with endothelial dysfunction and is subsequently associated with altered vasomotion, an early event in the development of atherosclerosis (Bonetti *et al*., 2003, Naseem, 2005). Shifting the phenotype of the vascular endothelium from a quiescent non-adherent surface, to one that induces the tethering of monocytes an early event in the atherosclerotic plaque formation.

Several lines of evidence currently support the loss of NO and the onset of endothelial dysfunction. Impaired vasoreactivity maybe the outcome of a direct decrease in L-arginine (Kamada *et al*., 2001) an increase in the number of endogenous vasoconstrictors such as endothelin-1 (ET-1) (de Andrade *et al*.,

2009) the opposing mechanism to NO mediated vasodilatation; eNOS loss by apoptosis of endothelial cells (Winn and Harlan, 2005) or the quenching of NO by ROS formation or a loss of one or more of the essential co-factors (Herrera *et al*., 2010, Alp and Channon, 2004).

Importantly evidence suggests that inflammation even at subclinical levels is correlated with a reduction in the bioavailability of NO and impaired endothelium-dependent vasodilatation (Clapp *et al*., 2004, Clapp *et al*., 2005). Research has shown pro-inflammatory molecules such TNF-α have a pivotal role in reducing the biological potency of NO (Zemse *et al*., 2010). Studies suggest that patients suffering from atherogenesis are likely to have widespread problems throughout the vascular system, with damage significantly affecting more than one vascular bed including endothelial dysfunction, neointimal proliferation and atheroma development, all which may be mediated by the loss of NO bioavailability (Tedgui and Mallat, 2006). The ability to test for endothelial function, as an early event in CVD has been used as a marker of vascular health and as a prognostic marker for future adverse cardiovascular events in humans.

In vivo Models of Endothelial Dysfunction

Methodologies for the assessment of endothelial function have been established to asses CVD risk in patients. Endothelial dysfunction remains the earliest detectable functional abnormality in vascular tissue and has been prominently reported in a wide range of clinical diseases including: diabetes (Jones and Dewan, 2003), RA (Galarraga *et al*., 2008) and in patients with known CVD risk factors (Hadi *et al*., 2005, Khan *et al*., 2000).

Invasive and non-invasive techniques have been described for the assessment of endothelial function in humans. Studies examining the role of coronary artery dysfunction in CVD have infused agents such as adenosine and papaverine to elicit endothelium-dependent responses in a technique called flow-mediated vasodilatation (FMD). The method evaluates coronary circulation, measuring changes in endothelium-dependent vasodilatation. In healthy individuals increased flow is associated with greater shear stress and a greater release of NO, inducing vasodilatation in proximal epicedial arteries; whereas reduced flow is indicative of endothelial dysfunction through altered NO bioavailability. The technique is limited by the assessment of flow through larger conduit coronary arteries, thus the technique does not distinguish between impaired function and obstructed flow. Flow may be impaired by the presence of atherosclerotic lesions, however impaired endothelial function contributes significantly to diseases such as hypertension through diminished vascular function in small vessels. Functional testing of the coronary bed can be performed through insertion of a Doppler wire into a coronary artery and followed by the infusion of vasoactive chemicals i.e. ACh and bradykinin, delineating impaired flow to specific agonist as impaired endothelial function. The major limitation to the assessment of coronary macro and microcirculation is the invasive nature of the technique and thus these patients are often pre-selected and studied under a routine clinical screen, introducing selection bias for research studies.

Techniques for the assessment of the peripheral circulation are therefore favoured. Blood vessels can be imaged non-invasively using high frequency ultrasound and there is no need for radioactive tracers. FMD can be used to assess function in numerous vascular beds including the brachial or femoral arteries. Similarly, peripheral FMD monitors the changes in vessel diameter,

before and after application of stimulant. A sphygmomanometer cuff is placed above the anterior cubital fossa and inflated to induce vascular occlusion, pre- and post-vessel diameters are compared and nitro-glycerine, a NO donor can be used as an internal control for endothelium-independent vasodilatation. This technique has been used in large clinical trials for the assessment of CVD. Although non-invasive, the technique is highly operator dependent and values can vary considerably, a period of months is needed for training and there is currently no agreement on a standardised protocol. Images are prone to artefact and image quality is of key importance, high resolution images must be obtained to accurately evaluate changes in vessel diameter (Barac *et al*., 2007).

In an effort to reduce operator variation and to reduce image artefacts the skin, microcirculation has been used as alternative method to assess systemic CVD burden and endothelial function. The small vessels in the skin can be assessed through laser scattering methods that are comparatively cheaper and more operator friendly than brachial FMD, but maintain the advantage of being non-invasive. Laser Doppler flowmetry (LDF) has been used to assess endothelial function in a range of clinical diseases including chronic kidney disease(Babos *et al*., 2013, Wilson *et al*., 1992, Khan *et al*., 1999, Khan *et al*., 1991). The technique is founded upon the static scattering of a stable laser beam by the movement of red blood cells in the skin microcirculation. Using a similar principle to FMD, perfusion can be increased with the use of vasodilators and decreased with vasoconstrictors. Changes in perfusion can be related to underlying pathobiology, with attenuated responses to ACh associated with decreased NO bioavailability. The technique has previously been compared to FMD and has shown good correlation (Debbabi *et al*., 2010). Although cheaper and more user friendly, LDF is not the optimal technique. The technique suffers

from the poor spatial and temporal heterogeneity of skin microcirculation. The small region of interest measured by the LDF probe can often represent local changes, and/or variation in the skin microenvironment and not necessary be indicative of any underlying pathophysiology. As an alternative, Laser Doppler Imaging (LDI) uses a scanning stable laser, which assesses a larger region of interest than LDF, reducing spatial heterogeneity. LDI has shown good correlation with underlying cardiovascular function in humans (Khan *et al*., 2008) and has shown good temporal reproducibility. Importantly, LDI in combination with vasoactive chemicals has allowed researchers to non-invasively assess disease severity before the onset of overt clinical disease (Khan *et al*., 2005, Khan *et al*., 2000).

Endothelial function testing has been used as a prognostic marker for adverse future cardiovascular events in clinical trials; an intimate relationship between systemic inflammation and cardiovascular health has been reported. However the initial pathological events that lead to endothelial dysfunction remain poorly defined. The ability to interrogate specific cellular signalling pathways of pathophysiology is limited in human clinical trials. Often patients are selected from pre-requisite criteria for inclusion or exclusion and therefore clinical trials measure outcome based on assessment of risk factors or mortality. Research groups over the past two decades have shifted their research interests away from the patient scenario and capitalised on the ability to genetically modify rodents, altering their risk profile to CVD through diet and pharmacological intervention, exacerbating disease scenarios to model prevalence and severity, as observed in the human population.

Cardiovascular Disease: Human to Murine

Recombinant DNA technology in the 1970s gave rise to genetic manipulation, with the ability to test factors of many diseases observed in the human population including CVD. The relatively easy genomic application of DNA recombination to rodents, in harmony with their species specific attributes, such as short gestation periods (18-21 days) and low maintenance costs, reinstated the suitability of mice as experimental models (Russell, 2003).

Numerous groups have used experimental mouse models of CVD to better understand a variety of cellular changes in the myocardium and vascular system. Operator interventions have been used to mimic established cardiovascular risk factors as observed in the human population. For example, the effects of oxidative stress are associated with the attenuation of endothelium-dependent vasodilatation in humans and rodents (Lesniewski *et al*., 2009, George *et al*., 2006). Talukder *et al* (2011) (Talukder *et al*., 2011) demonstrated the pathophysiological effects of oxidative stress in wild-type (WT) C57Black/6 (C57BL/6) mice, a routinely used experimental mouse model. Animals exposed to cigarette smoke showed cardiac hypertrophy, hypertension, leucocyte activation, ROS generation and a significant reduction in NO availability, a multimodal risk factor for CVD originally described by the Framingham Heart Study.

During the 1990s the development of homologous apolipoprotein E (ApoE) gene targeted knock-out (KO) mouse by Jan Breslow (Nakashima *et al*., 1994, Plump *et al*., 1992) resulted in a plethora of studies looking at CVD and lipid homeostasis. Apolipoprotein transport lipids in the blood and deficiency in humans is associated with atherosclerosis. Breslow and his team generated animals deficient in ApoE, and studies showed significant differences between

gene targeted KO and control groups in plasma cholesterol. Importantly, ApoE KO animals had significantly greater plasma lipids and these hypercholesterolaemia changes were supported by atherosclerotic lesion presentation in KO mice (Nakashima *et al*., 1994).

In addition to the generation of ApoE KO mouse, the low density lipoprotein receptor (LDLr) deficient mouse was developed (Ishibashi *et al*., 1993). LDLr receptor mice show significant elevation for plasma cholesterol when compared to WT control mice and the onset of atherosclerotic lesions, similar to ApoE KO mice (Ishibashi *et al*., 1994a). ApoE KO mice display significantly greater plasma lipids when compared to LDLr KO mice on a chow diet (Ishibashi *et al*., 1994b). However, double KO of ApoE and LDLr failed to show a greater onset of hypercholesterolaemia when compared to single ApoE KO animals (Ishibashi *et al*., 1994b).

Although the two genetic models of CVD (ApoE and LDLr KO) have provided insight into the manifestation of CVD, ApoE and LDLr deficient mice only serve as an experimental model for an aggressive form of CVD, induced by high physiological hypercholesterolaemia. The study of genes, proteins and pathways that are not innately based on irregularities in cholesterol metabolism are then unfavourably tested using these models. Genetic irregularities in lipid metabolism result in plaque formation in humans, in the absence of high dietary cholesterol. Thus, these models of CVD are inherently based on genetic abnormalities in lipid metabolism, a factor which limits the contribution to the overall CVD cases in the human population and limits translational science.

The aggressive phenotype observed in ApoE and LDLr KO mice is more indicative of a latent stage of CVD in humans, one where early intervention is

less applicable. The spontaneous lipid accumulation in the plasma of these animals is not necessarily representative of health in the human population. Individuals may consume high levels of dietary cholesterol intermittently and not necessarily repeatedly or for prolonged durations, such as a single high cholesterol meal at breakfast, lunch and dinner. Thus, the ApoE and LDLr KO mouse models are representative of a chronic state of hypercholesterolaemia. Animal studies using these models have however highlighted the importance of initial dyslipidaemia and its contribution to future adverse CVD events. Crucially, plaque progression can be observed after plasma lipids have normalised through the cessation of dietary cholesterol in animal models (Khanna *et al*., 2013), suggesting significant modulation of pathological processes within physiological systems that are not based on elevated plasma levels; this is believed to be inflammation. Importantly, patients who do not display elevated plasma levels of cholesterol display elevated CVD risk profiles; this is potentially mediated through inflammation.

Inflammation and Endothelial Dysfunction

The generation of pathophysiological signals involved in the development and progression of CVD remains poorly defined. Although plaque formation is known to span many decades, the initial pathological events leading to lesion formation remain poorly understood. Cellular communication is achieved through conserved evolutionary biological signalling pathways responsible for cell growth, cell survival as well as the expression of inflammatory genes. Inflammation and its propagation involve the interplay of many molecules; this in turn mediates numerous cell responses and contributes to the development of

atherosclerosis. Scientific manipulation of animal models to study this process continues to provide invaluable knowledge, aiding both the basic understanding of disease evolution and supporting the innovation of new therapies.

Pre-clinical studies have used gene targeted models, manipulating the expression of inflammatory cytokines such as IL-10, IL-1 (Mallat *et al*., 1999, Mallat and Tedgui, 2007, Isoda *et al*., 2003) and TNF-α (Branen *et al*., 2004) to better understand their role in endothelial dysfunction, as a surrogate marker for CVD. Researchers have developed numerous techniques to assess CVD disease burden in both, clinical medicine and in investigative cardiovascular physiology. Physiological studies of CVD are ordinarily performed post mortem using histological techniques for the assessment of atherosclerotic lesions or *ex vivo* in organ baths, without the control of tissue and system homeostasis. Furthermore, there remain limited translational techniques that are both applicable to human clinical medicine for the interrogation of CVD and for aiding research utility in animal models. Therefore, the translational efficacy of inflammatory molecules as prognostic markers for future adverse cardiovascular events, such as MI or stroke, is unclear. There is uncertainty due to a lack of standardisation amongst research groups, a number of methodological differences such as the use of plasma or serum, differences in the use of anti-coagulations such as heparin or EDTA (ethylene diamine tetra acetic acid), the time frame of measurements (i.e. baseline, monthly, bi-annually, annually) and which inflammatory markers to use (TNF-α, IL-6, IL-10, IL-1, CRP and high sensitive-CRP (hs-CRP)). Furthermore, there are inconsistencies in the large scale epidemiological studies and the evidence for novel markers as accurate predictors above and beyond that of traditional factors, such as blood pressure and plasma cholesterol, for future adverse

cardiovascular events continue to be uncertain, largely due to differences observed in individuals during repeated testing (Pearson *et al*., 2003, Evora *et al*., 2013).

In particular, TNF-α has produced conflicting results, although established as a pro-inflammatory cytokine with an integral role in immunity, bacterial clearance and clinical conditions including diabetes, RA and atherosclerosis (Popa *et al*., 2007) evidence from human studies varies considerably. TNF-α polymorphic analysis suggests a strong, weak or no association to CVD for various TNF alleles (Cho *et al*., 2013, Asifa *et al*., 2013, Keso *et al*., 2001). This is further complicated by research studying the contribution of TNF-α in atherogenesis. Mice deficient in both TNF-α and ApoE display a 50% reduction in atherogenic lesions after 10 weeks on a western type diet (Branen *et al*., 2004), suggesting a role for this cytokine in CVD, when risk factors are combined.

To better understand the role of cytokines in CVD is therefore necessary to study the pathways that stimulate inflammatory cytokines. Cytokine expression can be induced through numerous pathways, such as macrophage toll-like receptors (TLRs) that are able to signal pro-inflammatory gene expression associated with atherosclerosis (Tobias and Curtiss, 2007). As previously discussed, macrophages are highly abundant in atherogenic plaques and contribute to the latent stage of atherosclerosis, with the formation of a necrotic core that is densely filled with lipid. TLRs transduce signals through numerous mediators of inflammation, including p38 mitogen-activated protein kinase (MAPK), suggesting a role for this pathway in atherogenesis. Inhibition of p38 in a model of atherosclerosis has shown to reduce plaque formation (Seeger *et al*., 2010). Therefore, a greater study of the pathways controlling the expression

of inflammatory genes may aid the current understanding of inflammation-induced CVD and the increased CVD risk associated with inflammation as evidenced in patients suffering from RA and SLE.

Toll-like Receptors and Inflammation

Innate immune signalling is dependent on cell surface receptors, providing an interface between the extracellular space and the intracellular domain of cells. TLRs were initially documented for their role in the recognition of invading microbial pathogens. More specifically, TLRs are able to recognise pathogen associated molecular patterns (PAMPs) on the cell surface of microbes, which are absent from mammalian tissue. Lipopolysaccharide (LPS) is released by gram negative bacteria during cell lysis and recognised by a specific type of TLR (TLR-4). There are many documented members of the TLR family (TLR 1-13 in mouse and TLRs1-10 in man (Falck-Hansen *et al*., 2013). The extracellular TLRs are: TLR1-2, TLR4-6 and TLR11, for the detection of lipoproteins. Conversely, the TLRs expressed in the cell cytoplasm include: TLR3, TLR7-9 and the mouse TLR12-13 (**Figure 1.4**), these intracellular TLRs are involved in the detection of bacterial and viral nucleic acids. Intracellular TLRs are expressed on cellular organelles such as the endoplasmic reticulum, endosomes and lysosomes, suggesting specific extracellular and intracellular function for each of these receptors (**Figure 1.4**).

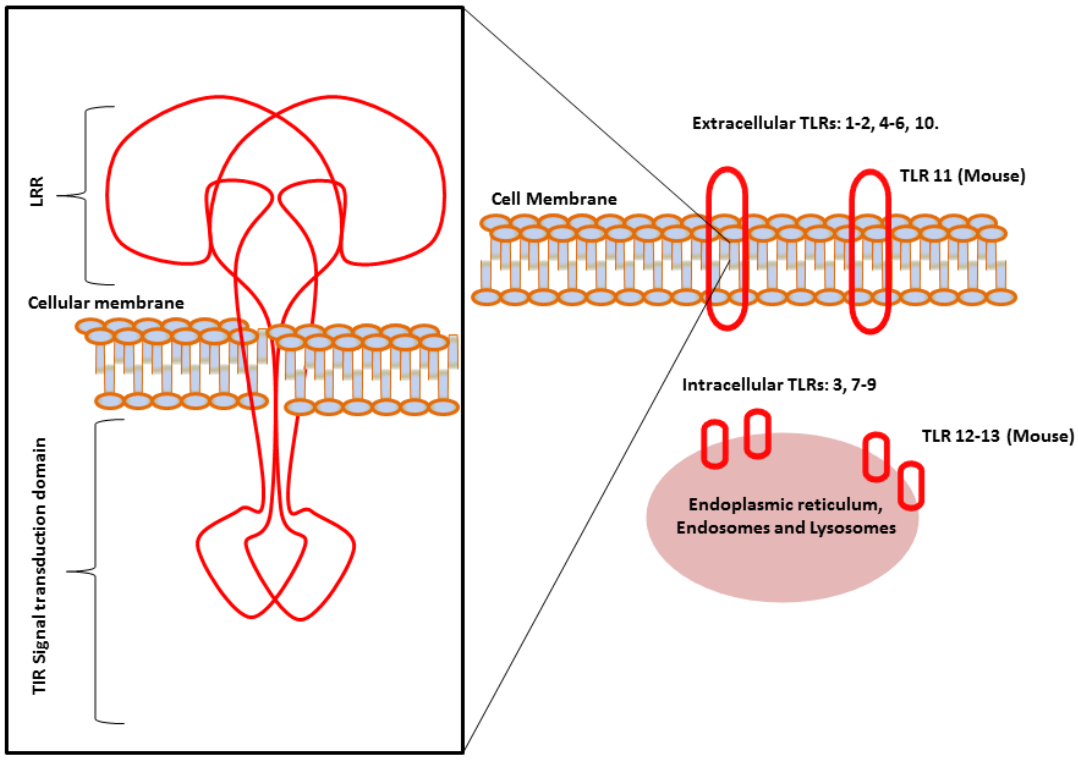

Figure 1.4. Extracellular and intracellular expression of TLRs: Extracellular TLR's are 1-2,4-6,10 and the mouse TLR11, intracellular TLRs are 3,7-9 and the mouse 12-13, species differences between man and mouse as denoted. LRR= leucine-rich repeat. TIR= toll\IL-1 receptor domain.

TLRs are membrane-spanning receptors with a leucine-rich repeat (LRR) extracellular motif. TLRs have a horse-shoe like ectodomain that can interact with agonists such as LPS through a string of LRR. The copy number of LRR varies and is typically between 20-25 amino acids in length which maintain the horse-shoe like structure. The ectodomain is followed by a trans-membrane helix and initiates downstream effects through a toll\IL-1 receptor (TIR) domain. This LRR repeated domain serves as an integral part for recognition of PAMPS and danger associated molecular patterns (DAMPs), forming protein-to-protein interactions activating downstream events.

The physiological relevance of TLRs have previously been studied. TLRs show specificity to particular pathogen components, demonstrating the highly

specialised nature of the mammalian immune system, with an ability to distinguish between pathogens and pathogenic components i.e. PAMPs and LPS.

Transmembrane signalling via TLRs causes homodimer formation, except for TLR1/2, 2/6, 4/6/CD36 that forms heterodimers. The TLRs share LRR and a TIR domain for signalling downstream, which is achieved through adaptor molecules. The cytoplasmic TIR domain that governs the TLR signalling pathway for all TLRs except TLR-3 rely on a proline residue. Trans-cytoplasmic signalling by TLRs is achieved by TIR and myeloid primary response gene 88 (MyD88).

MyD88 is a universal adaptor molecule and is used by all TLRs, except TLR-3 and thus TLR-3 activation is regarded as being MyD88 independent, as opposed to MyD88 dependent signalling. Other adaptors include TIR domain-containing adaptor inducing interferon (IFN-β) (TRIF), MyD88-like adaptor (Mal)/TIR domain containing adaptor protein (TIRAP), and TRIF-related adaptor molecule (TRAM) (Cole *et al*., 2013).

TLR2 and TLR4 require Mal/TIRAP to bridge the TIR domain with MyD88. MyD88 also has a TIR and death domain (DD); following TLR activation, the MyD88 DD interacts with the DD of intracellular receptor associated kinase-4 (IRAK-4), IRAK-1 and IRAK-2. IRAK kinases phosphorylate tumour necrosis factor receptor associated factor-6 (TRAF-6) and E3 ligase (**Figure 1.5**) (Cole *et al*., 2013). Polyubiquitin binding results in transforming growth factor TGF-β-activated kinase-1 (TAK-1) binding proteins (TAB2-3) activating TAK-1. Activation of TRAF-6 causes polyubiquitination of TAK-1 as well as itself (TRAF-6) assisting binding to the inhibitors of kB (IκB). Phosphorylation of IκB

promotes its degradation. The loss of IκB induces nuclear translocation of nuclear factor kappa B (NF-κB) from the cytoplasm, activating transcription and induces the expression of inflammatory genes (**Figure 1.5**). This innate signalling cascade causes the production of many inflammatory genes that are non-specific and thus, this is regarded as an early phase response in immunity.

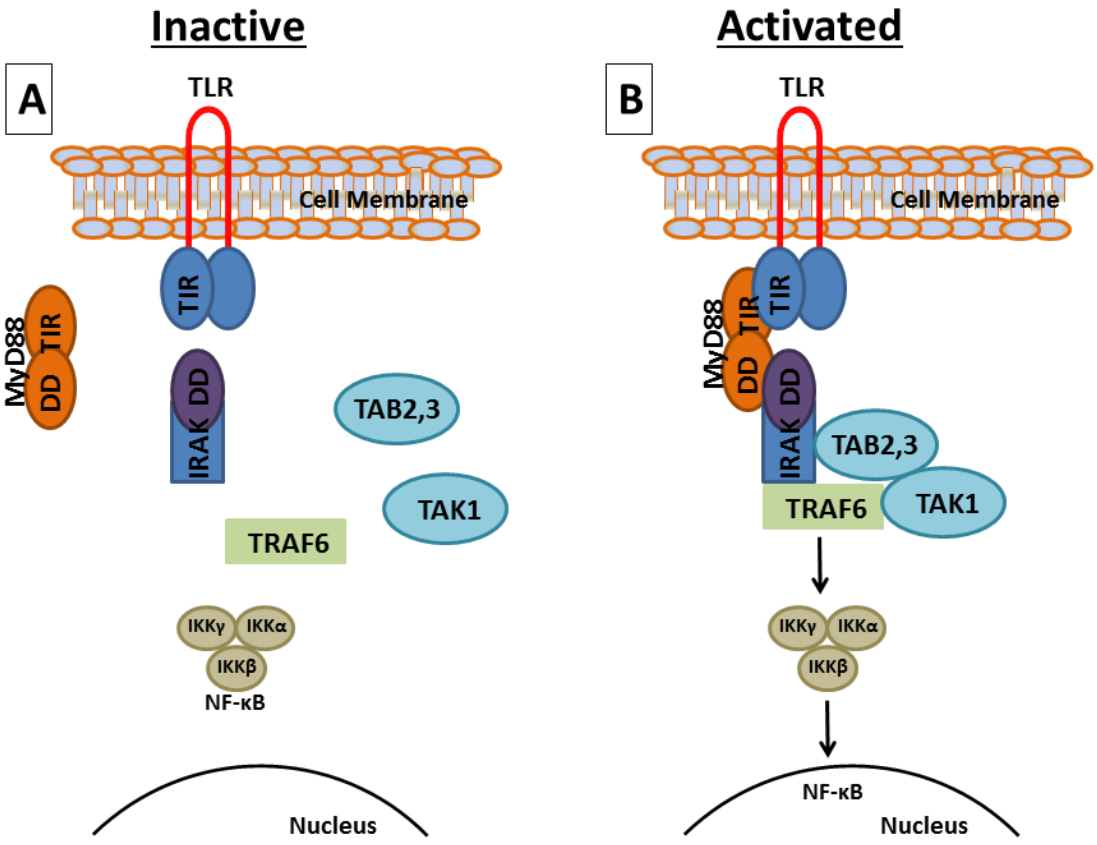

Figure 1.5. MyD88-dependent TLR Signalling: A: inactive, resting cell and B: activated/stimulated cell Toll-like receptor (TLR), interactions with toll/interlukein-1 receptor (TIR) and MyD88 for NF-κB activation. Adapted from (Han, 2006).

The integral role of MyD88 in the inflammatory responses has previously been established. Animals deficient in MyD88 show depleted inflammatory responses to LPS, peptidoglycan, imidazoquinoline and flagellin, specific TLRs agonists. Furthermore, animals deficient in MyD88 display depleted responses for the

production of IL-6 and TNF-α, supporting the role of MyD88 in the mediation of inflammatory responses via TLRs.

TLR signalling, specifically TLR1/2, TLR4 and TLR5 expression is highly evident in atherogenic lesions. TLR4 accumulation can be specifically observed in regions that are prone to rupture through the increased expression and release of matrix metalloproteinase-9 (MMP-9), that possess the ability to instigate plaque rupture through protein lysis. Within atherogenic lesions, numerous research groups have shown increased expression of TLR4, which is specifically up regulated in macrophages in responses to oxLDL (Bjorkbacka *et al*., 2004, Cole *et al*., 2013, Tobias and Curtiss, 2007).

The ability of TLRs to detect oxLDL makes them important signalling molecules in CVD. Elevated plasma cholesterol is an established risk factor for future adverse cardiovascular events, and thus blockade of TLRs may provide a novel avenue for attenuating/ alleviating early CVD. TLR4 further signals for a number of pro-inflammatory molecules, including adhesion molecules, VCAM-1 and ICAM-1 that are relevant to CVD in the capture and transmigration of monocytes into the sub-endothelial space.

Animals deficient in the adaptor MyD88 display reduced atherosclerosis and a significant reduction in the infiltration of macrophages into the arterial lumen, when backcrossed onto the ApoE KO CVD-prone mouse (Bjorkbacka *et al*., 2004). Under shear flow, where flow is laminar, the production of NO maintains a non-adherent, quiescent phenotype. Duzendorfer *et al* (2004) (Dunzendorfer *et al*., 2004) demonstrated the up regulation of TLRs during disturbed laminar flow or static flow (no flow), representative of no/low flow conditions during MI.

Without MI, endogenous flow differences exist throughout the cardiovascular system, due to the natural curvature of the aorta. Flow differences produce sites that are either prone to atherogenesis and those that are essentially athero-protective (mid-thoracic aorta) early in atherosclerosis development. Pulsated blood from the left ventricle remains laminar until the aortic arch; here the flow and direction of blood changes and a more turbulent pattern can be observed (**Figure 1.6**). Thus a reduction in laminar flow reduces shear stress and depletes NO bioavailability, promoting an altered vascular phenotype that is pro-inflammatory and activated, inducing the adherence of monocytes for subsequent infiltration, a pre-requisite for the development of atherosclerosis.

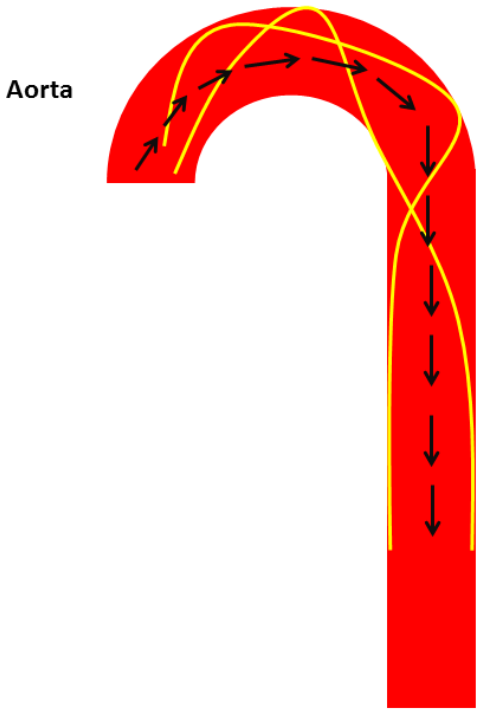

Figure 1.6. Aortic blood flow: Blood entering the aorta remains laminar until the aortic arch; the curvature of the aortic arch induces turbulent flow producing haemodynamic variation and reduces shear stress. Yellow lines denote turbulent flow; black arrows show median direction of blood flow without disruption.

TLR2 inhibition has shown promising results with a reduction in infarct size in an ischaemic model of reperfusion injury in the pig (Arslan *et al*., 2012). Inhibition

of TLR2 in the study by Arslan *et al* demonstrated reduced inflammation and macrophage infiltration with a significant reduction in MMP-9. Further to this, experimental groups that are double KO for ApoE and MYD88 displayed no significant changes in plasma triglycerides and total plasma cholesterol when compared to controls ApoE KO mice (Bjorkbacka *et al*., 2004). Supporting the notion that pathophysiology in atherogenesis are a direct results of the innate immune response, as opposed to a secondary outcome or change in plasma lipid metabolism, mediated through a similar pathway. The role of MyD88 activation in endothelial dysfunction has not previously been described. Importantly, MyD88 inactivation early in CVD may be a novel therapeutic avenue to limit inflammatory responses, protecting against overt inflammatory-mediated diseases, such as atherosclerotic plaque formation. There are other regulators of inflammation after TLR activation that can induce the synthesis of inflammatory genes associated with CVD; these include the MAPK pathway (Muslin., 2008).

Mitogen Activated Protein Kinases in Inflammation

MAPKs are involved in a large number of biological functions from cell proliferation, differentiation, cell survival and programmed cell death. Biological signalling in this group relays extracellular events to the intracellular domain of cells, a process which is underpinned by phosphorylation cascades and negatively regulated by MAPK phosphatases. Activation of MAPK can be induced by TLR stimulation. There are three well established MAPKs family groups; extracellular signal-regulated kinases (ERK) isoforms 1 and 2; the c-Jun-N terminal kinases (JNK) of which there are isoforms 1-3 and MAPKs p38,

isoforms α, β, γ and δ (**Figure 1.7**). Because these pathways are involved in the development, growth and apoptosis of cells, the tight regulation of phosphorylation cascades is essential to ensure cell survival, as unabated signalling could result in excessive cell proliferation and/or cell death.

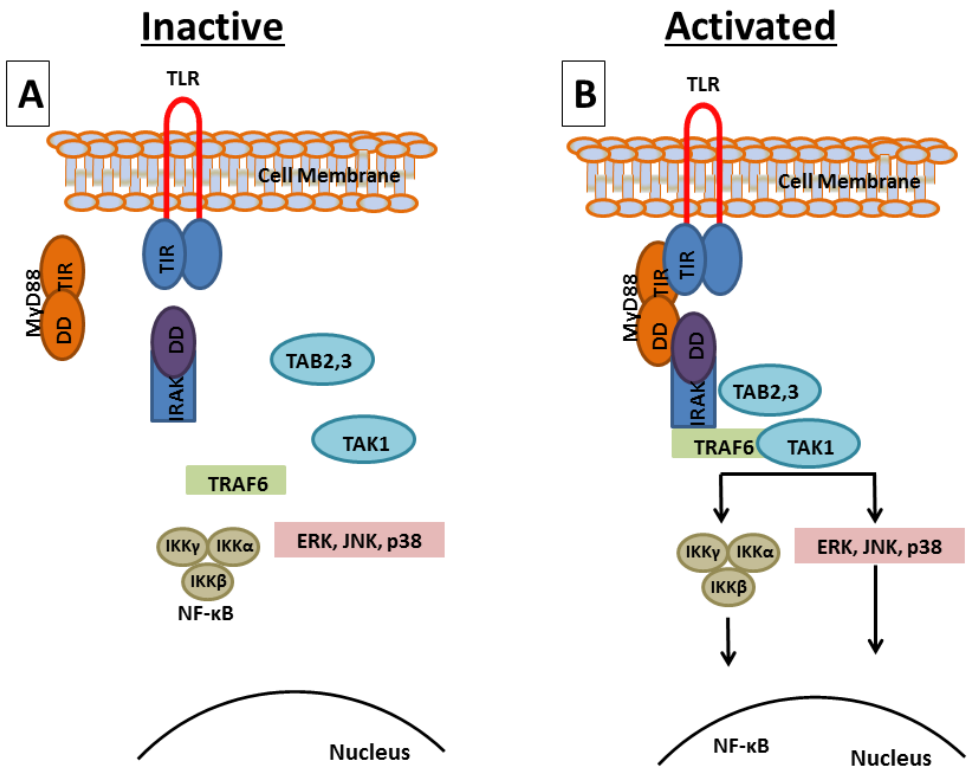

Figure 1.7. MAPK activation: A: inactive, resting cell and B: activated/stimulated cell. MAPK; ERK, JNK and p38 kinases are activated after TLR stimulation.

Activation of ERK 1/ 2 is associated with the development of cardiovascular hypertrophy (Zhang *et al*., 2003). The involvement of JNK and MAPK p38 pathways in physical/chemical stress, infections and cytokine release makes them an effective target for vascular study. JNK subfamilies JNK1&2 are ubiquitously expressed in physiology: signalling immune activation, cytokine production and inflammation. Additionally, physiological roles of JNKs in atherosclerosis have been documented (Sumara *et al*., 2005).

MAPK p38 is of particular interest due to its subfamily expression of p38α. Like the JNK pathway, p38 kinases are concerned with immunity, triggered by the inflammation cascade which in turn leads to the signalling promotion of inflammatory molecules including: IL-1, TNF-α, IL-6, VCAM-1, proliferation, differentiation and the function of leucocytes. Physiologically, the regulatory functions of the p38 pathways make it an important precursor in chronic inflammatory conditions such as atherosclerosis (Mei *et al*., 2012, Yang *et al*., 2014) .

While p38α is known to have inflammatory roles, recent work has also revealed that it can also have anti-inflammatory functions (Arthur and Ley, 2013, Guma *et al*., 2012). For example, mice with a myeloid specific deletion in p38α show increased pathology in an ultraviolet-B (UV-B) induced skin inflammation model (Kim *et al*., 2008) and in a model of RA (Guma *et al*., 2012). The anti-inflammatory effects of p38α are mediated, in part, via the activation of mitogen and stress kinase (MSK) 1 and 2 (Kim *et al*., 2008). MSK1 and MSK2 are nuclear kinases that are activated downstream of the ERK1/2 and p38α MAPKs and serve to help regulate the induction of immediate early genes (Arthur, 2008) (**Figure 1.8**).

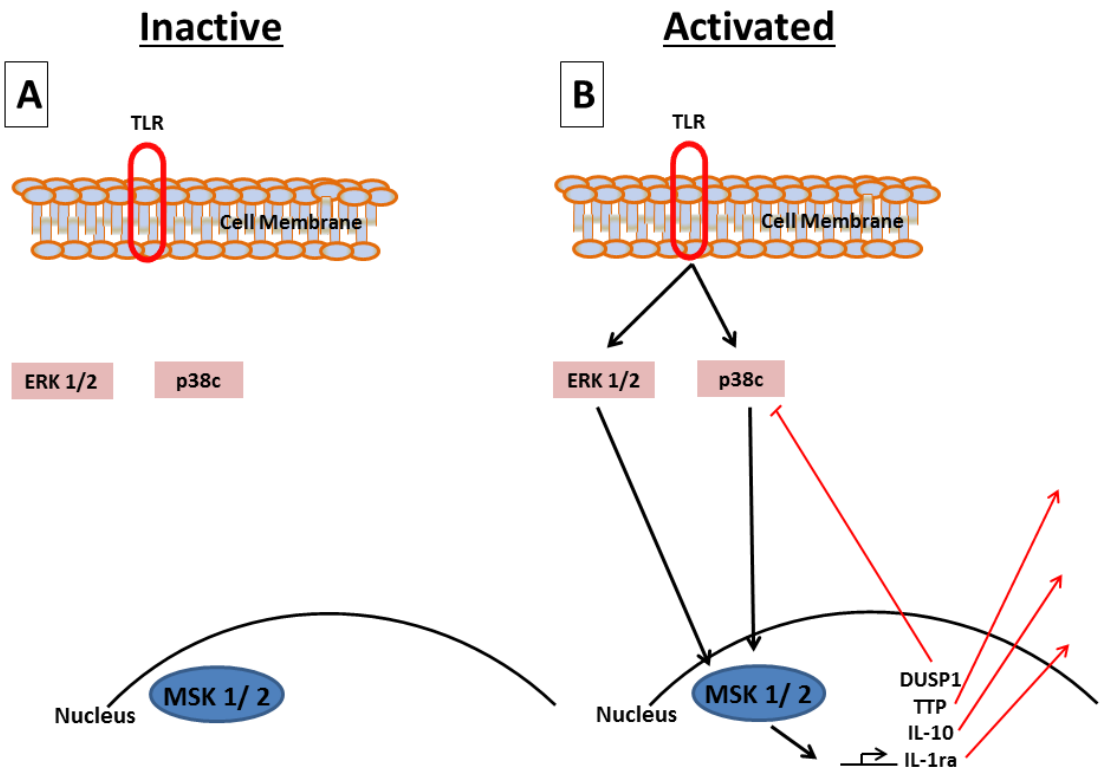

Figure 1.8. MSK 1/ 2 induction of anti-inflammatory genes: A: inactive resting cell and B: stimulated cell. TLR stimulation stimulates MAPK p38 and ERK phosphorylation of MSK 1/ 2 and the induction of anti-inflammatory genes.

TLR signalling in macrophages has shown to activate MSKs and this promotes the transcription of several genes with anti-inflammatory functions, including the cytokines IL-10 and IL-1ra (Kim *et al*., 2008, Darragh *et al*., 2010) (**Figure 1.8**). MSKs also regulate the induction of a dual specificity phosphatase (DUSP1) (Kim *et al*., 2008) (**Figure 1.8**), involved in deactivation of p38α and JNK, downstream of TLR signalling (Wang and Liu, 2007). As a result of this, MSK1/2 double KO mice exhibit increased sensitivity to LPS-induced endotoxin shock, which is accompanied by an increase in TNF-α, IL-6 and IL-12 relative to WT animals (Kim *et al*., 2008). The role of MSK 1/ 2 in CVD has not previously been addressed. TNF-α, IL-6, -10 have previously been reported in the pathogenesis of CVD. The MSK 1/ 2 kinases may provide novel insights into the downstream

signalling of inflammation in the development of CVD.

Mitogen Activated Protein Activated-protein kinases in Inflammation

The ability to modulate inflammation holds the potential to alleviate inflammatory disease burden. In particular, it may stop the progression of inflammatory diseases, such as SLE, RA and inflammation induced CVD. The MAPK p38 inhibitor SB-203580 has shown favourable results in limiting inflammation. Koyo *et al* (Kyoi *et al*., 2006) reported an improvement in heart failure in a hamster model using the SB-203580 compound and exacerbated damage when a JNK inhibitor (SP600125) was used. It is important to remember that MAPK p38 has numerous roles; as previously discussed, it is able to phosphorylate MSK 1/ 2 that have anti-inflammatory properties, a loss may lead to undesired effects such as the perpetuation of inflammation as observed in the MSK 1/ 2 KO mouse when compared to WT cells. The genetic deficiency of MAPK p38 emphasises the incompatibility of this molecule as a target for inflammatory mediated diseases, as MAPK p38 KO murines are embryonic lethal (Allen *et al*., 2000).

Mitogen activated protein activated-protein kinases (MAPKAP) 2/ 3 are downstream substrates of p38. These two kinases are important messengers in the inflammation cascade, and their involvement is mainly in regulation of gene expression (Ronkina *et al*, 2010). Deficiency of either MAPKAP 2 or 3 does not produce a discernible phenotype and off-spring are otherwise healthy.

As discussed previously, macrophages are able to recognise both exogenous and endogenous molecules, and elicit an inflammatory response through TLRs, acting downstream on NF-kB or MAPK p38 respectively, giving rise to the release of inflammatory cytokines.

Importantly MAPKAP 2 deficient animals display a significant attenuation of TNF-α production in response to LPS, a response which is a fraction of that observed in WT animals (10% of WT response) (Ronkina et al., 2007. The MAPKAP 2 KO model has shown translational potential, with resistance to the development of RA in an animal model (Hegen *et al* 2007).

Although MAPKAP 2 is physiologically more abundant than MAPKAP 3, there remains some compensatory mechanisms. In the absence of MAPKAP 2, MAPKAP 3 will induce TNF-α synthesis (Ronkina *et al* 2007). The double homologous KO yields a TNF-α response that is 1-3% when compared to the single MAPKAP 2 KO in macrophages, a >90% decreased in comparison to WT cells. The double KO does not yield an alternative phenotype, suggesting that the physiological function of these kinases is similar, although their expression levels vary considerably.

MAPKAP 2 is essential for the generation of inflammatory cytokines; however mRNA levels for TNF-α do not vary considerably from WT mice (Ronkina *et al* 2010). Under basal conditions these kinases are localised in the nuclear envelope. Upon an appropriate signal from MAPKP p38, MAPKAP 2/3 are activated and exported from the nucleus. MAPKAP 2/3 equally lead to stabilisation of MAPK p38.

One mechanism by which MAPKAP prolongs inflammation is by the modulation of inflammatory mRNA-stability of cytokines such as TNF-α. MAPKAP 2/3 target specific adenosine and uridine(AU)-rich elements (ARE) of TNF-mRNA that were shown to be essential for the post-translational regulation of TNF synthesis, suggesting a modulatory role for MAPKAP 2/3 in ARE binding. One member of this group is tristetraprolin (TTP), important in TNFα-mRNA-ARE-

binding. TTP can act on the 3'-unsaturated region of the RNA of protein inflammatory mediators, via phosphorylation, thus inducing stability.

The regulation of inflammation is of key importance in physiological systems and this is largely achieved through activation of STAT3 (signal transducer and activator of transcription 3) through IL-10 synthesis. IFNs are regarded as key mediators of IL-10 production in macrophages and thus potent initiators of anti-inflammatory effects. Importantly, MAPKAP 2/3 activation suppresses IL-10 production..

MAPKAP 2 deficient mice have shown a reduction in atherosclerotic lesion presentation when back-crossed on to an LDLr KO mouse. These double KO animals show significantly reduced lipid deposition after 16 weeks on a cholesterol diet, with reduced expression of VCAM-1, macrophage infiltration and reduced foam cell formation (Jagavelu *et al* 2007). Although the role of these kinases has been assessed in atherosclerosis, their role in development of early endothelial dysfunction *in vivo* has not previously been reported.

NF-κB Regulation in Inflammation

As previously discussed, the activation of TLRs can induce the activation of NF-kB and mediate the release of pro-inflammatory genes relevant to CVD. In mammalian tissues, the NF-κB family consists of: RelA (p65), RelB (RelB), C-Rel (Rel), NF-κB1 (p50 and the precursor p105) and NF-κB2 (p52 and the precursor p100). These family members are involved in a wide range of biological activities including immune function and inflammatory responses. Under basal conditions, NF-κB is sequestered in the cytoplasm; however stimulation of appropriate receptors such as MyD88 dependent activation of

TLRs causes nuclear translocation, through a phosphorylation cascade where IκBs are degraded (Van der Heiden *et al*., 2010) (**Figure 5**).

All members of the NF-kB family share a conserved region called the N-terminal rel-homology-domain (RHD). The N-terminus of the RHD is the DNA-binding domain. The transportation of NF-κB from the cell cytosol to the nucleus is dependent on a nuclear localisation signal (NLS), which is situated at the C-terminal end of RHD. IκBs sequester NF-κB dimers in the cell cytosol by non-covalent interactions containing a repeated amino acid sequence termed ankyrin repeats. IκB inhibitors interact with the RHD region through the ankyrin repeats and conceal the NLS, maintaining the dimer in the cell cytosol.

The degradation of IκB permits the movement of NF-κB to the nucleus; however IκB activation is complex and involves phosphorylation by the Iκκ complex. This Iκκ complex is composed of an Iκκ-α, Iκκ-β and Iκκ-γ subunit; Both the Iκκ-α/β subunits possess catalytic properties whereas the Iκκ-γ is non-catalytic and is also termed NEMO (NF-kB essential modulator) (**Figure 1.9**).

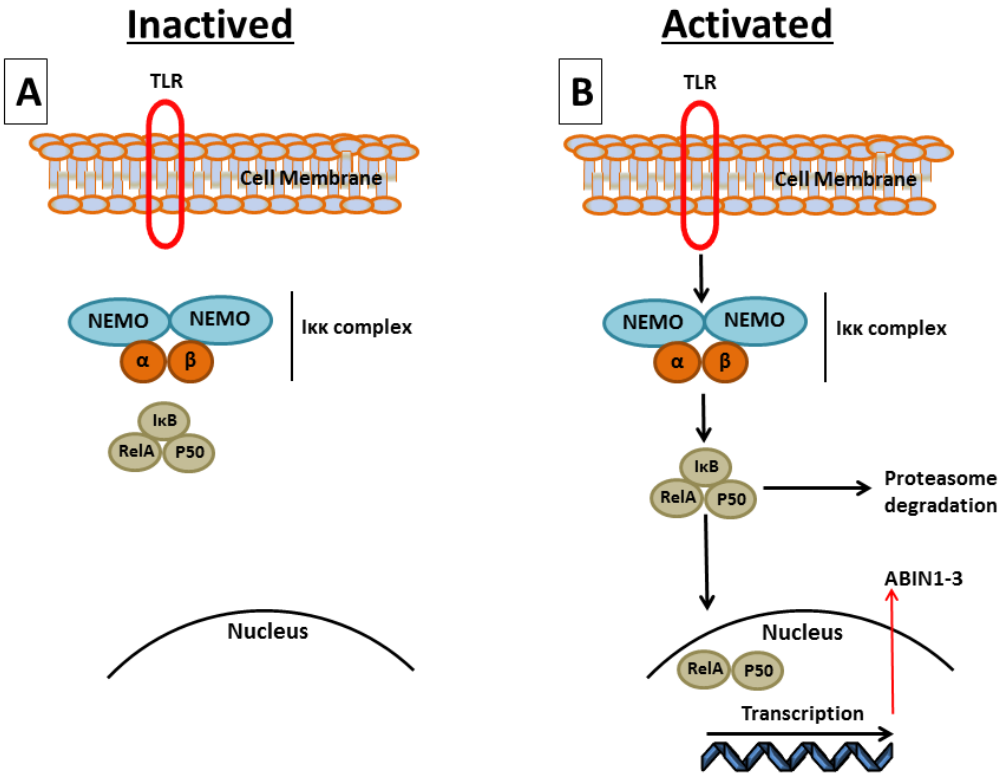

Figure 1.9. NF-κB activation: A: inactivated and B: activated cell. TLR activation through MyD88 induces IRAK4 phosphorylation of TRAF6 and the activation of IκK. IκK phosphorylates IκB and NF-κB translocate to the nucleus to stimulate transcription.

NF-κB activation mediates the release of inflammatory molecules associated with atherosclerosis, including IL-6, IL-10 and TNF (Mallat *et al*., 1999, Huber *et al*., 1999, Boesten *et al*., 2005). Under physiological conditions, NF-kB inhibitors maintain inflammatory homeostasis, silencing gene expression after appropriate receptor stimulation, such as the activation of TLRs. The A20-binding inhibitors of NF-κB (ABINs1-3) are suppressors of inflammation. Recent work suggests that ABIN1 restricts the activation of the canonical IKK complex and MAPK, by binding to Lys63-linked and linear ubiquitin chains (Nanda *et al*., 2011).

Human polymorphisms in the gene encoding the ABIN1 protein have been identified and are associated with a pre-disposition for autoimmune disease (Caster *et al*., 2013). The clinical manifestations of polymorphisms in ABIN1 are

wide spread and can resemble SLE (Vaughn *et al*., 2012, Adrianto *et al*., 2012). Mutations in ABIN1 are associated with psoriasis, psoriatic arthritis and importantly in the context of CVD, He *et al* (He *et al*., 2010) reported an enhanced risk of vasculitis. The TNIP1 (TNFAIP3-interacting protein 1) gene locus that encodes for the protein ABIN1 is associated with the predisposition to SLE (Adrianto *et al*., 2012), and it is also thought to be significantly associated with other inflammatory mediated pathologies including CHD and MI (Ozaki *et al*., 2002, Ozaki and Tanaka, 2005, Boonyasrisawat *et al*., 2007). Wolfrum *et al* (2007) (Wolfrum *et al*., 2007) studied mice that were haploinsufficient for A20, a protein that interacts with ABIN1, and backcrossed them on to the CVD prone apolipoprotein E KO mouse. These mice showed significant exacerbation in atherosclerotic lesion presentation, mediated through NF-κB activation (Wolfrum *et al*., 2007).

The important roles of ABINs in physiology are highlighted in gene targeted KO mice that display organ failure and premature death (Zhou *et al*., 2011). A knock-in mouse in which WT ABIN1 was replaced by the polyubiquitin-binding-defective mutant ABIN1[D485N] has previously been described (Nanda *et al*., 2011). Several types of immune cells from these mice show enhanced NF-κB and MAP kinase activation after TLR stimulation and display an SLE-like phenotype (Nanda *et al*., 2011). The ABIN1[D485N] knock-in mice show significant expansion of myeloid cells in various organs (Nanda *et al*., 2011). Caster *et al* (Caster *et al*., 2013) reported similarity between the ABIN1[D485N] mice and SLE patients in the context of lupus nephritis, a leading cause of morbidity and mortality in chronic inflammation. However, the onset of CVD relevant to this mutation has not been addressed.

In conclusion the development of CVD is attributed to CVD risk factors such as dietary cholesterol, smoking and physical inactivity. Risk factors share common physiological responses of inflammation. Through receptor stimulation of innate immune signalling pathways such as TLRs, transcription factors are activated and signal the synthesis and release of pro-inflammatory cytokines. Importantly, these cytokines are also present in chronic inflammatory disease conditions such as RA and SLE; two patient groups that display elevated risk profiles for CVD that is not fully explained by the Framingham risk score (Esdaile *et al*., 2001). Systemic cytokine expression in humans has suggested a causal relationship to the onset of CVD. Animal models of CVD, where inflammatory gene expression is in part abrogated have shown protection to CVD. There remains limited information on the role of intracellular signalling pathways and the development of endothelial dysfunction, an early event in CVD. Importantly the modulation of endothelial function by the expression of systemic cytokine expression remains understudied, with limited *in vivo* studies. Animal models of CVD for specific pathway analysis are further limited by the deployment of translational techniques, which would allow laboratory findings to be related to those in human clinical trials.

Thesis Aim

The overall aim of this thesis is to longitudinally measure vascular responses in the skin microcirculation of mice, using LDI and drug iontophoresis of vasoactive chemical *in vivo*, that have undergone genetic and dietary alterations. This thesis aims to assess the role of underlying signalling pathways that are responsible for the expression of inflammatory molecules early in the pathogenesis of CVD through the use of innate immune models of protein phosphorylation.

Hypothesis

The main hypothesis is that systemic cytokine expression is implicated in the pathogenesis of endothelial dysfunction and can be hindered/ exacerbated through alterations in innate immune pathways.

Specific Aims

1. To measure microvascular responses in the skin microcirculation of mice longitudinally, using LDI and iontophoresis of vasoactive chemicals *in vivo*.
2. To better understand the complexity between microvascular responses and systemic cytokine expression.
3. To better understand the role of mitogen and stress kinases (1/ 2) in the pathogenesis of endothelial dysfunction.
4. To better understand the role of TLR activation in the pathogenesis of endothelial dysfunction.

5. To better understand the role of MAPKAP 2/3 in the pathogenesis of endothelial dysfunction.

6. To better understand the role of ABIN1 in the pathogenesis of endothelial dysfunction.

Chapter 2

Materials and Methods

Mouse Generation

Breeding

Animal colonies were established by housing mice of appropriate age (minimum 6 weeks) for copulation. All mating animals were genotyped before pairings. First litters were also genotyped to confirm transgenic knock-in, KO or WT status. Offspring were weaned at 21 days of age and utilised in studies as described (Table 2.1). Additional WT C57BL/6 males were purchased from Charles River Laboratories at 8-10 weeks of age.

Table 2.1. Summary of mouse models and study groups used for investigations detailed in this thesis.

Study/Chapter	Animal group	Group 1	Group 2	Group 3	Group 4
Blood pressure/ Chapter 3	C57/black/6	WT-chow – Habitualization	WT-chow – Anaesthesia	-	-
Blood pressure and iontophoresis / Chapter 3	C57/black/6	Vehicle iontophoresis	ACh iontophoresis	SNP iontophoresis	-
Blood Glucose/ Chapter 3	C57/black/6	WT-chow	WT-cholesterol	-	-
MSK1/ 2 / Chapter 4	MSK 1/ 2	WT-chow	WT-cholesterol	KO-chow	KO-cholesterol
MyD88/ Chapter 5	MyD88	WT-chow	WT-cholesterol	KO-chow	KO-cholesterol
MAPKAP2/3 / Chapter 6	MAPKAP	WT-chow	WT-cholesterol	KO-chow	KO-cholesterol
ABIN1(D485N) / Chapter 7	ABIN1 (D485N)	WT-chow	WT-cholesterol	ABIN1(D485N)-chow	ABIN1(D485N)-cholesterol
Vitamin D supplementation/ Chapter 8	MSK 1/2	KO-cholesterol – Vehicle	KO-cholesterol - Calcitrol	-	-

Genotyping

The genotype of offspring and mating pairs was determined by polymerase chain reaction (PCR). Whole genomic DNA was obtained from tail biopsies and

genotyped according to previously published sequences and PCR methods as detailed in **Table 2.2** by animal facility personnel**.**

Table 2.2. References for genotyping sequences for genetically modified mice.

Animal Strain	Primer sequences	Reference
Mitogen and stress kinases activated (MSK) 1/ 2	MSK1 knockout mice, primers: CACTTCGCCCAATAGCAGCCAGTCCCTTCC (targeted), TCCGCAGCTCGTGCTTGACAGTAAGGAGC (wild type), and AATAGCGCTGGTGGCTCAGGGCTGT. Genotyping for MSK2 knockout mice, primers: CGTTGGCTACCCGTAATATTGCTGAAGAGC (targeted), AAGATCTTCAGGGCATCTCTTTATCCTACG (wild type), and TTGTGCTCCCCATGCTGCAGCCCGGCCTTC (targeted or wild type).	(Wiggin *et al*., 2002)
Myeloid differentiation primary response gene-88 (MyD88)	FORWARD (K/W) = 5'GGT CCA TTG CCA GCG AGC TAA TTG AG 3' REVERSE (W) = 5' CTG GGA AAG TCC TTC TTC ATC GCC TTG T 3' REVERSE (KO) = 5' ATC GCC TTC TAT CGC CTT CTT GAC GAG 3'	(Adachi *et al*., 1998)
Mitogen activated protein kinase activated-protein (MAPKAP) 2/3	MK2 forward (5'-CATGCCATGATGAGGTGCCTCTGC-3') and MK2 reverse (wild-type allele, 5'-CCCTCTCTACCTCTTTCTGTGAATGCC-3'; knockout allele, 5'-CTGTTGTGCCCAGTCATAGCCG-3'); and MK3 forward (5'-GCCAATGTCCCGCATTATCTCTGC-3') and MK3 reverse (wildtype allele, 5'-CAGGGAGCACTCACAGAGCAGTGGGC-3'; knockout allele, 5'-CTGTTGTGCCCAGTCATAGCCG-3')	(Ronkina *et al*., 2007)
A20 binding inhibitor of NF-κB-1 (ABIN-1)(D485N)	P1 5′ LoxP sense (5′-ATCCAACTCTCCAGCCAATAACC-3′), P2 5′ LoxP antisense (5′-GAGGCGTGTGGAAGTCTGC-3′), P3 mRNA sense (5′-CGTTGTGAGTTGGATAGTTGTGG-3′), P4 mRNA antisense (5′-AGCTGGCTCTGAAAGATGAAGG-3′), P5 3′ LoxP sense (5′-CCTATCCCTATGCCTACCCACCCATG-3′), P6 3′ LoxP antisense (5′-AGCTGACTCGGCAGCCGATGGTACTC-3′), and P7 *neo*-IRES sense (5′-CGTATTCAACAAGGGGCTGAAGGATGC-3′).	(Nanda *et al*., 2011)

Animal Housing and Husbandry

All listed procedures were carried out under the authority of a U.K. Home Office project license by Personal License Holders. Prior approval was granted by the institutions ethics committee for all studies (University of Dundee). Animals were generated in specific pathogen free conditions within the transgenic laboratories at the Wellcome Trust (University of Dundee) and were specifically all C57BL/6 male mice.

Animals were housed together in groups of up to six. Diets consisted of standard rodent chow (Special Diets Services: Rat&Mouse diet number 1 fed as a standard or Rat&Mouse diet number 3 for breeding animals, United Kingdom) and sterilised distilled water fed *ad libitum* after weaning, for all animals and for the total study duration unless otherwise stated. Cages were kept in a room that maintained a 12hour light/dark cycle and a constant temperature of 22±2 ^{o}C.

Animals were transferred from a barrier breeding facility to the experimental facility (in which the necessary equipment was installed) at least one week before vascular function testing, to allow acclimation and to avoid stress**.** Upon arrival animals were acclimated to the Medical School Resource Unit (MSRU) at Ninewells Hospital unit for at least 7 days prior to any experimental testing.

A specifically tailored pro-atherogenic diet (TD.01383 diet, Harlan-Teklad) (18% protein rodent chow with added cholesterol, 2% by weight) that has been used in previous studies (Singer *et al*., 2013) was used for all cholesterol challenged experiments. The diet consisted of (by weight) 18% protein, 47% carbohydrates and 6% fat. Previous studies have reported the presence of hypercholesterolaemia after one week of cholesterol feeding (Tsuda *et al*., 1983).

In Vivo Vascular Assessment

Laser Doppler Imaging (LDI)

LDI was the primary technique used in all experimental study chapters for assessment of endothelium-dependent responses to vasoactive chemicals (Belch *et al*., 2013). LDI is an automated computerised system that allows the assessment of perfusion in very fine arterioles, venules and capillaries supplying the skin. LDI allows changes in blood flow to be monitored overtime or in relation to particular stimuli i.e. agonist drugs.

Numerous animal studies have used ApoE KO mice that spontaneously show dyslipidaemia on a standard rodent chow diet (Boesten *et al*., 2005, Bjorkbacka *et al*., 2004, Nakashima *et al*., 1994. These investigations have largely focused their studies on medium-large sized vessels, showing lipid streaks within the aorta, carotid and brachial artery. Johansson *et al* (2005) effectively communicated the importance of intra-vascular differences in endothelial dysfunction in the presence of hypercholesterolaemia in large vessels. Impaired endothelial function is apparent in lipid prone regions of the aorta including the proximal ascending aorta and the aortic roots in cholesterol fed animals. However, the mid-thoracic aorta does not show impairment and is effectively preserved in the same mice early in the disease process. These differences hinder the effective study of early changes relevant to endothelial dysfunction using traditional technologies such as the tension based organ bath system (Akbar *et al*., 2011). Vascular rings cut from the aortic arch, thoracic and abdominal aorta may produce significantly different responses early in pathophysiology. The uncertainty of intravascular pathology results in tissue homogeneity, an experimental limitation in *ex vivo* studies. Most importantly

vessel segments may not represent the entire vascular system and may only be representative of turbulent flow, an established factor for atherogenesis (Prado *et al*., 2008). As previously discussed in the *Introduction (Toll-like Receptors and Inflammation),* turbulent flow is associated with reduced shear stress. Turbulent flow is progressively lost and becomes less significant as blood is ejected from the left ventricle and travels through the arterial system, producing the least hemodynamic variation in peripheral blood. Shear flow is a stimulator of NO production, inducing basal vasomotion and maintains the endothelium as a quiescent no adherent surface.

The skin microcirculation has been utilised in numerous clinical studies and has shown good correlation with central cardiac function (Khan *et al*., 2008), and has been used as a biomarker in CVD (Galarraga *et al*., 2008, Khan *et al*., 2000). The small vessels in the skin microvasculature are relevant to whole body physiology and the cardiovascular system as important regulators of blood pressure through the modulation of peripheral resistance.

Although LDI has been used successfully in numerous clinical trials to interrogate the skin microcirculation in humans (Kruger *et al*., 2006), the use of LDI in animal studies is limited (Turner *et al*., 2008). Numerous groups have utilised the single LDF system that is not the optimal technique due to significant perfusion heterogeneity in the skin (Turner *et al*., 2008, Sigaudo-Roussel *et al*., 2004). Furthermore, previously described studies have utilised experimental methods (anaesthetic agents) that do not easily permit the recovery of animals after scientific interrogation, such as the use of pentobarbital (Sigaudo-Roussel *et al*., 2004).

LDI uses a stable helium neon (HeNe) laser source (633nm and a 2mW nominal power), coupled with a diode laser source (780nm at a 1mW nominal power). The HeNe laser beam undergoes scattering by movement of red blood cells (RBCs), producing frequency broadened light (**Figure 2.1**). The movement of a 10cm mirror with rotation of two axes provides dexterity for optimal scanning within the laser head. Collected light is returned to an imaging lens and focused on two photo bodies. Laser speckle differences are automatically normalised by the software. Scattered light from moving RBCs and static scattering from the skin surface are detected and processed as a photocurrent, providing a relative measurement of blood flow. The average Doppler frequency shift is proportional to the average speed of RBCs in tissue and their concentration, output as an arbitrary value (AU) (Doppler Flux) in skin perfusion maps. Low flow is represented as blue and purple whilst increased or high flow is yellow, green and red (**Figure 2.2**). Colour coded maps are then converted into arbitrary perfusion values (0-1000 AU) (**Figure 2.2**). The laser was positioned 50cm above the animal, the internal mirror distance was accounted for and a height of 32cm from laser hood to tissue was maintained for all studies (**Figure 2.3**). The LDI was routinely calibrated at 4 week intervals, according to the manufacturer's instructions.

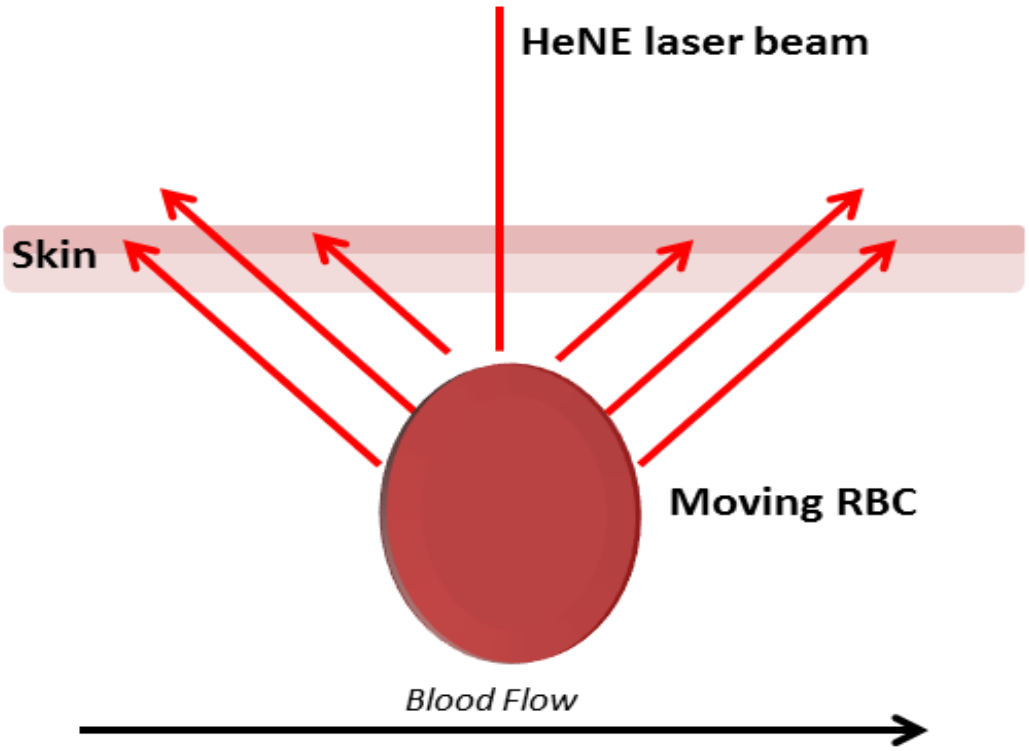

Figure 2.1. Laser beam scattering by moving red blood cells: Helium Neon (HeNe) laser beam undergoing scattering by the movement of red blood cells (RBCs) in the peripheral skin microcirculation.

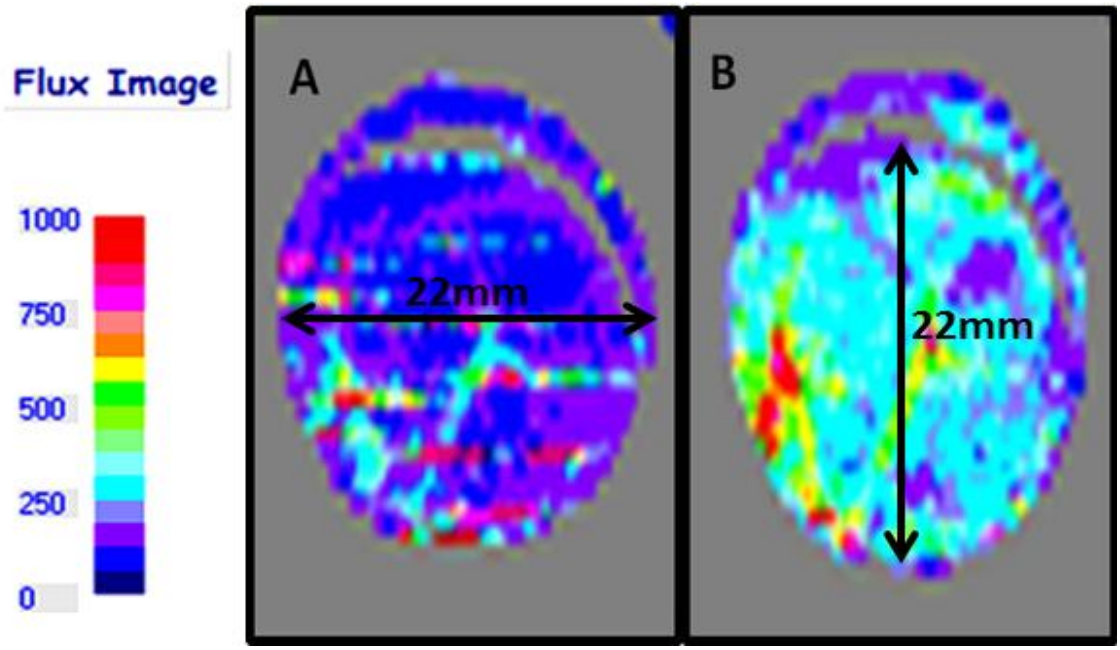

Figure 2.2. Perfusion map of blood flow: Colour coded maps of skin perfusion from the laser Doppler imager software v5.3 (Moor Instruments). (A) representative of low perfusion and (B) increased perfusion. Circular dimension (22mm) for region of interest and a flux scale showing arbitrary values of intensity for perfusion measurements (0-1000 arbitrary units).

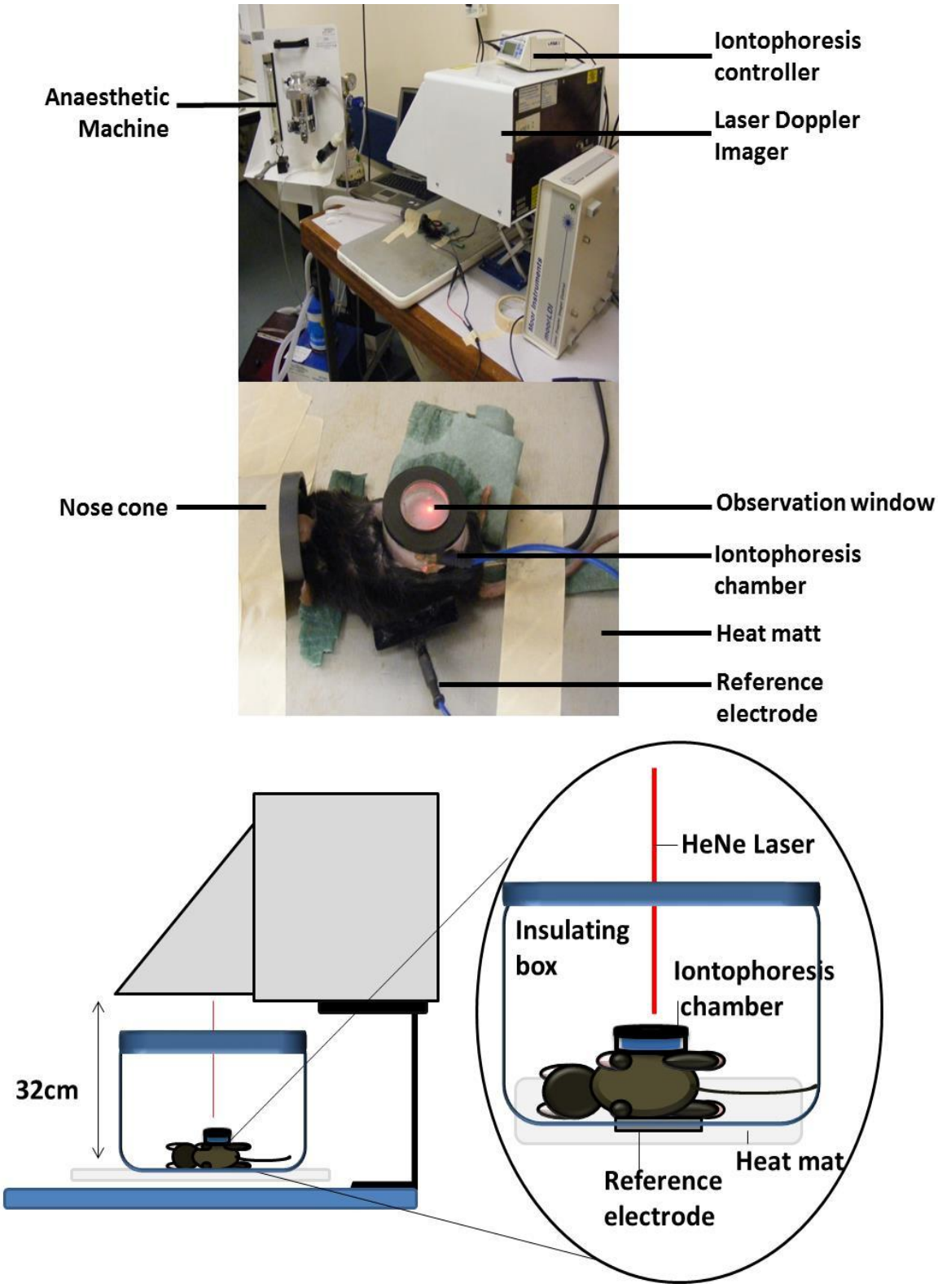

Figure 2.3. **LDI and iontophoresis:** Laser Doppler imaging and drug iontophoresis set up for *in vivo* studies, detailing anaesthetic machine and nose cone for delivery of Isoflurane during peripheral assessment of skin microvascular responses in mice.

LDI Acquisitions Parameters

For image acquisition the following parameters were set in the propriety software (Moor Instruments v5.3) for all acquired images.

- Direct current (DC), flux (Flux) and concentration (Conc): **Zero**
- Image scan: **X0=90, Y0=90, dX=60,dY=60 (scan area** 56mm^2**)**
- Scan resolution: **X=60, Y=60, scan speed 10ms/pixel**
- Average scan time: **49seconds**
- Time between scans: **5seconds**
- Total scan time: **55seconds**

Anaesthesia

Anaesthesia was necessary to prevent artefact movement confounding results during peripheral vascular assessment. Animals were weighed on an electronic balance (grams (g)) before all experimental procedures. Anaesthesia was achieved using a 5% combination of Isoflurane (Abbott Laboratories) in medical oxygen (BOC gases) (1.5-2 litres/minute), delivered using a standard Boyle's Apparatus (Fluovac, Harvard Appratus Ltd.) intended for small animal/rodent use (**Figure 2.4**)**.** Induction of anaesthesia was confirmed when the animal was supine and non-responsive (absence of rear foot reflexes). Anaesthesia was maintained by inhalation of 1.5-2.0 % concentration of Isoflurane in oxygen (1.5-2 litres/minute), delivered via a nose cone covering the mandible/nasal area (**Figure 2.3**). Depth of anaesthesia was continually monitored, by observing the absence of rear foot reflexes to toe pinching. The animals body temperature was maintained at 37 ^{o}C using a heat mat (VetTech Solutions). Core body temperature was monitored using a lubricated (KY Jelly) electrical probe inserted into the animal's rectum (VetTech Solution); peripheral skin

temperature was monitored by using an infrared thermometer (ThermoWorks). All experiments were carried out in a laboratory with a standardised room temperature of 22±2 ^{o}C.

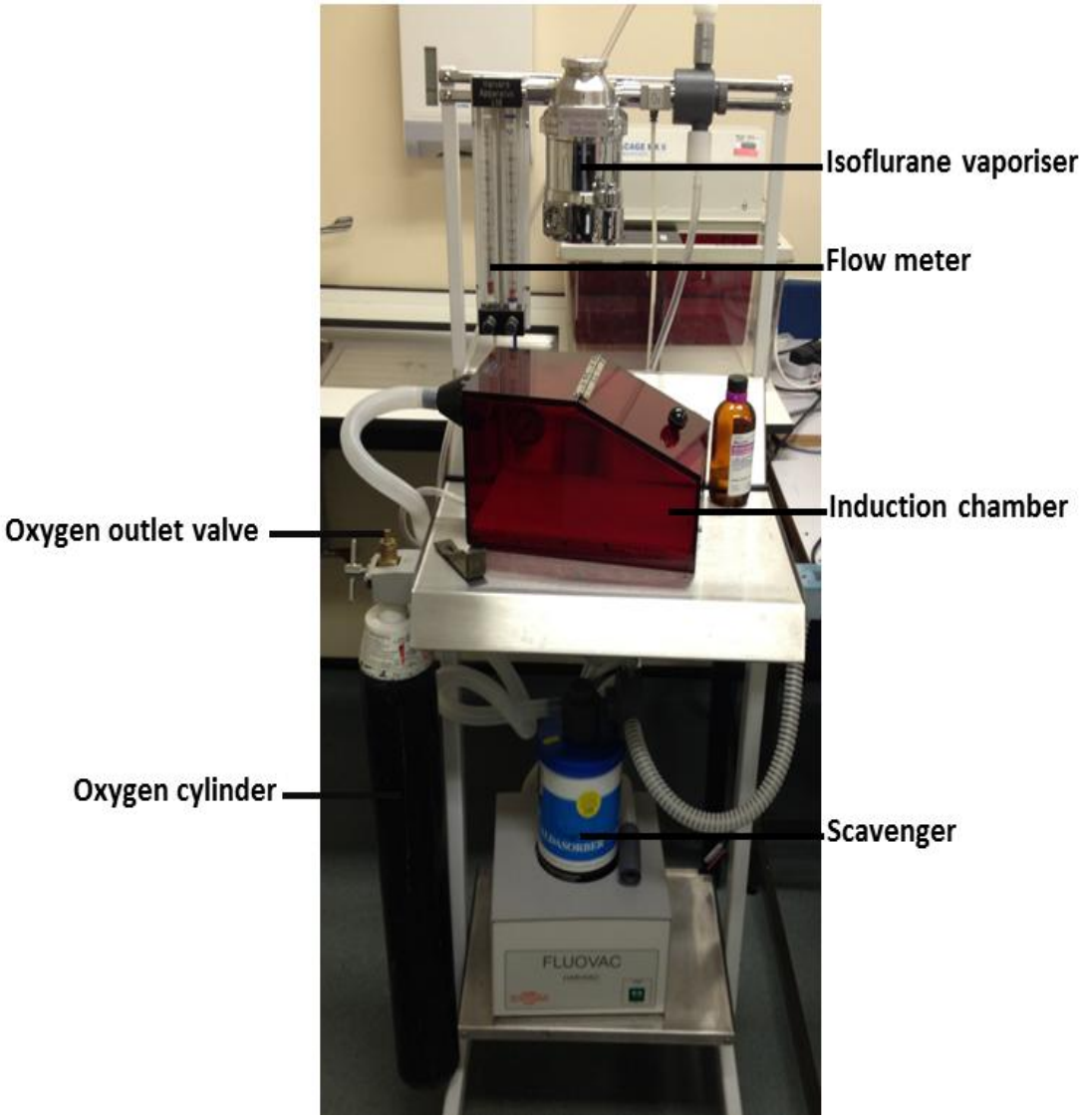

Figure 2.4. Anaesthetic machine: Standard Boyle's apparatus and induction chamber intended for small rodent use.

Anaesthetic recovery

Animals were recovered from anaesthesia after vascular assessment for longitudinal studies by turning off the supply of inhalant Isoflurane and allowing the animal to breathe oxygen alone for one minute (1.5-2Litres/minute). Animals were then briefly transferred to a Thermacage (MK II, Datesand Ltd.) (30 ^{o}C) until fully motile. Animals were returned to their housing cages and monitored

for at least 48 hours for any signs of ill health, including but not limited to: restlessness, fatigue, hunched back, ruffled coats and weight loss.

Iontophoresis

Non-invasive drug delivery of vasoactive chemicals for all studies was achieved by iontophoresis. Iontophoresis is the unidirectional transportation of ions in a solution across the epidermal *stratum corneum* layer by a direct continuous current (**Figure 2.5**). A chamber containing an incorporated internal platinum ring electrode produces a painless, sterile and non-invasive technique, where drug delivery to specific areas is achieved and provides a safer alternative to intravenous injection.

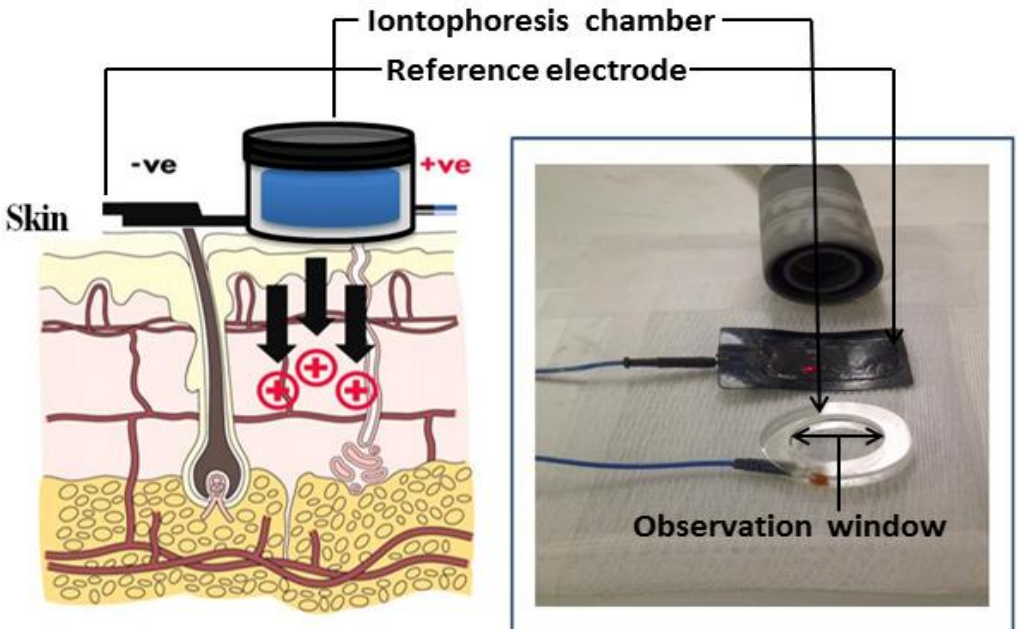

Figure 2.5. Iontophoresis: Iontophoresis chamber and gel electrode for non-invasive drug delivery.

Ion transportation during iontophoresis maintains a relatively constant concentration of drug within the intended tissue for a specified period of time (dependent on current duration). Ions are actively transported by repulsion of electrochemical forces; however, transfer is dependent upon a number of

factors including: ionic concentration, molecular size, treatment duration (current duration) and pH.

Ion movement is determined by polarity; the negatively charged electrode (cathode) repels negatively charged ions, attracts positively charged ions and accounts for the highest concentration of electrons. A positive charged electrode (anode) repels positively charged ions and attracts negatively charged ions and has a lower concentration of electrons.

Ion movement into tissues is determined by electrical strength and electrical impedance of tissue to current flow (resistance); where the electrical field is a result of current density. A difference in current density between the active repelling electrode and its inactive counterpart produces a gradient potential encouraging ion migration. Current densities may be tainted by fluctuating current intensities and chamber size, an inverse relationship between chambers size and current density exists.

Sweat ducts are ideal routes for ion movement through the dermis and decrease impedance by facilitating current flow and ion movement. Ion movement in iontophoresis is dependent on: current densities at the active electrode (repelling), the duration of current and the purity of the solution.

Lower currents are recommended for an active repelling force, higher currents carry a greater risk of electrical burns, current intensity should be determined by chamber size (active electrode) and treatment duration which is standardised so that current density falls between 1-0.5 mA/cm^2 of the active electrode surface.

Belanger (B©*langer, 2009) stated that current densities should not exceed 0.5mA/cm^2 at the anode and 1.0mA/cm^2 at the cathode to safe guard against electrical burns and the following transposition provides a safe treatment.

Maximum current (mA) =

Maximum safe current density (mA/cm^2) x Electrode area (cm^2)

Electrodes should be adequately separated, wider differences ensures minimal differences in current densities and reduces the likelihood of burns. Negative ions accumulating at the positive pole produce acidic reactions through the formation of hydrochloric acid. This in turn produces tissue softening. Positive ions accumulating at the negative pole produce alkaline reactions with the formation of sodium hydroxide and may produce hardening of the skin. Continuous direct currents create an altered skin pH through the migration of ions, with chemical burns being the results of sodium hydroxide at the cathode. Thermal irritation and burns may be a result of poor skin contact between the active and inactive electrodes

Skin presents high electrical resistances to current flow, conversely the underlying flesh and blood show a much lower electrical resistance. The nonspecific effect of blood flow on electrical activity is termed the galvanic effect, which is stronger at the cathode than the anode. Lower currents are recommended, however the therapeutic doses can be adequately achieved with a longer duration.

Skin preparation

Vascular measurements were made on the flanks of anesthetised mice (**Figure 2.6**). Maximum contact between skin and iontophoresis electrodes was achieved through shaving (Carmen 11740 Top to Toe Trimmer) and application of a depilatory lotion (Veet®, Reckitt-Benckiser) **(Figure 2.6)** 24-48 hours prior to vascular measurements to minimise skin irritation. Excess lotion was thoroughly washed off with warm water and cotton wool. Animals were then allowed to dry in a Thermacage (MK II), before being returned to their respective housing cages. A small amount of extra bedding was provided to all cages for insulation after fur removal. Care was taken to avoid excessive abrasion during fur removal, as broken/damaged skin is more susceptible to burns. In human studies, skin resistance can be improved by gently removing dead skin cells by applying and removing an adhesive strip and natural oils may be cleansed with alcohol wipes. To avoid unnecessary irritation and to avoid the application of alcohol to the skin of mice, this was not carried out in all studies.

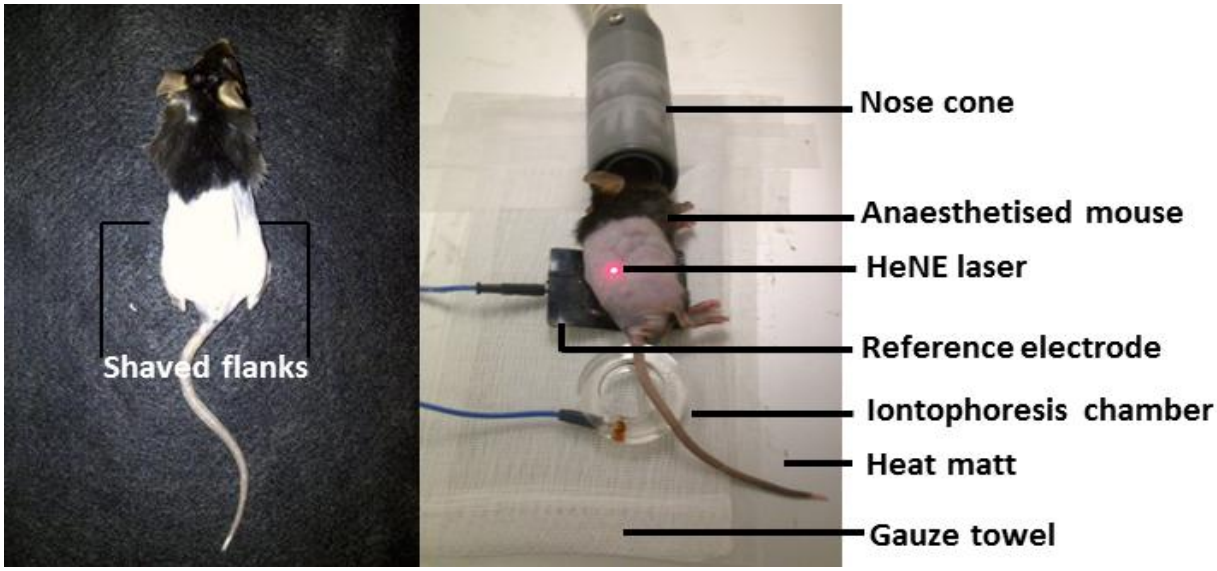

Figure 2.6. Exposed mouse flanks: C57BL/6 mouse prepared for laser Doppler Imaging and drug iontophoresis.

Iontophoresis chambers were obtained from Moor Instruments (ION6 probe, Moor Instruments Ltd, Devon, U.K.). Each chamber had an internal diameter of 20mm, providing a total surface area of 3.2cm^2 and was securely attached to the flank of each animal, using doubled-sided adhesive rings (IAD, Moor Instruments) producing a water tight seal. A second reference electrode (MIC-CP, Moor Instruments) was positioned on the opposite flank of each animal to complete the circuit (**Figure 2.6**) and attached to the iontophoresis controller (MIC2 Iontophoresis Controller, Moor Instruments).

Normalisation of baseline perfusion

Iontophoresis chambers were initially filled with ~2ml of 1% solution of phenylephrine (PE) (Sigma-Aldrich) and sealed with a Perspex cap (MIC-ION6 CAP, Moor Instruments). Three initial baseline measurements were taken without current; after this period, an anodal current of 100μA was applied to induce vasoconstriction of the peripheral vasculature, standardising baseline perfusion.

Following constriction, microvessels were dilated using a 2% solution of endothelium-dependent agonist ACh (Sigma-Aldrich) with an anodal current of 100μA (**Figure 2.7).**

SCAN 1	SCAN 2	SCAN 3	SCAN 4	SCAN 5	SCAN 6
Phenyleprine (1%) 0µA	Phenyleprine (1%) 0µA	Phenyleprine (1%) 0µA	Phenyleprine (1%) 100µA	Phenyleprine (1%) 100µA	Phenyleprine (1%) 100µA
SCAN 7	**SCAN 8**	**SCAN 9**	**SCAN 10**	**SCAN 11**	**SCAN 12**
Phenyleprine (1%) 100µA	Phenyleprine (1%) 100µA	Phenyleprine (1%) 100µA	Acetylcholine (2%) 100µA	Acetylcholine (2%) 100µA	Acetylcholine (2%) 100µA
SCAN 13	**SCAN 14**	**SCAN 15**	**SCAN 16**	**SCAN 17**	**SCAN 18**
Acetylcholine (2%) 100µA	Acetylcholine (2%) 100µA	Acetylcholine (2%) 100µA	Acetylcholine (2%) 100µA	Acetylcholine (2%) 100µA	Acetylcholine (2%) 100µA
SCAN 19	**SCAN 20**	**SCAN 21**	**SCAN 22**		
Acetylcholine (2%) 100µA	Acetylcholine (2%) 100µA	Acetylcholine (2%) 100µA	Acetylcholine (2%) 100µA		

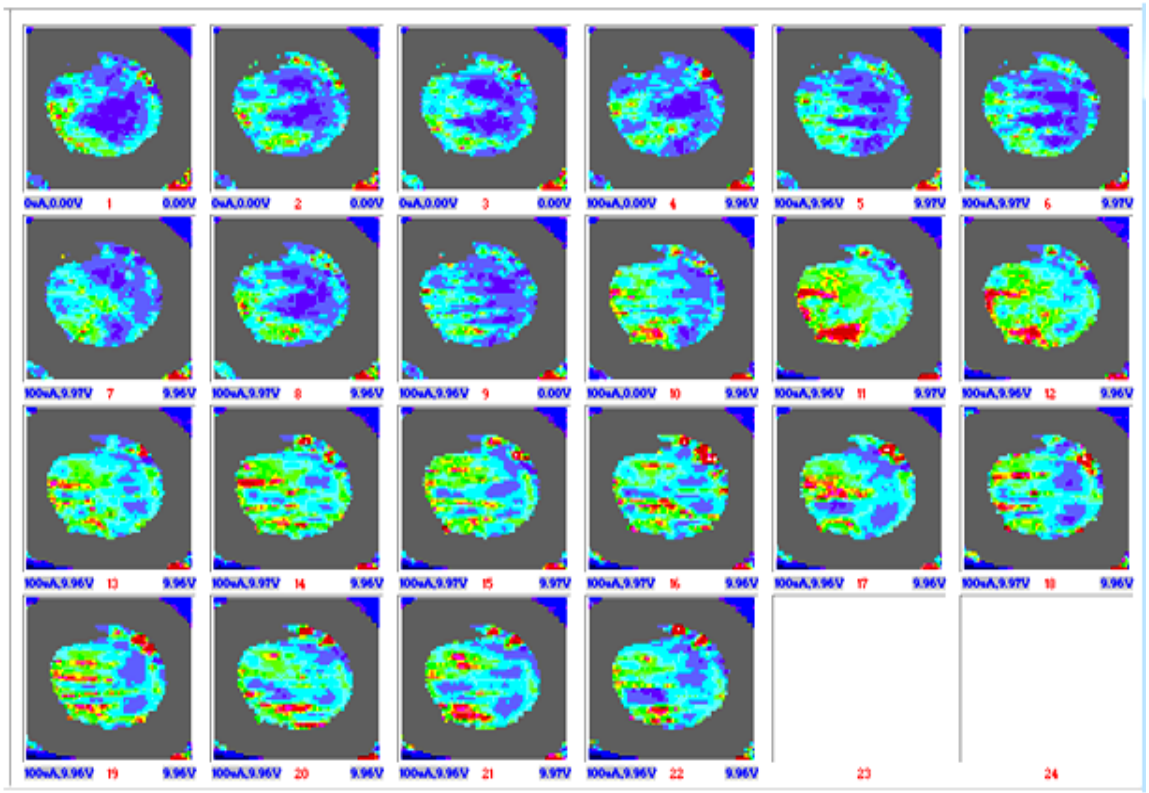

Figure 2.7. Endothelium-dependent iontophoresis protocol: Acetylcholine (ACh) protocol and representative trace for vasodilator responses.

Endothelium-dependent vasodilatation to acetylcholine

ACh is an ester of acetic acid and choline produced endogenously as a neurotransmitter in both the peripheral and central nervous systems. It is also well documented as an endothelium-dependent vasodilator. Studies conducted by Furchgott and Zadawski (1980) demonstrated the importance of the endothelium, by observing attenuated vasodilator responses in sections of rabbit aorta that had their lumens braised. ACh stimulates the release of NO (**Figure 2.8**) from endothelial cells and induces VSMCs cell vasodilatation.

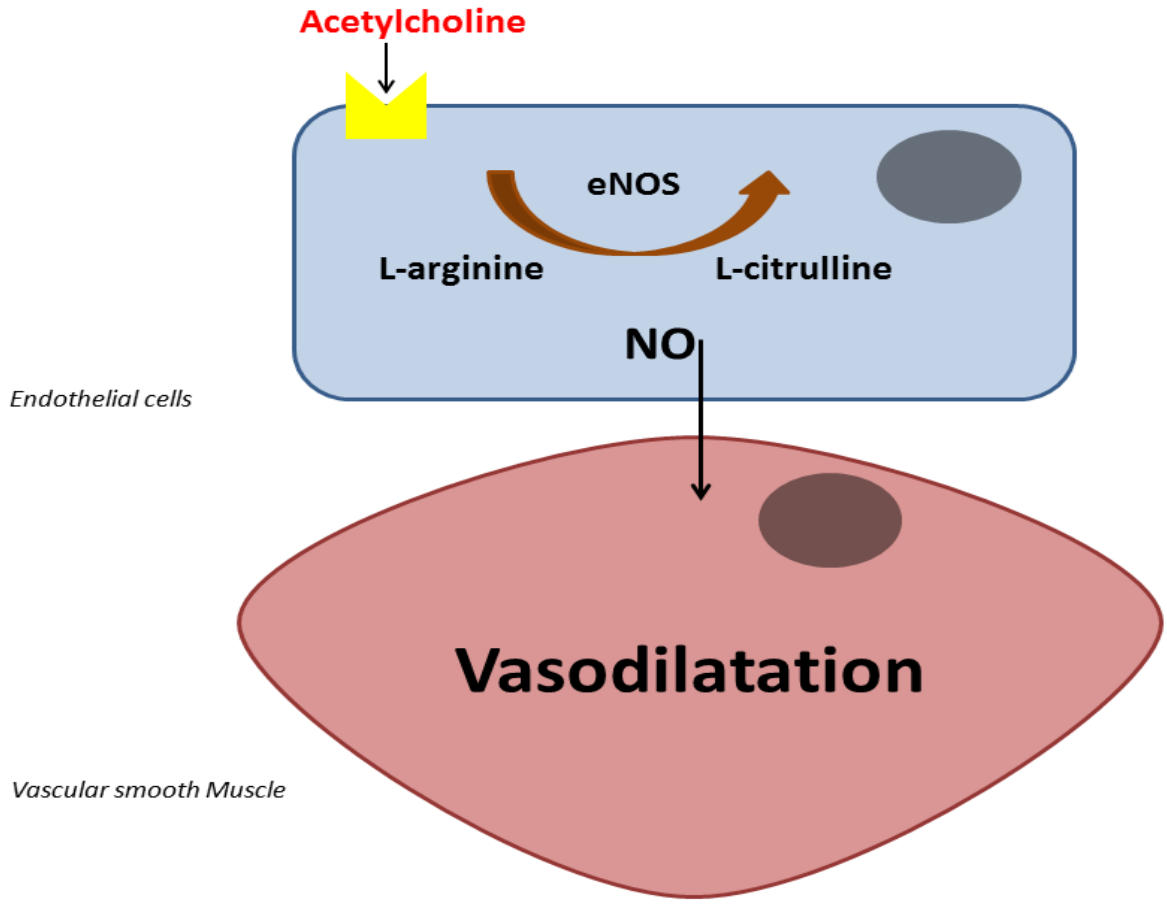

Figure 2.8. Endothelium-dependent release of NO: Acetylcholine (ACh) induced endothelium-dependent vasodilatation.

Endothelium-independent vasodilatation to sodium nitroprusside

During vascular assessment it is necessary to obtain a maximal vasodilator reference value for comparison to endothelium-dependent vasodilatation. Sodium nitroprusside (SNP) is a complex inorganic anion that is a potent vasodilator. The octahedral molecule features a central ferrous core, surrounded by five tightly bound cyanide groups and one linear nitric oxide group. Upon metabolism, the five cyanide ions are cleaved and the NO group is released, that is able to diffuse to VSMCs and instigate vasodilatation irrespective of the endothelial lining, producing an endothelium-independent vasodilator response **(Figure 2.9)**. To minimise drug exposure to experimental animals, SNP responses were only conducted under terminal measurements, after which animals were euthanized.

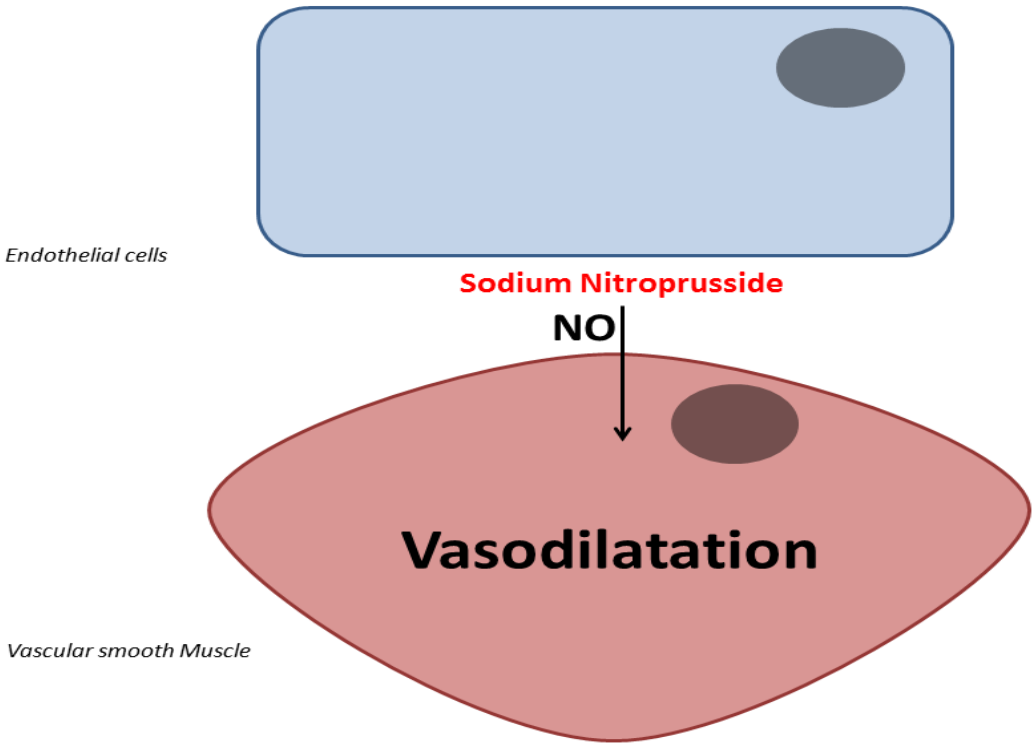

Figure 2.9.Endothelium-independent iontophoresis protocol: Sodium nitroprusside (SNP) induced endothelium-independent vasodilatation.

Similar to the ACh protocol, three initial baseline measurements were taken without current, after this period an anodal current of 100μA was applied to induce vasoconstriction of the peripheral vascular network with PE, standardising baseline perfusion. Following constriction, microvessels were dilated using a 2% solution of endothelium-independent agonist SNP (Sigma-Aldrich) with an anodal current of 100μA (**Figure 2.10**).

SCAN 1 Phenyleprine (1%) 0µA	SCAN 2 Phenyleprine (1%) 0µA	SCAN 3 Phenyleprine (1%) 0µA	SCAN 4 Phenyleprine (1%) 100µA	SCAN 5 Phenyleprine (1%) 100µA	SCAN 6 Phenyleprine (1%) 100µA
SCAN 7 Phenyleprine (1%) 100µA	SCAN 8 Phenyleprine (1%) 100µA	SCAN 9 Phenyleprine (1%) 100µA	SCAN 10 SNP (2%) 100µA	SCAN 11 SNP (2%) 100µA	SCAN 12 SNP (2%) 100µA
SCAN 13 SNP (2%) 100µA	SCAN 14 SNP (2%) 100µA	SCAN 15 SNP (2%) 100µA	SCAN 16 SNP (2%) 100µA	SCAN 17 SNP (2%) 100µA	SCAN 18 SNP (2%) 100µA
SCAN 19 SNP (2%) 100µA	SCAN 20 SNP (2%) 100µA	SCAN 21 SNP (2%) 100µA	SCAN 22 SNP (2%) 100µA		

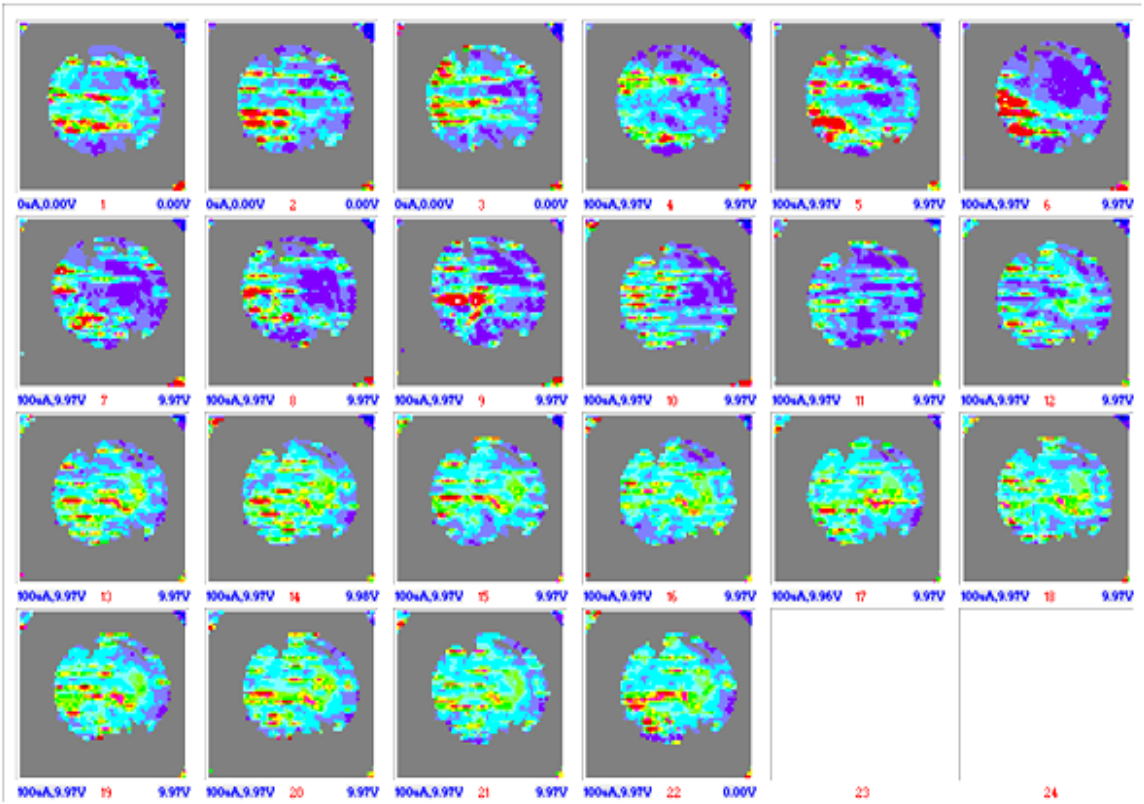

Figure 2.10. Endothelium-independent iontophoresis protocol: Sodium nitroprusside (SNP) protocol and representative trace for vasodilator responses.

Nitric oxide

N_ω-Nitro-L-arginine methyl ester hydrochloride (L-NAME) is a nonspecific NO inhibitor. Where appropriate, animals received L-NAME (Sigma-Aldrich) by intraperitoneal injection (20mg/kg) in deionised water (European Pharmacopoeia) 30 minutes prior to vascular assessment. The ACh protocol was then rerun to establish the role of NO in ACh mediated vasodilatation. This concentration has been previously reported and has shown attenuation of NO mediated responses *in vivo* (Sigaudo-Roussel *et al*., 2004).

Maximal dilator capacity (localised skin heating)

A maximal hyperaemic response was required from each animal for reference value of maximal dilator capacity at study baseline. This was achieved by localised heating of the skin using a specially designed heating probe (SH02™ Skin Heating Unit and SHP3 probe, Moor Instruments).

A skin heating probe had an internal diameter of 20mm and an inner ring heating electrode provided a total surface area of 3.2cm^2 and was attached using double sided adhesive rings (IAD, Moor Instruments) (**Figure 2.11**).

Figure 2.11. Localised heating chamber: Anaesthetised C57BL/6 mouse for assessment of maximal dilator capacity.

A localised heating protocol was followed (**Figure 2.12**). Baseline measurements were taken for five minutes by LDI, followed by the continual assessment of microvascular responses to localised heating of the skin as the temperature within the heating chamber was increased at a rate of 1 ^{o}C/minute until a maximum temperature of 44 ^{o}C was achieved. This was then maintained for a period of >ten minutes to assess maximal dilator response in the skin microcirculation (**Figure 2.12**).

During localised skin heating experiments animal's core body temperature was not acclimated to 37 ^{o}C for baseline scans. 37 ^{o}C was achieved through a combination of applied heat from the heat mat and the localised heating of the skin. Core body temperature was acclimated to 37 ^{o}C for maximal responses (44^{0}C). This combined approach to heating, allowed the capture of accurate data without lengthening the procedure and reduced prolonged anaesthetic exposure to experimental mice.

SCAN 1 25-30°C	SCAN 2 25-30°C	SCAN 3 25-30°C	SCAN 4 25-30°C	SCAN 5 25-30°C	SCAN 6 30°C
SCAN 7 31°C	SCAN 8 32°C	SCAN 9 33°C	SCAN 10 34°C	SCAN 11 35°C	SCAN 12 36°C
SCAN 13 37°C	SCAN 14 38°C	SCAN 15 39°C	SCAN 16 40°C	SCAN 17 41°C	SCAN 18 42°C
SCAN 19 43°C	SCAN 20 44°C	SCAN 21 44°C	SCAN 22 44°C	SCAN 23 44°C	SCAN 24 44°C
SCAN 25 44°C	SCAN 26 44°C	SCAN 27 44°C	SCAN 28 44°C	SCAN 29 44°C	SCAN 30 44°C
SCAN 31 44°C	SCAN 32 44°C	SCAN 33 44°C	SCAN 34 44°C	SCAN 35 44°C	

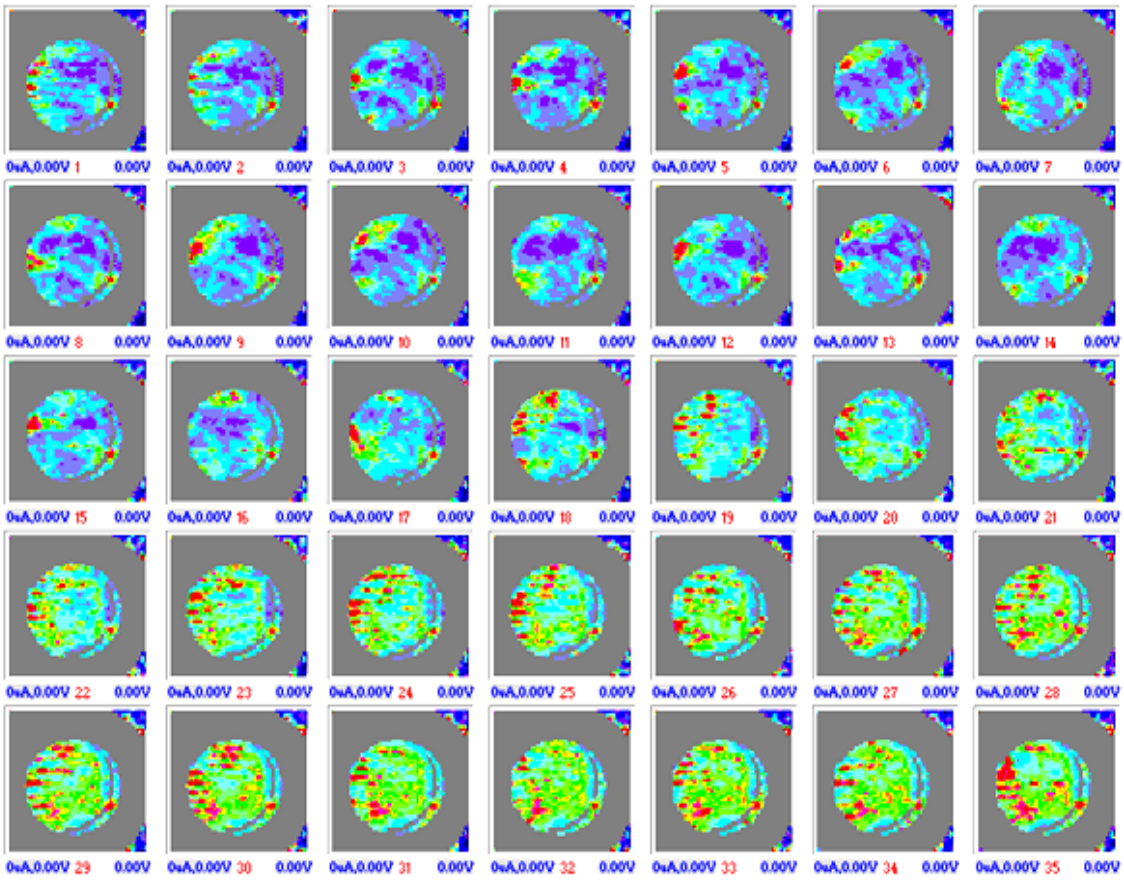

Figure 2.12. Maximal dilator capacity: Protocol for localised skin heating (maximal dilator response) and representative trace for vasodilator responses.

Blood Flow Analysis

Blood flow images were analysed using propriety software (Moor Instruments, Version 5.3) and are expressed as group means in AU± standard error of the mean (SE). In certain circumstances, % change ±SE was used to express perfusion data (percentage change = (peak response (AU) – baseline (AU)/baseline (AU) x 100) where described.

LDI validation with wire myography

Belch *et al* (2013) previously demonstrated a correlation between LDI ACh, endothelium-dependent mediated vasodilatation in the skin micro circulation of mice after 24 weeks of cholesterol feeding when compared to post-mortem analysis of the tail artery by wire myography ($r= 0.699$, $P<0.05$). WT-chow and WT cholesterol fed mice were compared and no significant differences were found for vasoconstriction or endothelium-independent vasodilatation, confirming *in vivo* observations of endothelial dysfunction. Importantly the small resistance vessels used in this *ex vivo* study are comparable to the small resistance vessels found in the skin microvasculature.

Blood Sampling

Blood samples were collected after LDI and ACh iontophoresis. Animals were gently heated in a Thermacage (MK II) to promote peripheral vasodilation of the tail artery. Animals were then placed in a small rodent restrainer of appropriate size (VetTech solutions Ltd). A small incision was made to the lateral tail vein (located one-third along the tail from the tip) using a scalpel blade, gentle pressure was applied to promote bleeding.

Upon terminal measurements, larger blood samples were collected by cardiac puncture using a 2ml syringe attached to a 25 gauge needle. For cardiac puncture, animals were maintained under terminal anaesthesia by nose cone (3-5% Isoflurane in oxygen 1.5-2Litres/minute). The syringe was held at a 45^{o} angle to the sternum and the needle inserted into the thoracic cavity at the region of maximum pulsation, maintaining a depth of 5-10mm. The presence of blood within the needle confirmed ventricle puncture; a vacuum was created by withdrawing air into the syringe and this was then allowed to fill with blood. All blood was collected in heparinised micro tubes (BD Microtainer^{TM} Lithium Heparin) and kept on ice until centrifuged at 1500 rounds per minute (RPM) (Hermle Z 230 M Centrifuge) for five minutes; plasma was decanted into freezer suitable tubes and stored at -80^{o}C until analysed.

Plasma Cholesterol

Plasma was used to quantify total plasma cholesterol (mg/dl ±SE) (Biovision, catalog#: K603-100); or a specialist cholesterol assay kit which measured high density lipoproteins (HDL), low density lipoproteins and very low density lipoproteins (LDL/vLDL) (mg/dl ±SE) (AB65390, Abcam), as detailed in the manufacturer's instructions. Assays were conducted under the supervision of Dr. Gwen Kennedy within the Core Facility, Ninewells Hospital, Dundee.

Plasma Cytokines

Plasma was analysed by Luminex multiple bead-based assays using Bio-Plex® Precision Prokits™ from BIO-RAD laboratories for: IL-1α, IL-6, IL-10, TNF-α, E-selectin, soluble ICAM-1 (sICAM-1), and soluble VCAM-1 (sVCAM-1) (pg/ml ±SE) as detailed in the manufacturer's instructions. Assays were conducted under the supervision of Dr. Gwen Kennedy within the Core Facility, Ninewells Hospital, Dundee.

Blood Pressure

The CODA non-invasive blood pressure system (Kent Scientific, USA) was used to measure systolic blood pressure, diastolic blood pressure, mean arterial blood pressure (MAP) in millimetres of mercury (mmHg) and heart rate in beats per minute (bpm) in mice. The system has previously been used for the *in vivo* assessment of blood pressure in mice (Talukder *et al*., 2011).

CODA is a volume pressure recording (VPR) system. The two system cuff: occlusion cuff (O-cuff) and VPR cuff utilise tail volume (swelling) to determine parameters of blood pressure. The CODA system was validated against radiotelemtery and has demonstrated 99% accuracy (Feng *et al*., 2008a). The O-cuff is placed at the base of the tail and the VPR-cuff immediately below it (2mm distance) (**Figure 2.13**).

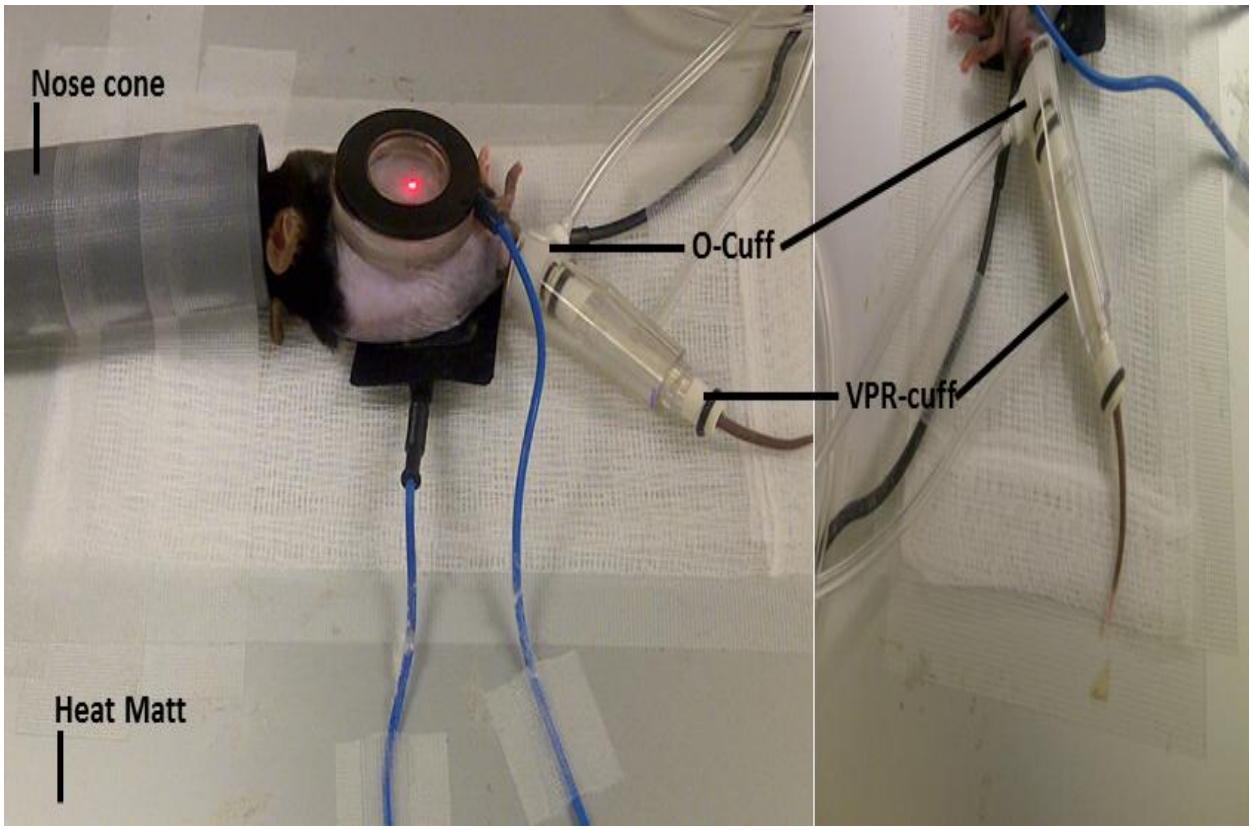

Figure 2.13. Blood pressure measurements: *In vivo* measurement of blood pressure using a tail cuff system: occlusion cuff (O-cuff) and volume pressure recording cuff (VPR-cuff).

Session parameters on the propriety software were set as: 0 acclimation cycles, one set of cycles, 20 cycles per set (5 seconds between cycles); maximum occlusion pressure was 250 mmHg, deflation time was 20 seconds and a minimum detection of blood volume of 15µl was set. Results are expressed as group mean in mmHg for blood pressure parameters and bpm for heart rate ±SE.

Tissue Extraction

Immediately preceding cardiac puncture, the animal was pinned to a polystyrene dissection board through its paws using 23 gauge needles. A small superficial cut was made at the level of the pubis and a median longitudinal cut superiorly to the chin, carefully separating underlying muscle to the skin using blunt dissection and exposing the thoracic and abdominal cavities.

To gain access to the thoracic cavity, the xiphoid process was gripped by forceps and the diaphragm carefully removed by making two cuts on either side of the rib cage, to reveal the posterior thoracic cavity. Perfusion of all tissues was achieved by insertion of a 23 gauge needle into the left ventricle, at an angle parallel to the septum of the heart. 20ml of ice cold heparinised (sodium heparin) (10 unit/ml) (Wockhard, United Kingdom) phosphate-buffered saline (PBS) (Fisher Bioreagents) was perfused gradually. The right ventricle was cut to allow blood/PBS to flush out of the animal. After perfusion, tissues were extracted.

Heart and Aorta

The abdominal aorta is the first section of the aorta to be dissected; it is freed from the region of the renal branches initially and this dissection is continued to the iliac bifurcation and up to the diaphragm. The thoracic aorta and heart are removed as an entire unit. With forceps, the heart is slightly lifted by grasping adipose tissue ordinarily found at the base of the heart (pericardial fat), with fine dissection scissors the aorta is cut free from the thoracic cavity by making gradual longitudinal cuts down the aorta moving towards the abdominal area. The aorta and heart were placed in ice cold heparinised PBS.

The heart was cut free of the aorta at the base of the aortic arch. Remaining adipose and connective tissue were carefully removed with fine forceps and scissors. Hearts were momentarily blotted and rolled on gauze to eject any residual heparinised PBS and/or blood. Hearts were then weighed on an electronic balance (mg) and snap frozen in liquid nitrogen and stored at -80^{o}C.

Perivascular tissue surrounding the adventitial layer of the aorta was meticulously removed under a stereomicroscope. The aorta was fixed in 10% buffered formalin overnight and then transferred to PBS for storage.

Cardiac Hypertrophy

Cardiac mass was analysed to assess cardiac hypertrophy. Hearts were excised as described above. In order to standardise measurements, tibias were dissected out from the hind limbs, measured in millimetres (mm) using a digital calliper (Silverline 380224 Digital Vernier Professional Caliper, ToolBox, UK) and a ratio obtained (cardiac hypertrophy = total heart weight (mg)/ average length of tibia (mm)).

***En Face* Staining of the Aorta**

In order to assess the level of lipid deposition within the aorta, the aorta was opened longitudinally and pinned down on to a paraffin wax block for *en face* analysis. Aortic tissue was stained with oil red O (0.5%) (Sigma-Aldrich) in 1, 2-Propanediol (100%) (Sigma-Aldrich) according to the following protocol. Aortas were placed in absolute 1, 2-Propanediol for 5 minutes to avoid carrying water into the oil red O stain. Aortas were incubated in pre-warmed oil red O for 10 minutes (60 ^{o}C in a water bath), after this tissues were differentiate in an 85% 1, 2-Propanediol solution for 1 minute and rinsed in two changes of distilled water. *En face* tissues were digitally analysed by photographs and quantified by image software analysis (Volocity, PerkinElmer). Lipid deposition is analysed as a percentage of total analysed area (results are group means ±SE). Aortic tissue was processed by Tayside Tissue Bank, Ninewells Hospital, Dundee.

Power calculation

A power calculation was performed for determination of sample size for LDI studies. Preliminary in house studies showed that WT chow fed animals display an endothelium-dependent response that is 350±24 (SD) AU n =19, a minimum difference of 16 AU is needed for statistical significance ($P<0.05$). Test value 350 AU, sample average 335±24 SD, α error level 1% (confidence level) and a statistical power (1 - beta) sample size (n) = 14 . This reflects previously published group size for LDI of small rodents (Sigaudo-Roussel *et al*., 2004).

Statistical Analysis

All data are expressed as group means ±SE. Within and between group differences were compared using paired and unpaired t-tests. One-way and two-way ANOVA was used for comparisons of 3 or more groups. The associations between skin microvascular responses and plasma measures of cholesterol, cytokines and lipid deposition, parameters of cardiovascular hypertrophy and blood pressure were tested using Pearson correlation coefficients in the software package PASW Statistic (Version 18). Furthermore a step wise multiple linear regression model to ascertain the determinants of vascular dysfunction was conducted. The null hypothesis was rejected at $P<0.05$.

Chapter 3

Development of Methods

Measurements of blood pressure in conscious trained and anaesthetised mice, an *in vivo* comparison.

Introduction

Blood pressure measurements are often made in conscious mice following a programme of training. In this study animals were acclimated to blood pressure measurements by implementation of a 7 day training programme. Blood pressure measurements were taken longitudinally (over several days) in the same mice and compared to blood pressure measurements obtained from anaesthetised mice. The study sought to establish whether the extensive training programme involved in blood pressure recordings could be avoided through the use of an inhalant anaesthetic, and secondly to establish the impact of an inhalant anaesthetic on blood pressure and heart rate in mice.

Methods

The methods description below is intended to provide an overview of experimental techniques used in this study. Further experimental details are described in *Materials and Methods Pages 62-92.*

Training

WT C57BL/6 male mice (12 weeks of age) were trained to blood pressure measurements over a 7 day protocol. Each day, simultaneous (n =20) blood pressure measurements were made in the same animals (n =12). On days one and two, animals were placed in specifically designed blood pressure holders **Figure 3.1** and placed on a heated platform that held the holder in place **Figure**

3.1. Animals were acclimated to the holder for 5 minutes and tail cuffs attached. On experimental days one and two sham measurements were made and animals returned to their housing cages. Following this, on days three to seven (measurement days 1-5) animals were placed in holders on the heated platform and allowed to acclimatise for 5 minutes, tail cuffs were mounted and measurements recorded using the propriety software

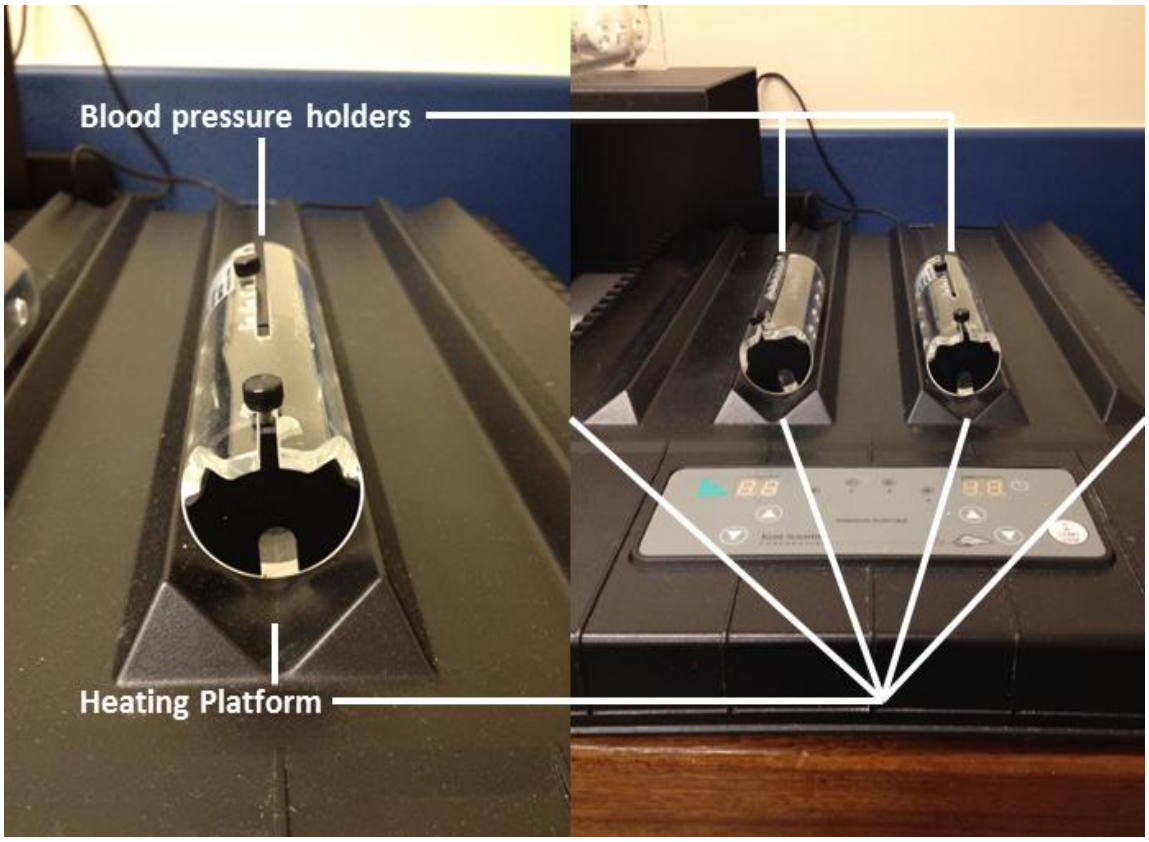

Figure 3.1. Heated platform for blood pressure measurements: Blood pressure heating platform and tube holders for mice.

Anaesthetic

The same mice from the training study (above) were anaesthetised (1.5-2% isoflurane in oxygen) without recovery, core body temperature was maintained at 37 ^{o}C. Blood pressure measurements were made by tail cuff and animals euthanised by cervical dislocation at the end of the procedure.

Results

Training

There were no significant differences between measurements on experimental recording day 1 (start of training) and day 5 (end of training) for all parameters: diastolic blood pressure (75±2 mmHg VS. 74±2 mmHg, P>0.05), systolic blood pressure (99±2 mmHg VS. 103±2 mmHg, P>0.05), MAP (83±2 mmHg VS. 84±2 mmHg, P>0.05) and heart rate (671±41 bpm VS. 694±13 bpm, P>0.05), respectively **Figure 3.2 A-D**.

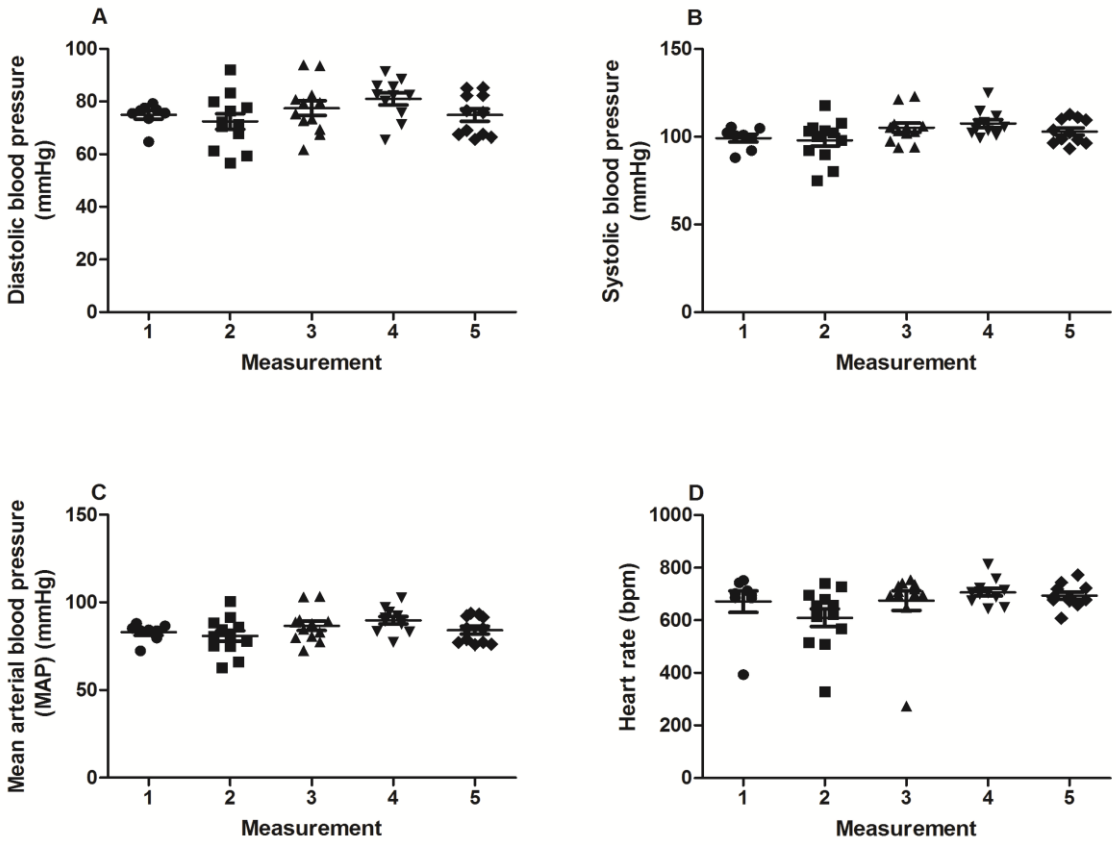

Figure 3.2. Blood pressure training: Training measurements of wild-type mice over five consecutive days (n =12) for (A) diastolic blood pressure (mmHg), (B) systolic blood pressure (mmHg), (C) mean arterial blood pressure (MAP) (mmHg) and (C) heart rate (beats per minute) (bpm). Results are group means ±SE. One-way ANOVA with post-hoc Bonferroni correction.

Training VS. anaesthesia

Training data (experimental training day 5) data were compared to measurements obtained from anaesthetised mice. No significant differences were found for diastolic blood pressure (78±2 mmHg, P>0.05) or mean arterial pressure (89±2 mmHg, P>0.05) between the two groups **Figure 3.3 A and B** respectively. A significant differences was found for systolic blood pressure (111±2 mmHg, P<0.05) and heart rate 614±12 bpm, P<0.001) between the two groups (**Figure 3.3 C** and **D** respectively).

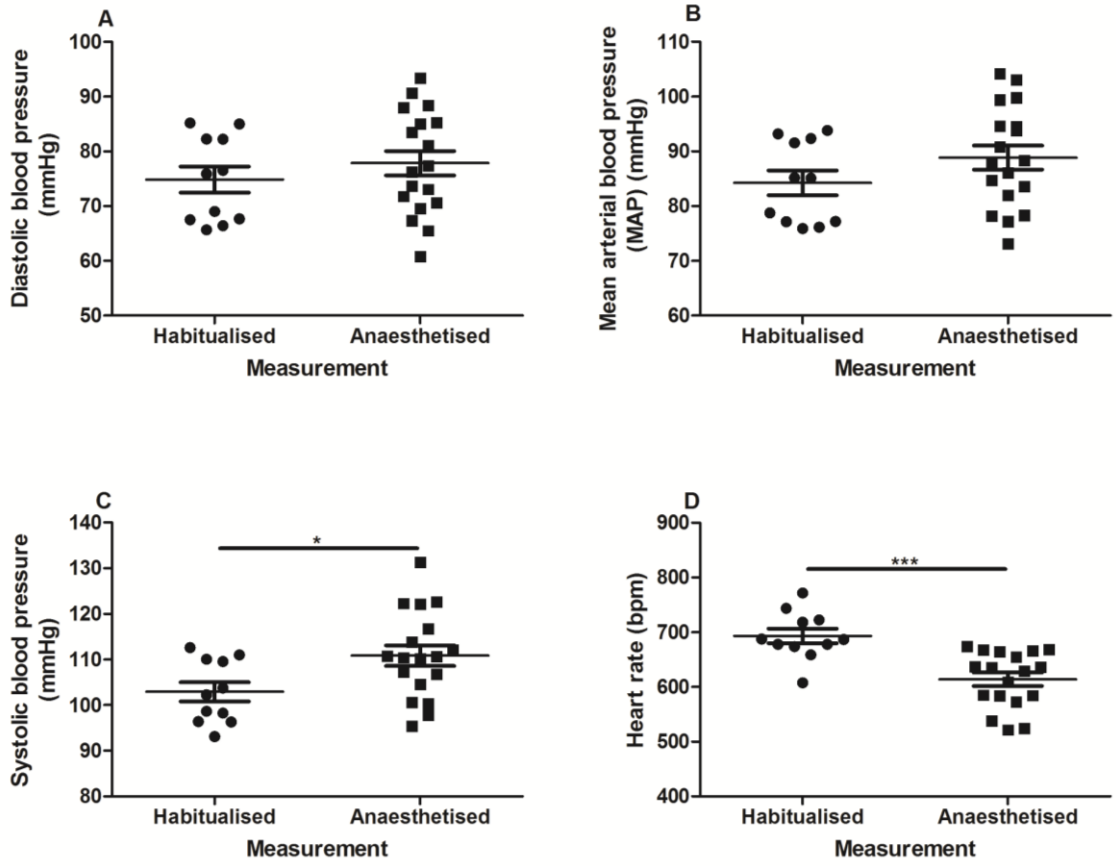

Figure 3.3. Training VS. anaesthesia: Comparison of blood pressure parameters obtained from trained conscious wild-type mice (n =12) to those obtained from the same animals under anaesthesia (Isoflurane). (A) diastolic blood pressure (mmHg), (B) mean arterial blood pressure (MAP) (mmHg), (C) systolic blood pressure (mmHg), (D) heart rate (beats per minute) (bpm). Results are group means ±SE. Unpaired Student's t-test. *P<0.05, ***P<0.001.

Discussion/conclusion

A strict 7 day training programme in conscious mice does not significantly improve the efficacy of blood pressure data, suggesting the restraint needed to perform measurements in conscious mice does not subside over a period of training.

There were no significant differences between diastolic and mean arterial blood pressures between conscious mice and anaesthetised animals; however, a significant reduction in heart rate and systolic blood pressure was observed in

anaesthetised mice. Values obtained from anaesthetised mice are in agreement with published radio telemetry values (Peotta *et al*., 2014).

The measurement of blood pressure *in vivo* in anaesthetised mice may help reduce stress induced by animal handling that is otherwise associated with restraint and repeated handling. The measurement of blood pressure in anaesthetised mice using an inhalant anaesthetic is in line with radio telemetry published recordings, and thus maybe used as a suitable alternative.

Study of blood pressure changes and heart rate during the iontophoresis of vasoactive chemicals *in vivo*.

Introduction

LDI and the iontophoresis of vasoactive chemicals has previously been described in small rodents (Belch *et al*., 2013, Sigaudo-Roussel *et al*., 2004). Iontophoresis can be used to locally deliver drugs such as PE, ACh and SNP, agents that can significantly affect the cardiovascular system by inducing vasoconstriction and vasodilatation, respectively. Current methodologies have not established whether the iontophoresis of PE, ACh and SNP significantly affects heart rate and blood pressure *in vivo*. Blood pressure parameters were measured non-invasively before and after the iontophoresis of PE, ACh and SNP *in vivo,* to establish whether the iontophoresis of vasoactive chemicals induced systemic changes in the cardiovascular system.

Methods

The methods description below is intended to provide an overview of experimental techniques used in this study. Further experimental details are described in *Materials and Methods Pages 62-92.*

Iontophoresis and Blood pressure

Blood pressure measurements were made in WT C57BL/6 (12 weeks of age) anaesthetised mice (1.5-2% isoflurane in oxygen) without recovery (n =6 per group) non-invasively by tail-cuff. Deionised water was used as a vehicle control for PE, ACh and SNP iontophoresis. Three sets of measurements were made

throughout the iontophoresis protocol: at baseline, before PE iontophoresis, mid-point (after PE iontophoresis but before iontophoresis of ACh and SNP) and after the iontophoresis of vasodilators ACh and SNP.

Results

Baseline Iontophoresis

There were no significant differences for parameters between vehicle and drug iontophoresis groups at baseline **Table 3.1 and Figure 3.4 A-D**, before commencement of the iontophoresis protocol.

Table 3.1. **Baseline blood pressure parameters**: Baseline blood pressure parameters in wild-type mice (n =6 per group) before the iontophoresis of phenylephrine (PE) in study groups vehicle, acetylcholine (ACh) and sodium nitroprusside (SNP). Diastolic blood pressure (mmHg), systolic blood pressure (mmHg), mean arterial blood pressure (MAP) (mmHg), heart rate (beats per minute) (bpm). Results are group means ±SE. One-way ANOVA.

Baseline Parameters	Vehicle	ACh	SNP	P value
Diastolic blood pressure (mmHg)	80±5	74±3	80±4	>0.05
Systolic blood pressure (mmHg)	116±5	106±3	111±3	>0.05
Mean arterial blood pressure (mmHg)	92±5	84±3	90±3	>0.05
Heart rate (bpm)	616±22	609±24	618±21	>0.05

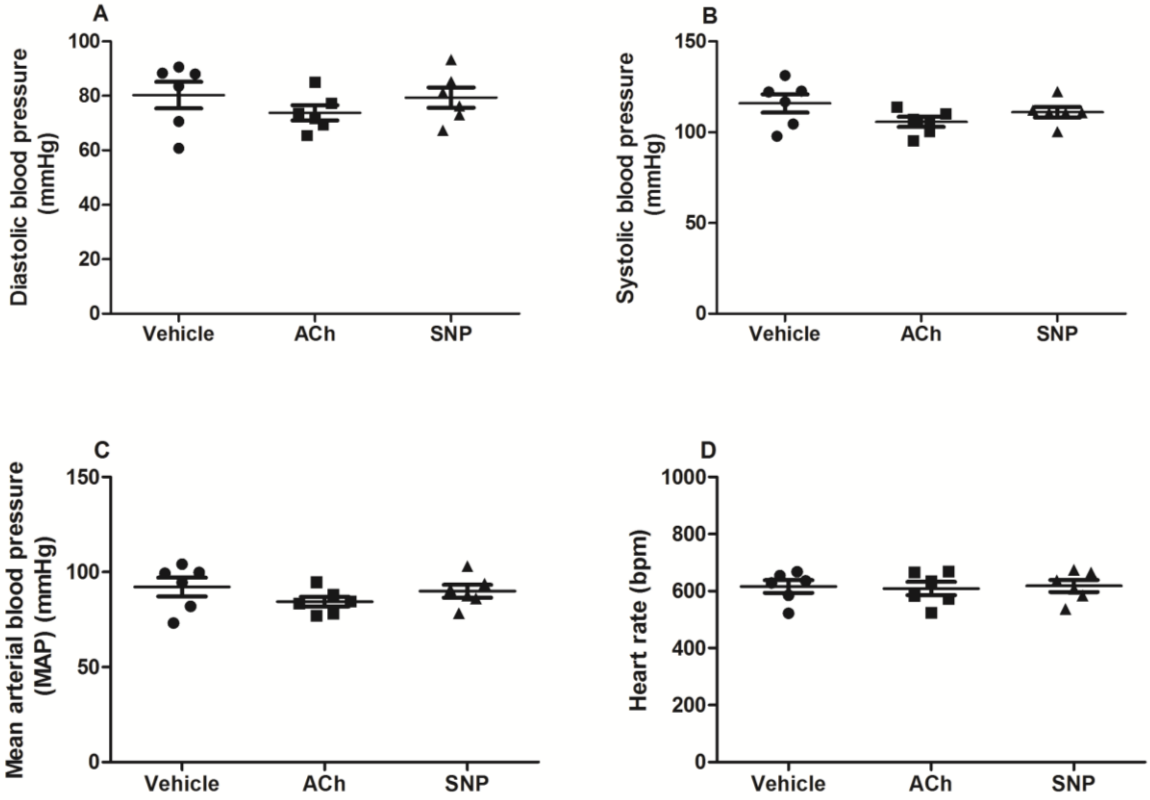

Figure 3.4. Baseline blood pressure parameters: Baseline blood pressure parameters in wild-type mice (n =6 per group) before the iontophoresis of phenylephrine (PE) to study groups vehicle, acetylcholine (ACh) and sodium nitroprusside (SNP). (A) diastolic blood pressure (mmHg), (B) systolic blood pressure (mmHg), (C) mean arterial blood pressure (MAP) (mmHg), (D) heart rate (beats per minute) (bpm). Results are group means ±SE. One-way ANOVA.

Mid-point Iontophoresis

After the iontophoresis of PE, blood pressure and heart rate parameters were recorded to establish whether the described PE iontophoresis protocol impacted on blood pressure parameters and heart rate. There were no significant differences between the groups for all parameters **Table 3.2 and Figure 3.5 A-D**.

Table 3.2. Mid-point blood pressure parameters: Blood pressure parameters in wild-type mice (n =6) after the iontophoresis of phenylephrine (PE) in study groups vehicle, acetylcholine (ACh) and sodium nitroprusside (SNP). Diastolic blood pressure (mmHg), systolic blood pressure (mmHg), mean arterial blood pressure (mmHg), heart rate (beats per minute) (bpm). Results are group means ±SE. One-way ANOVA.

Midpoint Parameters	Vehicle	ACh	SNP	P value
Diastolic blood pressure (mmHg)	82±3	75±4	73±3	>0.05
Systolic blood pressure (mmHg)	118±3	108±5	107±2	>0.05
Mean arterial blood pressure (mmHg)	94±3	86±4	84±3	>0.05
Heart rate (bpm)	632±19	630±10	621±55	>0.05

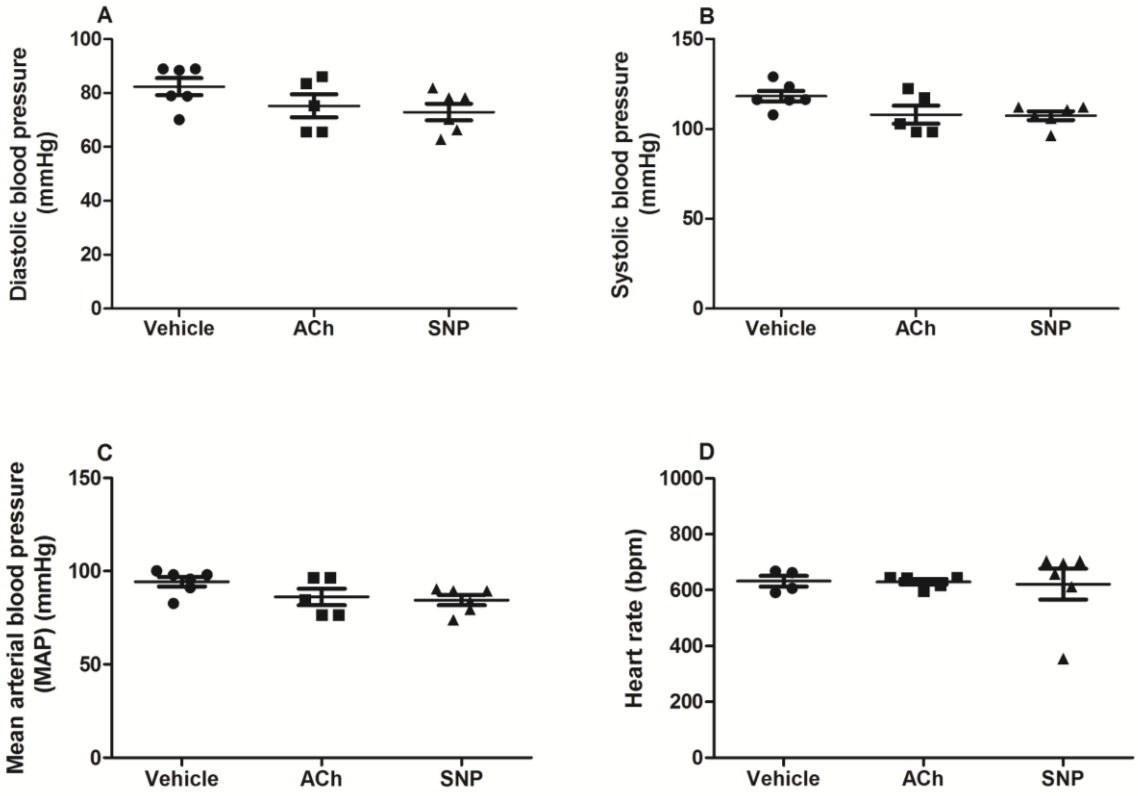

Figure 3.5 Mid-point blood pressure parameters: Blood pressure parameters in wild-type mice (n =6 per group) after the iontophoresis of phenylephrine (PE) in study group's vehicle, acetylcholine and sodium nitroprusside. (A) diastolic blood pressure (mmHg), (B) systolic blood pressure (mmHg), (C) MAP (mmHg), (D) heart rate (beats per minute) (bpm). Results are group means ±SE. One-way ANOVA.

End of Iontophoresis Protocol

There were no significant differences for parameters between vehicle, ACh and SNP treated animals at the end of the iontophoresis protocol **Table 3.3, Figure 3.6 A-D.**

Table 3.3. After iontophoresis blood pressure parameters: Blood pressure parameters in wild-type mice (n =6) after the iontophoresis of vehicle, acetylcholine (ACh) and sodium nitroprusside (SNP). Diastolic blood pressure (mmHg), systolic blood pressure (mmHg), mean arterial blood pressure (mmHg), heart rate (beats per minute) (bpm). Results are group means ±SE. One-way ANOVA.

End Parameters	Vehicle	ACh	SNP	P value
Diastolic blood pressure (mmHg)	69±5	68±5	69±4	>0.05
Systolic blood pressure (mmHg)	104±6	100±6	106±2	>0.05
Mean arterial blood pressure (mmHg)	81±5	79±5	81±3	>0.05
Heart rate (bpm)	643±70	673±17	658±46	>0.05

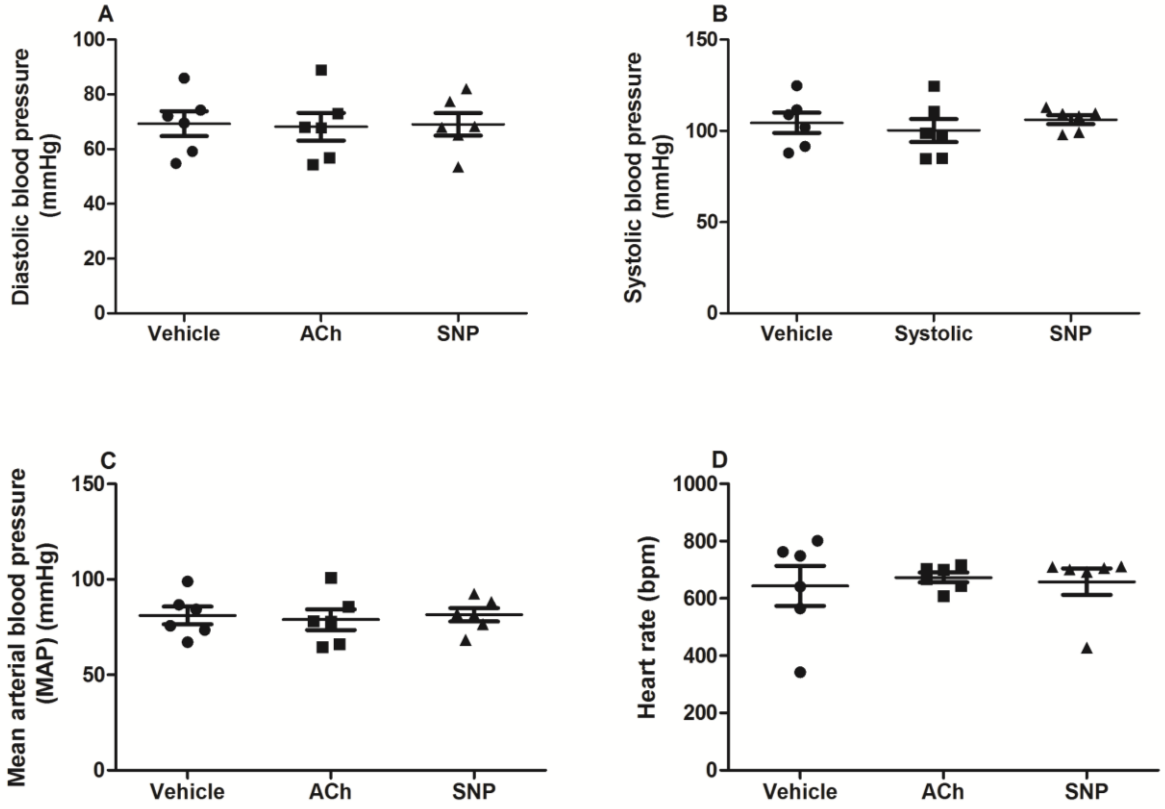

Figure 3.6. After iontophoresis blood pressure parameters: Blood pressure parameters in wild-type mice (n =6 per group) after the iontophoresis of vehicle, acetylcholine (ACh) and sodium nitroprusside (SNP). (A) diastolic blood pressure (mmHg), (B) systolic blood pressure (mmHg), (C) MAP (mmHg), (D) heart rate (beats per minute) (bpm). Results are group means ±SE. One-way ANOVA.

Discussion/conclusion

The use of vasoactive chemicals does not significantly affect cardiovascular function as measured by diastolic blood pressure, systolic blood pressure, mean arterial blood pressure and heart rate in WT mice undergoing iontophoresis. Microvascular function changes observed during the iontophoresis of PE, ACh and SNP in small rodents are representative of local changes in the peripheral skin microvascular network and not systemic, generalised changes in systemic blood pressure or heart rate.

Study of blood glucose in wild-type mice fed a cholesterol diet (2%).

Introduction

Chronic high fat feeding results in significant irregularities in glucose homeostasis in WT C57BL/6 mice and the onset of type two diabetes (Surwit *et al*., 1988, Park *et al*., 2005). Diabetes is an established risk factor for CVD in humans (D'Agostino *et al*., 2013) and has been previously studied through high fat feeding in WT mice relevant to CVD (Calligaris *et al*., 2013). The longitudinal studies detailed in this thesis endeavoured to answer whether dietary cholesterol could propagate CVD through activation of innate immune inflammatory cascades, without the presence of diabetes. This study sought to establish the suitability of a 2% added cholesterol diet in WT mice, and establish whether chronic feeding would results in significant plasma glucose elevations after 20 weeks of feeding.

Methods

The methods description below is intended to provide an overview of experimental techniques used in this study. Further experimental details are described in *Materials and Methods Pages 62-92.*

Measurements

WT C57BL/6 male mice (12 weeks of age) (n =7 per group) were fed either normal rodent chow or a cholesterol diet for 20 weeks. Study end point body weight (g), plasma cholesterol (mg/dl) and blood glucose were measured. Blood collected from the tail vein was used for glucose measurements using a

blood glucose meter (mmol/l) (Ascensia Contour). Results are group means ±SE.

Results

There were no significant differences between WT-chow (29±1g) and WT-cholesterol (31±1g) fed animals in body weights at study end point (P>0.05) **Figure 3.7A**.

There were no significant differences between WT-chow (5±1 mmol/L) and WT-cholesterol (5±1 mmol/L) fed animals for blood glucose (P>0.05) **Figure 3.7B**.

Cholesterol fed animals had significantly greater plasma LDL/vLDL (13±1 mg/dl) compared to WT-chow fed animals (5±1 mg/dl) (P<0.001) **Figure 3.7C**.

However levels of HDL were not significantly different between the groups (WT-chow 18±1 mg/dl VS. WT-cholesterol 19±1 mg/dl, P>0.05) **Figure 3.7D**.

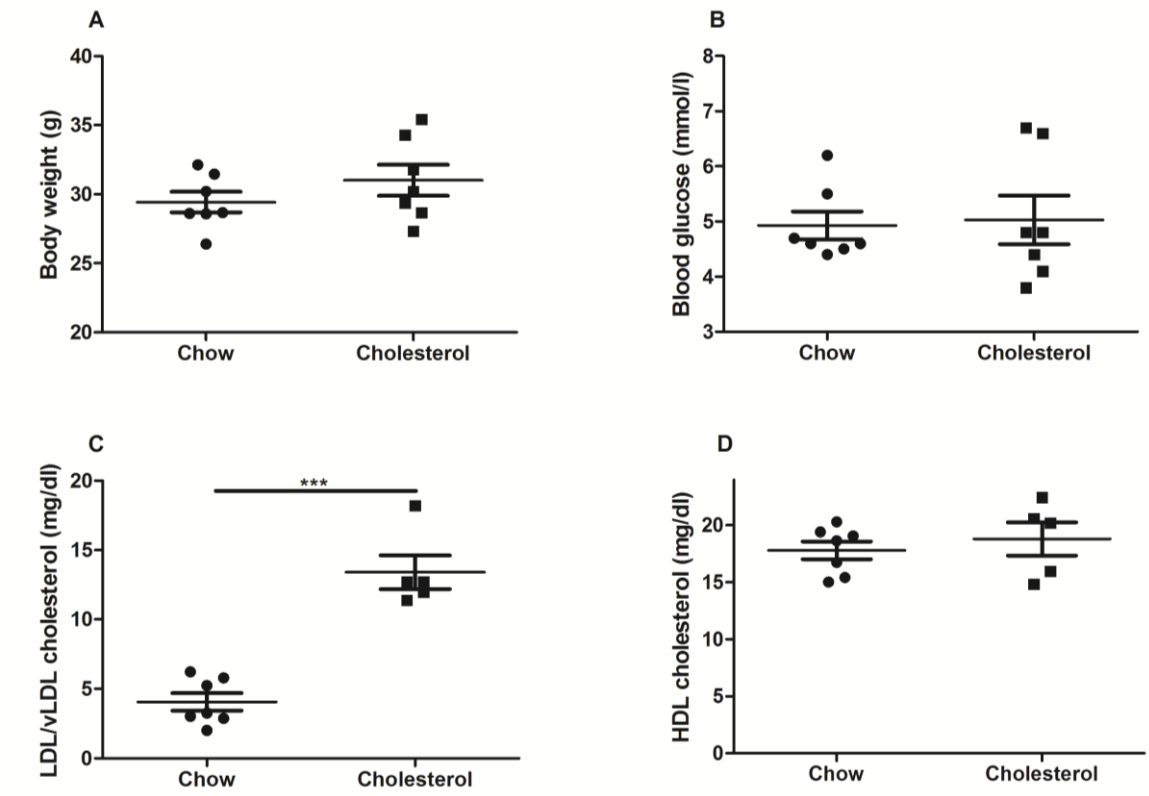

Figure 3.7. **Cholesterol feeding effect on body weight, blood glucose and plasma cholesterol:** Study week 20 measurements of (A) body weight (g), (B) blood glucose (mmol/l), (C) LDL/vLDL and HDL (D) in wild-type chow (n =7) and cholesterol fed mice (n =7). Results are group means ±SE. Unpaired Student's t-test. ***P<0.001

Discussion/conclusion

2% added cholesterol feeding in WT mice does not significantly alter body weight, blood glucose or HDL plasma cholesterol. Cholesterol feeding significantly induces dyslipidaemia through elevation of LDL/vLDL. The use of a 2% cholesterol diet that is adjusted for calories is suitable for longitudinal *in vivo* studies, and does not result in a significantly altered plasma glucose level that is otherwise associated with diabetes, a risk factor for CVD. Nonetheless glucose homeostasis is tightly regulated by catabolic (glucagon, cortisol and catecholamines) and anabolic (insulin) hormones and further investigation is needed into the suitability of a 2% added cholesterol diet for endothelium-dependent investigations to ensure against hyperinsulinemia, an early event in diet induced diabetes.

Chapter 4

Deficiency of Mitogen and Stress-Activated Kinase 1 and 2 (MSK 1/2) Promotes Endothelial Dysfunction *in vivo*.

Introduction

As previously discussed in the *introduction (Mitogen and Protein Activated Kinases)* the anti-inflammatory effects of p38α are mediated in part via the activation of MSK 1 and 2 (Kim *et al*., 2008, Darragh *et al*., 2010). MSK1/2 double KO mice show increased sensitivity to LPS induced endotoxin shock, which is accompanied by an increase in the induction of TNF, IL-6 and IL-12 relative to WT animals (Kim *et al*., 2008). TNF, IL-6, IL-1 and IL-6 are cytokines implicated in the pathogenesis of CVD, but the role of these kinases early in the development of CVD has not been studied.

Aim

The aim of this chapter was to assess endothelial function in MSK 1/ 2 gene targeted KO mice fed rodent chow or a cholesterol supplemented diet, and to explore the potential role of systemic cytokine expression early in the pathogenesis of CVD.

Methods

The methods description below is intended to provide an overview of experimental techniques used in this study. Further experimental details are described in *Materials and Methods Pages 62-92.*

Animals

Animals from the breeding strain MSK 1/ 2 were randomly allocated into four groups: WT control mice fed normal rodent chow, WT mice on a pro-atherogenic diet and MSK 1/2 KO mice on normal rodent chow and on the pro-atherogenic diet.

Longitudinal Assessment of Vascular Function

The following time points were used for vascular function testing: baseline (study week 0), 4 weeks, 8 weeks, 12 weeks, 16 weeks, 20 weeks and 24 weeks for *in vivo* assessment of endothelium-dependent, endothelium-independent and maximal vasodilator capacity as described. The role of NO was further explored through application of L-NAME.

Body Weight

Animals were weighed at study baseline and week 24.

Plasma Cholesterol

Measurements were made at study baseline and 24 weeks.

Cytokine Expression

Measurements were made at study baseline and 24 weeks.

Lipid Staining of the Aorta

Lipid deposition within the aorta was achieved by oil red O staining at study week 24 weeks.

Results

Baseline Body Weights

Baseline body weights at 16 weeks of age were significantly greater in WT than in MSK1/2 KO mice (28±1g VS. 26±1g respectively, P<0.01.) (**Figure 4.1A**). This translated to a mean difference of 2g.

Week 24 Body Weights

WT-chow (baseline 27±1g VS. week 24 32±1g, P<0.001), WT-cholesterol (baseline 30±1g VS. week 24 36±1g, P<0.001), KO-chow (baseline 27±1g VS. week 24 32±1g, P<0.001) and KO-cholesterol (baseline 26±1g VS. week 24 35±1g, P<0.001) fed mice significantly increased in body weight over the study duration.

End-point body weights were significantly greater in cholesterol fed WT and MSK 1/ 2 KO mice (P<0.001) when compared to control chow fed mice (**Figure 4.1 B**).

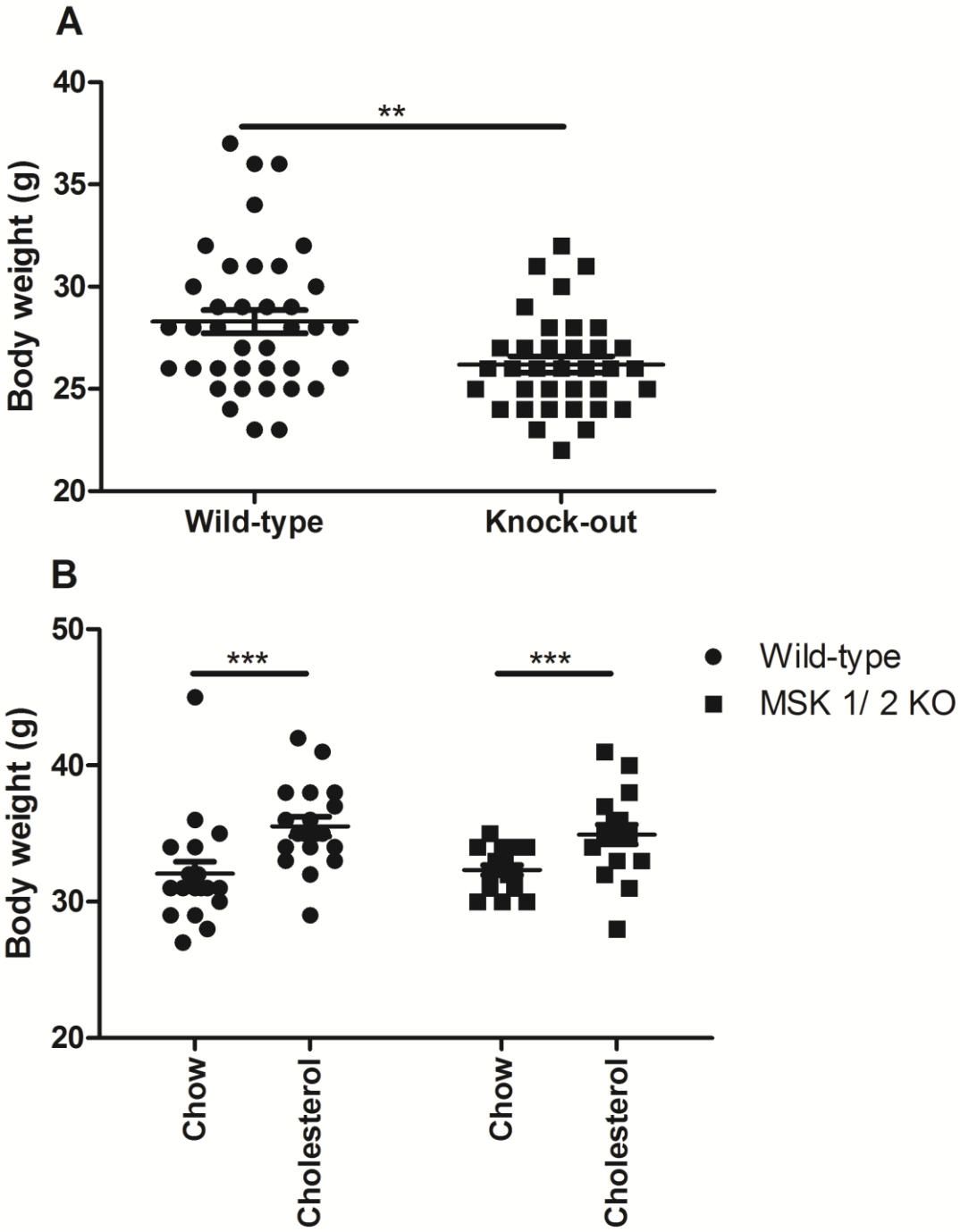

Figure 4.1. Body weights: (A) Baseline body weights (16 weeks of age) in WT (n =38) and MSK 1/ 2 KO (n =36) mice. Unpaired Student's t-test. (B) week 24 weights in WT-chow (n =19), WT-cholesterol (n =19), MSK 1/2 KO-chow (n =18) and MSK 1/2 KO-cholesterol (n =18) fed mice. Two-way ANOVA . Results are group means ±SE in grams (g). **P<0.01, ***P<0.001.

Baseline Vascular Responses

WT and MSK 1/2 KO mice showed skin microvascular responses to ACh and localized heating to 44ºC that were not significantly different between the groups (ACh: WT 349±4 AU VS. KO 338±6 AU P>0.05; localised skin heating: WT 394±4 AU VS. KO 396±6 AU P>0.05) (**Figure 4.2 A/B** respectively).

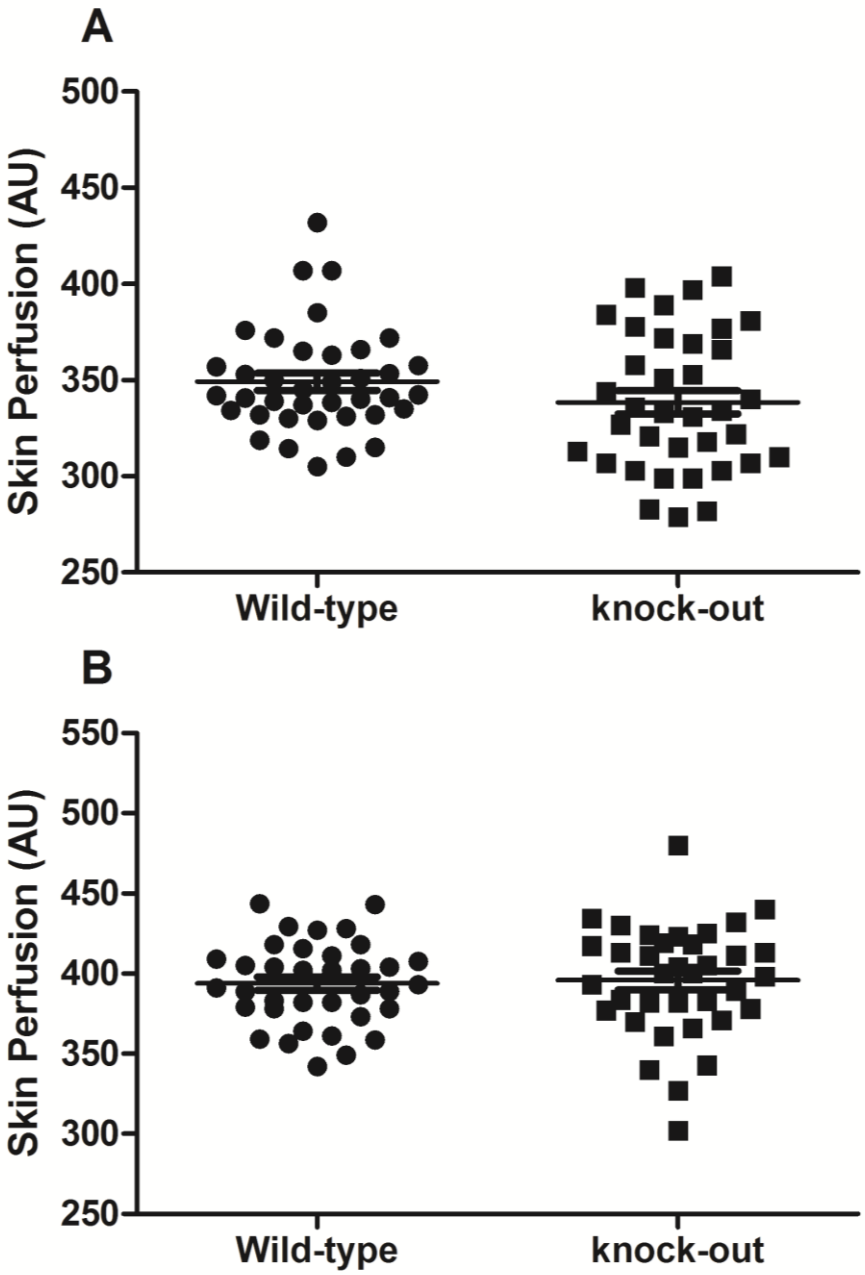

Figure 4.2. Baseline vascular responses: Baseline (study week 0) microvascular responses in WT (n =38) and MSK 1/ 2 KO (n =36) animals: (A) endothelium-dependent responses and (B) maximal dilator capacity. Results are group means ±SE arbitrary units of skin perfusion (AU). Unpaired Student's t-test.

Baseline Cytokines

Cytokine analysis showed several differences in baseline levels between WT and MSK 1/2 KO mice. MSK 1/ 2 KO mice had significantly greater IL-1α, IL-6, reduced levels of IL-10 and higher sE-selectin when compared to WT mice (**Table 4.1, Figure 4.1A-D**). Whilst levels of TNF-α and sICAM-1 were not significantly different between the groups (**Table 4.1, Figure 4.1 E/F** respectively).

Table 4.1. Baseline inflammatory markers. Baseline (study week 0) in WT (n =38) and MSK 1/ 2 KO (n =36) mice. Unpaired Student's t-test.

Cytokine	WT	MSK 1/ 2 KO	P value
IL-1α (pg/ml)	476±29	629±44	<0.01
IL-6 (pg/ml)	392±49	660±45	<0.001
IL-10 (pg/ml)	570±29	213±11	<0.001
sE-selectin (pg/ml)	5±0.3	8±1	<0.01
TNF-α (pg/ml)	4940±622	5628±442	>0.05
sICAM-1 (pg/ml)	2±0.2	2±0.2	>0.05

Plasma Cholesterol

Total plasma cholesterol levels were similar in WT and MSK 1/2 KO mice at study week 0 (72±1 and 74±1 mg/dl, respectively) (**Figure 4.4A**).

Chow fed WT mice showed no significant changes in total plasma cholesterol over the study duration (WT chow-fed week 0: 72±1 and 24 weeks: 71±1 mg/dl). Whereas WT-cholesterol fed mice had significant elevations in plasma cholesterol (**Figure 4.4B**). MSK 1/ 2 KO-chow fed mice displayed similar levels of plasma cholesterol when compared to WT-chow fed mice (**Figure 4.4B**) and

MSK 1/ 2 KO-cholesterol fed mice displayed the greatest onset of dyslipidaemia (**Figure 4.4)**.

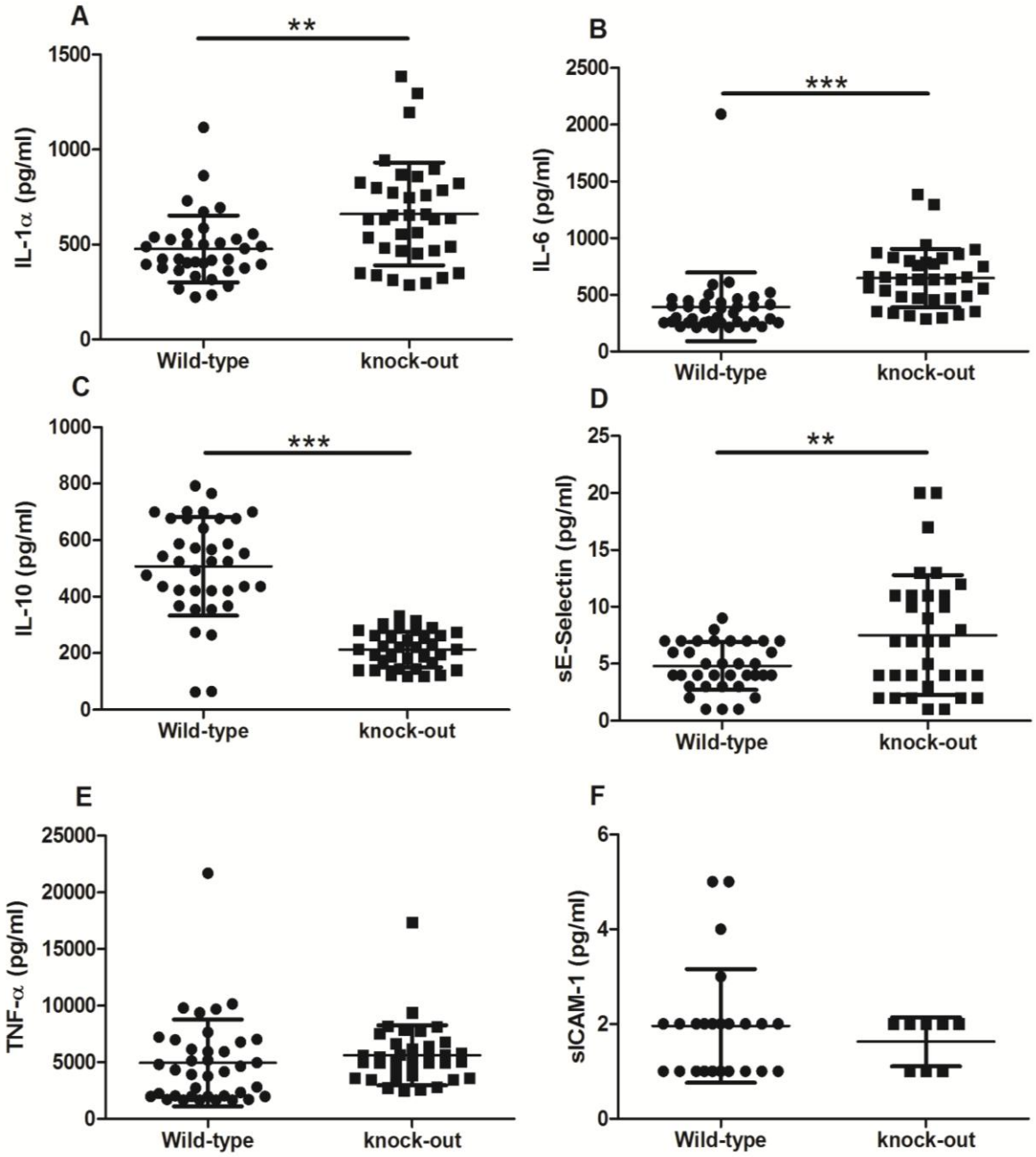

Figure 4.3. Baseline inflammatory markers. Baseline (16 weeks of age) plasma cytokines for (A) IL-1α (B) IL-6, (C) IL-10 (D) E-selectin (E) TNF-α and (F) sICAM-1 in WT (n =38) and MSK 1/ 2 KO (n =36). Results are group means ±SE (pg/ml). Student's t-test. **P<0.01, ***P<0.001.

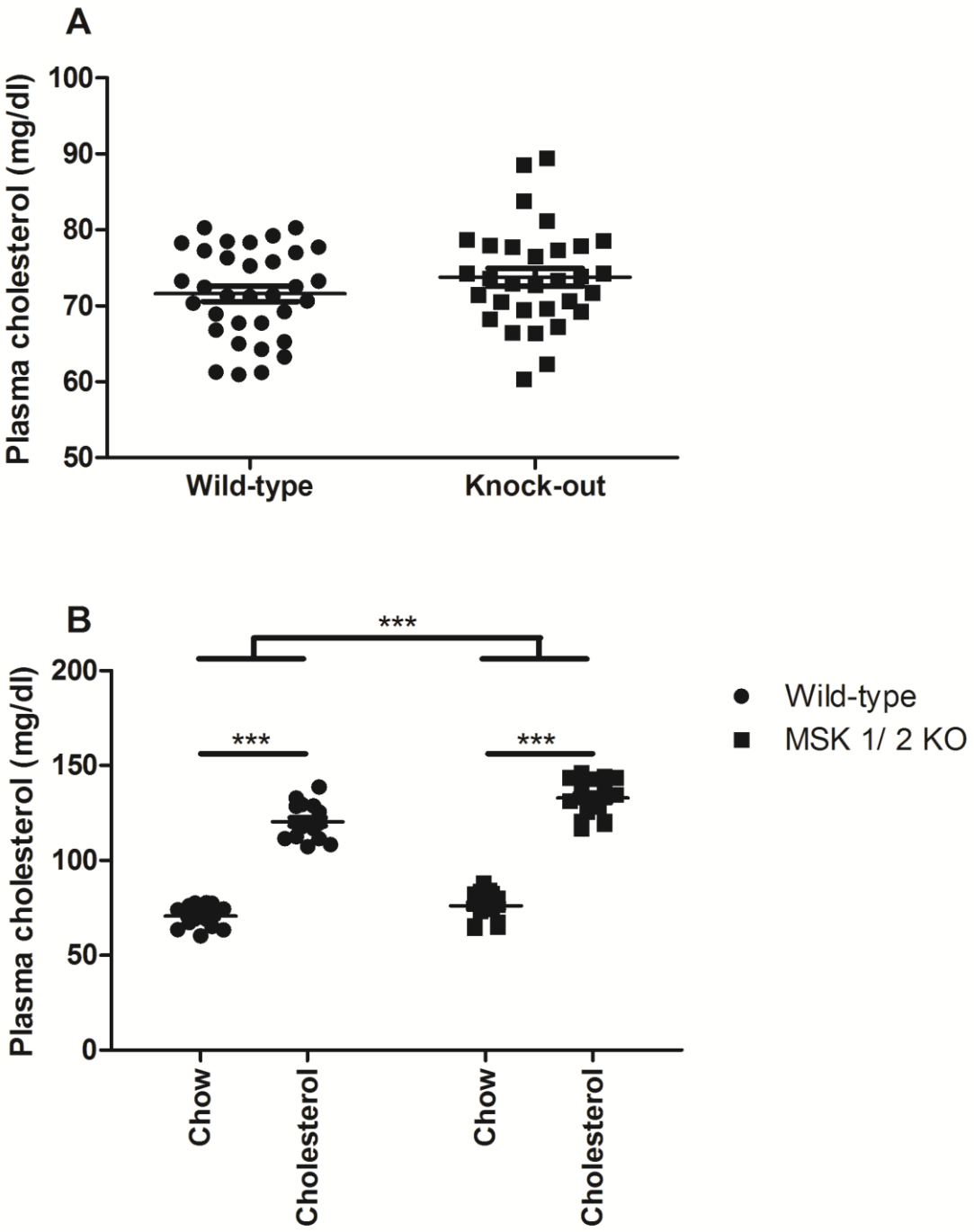

Figure 4.4. Plasma cholesterol: Total plasma cholesterol, values are group means ±SE (mg/dl) at (A) study baseline (WT n =38, KO n =36), unpaired Student's t-test and (B) 24 week measurements in WT-chow (n =19) WT-cholesterol (n =19), MSK 1/2 KO-chow (n =18) and MSK 1/ 2 KO-cholesterol (n =18) fed mice, two-way ANOVA. ***P<0.001.

Changes in Endothelium-dependent Responses Over 24weeks

WT mice on a chow diet showed no significant changes in skin microvascular responses to ACh over 24 weeks (**Table 4.2**), supporting the view that these mice show no signs of endothelial dysfunction (**Figure 4.5A**). In contrast, WT mice on a cholesterol diet showed significant attenuation of microvascular responses to ACh from 4 week onwards compared with baseline measurements ($P<0.001$ all time-points) (**Figure 4.5A**). Furthermore MSK 1/2 KO mice both on chow and cholesterol showed significant attenuation of ACh responses from week 4 onwards compared with week 0 measurements ($P<0.001$ all time-points) (**Figure 4.5A**). Over the 24 week period, ANOVA showed that WT-chow mice had significantly greater ACh responses than WT-cholesterol, MSK 1/2 KO-chow and MSK 1/2 KO-cholesterol fed mice ($P<0.001$ for all, **Figure 4.5A**). Additionally, MSK 1/2 KO mice on a high cholesterol diet had significantly poorer microvascular responses to ACh compared with WT mice on a cholesterol diet ($P<0.01$) and MSK 1/2 KO on chow ($P<0.01$) (**Figure 4.5A**).

Table 4.2. Longitudinal endothelium dependent responses: Skin microvascular responses to ACh in WT-chow (n =19), WT-cholesterol (n =19), MSK 1/ 2 KO-chow (n =18) and MSK 1/ 2 KO-cholesterol (n =18) fed mice. Results are group means in arbitrary units (AU) ±SE.

Group	Baseline (Week 0) (AU)	4 weeks (AU)	8 weeks (AU)	12 weeks (AU)	16 weeks (AU)	20 weeks (AU)	24 weeks (AU)
WT-chow	348±6	356±7	338±7	343±7	354±8	350±6	349±7
WT-cholesterol	351±6	306±12	262±12	248±9	248±6	248±5	247±5
KO-chow	339±8	284±8	279±7	254±8	225±10	239±6	230±6
KO-cholesterol	338±9	294±6	222±6	213±4	235±11	216±4	233±6

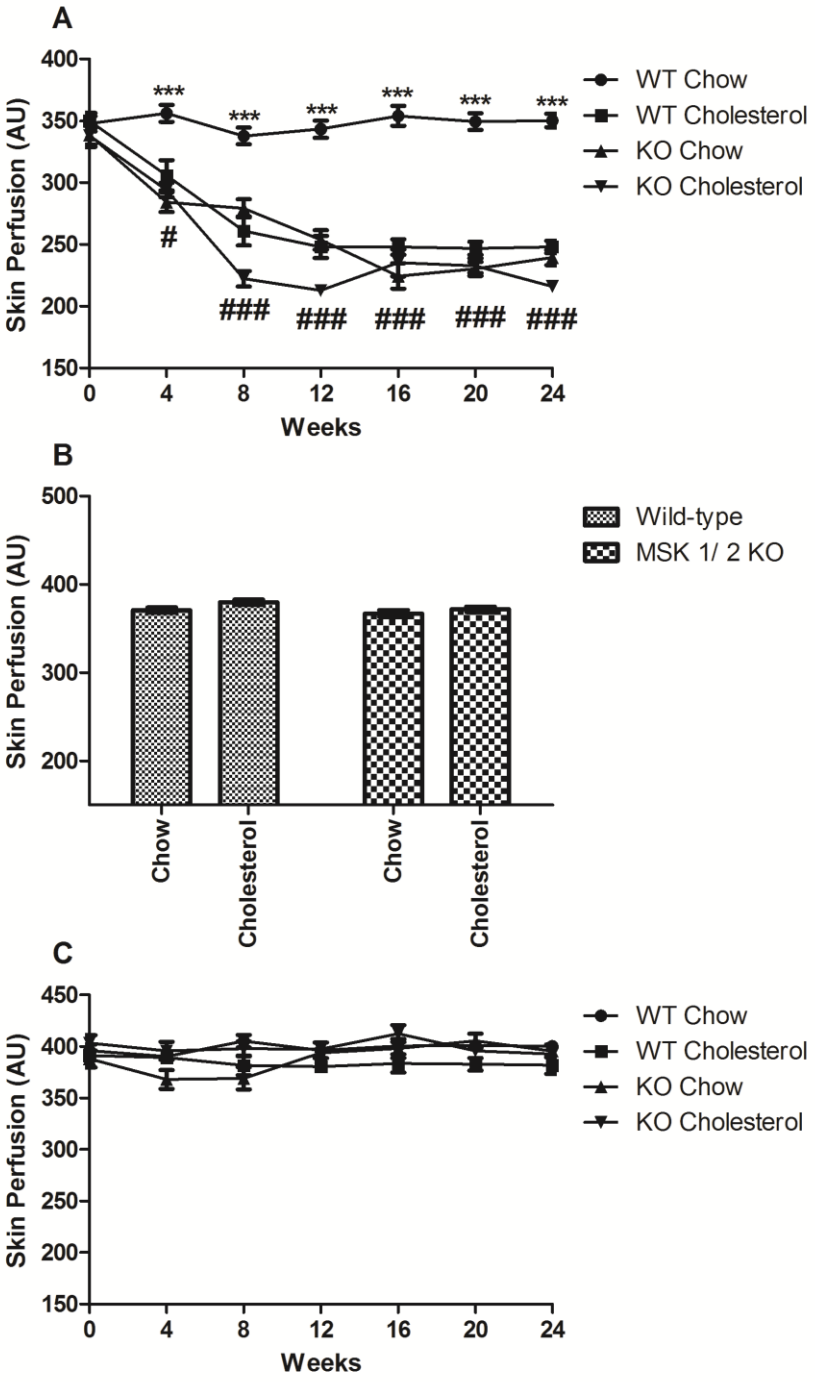

Figure 4.5. Longitudinal microvascular responses: Microvascular responses in arbitrary units (AU), results are group means ±SE over 24 weeks to (A) ACh, (B) SNP at 24 weeks only and (C) localised 44°C heating (over 24 weeks) in WT-chow (n =19), WT-cholesterol (n =19), MSK 1/2 KO-chow (n =18) and MSK 1/2 KO-cholesterol (n =18) fed animals. Changes were analysed by two-way ANOVA.
***P<0.001 comparing genotype.
(P<0.05), ### (P<0.001) P<0.01 comparing diet

Effect of NO Inhibition on Endothelium-dependent Responses

At week 0, administration of the NO synthase inhibitor, L-NAME produced a significant reduction in the peak ACh response (320±56 AU VS. 257±60 AU, $P<0.05$ in WT mice and 318±60 AU VS. 243±65 AU, $P<0.05$ in MSK 1/2 KO mice), supporting a role for endothelium-derived NO in ACh-mediated vasodilatation. L-NAME administration to chow fed WT mice at 12 weeks also caused significant attenuation in the peak ACh response compared with the response without L-NAME (248±51 AU VS. 310±65 AU, $P<0.05$), supporting the notion that NO in WT chow fed mice is preserved over time (with age).

In WT mice fed a high cholesterol diet, L-NAME administration produced a smaller, but significant reduction in the peak ACh response compared with the response without L-NAME (180±21 AU VS. 226±21 AU, $P<0.05$), suggesting NO was diminished in part by cholesterol feeding. L-NAME administration to MSK 1/2 KO mice fed chow or cholesterol did not show any significant reduction in the peak ACh response compared with the response without L-NAME (chow-fed 226±18 AU VS. 251±18 AU, $P>0.05$ and cholesterol-fed 235±19 AU VS. 237±38 AU, $P>0.05$), indicating that NO was depleted in these groups.

Endothelium-independent Responses to SNP at 24 Weeks

Endothelium-independent microvascular responses to iontophoresis of SNP at week 24 were not significantly different amongst the groups (**Figure 4.5B**). No significant differences were found for this measurement, which suggests that cholesterol feeding in WT mice and the MSK 1/2 deficiency (cholesterol and chow groups) affects endothelial function without affecting smooth muscle function.

Changes in Maximum Vasodilator Response to 44ºC heating over 24 weeks

Figure 4.5C shows that the maximum vasodilator response to localised 44ºC heating was not significantly different amongst the groups over 24 weeks. This further suggests that attenuated ACh responses are indicative of dysfunction at the level of the endothelium and not generalised vascular smooth muscle dysfunction.

Changes in Plasma Cytokines Over 24 Weeks

Compared with measurements at study baseline, IL-1α increased significantly over 24 weeks in WT cholesterol-fed ($P < 0.001$), MSK 1/2 KO chow-fed ($P<0.01$) and MSK 1/2 KO-cholesterol fed ($P<0.001$) mice. The extent of change at 24 weeks was greatest in MSK 1/2 KO cholesterol-fed mice. Levels of IL-1α in MSK 1/2 KO cholesterol-fed mice were significantly greater than in WT chow-fed ($P<0.001$), WT cholesterol-fed ($P<0.01$) and KO chow-fed ($P<0.001$) mice (**Figure 4.6A**).

IL-6 increased significantly over 24 weeks in WT cholesterol-fed, MSK 1/2 KO chow-fed and MSK 1/2 KO cholesterol-fed mice ($P<0.001$ for all) compared with levels at week 0. At 24 weeks, levels of IL-6 were significantly greater in WT cholesterol-fed, MSK 1/2 KO chow-fed and MSK 1/2 KO cholesterol-fed ($P<0.001$ for all) mice compared with WT chow-fed mice (**Figure 4.6B**).

Plasma IL-10 levels for WT-chow and KO chow-fed mice showed no significant change over the study duration (0 VS. 24 weeks). IL-10 levels were significantly lower at 24 weeks in cholesterol-fed mice (WT $P<0.01$ and MSK 1/2 KO $P<0.001$) compared with levels at week 0. **Figure 4.6C** shows the significant differences amongst the groups. These reductions were statistically significant

when groups were compared with WT-chow fed mice at study week 24, IL-10 levels were significantly reduced in WT cholesterol-fed (P<0.01), MSK 1/2 KO chow-fed (P<0.001) and MSK 1/2 KO cholesterol-fed(P<0.001) mice (**Figure 4.6C**). MSK 1/2 KO cholesterol-fed mice also had significantly lower levels than WT cholesterol-fed mice (P<0.001) (**Figure 4.6C**).

TNF-α increased significantly over 24 weeks in WT cholesterol-fed, MSK 1/2 KO chow-fed and MSK 1/2 KO cholesterol-fed mice (P<0.001 for all) compared with levels at week 0. At 24 weeks, compared with WT chow-fed mice, levels of TNF-α were significantly greater in WT cholesterol-fed (P<0.001), MSK 1/2 KO chow-fed (P<0.01) and MSK 1/2 KO cholesterol-fed (P<0.001) mice (**Figure 4.6D**). MSK 1/2 KO cholesterol-fed mice also had higher TNF-α levels than WT cholesterol-fed (P<0.01) and MSK 1/2 KO chow-fed (P<0.001) mice (**Figure 4.6D**). At 24 weeks, E-selectin levels were significantly higher in MSK 1/2 KO cholesterol-fed mice compared with WT chow-fed (P< 0.001) and WT cholesterol-fed (P<0.01) and MSK 1/2 KO chow-fed (P<0.01) mice (**Figure 4.6E**). No significant changes were seen in sICAM-1 from baseline levels or between the groups at 24 weeks (**Figure 4.6F**).

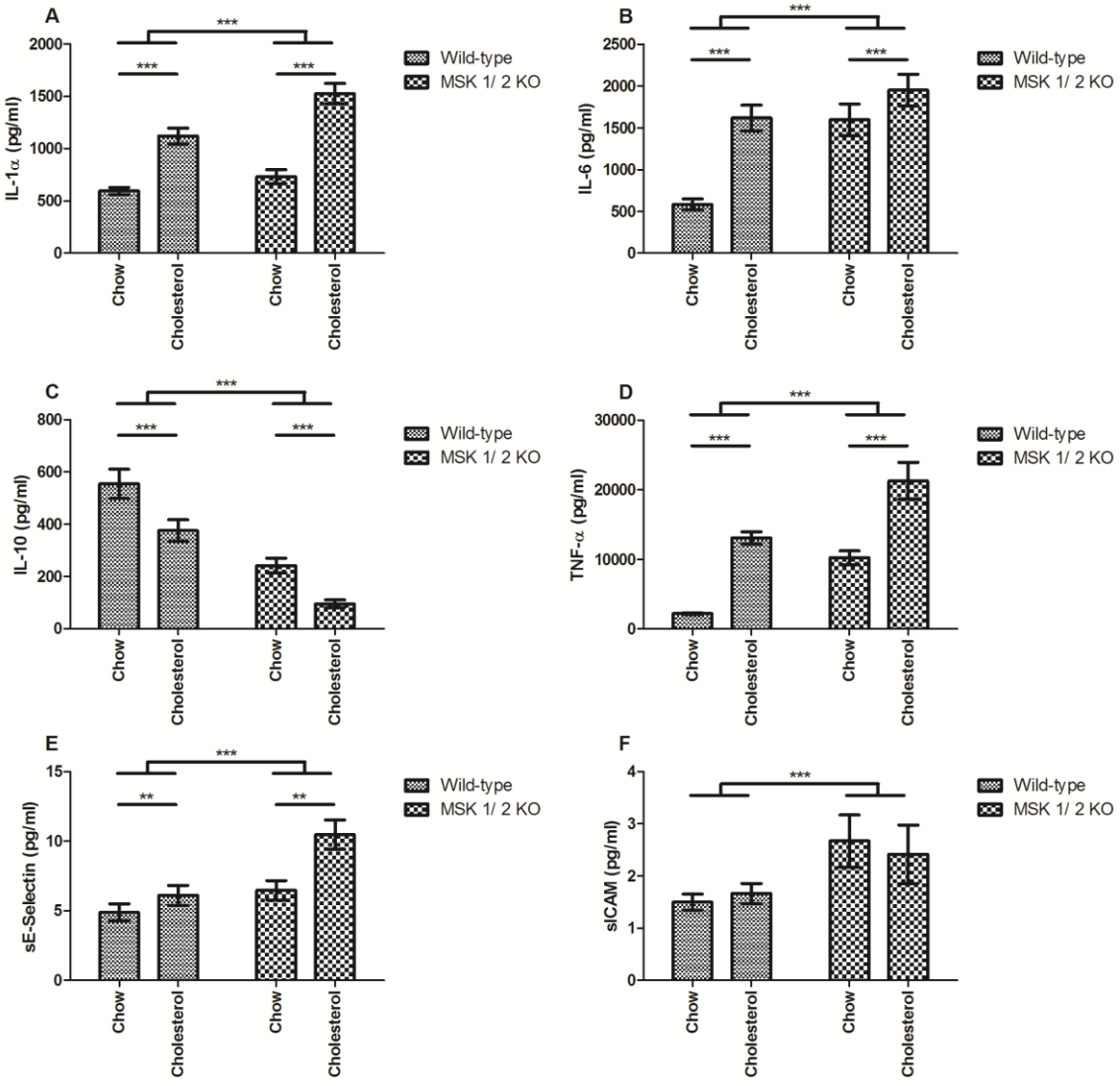

Figure 4.6. Week 24 inflammatory markers: Levels of inflammatory markers at week 24 in WT-chow (n =19), WT-cholesterol (n =19), MSK 1/2 KO-chow (n =18) and MSK 1/2 KO-cholesterol (n =18) fed mice. Results are group means ±SE (pg/ml) (A) IL-1α, (B) IL-6, (C) IL-10, (D) TNF-α, (E) sE-Selectin, (F) sICAM-1. Two-way ANOVA. **P<0.01 ***P<0.001

Aortic Lipid Deposition

In comparison with WT chow-fed mice (3.0±0.2%) cholesterol-fed WT mice showed a significantly higher lipid deposition (14.0±1.0%, P<0.001) (**Figure 4.7A**). Similarly, MSK 1/2 KO mice fed chow and cholesterol displayed higher lipid deposition than WT-chow fed mice (6±1%, P<0.05 and 20.0±0.8%, P<0.001, respectively) (**Figure 4.7A**). Increased levels of lipid deposition were associated with poorer vascular function as shown by the significant negative

correlation between lipid deposition and the peak ACh response (week 24) (r= -0.664, P<0.001) (**Figure 4.7B**).

Correlations between Vascular Responses and Blood Markers

Microvascular responses to ACh and localised heating at week 0 showed no significant correlations with cholesterol or any of the cytokines markers. In contrast, a number of significant correlations were observed at 24 weeks between blood markers and ACh responses, but not with the response to SNP or with the response to localised 44ºC heating. Peak ACh responses at 24 weeks significantly correlated with IL-1α (r= -0.514, P<0.001), IL-6 (r= -0.581, P<0.001), IL-10 (r= 0.651, P<0.001), TNF-α (r= -0.617, P<0.001), and E-selectin (r= -0.424, P<0.001) (**Figure 4.8**). From the univariate correlations above, these were entered into a stepwise linear regression model. Independent determinants of ACh responses were IL-10 (β= 0.483, P<0.001) and IL-1α (β= -0.286, P<0.01).

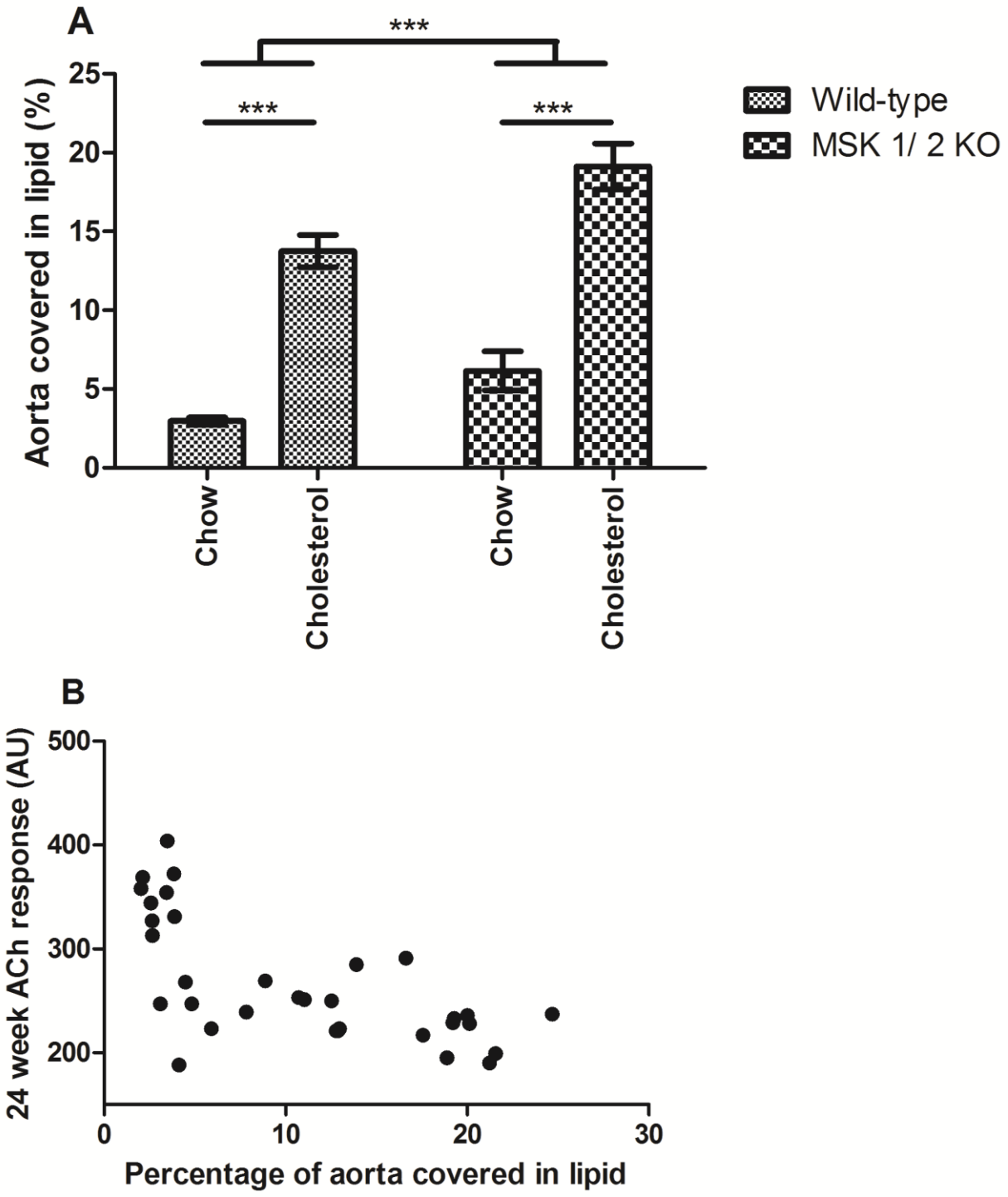

Figure 4.7. Aortic lipid deposition: Aortic lipid staining conducted by Jamie Turner. (A) Percentage (%) of aorta covered in lipid at 24 weeks in WT-chow (n =9), WT-cholesterol (n =8), MSK 1/2 KO-chow (n =8) and MSK 1/2 KO-cholesterol (n =8) fed mice. Values are group means ±SE, Two-way ANOVA. ***P <0.001 (B) Significant association between microvascular response to ACh in arbitrary units (AU) at study week 24 VS. Percentage lipid deposition in the aorta (r= -0.664, P<0.001) (in WT-chow (n =9), WT-cholesterol (n =8), MSK 1/2 KO-chow (n =8) and MSK 1/2 KO-cholesterol (n =8) fed mice).

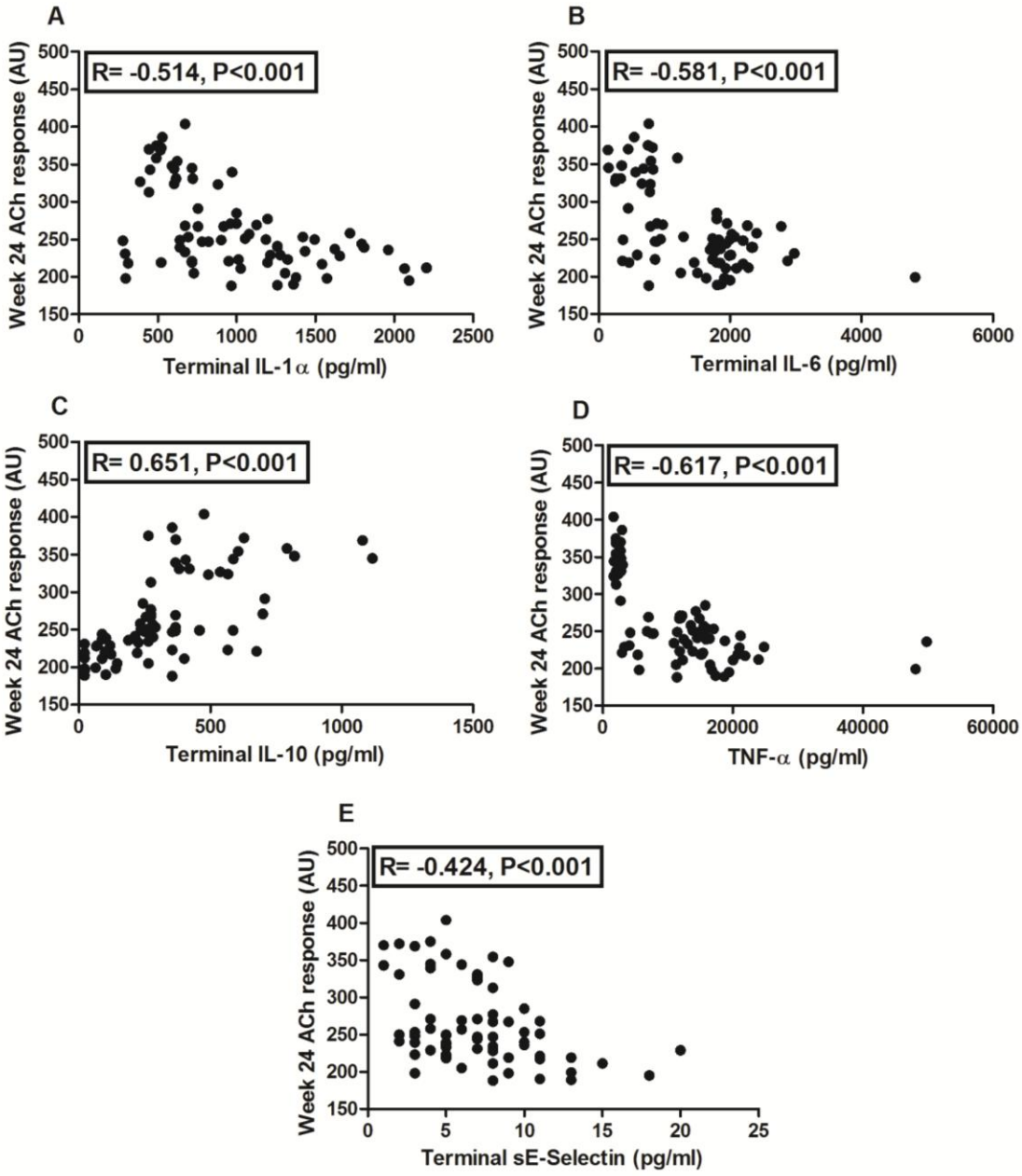

Figure 4.8. Correlations: The association between the ACh response (AU) at week 24 in WT-chow (n =19), WT-cholesterol (n =19), MSK 1/2 KO-chow (n =18) and MSK 1/2 KO-cholesterol (n =18) fed mice and (A) IL-1α, (B) IL-6, (C). IL-10, (D) TNF-α, (E) soluble E-selectin.

Discussion

The main findings from this study suggest that MSK 1/2 deficiency in mice causes significant impairment in endothelium-dependent vasodilatation with increased systemic cytokine production. L-NAME administration showed that ACh responses were in part mediated via the actions of NO, and therefore, a

decrease in ACh responses in MSK 1/2 deficient mice was mediated via reduced NO. In contrast, WT animals fed a normal chow diet maintained normal plasma lipids and exhibited no significant changes in basal levels of inflammatory markers and had preservation of endothelium-dependent vascular responses over the 24 week study. Generalised vascular function, tested by iontophoresis of the endothelium-independent vasodilator SNP and maximum vasodilator capacity to localised 44ºC skin heating was not significantly different amongst the groups, suggesting that elevation of pro-inflammatory cytokines was specifically affecting vascular function at the level of the endothelium. These data suggest a possible functional role of MSK1/2 in the development and progression of atherosclerosis through an interaction between regulation of inflammatory cytokines and endothelial dysfunction.

Baseline ACh responses were dependent on NO production in both WT and MSK 1/2 KO mice as shown by the significant reduction following pre-treatment with L-NAME. At 12 weeks however, while L-NAME still produced a significant decrease in WT mice on a chow diet (confirming dependency on NO production), WT mice on a high cholesterol diet showed a lesser decrease in ACh response following L-NAME, and MSK 1/2 KO mice (on either diet) demonstrated no significant change. Thus, 12 weeks of cholesterol alone (i.e. in WT only) did not inhibit NO completely, whereas in MSK 1/2 KO mice there was a more significant reduction in NO as shown by no further reduction in ACh responses following L-NAME. Interestingly, in spite of a greater reduction in NO in MSK 1/2 KO mice, ACh responses in the presence of L-NAME were not as low as responses in WT cholesterol-fed mice post L-NAME. It is possible that the higher level of perfusion in the MSK 1/2 KO mice might be related to a

compensatory increase in ACh-induced production of endothelium-derived hyperpolarising factor (Verma *et al*., 2003).

MSK 1/2 KO mice on a BALB/c Sv/129 mixed background do not reportedly display an altered phenotype, conversely in this study we report a lower age matched weight at 16 weeks of age on a C57BL/6 background. This translated to a mean difference of 2g which was considered negligible and would not significantly impact on the study outcome. At week 0, although elevations in pro-inflammatory markers in MSK 1/2 KO mice compared with WT mice were found (increased IL-1α, IL-6, E-selectin and reduced IL-10), there were no significant differences in ACh responses, perhaps indicating that the relative difference and potential duration of change in cytokine levels was not sufficient enough to impact significantly on vascular function at that time point. The difference in inflammatory cytokines between WT and KO strains at baseline may be mediated by environmental factors for example exposure to infectious agents. Mice were initially bred and maintained in a barrier facility and subsequently rehoused for vascular testing in a conventional unit, at which they could have been exposed to additional micro-organisms. The onset of CVD and induction of pro-inflammatory gene expression in immune compromised animals has previously been reported in non-pathogen free conditions when animals are challenged with high cholesterol feeding (Mallat *et al*., 1999). Previous findings show that high cholesterol feeding induces greater adverse changes in pro-inflammatory cytokines (Belch *et al*., 2013), with resultant endothelial dysfunction in WT mice compared with chow fed mice (Meyrelles *et al*., 2011). Interestingly, we found that MSK 1/2 KO mice fed a normal chow diet over 24 weeks also displayed elevations in pro-inflammatory cytokines and diminished responses to ACh. MSK 1/2 KO mice still can develop significant endothelial

dysfunction, to a degree similar to that seen with cholesterol feeding in WT mice. The exact mechanism for this dysfunction requires further scrutiny.

It has previously been reported that MSK 1/ 2 KO mice have decreased production of IL-1ra (Darragh *et al*., 2010). IL-1ra KO mice display a significant elevation in plasma cholesterol due to impaired cholesterol efflux through altered conversion of hepatic cholesterol to bile acids. This is mediated by reduced expression of 7α-hydroxylase (CY7A1) the rate limiting step in bile acid synthesis (Isoda and Ohsuzu, 2006). MSK 1/ 2 KO mice require further study to assess the exact mechanism of altered cholesterol homeostasis and the resultant impact on systemic cytokine expression and endothelial function, as evidenced by the significant elevation in plasma cholesterol of MSK 1/ 2 KO-cholesterol fed mice when compared to WT-cholesterol fed mice.

Ananieva *et al* (Ananieva *et al*., 2008) reported on the anti-inflammatory effects of the MSK 1/2 kinases. In response to LPS, MSK1/2 double KO macrophages produced elevated levels of TNF-α and IL-6 but decreased amounts of IL-10 relative to WT cells. Similar results were also obtained when plasma cytokine levels were measured following i.p. injection of LPS. These results are in agreement with our findings in which animals with compromised immune function (MSK 1/2 KO mouse) display higher plasma levels of pro-inflammatory molecules and a decreased IL-10 capacity compared with WT (chow-fed) control mice.

Ananieva *et al* (Ananieva *et al*., 2008) also demonstrated that the increased production of IL-6, and to a lesser extent TNF, was dependent on the ability of MSKs to regulate IL-10 production. IL-10 has a potential protective role in atherosclerosis and can be produced by macrophages. IL-10 inhibits pro-

inflammatory cytokine expression through a JAK/STAT3 dependent pathway (Pattison *et al*., 2012). Aortic ring relaxation from IL-10 KO mice display significantly blunted endothelium-dependent responses to ACh, mediated by a decrease in eNOS expression after incubation with TNF-α (Zemse *et al*. 2010). Zimmerman *et al* (Zimmerman *et al*., 2004) demonstrated the potential therapeutic benefits of exogenous IL-10 in WT animals subjected to carotid injury, and observed amplified intimal hyperplasia in WT controls that did not receive exogenous IL-10. Other studies *in vitro* have demonstrated that increased IL-10 levels appear to be anti-atherogenic by increased uptake and efflux of cholesterol, reducing levels of cell death and progression of atherosclerotic lesions (Han *et al*., 2010). Loss of the protective role of IL-10 in the silencing of inflammatory responses in our MSK 1/2 KO mice and WT cholesterol fed mice may indirectly lead to the perpetuation of inflammation.

Although IL-6 was not an independent determinant of ACh responses, it did exhibit a univariate association with endothelium-dependent responses. IL-6 has been linked to an increased risk of adverse cardiovascular events (Naya *et al*., 2007, Ridker *et al*., 2000a) and can be synthesized by a number of cells including macrophages. IL-6 inhibits eNOS activation and attenuates vasodilation by increasing caveolin-1, resulting in more eNOS binding, leading to reduced NO (Hung *et al*., 2010).

Although MSK 1/ 2 KO mice demonstrated a similar degree of endothelial dysfunction to WT mice fed on high cholesterol, they displayed a greater extent of lipid deposition within the aorta, indicating that elevation of pro-inflammatory cytokines together with high cholesterol produces a more profound effect on lipid accumulation within vessel walls than elevations in pro-inflammatory

cytokines alone. Thus, early intervention to promote the MSK 1/2 pathway could potentially limit or restore to some extent, alterations in endothelial function before excessive lipid accumulation within the vessel wall.

One possible explanation for this observed differences between MSK 1/2 chow and cholesterol fed mice could be secreted IL-1α. IL-1α is synthesised by activated endothelial cells and is released early in the atherosclerotic process and mediates the expression of cell adhesion molecules responsible for capture, rolling and subsequent transmigration into the sub-endothelial space (Shreeniwas *et al*., 1992). IL-1α levels are specifically up regulated in cholesterol fed animals. These regulatory and synthetic roles of IL-1 are associated with a number of physiological events including macrophage activation, endothelial proliferation (Hoge and Amar, 2007), myocardial cell damage and endothelial dysfunction through increased oxidative stress and inflammation (Chi *et al*., 2004, Chamberlain *et al*., 2006). Thus the cholesterol diet may further stimulate IL-1α release, resulting in a greater accumulation of macrophages in the arterial wall and a greater accumulation of lipid (Isoda and Ohsuzu, 2006, Isoda *et al*., 2004, Isoda *et al*., 2003).

Significant correlations between microvascular responses to ACh and levels of cytokines at 24 weeks were observed. Demonstrating that this methodology for assessment of microvascular function in the skin is sensitive and reflective of systemic inflammation and similar to what we have reported in patients. We additionally found a significant correlation between impairment in ACh-mediated vascular responses and the percentage of lipid deposition in the aorta at 24 weeks which provides supportive evidence that early measurements of endothelial dysfunction in the skin microcirculation reflect early atherosclerosis

burden using this mouse model. Of the significant univariate correlations between microvascular responses to ACh and cytokine levels, IL-10 proved to be the strongest independent determinant of ACh response in a multivariate regression model with IL-1α also proving to be an independent determinant, albeit to a lesser degree.

In conclusion MSK 1/2 plays an important role in limiting pro-inflammatory signalling downstream of TLRs, and the present study shows that deletion of MSK 1/2 produces a marked inflammatory state with consequent early endothelial dysfunction, reduced NO and increased early atherosclerotic burden. This study also shows that the changes in skin microvascular function are representative of early atherosclerotic burden and therefore the experimental set-up can provide a useful tool for exploring specific pathways and mechanisms underlying development and progression of CVD. Targeting the MSK 1/2 pathway, and in particular with agents that selectively activate MSK1 and MSK 2, might provide a useful therapeutic option for combating inflammation-induced endothelial dysfunction and atherosclerosis.

Chapter 5

MyD88 Activation in Inflammation Induced Endothelial Dysfunction

Introduction

The previous chapter detailed the onset on endothelial dysfunction *in vivo* in MSK 1/2 KO mice on rodent chow and when challenged with a cholesterol rich diet. MSK 1/ 2 can be are activated downstream of TLRs. TLR activation is complex and is dependent on trans-cytoplasmic signalling. As previously discussed in the *Introduction (Toll-like Receptors)*, MyD88 is a universal adaptor molecule and is used by TLR2/4 to induce pro-inflammatory gene expression. TLR activation is associated with CVD and atherosclerotic lesions (Ananieva *et al*., 2008, Arthur, 2008, Darragh *et al*., 2010, Kawai *et al*., 1999, Mullick *et al*., 2005, Tobias and Curtiss, 2007). Abrogation of TLR signalling by amelioration of MyD88 is atheroprotective (Bjorkbacka *et al*., 2004), however the role of MyD88 in endothelial dysfunction and systemic cytokine expression *in vivo* has not been described.

Aim

To address the role of MyD88 activation in endothelial dysfunction *in vivo* and to better understand how TLR activation is mediated through MyD88 activation and the systemic release of cytokines.

Methods

The methods description below is intended to provide an overview of experimental techniques used in this study. Further experimental details are described in *Materials and Methods Pages 62-92.*

Animals

Animals from the breeding strain MyD88 were randomly allocated into four groups: WT control mice fed normal rodent chow, WT mice on a pro-atherogenic diet and MyD88 KO mice on chow and pro-atherogenic diet.

Body Weight

Animals were weighed at study baseline and at 20 weeks.

Longitudinal Assessment of Vascular Function

In vivo assessment of endothelium-dependent, endothelium-independent and maximal vasodilator capacity were assessed, the following time points were used for vascular function testing: baseline (study week 0), 8 weeks, 12 weeks and 20 weeks as described.

Spleen Mass

Spleen mass was assessed at study end point (20 weeks). Spleen mass has previously been used to assess systemic inflammatory burden (Nanda *et al*., 2011) and enlarged spleens are associated with chronic inflammatory diseases such as SLE. Spleen mass was used to assess systemic inflammatory burden in this and subsequent studies.

Cardiac Hypertrophy

Cardiac hypertrophy was assessed at study end point (20 weeks)

Plasma Cholesterol

LDL/vLDL and HDL measurements were made at 20 weeks only.

Cytokine Expression

Measurements were made at study baseline and 20 weeks.

Results

Baseline Body Weight

MyD88 KO (27±1g) mice were significantly heavier than WT (25±1g) animals at study baseline (P<0.01) (**Figure 5.1**). The mean group difference was 2g.

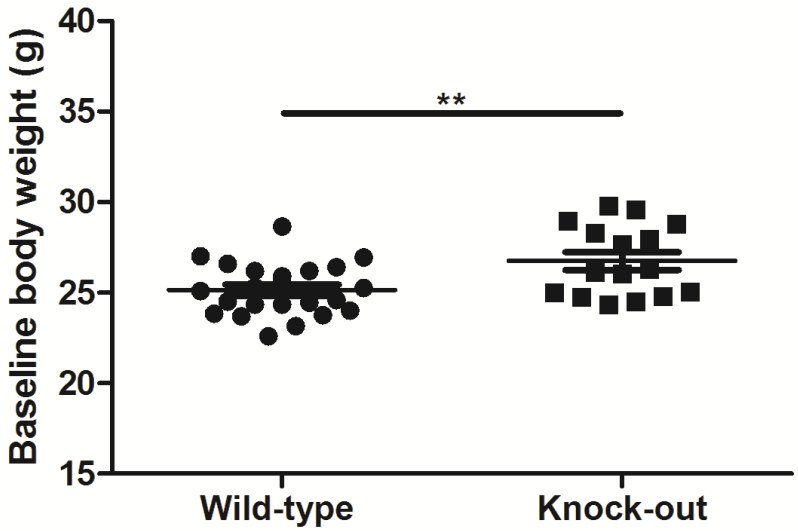

Figure 5.1. Baseline body weight: Baseline body weight in (12 weeks of age) WT (n =23) and MyD88 KO (n =16) animals. Results are group means ±SE in grams (g). Unpaired Student's t-test. ** P<0.01

20 Week Measurement of Body Weight

Animals in all groups significantly increased in body weight over the study duration: WT-chow (baseline 26±1 g VS. week 20 29±1g, P<0.001), WT-cholesterol (baseline 25±1g VS. week 20 30±1g, P<0.001) KO-chow (baseline 27±1g VS. week 20 32±1g, P<0.05) and KO-cholesterol (baseline 26±1g VS. week 20 30±1g, P<0.001).

Week 20 body weights were not significantly different amongst the groups (**Figure 5.2**).

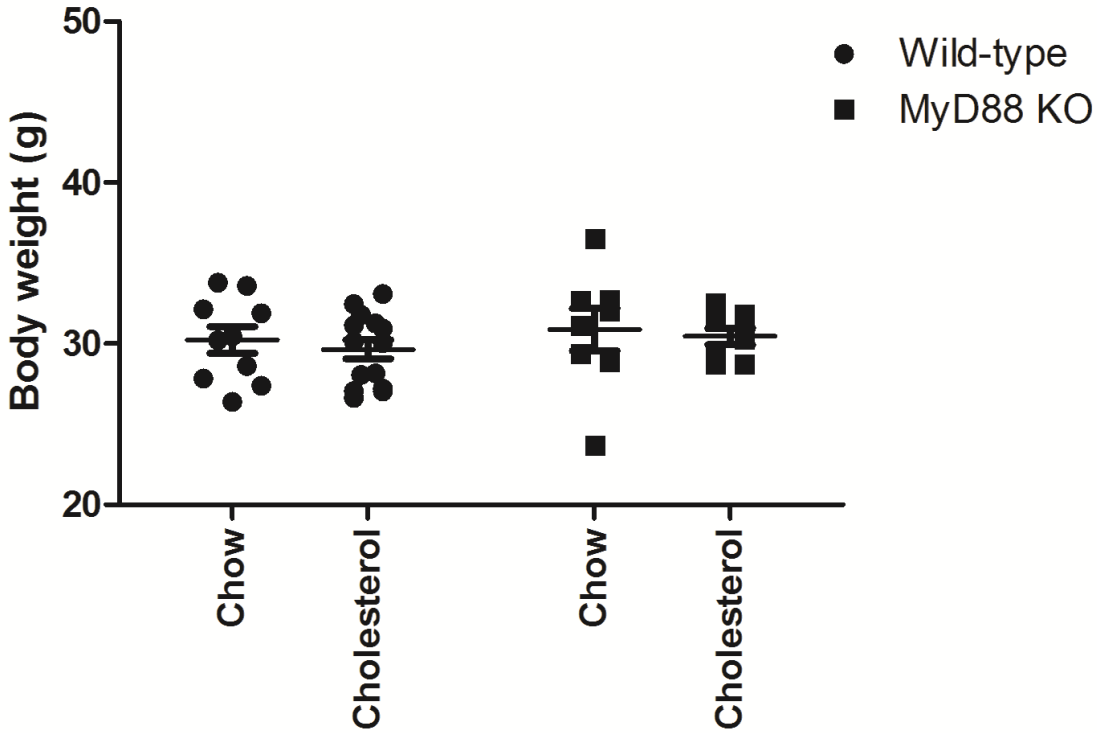

Figure 5.2. Week 20 body weights: Week 20 measurements of body weights in WT-chow (n =10), WT-cholesterol (n =14), MyD88 KO-chow (n =8) and MyD88 KO-cholesterol (n =8) fed animals. Results are group means ±SE in grams (g). Two-way ANOVA.

Baseline Vascular Function

There were no significant differences for baseline vascular responses to endothelium-dependent agonist ACh (WT 334±8 AU VS. KO 327±7 AU, P>0.05) (**Figure 5.3A)** or maximal dilator capacity (WT 453±15 AU VS. 467±13 AU, P>0.05) between WT and MyD88 KO animals (**Figure 5.3B**).

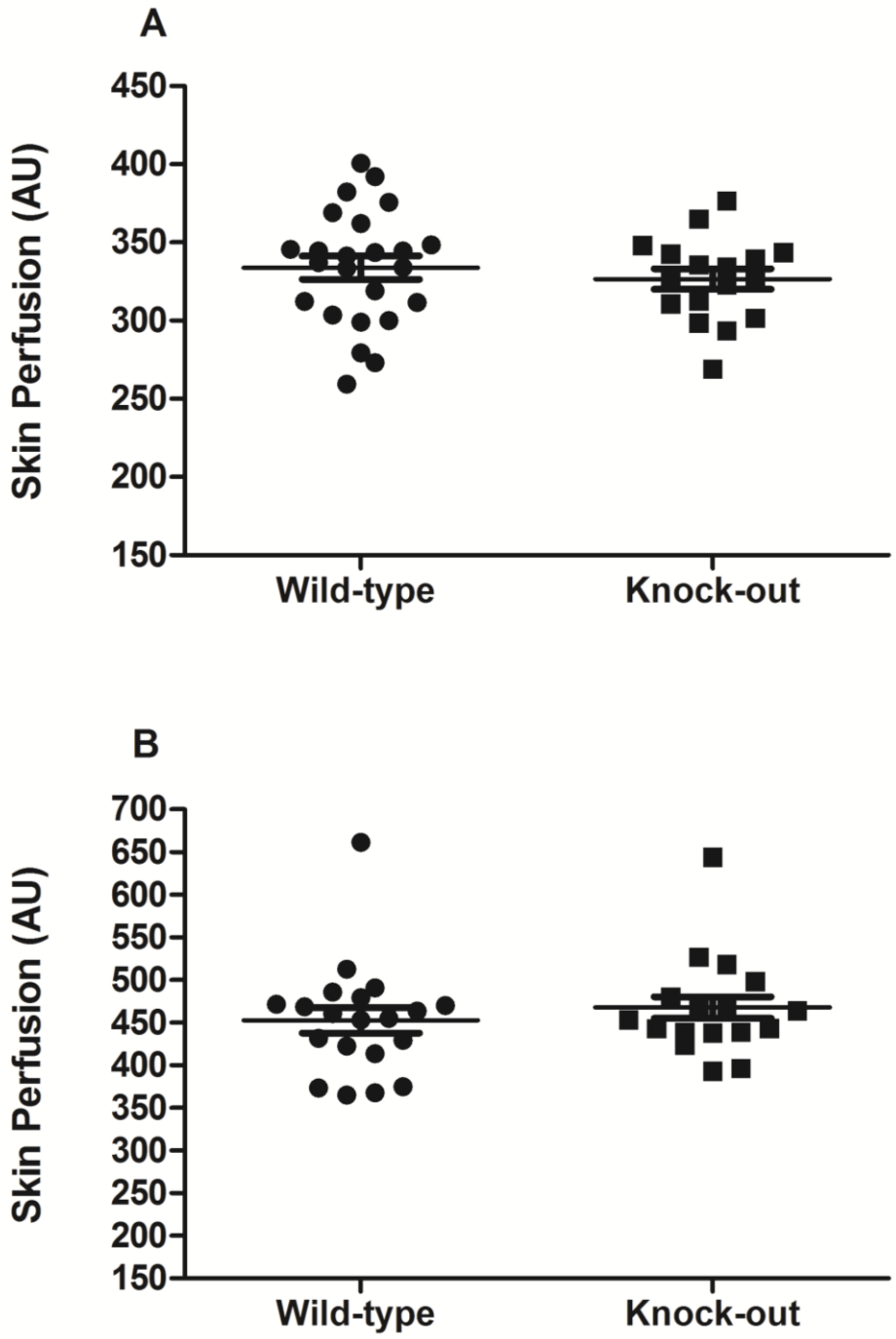

Figure 5.3. Baseline vascular function: Microvascular responses in arbitrary units (AU) at study baseline (week 0) to (A) endothelium-dependent ACh and (B) maximal dilator capacity in WT (n =24), MyD88 KO (n =17) animals. Results are group means ±SE. Unpaired Student's t-test.

Baseline Cytokines

There were no significant differences for baseline inflammatory markers between WT and KO animals: IL-1α, IL-6 and IL-10 (**Figure 5.4A-C respectively**).

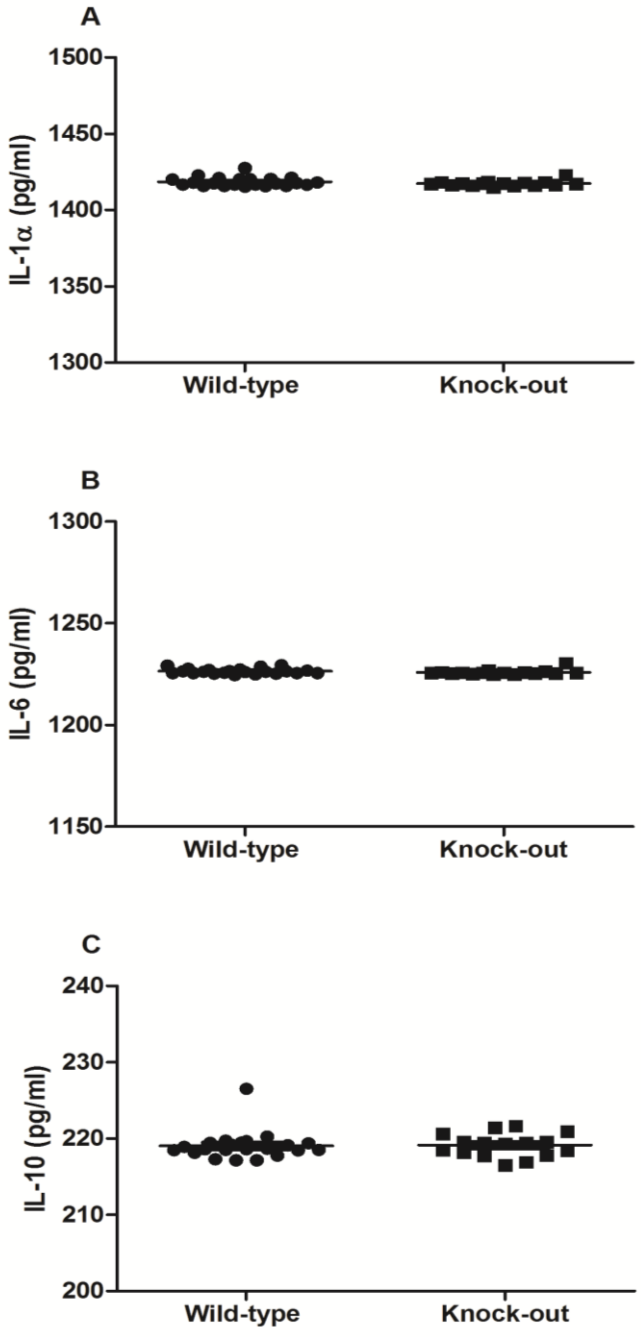

Figure 5.4. Baseline inflammatory markers: Baseline plasma cytokines for (A) IL-1α (B) IL-6, and (C) IL-10 in WT (n =20) and MyD88 KO (n =20) mice (pg/ml). Results are group means ±SE. Unpaired Student's t-test.

Spleen Mass

There were no significant differences between groups for spleen weight (WT-chow 105±28 mg, WT-cholesterol 107±10 mg, KO-chow 124±19 mg and KO cholesterol 161±37 mg) (**Figure 5.5**).

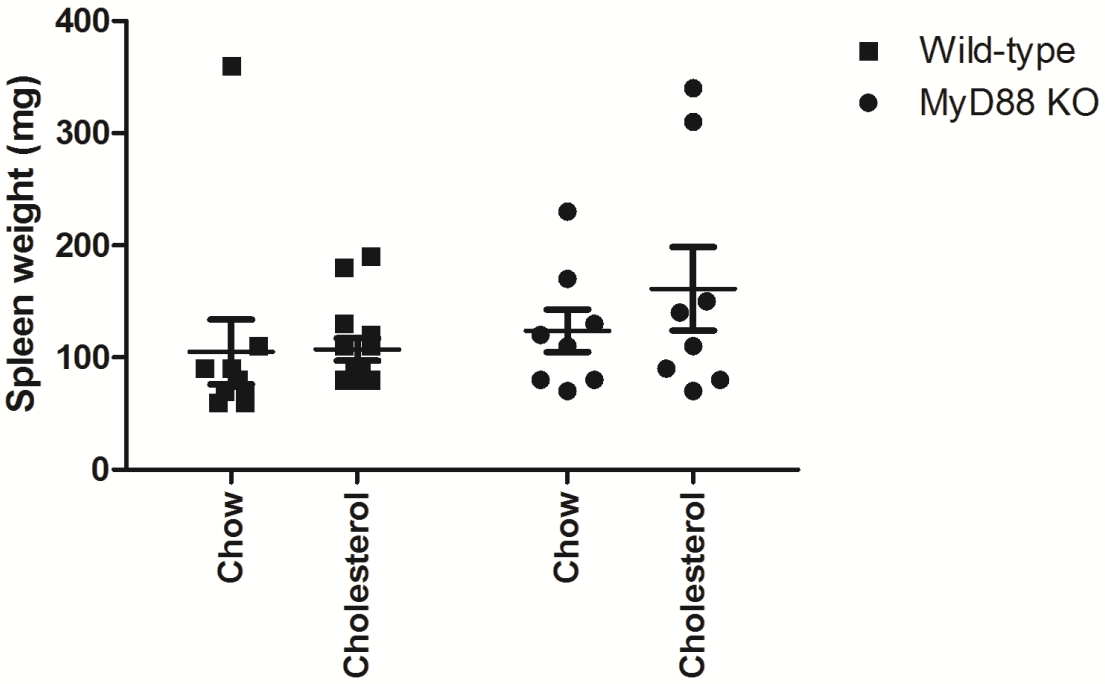

Figure 5.5. Spleen mass: Spleen weight (mg) in WT-chow (n =10), WT-cholesterol (n =14), MyD88 KO-chow (n =8) and MyD88 KO-cholesterol (n =8) fed animals. Results are group means ±SE. Two-way ANOVA.

Cardiac Hypertrophy

Cardiac mass was similar between the groups (WT-chow 160±5 mg, WT-cholesterol 146±3 mg, KO-chow 162±6 mg and KO-cholesterol 150±4 mg) (**Figure 5.6A**).

There were no significant differences amongst the groups for tibia length (WT-chow 18.0±0.2mm, WT-cholesterol 18.0±0.1mm, KO-chow 18.0±0.1mm, KO-cholesterol 18.0±0.4mm) (**Figure 5.6B**).

No significant differences were found for measurements of cardiac hypertrophy amongst the groups (WT-chow 9.0±0.3 ratio, WT-cholesterol 8.0±0.2 ratio, KO-chow 9.0±0.4 ratio, and KO-cholesterol 8.0±0.3 ratio) (**Figure 5.6C**).

Longitudinal Vascular Responses

Endothelium-dependent

There were no significant differences between the groups for ACh mediated vasodilatation at study baseline (week 0) (WT-chow 329±11 AU, WT-cholesterol 337±11 AU, KO-chow 331±12 AU and KO-cholesterol 322±5 AU).

Significant differences were found at study week 8; WT-cholesterol fed mice had significantly poorer microvascular responses to endothelium dependent agonist ACh (292±7 AU) when compared to age matched WT-chow fed (342±6 AU, $P<0.05$) animals. Responses to ACh at study week 8 were greater in MyD88 KO-chow (330±22 AU) and KO-cholesterol fed mice when compared to WT-cholesterol animals, however these observations did not reach statistical significance ($P>0.05$) (**Figure 5.6A**).

WT-cholesterol fed mice had significantly poorer microvascular responses to ACh at study week 12 (275±8 AU) when compared to WT-chow (324±12 AU, $P<0.05$), KO-chow (336±4 AU, $P<0.01$) and KO-cholesterol (331±23, $P<0.05$ AU) fed mice (**Figure 5.6A**).

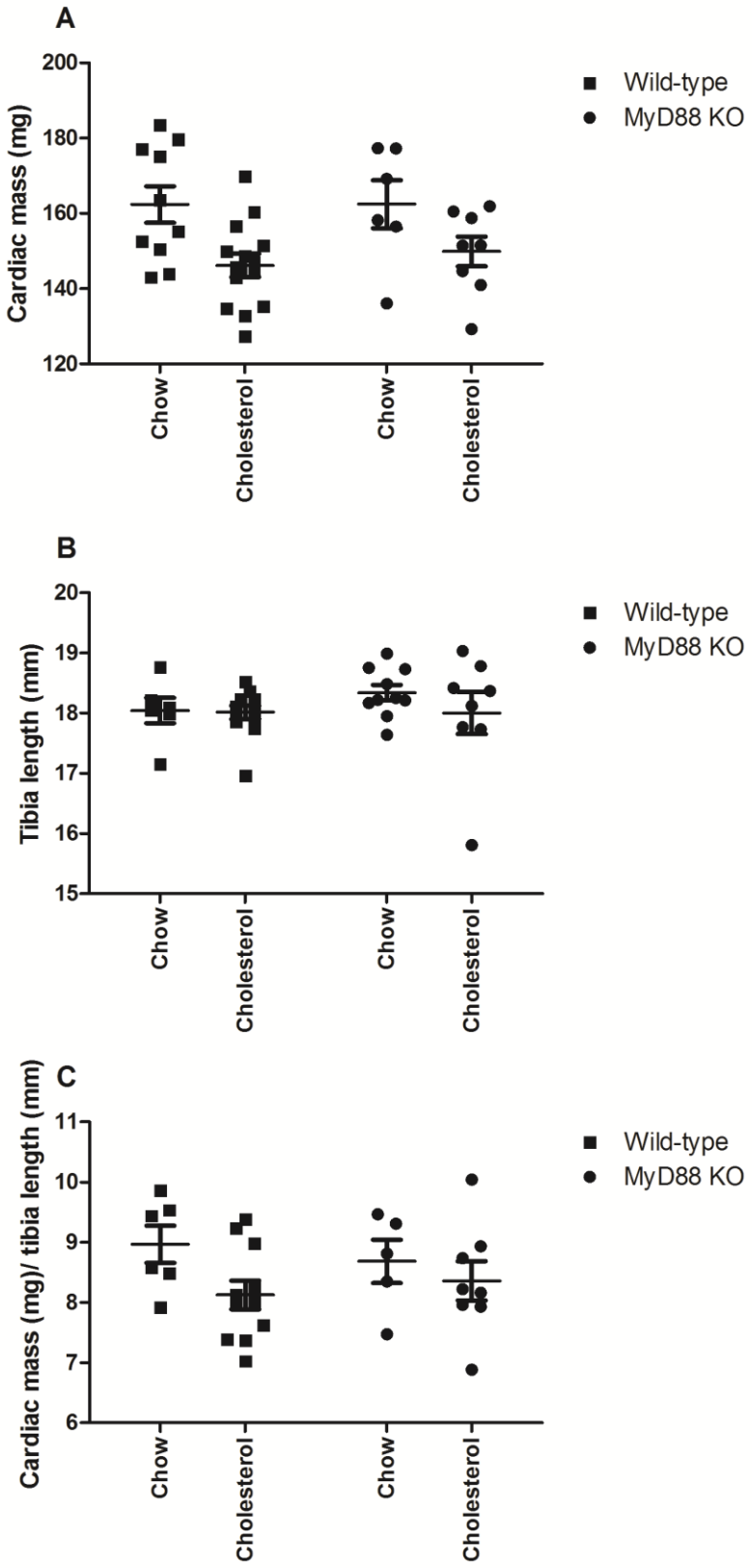

Figure 5.6. Cardiac hypertrophy: Cardiac mass (mg) (A), tibia Length (mm) (B) and cardiac hypertrophy (cardiac mass (mg)/average tibia length (mm)) (C) in WT-chow (n =9), WT-cholesterol (n =11), MyD88 KO-chow (n =6) and MyD88 KO-cholesterol (n =8) fed mice. Results are group means ±SE. Two-way ANOVA.

12 measurements of vascular function remained statistically significant at week 20. WT-cholesterol fed mice had poorer microvascular responses (275±5 AU) when compared to WT-chow (320±7 AU, P<0.001), KO-chow (333±8 AU, P<0.001) and KO-cholesterol fed (336±6 AU, P<0.001) mice (**Figure 5.6A**).

Endothelium-Independent

There were no significant differences in responses to endothelium-independent responses to SNP amongst the groups (WT-chow 351±21 AU), WT-cholesterol (371±22 AU), KO-chow (348±15 AU) and KO-cholesterol (331±9 AU) (**Figure 5.6B**).

Plasma Cholesterol

LDL/vLDL

Cholesterol feeding (14±2 mg/dl) in WT mice significantly increased plasma levels of LDL/vLDL lipoproteins when compared to WT-chow fed animals (3±1 mg/dl) (P<0.01) (Figure A). MyD88 KO-chow (6±1 mg/dl) fed animals had similar LDL/vLDL plasma cholesterol when compared to WT-chow fed animals. MyD88 KO-cholesterol (24±4 mg/dl) fed mice had significantly greater LDL/vLDL plasma lipoproteins when compared to WT-chow (P <0.001), WT-cholesterol (P<0.05) and KO-chow (P<0.001) (**Figure 5.8A**).

HDL

There were no significant differences for week 20 plasma HDL measurements amongst the groups (**Figure 5.8B**) (WT-chow 18±1 mg/dl, WT-cholesterol 15±2 mg/dl, MyD88 KO-chow 15±2 mg/dl and MyD88 KO-cholesterol18±1 mg/dl).

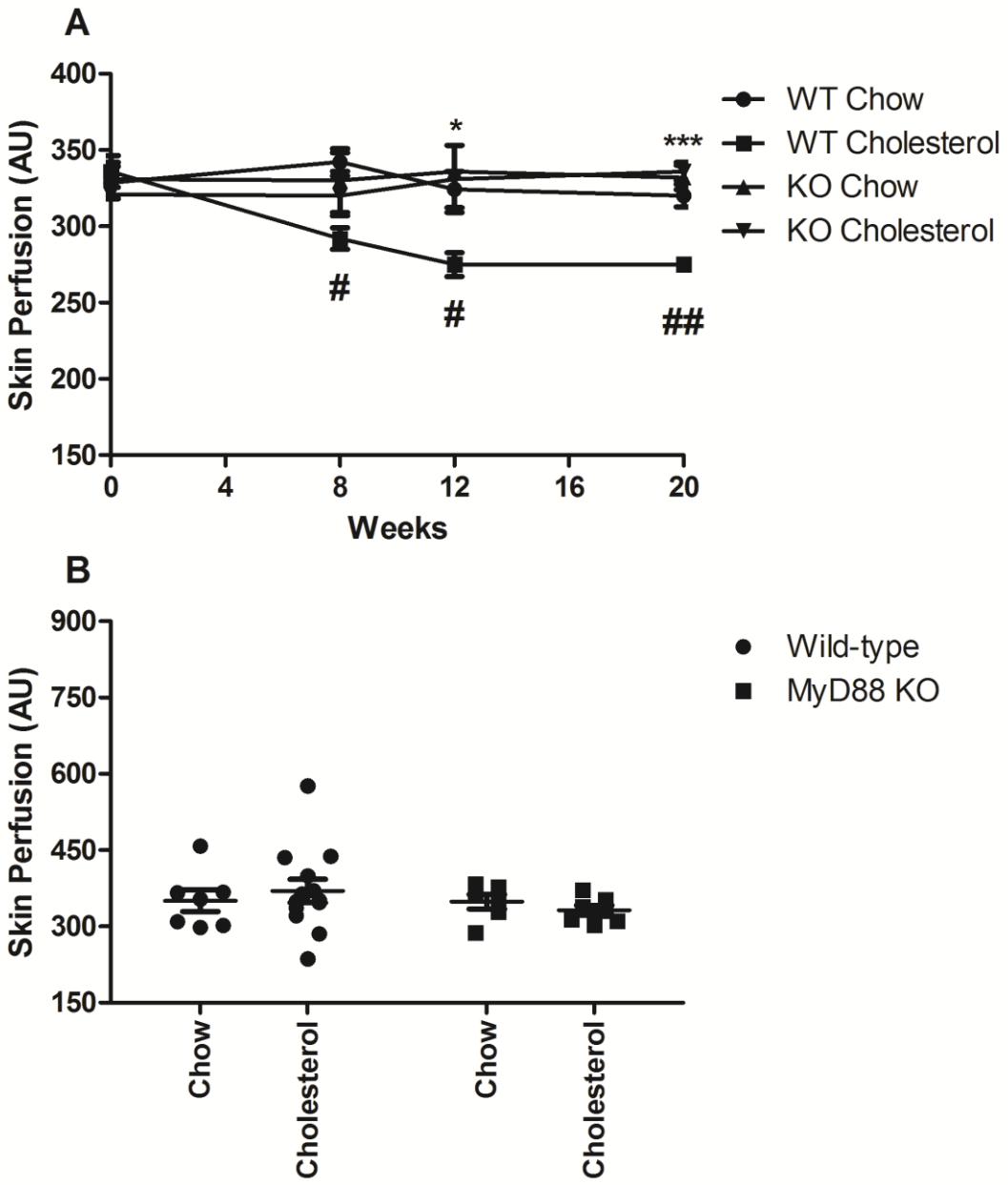

Figure 5.7. Longitudinal microvascular responses: (A) Microvascular responses in arbitrary units (AU) over 20 weeks to (B) endothelium-dependent ACh and (B) week 20 responses to endothelium-independent SNP in WT-chow (n =9), WT-cholesterol (n =15), MyD88 KO-chow (n =9) and MyD88 KO-cholesterol (n =8) fed animals. Results are group means ±SE. Two-way ANOVA.
*P<0.05, ***P<0.001 comparing genotypes
#P<0.05, ##P<0.01 comparing diet.

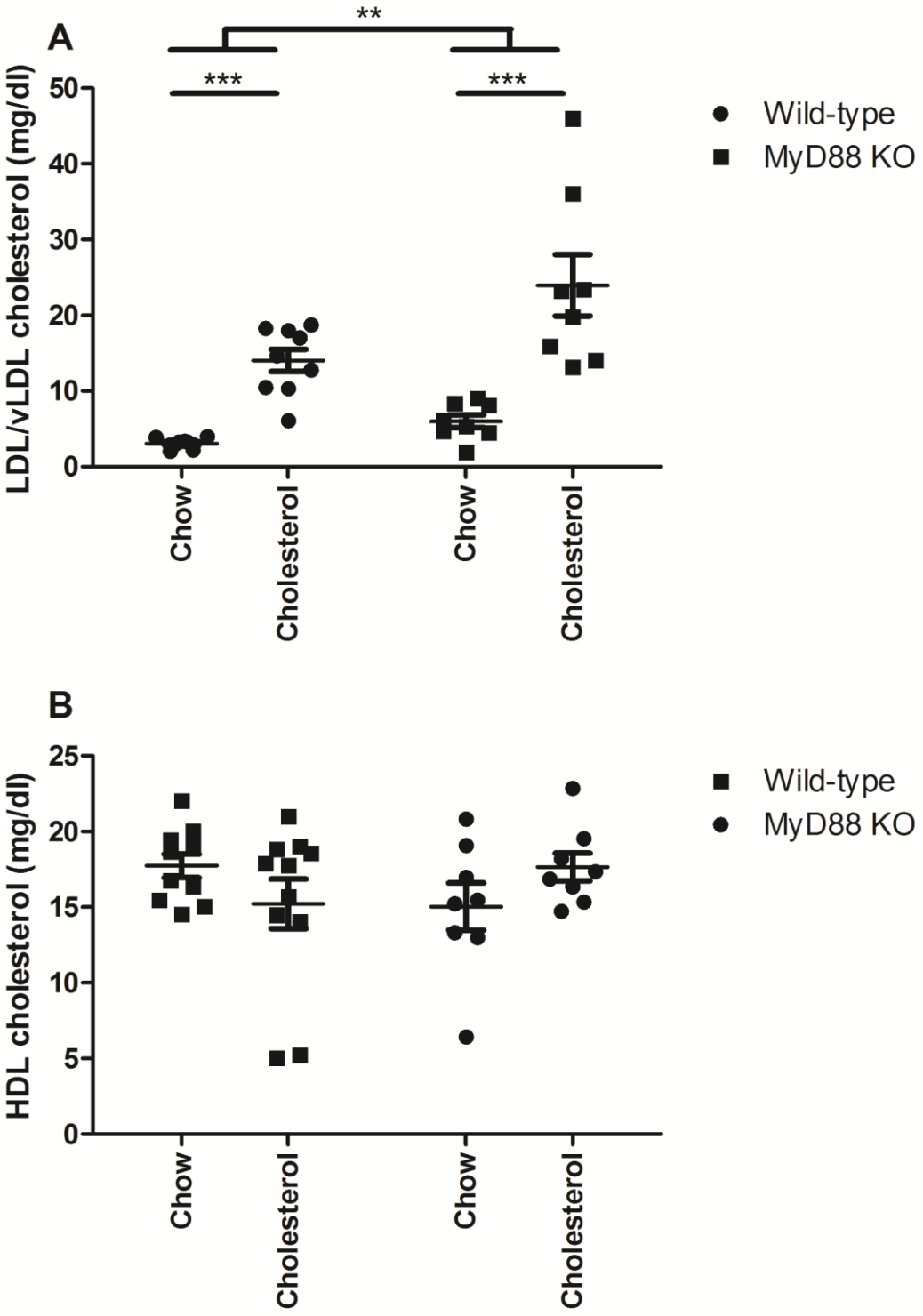

Figure 5.8. Plasma cholesterol: Week 20 measurements of (A) low density lipoproteins and very low density lipoproteins (LDL/vLDL) and high density lipoproteins (HDL) in the plasma of WT-chow (n =10), WT-cholesterol (n =11), MyD88 KO-chow (n =8) and MyD88 KO-cholesterol fed mice (n =8) (mg/dl). Results are group means ±SE. Two-way ANOVA. **P<0.01, ***P<0.001.

20 Week Measurement of Plasma Cytokines

WT-cholesterol fed mice (3042±120 pg/ml) had significantly greater levels of IL-1α at 20 weeks when compared to WT-chow (1524±23 pg/ml, P<0.001), MyD88 KO-chow (1470±22 pg/ml, P<0.001) and MyD88 KO-cholesterol (1505±25 pg/ml, P<0.001) mice (**Figure 5.9A**).

IL-6 at 20 weeks were significantly greater in WT-cholesterol fed mice (3109±120 pg/ml) compared to WT-chow (1374±9 pg/ml, P<0.01), MyD88 KO-chow (1592±187 pg/ml, P<0.01) and MyD88 KO-cholesterol (1425±223 pg/ml, P<0.01) mice (**Figure 5.9B**).

Plasma levels of IL-10 at 20 weeks were not significantly different between WT-chow (212±6 pg/ml) and WT-cholesterol (219±6 pg/ml) fed mice or between MyD88- KO-chow (227±9 pg/ml) and MyD88 KO-cholesterol (249±16 pg/ml) fed mice (**Figure 5.8C**).

Correlations

Microvascular responses to ACh and localised heating at week 0 showed no significant correlations with any of the cytokines markers. In contrast a negative association was found for ACh and plasma levels of IL-1α (r= -0.826, P<0.001) and IL-6 (r= -0.804, P<0.001) at 20 weeks.

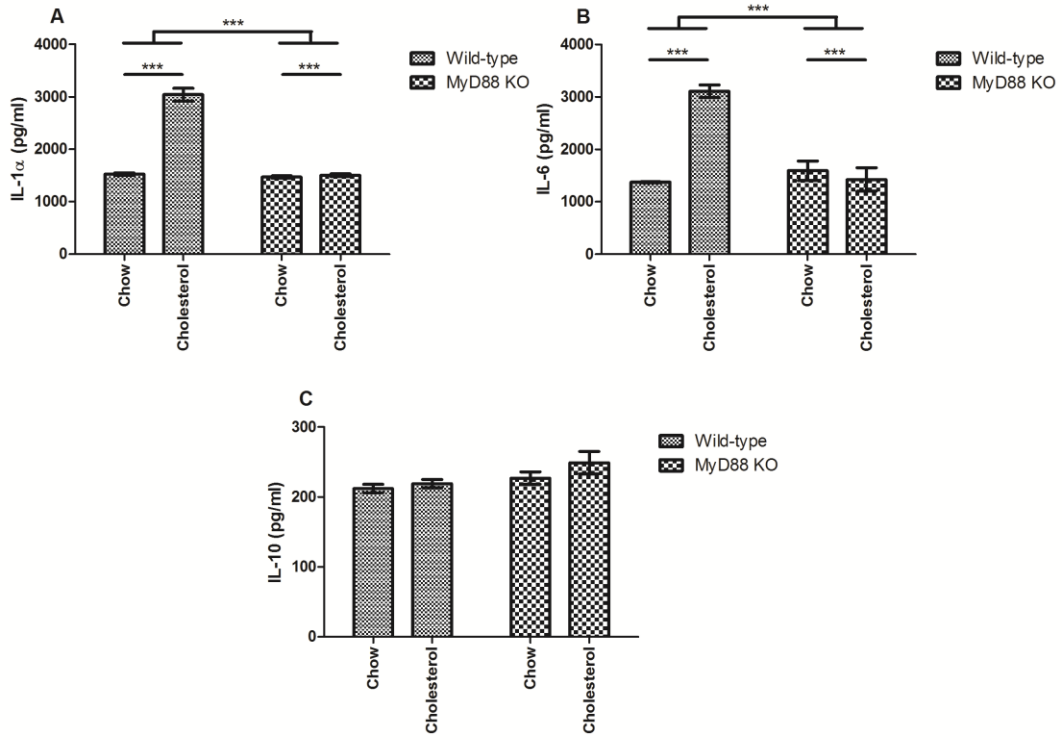

Figure 5.8. Week 20 measurements of inflammatory markers: Plasma cytokines (pg/ml) (A) IL-1α, (B) IL-6 and (C) IL-10 WT-chow (n =10), WT-cholesterol (n =10), MyD88 KO-chow (n =10) and MyD88 KO-cholesterol fed (n =10) mice. Results are group means ±SE. Two-way ANOVA. ***P<0.001.

Discussion

The main findings from this study show that MyD88 KO mice fed a cholesterol diet maintain endothelium-dependent vasodilatation *in vivo* over 20 weeks, unlike WT-cholesterol fed mice. Cholesterol feeding in WT mice reduces NO, as evidenced in the previous chapter. Generalised vascular function testing by the iontophoresis of endothelium-independent vasodilator SNP was not significantly different amongst the groups, suggesting that the elevation in inflammatory markers observed in WT-cholesterol fed mice was significantly affecting the endothelium. These data suggest that there is a potential functional role for MyD88 in the development and progression of CVD, an interaction that is potentially mediated by MyD88, cholesterol, cytokine synthesis and the endothelium.

Despite this apparent protection against CVD MyD88 KO-cholesterol fed mice displayed significantly greater levels of LDL/vLDL in plasma, when compared to WT-cholesterol fed animals. Hosoi *et al* (2010) has previously reported a similar dyslipidaemia profile in MyD88 KO mice in the context of diabetes. MyD88 KO high fat diet (HFD) fed mice display significantly higher plasma cholesterol than WT animals on the same diet, (Hosoi *et al*., 2010), a phenotype that is not dependent on body weight, visceral fat, locomotion or food intake. In the same study Hosoi *et al* also showed up regulation of LDLr in the liver of MyD88 deficient mice when compared to WT controls on the same diet, suggesting a positive feedback mechanism, a potential autocrine attempt to clear lipids from the blood stream. The increased plasma levels of circulating lipid in MyD88 HFD fed mice are thought to be mediated by an increase in expression of HMG-CoA reductase, an enzyme that is rate limiting in the biosynthesis of cholesterol and targeting this pathway with statins has shown favourable results in human trials (Davignon, 2004) by reducing plasma cholesterol. In contrast Bjorkbacka *et al* (2004) (Bjorkbacka *et al*., 2004) has previously reported a modest elevation in plasma cholesterol that was not significantly different in MyD88/ApoE deficient mice. However in agreement with Bjorkbacka *et al*, the elevation observed by double KO ApoE/MyD88 mice was due to elevated LDL and not HDL (Bjorkbacka *et al*., 2004).

Previous studies have established the rate limiting step of MyD88 in atherosclerosis. This is in part mediated by reduced MCP-1 expression, an important chemoattractant protein in monocyte recruitment and a significant (53%) reduction in the MCP-1 receptor, CCR2. Previous studies have sought to establish the role of MCP-1 in monocyte infiltration into the aortic sinus and peritoneal cavity, deficiency of MyD88 produced an 80% and 45% reduction in

infiltration F4/80 positive cells respectively, showing that MyD88 activation is needed for monocyte recruitment.

MCP-1 can be synthesised by endothelial cells and is dependent on MyD88 (Yu *et al*., 2014). Thus deficiency of MyD88 in this study may have preserved vascular function through reduced recruitment of monocytes into the vessel wall, an established early event in plaque formation. In support of this it has previously been shown that MyD88 is not an essential mediator of foam cell formation, through no significant differences in uptake and degradation of oxLDL in MyD88 deficient cells when compared to controls (Bjorkbacka et al., 2004, Park *et al*., 2012).

MyD88 KO-cholesterol fed mice also displayed reduced plasma levels of IL-6 unlike WT-cholesterol fed mice in the present study. The role of IL-6 in endothelial dysfunction has previously been described (Barnes *et al*., Barnes *et al*., Esteve *et al*., 2007, Esteve *et al*., 2006, Fernandez-Real *et al*., 2000, Hashizume and Mihara, Huber *et al*., 1999, Hung *et al*., Mihara *et al*., Naya *et al*., 2007). Hung *et al* (2010) reported IL-6 can specifically inhibit the release of NO, by increasing the effects of calveolin-1. Increased caveolin-1 reduces eNOS activity by attenuating the eNOS activation pathway, though reduced phosphorylation at Ser1177, an established phosphorylation site implicated in endothelial dysfunction (Matsumoto *et al*., 2014).

MyD88 KO-cholesterol fed mice displayed reduced levels of IL-1α when compared to WT-cholesterol fed mice. IL-1α has been implicated in early atherosclerotic plaque formation through modulation of cell adhesion molecules. Damaged endothelial cells can release IL-1α and enhance VSMC proliferation. Conversely IL-1ra has shown favourable results by limiting plaque formation

and reducing plasma lipids in mouse models and reduced restenosis in humans after angiography (Chi *et al*., 2004, Francis *et al*., 2001, Isoda and Ohsuzu, 2006, Isoda *et al*., 2004, Isoda *et al*., 2003).

The release of inflammatory cytokines into the vessel wall after recruitment of myeloid cells has shown to perpetuate vascular inflammation and atherosclerotic plaque formation. MyD88 deficiency has previously shown protection in a model of myocardial reperfusion injury in mice. Feng *et al* (2008) (Feng *et al*., 2008b) studied the effects of MyD88 *in vivo* and *ex vivo* using a model of myocardial injury. The detrimental effects of MyD88 activation are dependent on blood components such as the presence of myeloid cells, a response that can be prevented by using an *ex vivo* system that is devoid of circulating white blood cells. These observations are consistent with the role of TLR4 in the pathogenesis of CVD (Riad *et al*., 2008a, Riad *et al*., 2008b, Riad *et al*., 2012, Tobias and Curtiss, 2007). TLR4 KO mice have shown improved left ventricle function after MI, through reduced left ventricle remodelling, and for this reason TLR4 inactivation is thought to be a promising future therapeutic tool (Riad *et al*., 2008b).

Yu *et al* (2014) (Yu *et al*., 2014) studied endothelial cell (EC) specific MyD88 KO and myeloid cell (MC) specific deficient mice and showed protection against diet induced insulin resistance. EC specific KO mice only showed partial protection against insulin resistance in adipose tissue when compared to MC-MyD88 KO mice. Unlike the present study these authors report no significant difference in plasma cholesterol of endothelial cell specific and MC-MyD88 KO mice. However the findings from Yu *et al* are consistent with Bjorkbacka *et al.* Both studies used the ApoE KO CVD-prone model for their experiments and the

altered lipid effect may be dependent on the ApoE KO mouse, unlike the observations in the present study.

EC and MC-MyD88 deficiency protected against atherosclerotic lesion formation on a chow diet in the study by Yu *et al*, with respective reductions in the expression of TNFα, IL-6 and IL-1 compared with littermate controls, findings that are consistent with the present study. MC-MyD88 deficient mice show greater protection to pro-inflammatory responses when compared to EC-MyD88 KO mice, this phenotype is potentially mediated through the differences in cells response to stimuli. MC are more susceptible to the production of inflammatory markers due to their role in phagocytosis and immunity, suggesting that MC are more central to the onset of systemic chronic inflammation as observed in WT-cholesterol fed mice in this study and subsequently more prone to endothelial dysfunction. OxLDL can activate TLR signalling and leads to the recruitment of MyD88, to initiate downstream signalling such as the activation of NF-kB and MAPK p38 to induce the production of pro-inflammatory cytokines associated with atherosclerosis. Yu *et al* reported MyD88 dependent signalling in EC, dependently releases granulocyte macrophage –stimulating factor (GM-CSF), which can induce pro-inflammatory polarisation of macrophages in the arterial wall, a phenomenon associated with atherosclerotic plaque formation. However, MyD88 deficiency in the present study preserved endothelial function in the presence of dietary cholesterol a known cardiovascular risk factor, potentially through a similar pathway (reduced cell recruitment). TLR downstream signalling is otherwise associated with the expression of pro inflammatory genes and atherosclerosis, the present study shows protection against endothelial dysfunction when this signalling pathway is blocked.

In conclusion, MyD88 plays a critical role in the development of endothelial dysfunction through the activation of innate inflammatory pathways. Targeting TLRs in particular MyD88 with agents that block its effects could provide a novel tool for combating inflammation-induced endothelial dysfunction, systemic cytokine expression and early CVD.

Chapter 6

Mitogen Activated Proteins Kinases Activated-protein 2/3 in Endothelial Dysfunction

Introduction

The previous chapter detailed protection against endothelial dysfunction in MyD88 KO mice fed dietary cholesterol, potentially through abrogation of trans cytoplasmic signalling. Other novel downstream protein kinase targets have been described to sequester inflammation. As previously described in the *Introduction (Mitogen Activated Protein Kinases Activated-protein)* the MAPKAP 2/3 are substrates of the stress activated MAPK p38. *In vitro* cell based assay studies have shown that these kinases are important in inflammatory gene expression, through regulation of cytokines including IL-6.

MAPKAP 2/3 induce prolonged expression of inflammatory cytokines by modulating the stability of mRNA. This is achieved through targeting of the 3'untranslated region of mRNA of cytokines such as IL-6 through phosphorylation of RNA stability regulators. MAPKAP 2/3 deficient mice have been previously described and do not show a discernible phenotype unlike the upstream target p38, that is embryonically lethal. Importantly MAPKAP 2/3 are potential targets for future therapy. *In vivo* models of inflammation such as the LPS induced septic shock model, the collagen-induced RA model and a neuroinflammation model of Parkinson's disease have conferred protection from the onset of pathophysiology in MAPKAP deficient mice (Hegen *et al*., 2006, Kotlyarov *et al*., 1999, Thomas *et al*., 2008). The role of this pathway in the development of endothelial dysfunction and systemic cytokine expression has not been described.

Aim

To explore the role of MAPKAP 2/3 activation in the release of systemic cytokine expression and endothelial function *in vivo*.

Methods

The methods description below is intended to provide an overview of experimental techniques used in this study. Further experimental details are described in *Materials and Methods Pages 62-92.*

Animals

Animals from the breeding strain MAPKAP 2/3 were randomly allocated into four groups: WT control mice fed normal rodent chow, WT mice on a pro-atherogenic diet and MAPKAP 2/3 KO mice on chow and pro-atherogenic diet.

Body Weight

Animals were weighed at study baseline and 20 weeks.

Longitudinal Assessment of Vascular Function

In vivo assessment of endothelium-dependent, endothelium-independent and maximal vasodilator capacity were assessed, the following time points were used for vascular function testing: baseline (study week 0), 8 weeks, 12 weeks and 20 weeks as described.

Spleen Mass

Spleen mass was assessed at study end point (20 weeks).

Cardiac Hypertrophy

Cardiac hypertrophy was assessed at study end point (20 weeks)

Plasma Cholesterol

LDL/vLDL and HDL measurements were made at 20 weeks only.

Cytokine Expression

Measurements were made at study baseline and 20 weeks.

Results

Baseline Body Weight

WT (27±1g) animals were significantly heavier than KO mice at study baseline (23±1g) (12 weeks of age) (P<0.001) (**Figure 6.1**). The mean group difference was 4g.

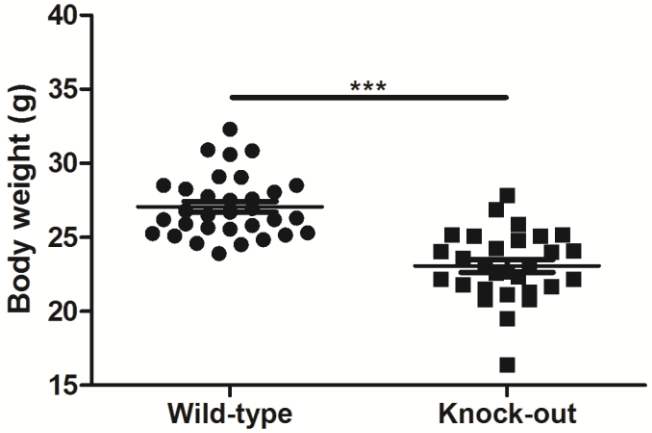

Figure 6.1. Baseline body weight: Baseline body weight in (12 weeks of age) WT (n =32) and MAPKAP 2/3 KO (n =29) mice. Results are group means ±SE in grams (g). Unpaired Student's t-test. *** P<0.001

20 Week Measurement of Body Weight

WT-chow (20 week weight 27±.1g, P<0.01), WT-cholesterol (20 week weight 31±1g, P<0.001) and KO-cholesterol (20 week weight 26±1, P<0.001) fed mice significantly increased in body weight over the study duration. KO-chow (20 week weight 25±1g) fed animals did not significantly increase in body weight over the study duration (P>0.05). Body weights between KO-chow and KO-cholesterol were not significantly different.

WT- cholesterol fed animals were significantly heavier than WT-chow (P<0.01), KO-chow (P<0.001) and KO-cholesterol fed animals (P<0.001) (**Figure 6.2**)

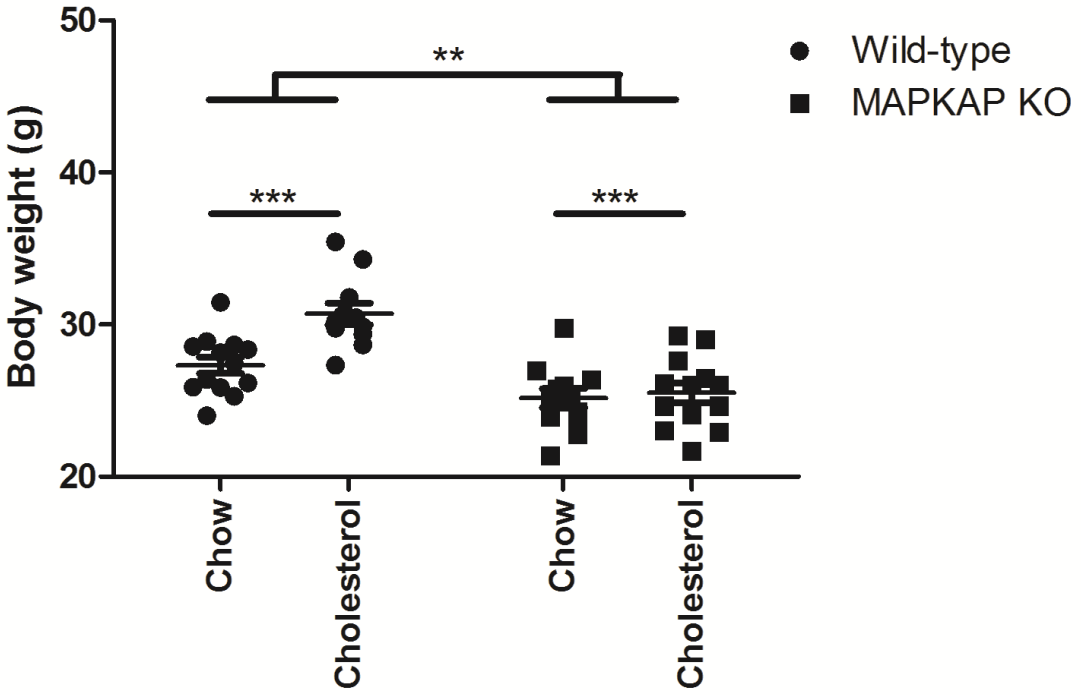

Figure 6.2. Week 20 measurements of body weights: WT-chow (n =13), WT-cholesterol (n =11), MAPKAP 2/3 KO-chow (n =12) and MAPKAP 2/3 KO-cholesterol (n =13) fed animals body weights at 20 weeks. Results are group means ±SE. Grams (g). Two-way ANOVA. **P<0.01, *** P<0.001

Spleen Mass

There were no significant differences for spleen mass amongst the groups (WT-chow 120±10 mg, WT-cholesterol 110±8 mg, MAPKAP 2/3 KO-chow 149±49 mg and MAPKAP 2/3 KO-cholesterol 133±19 mg (**Figure 6.3**).

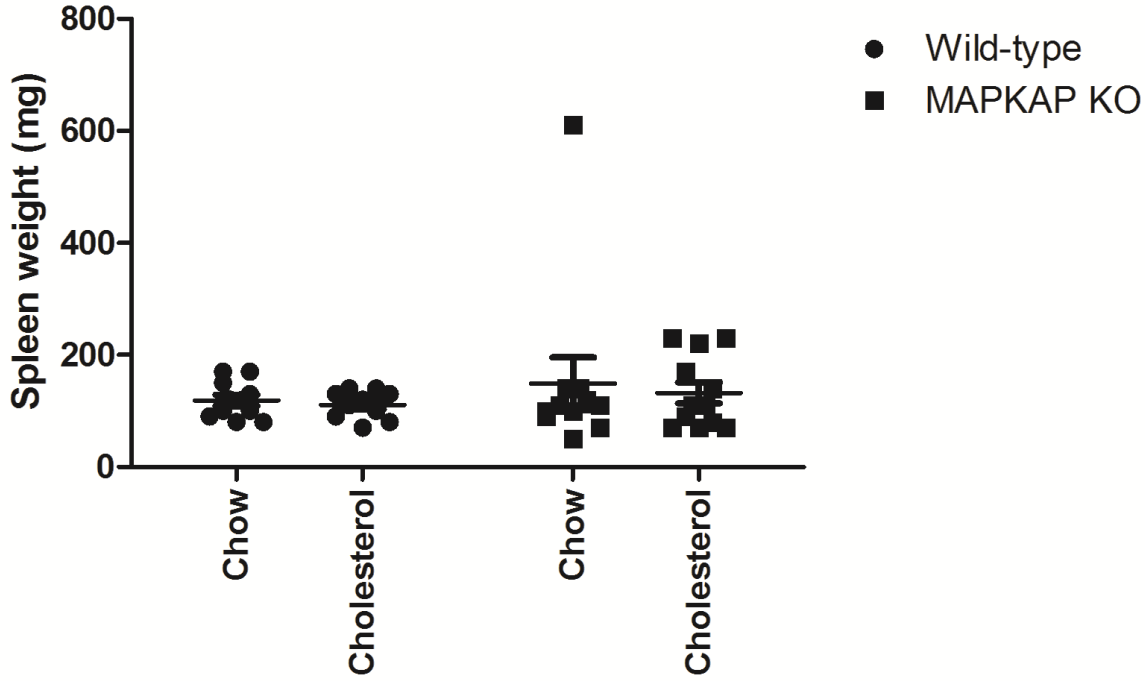

Figure 6.3. Spleen mass: Spleen weight (mg) in WT-chow (n =11), WT-cholesterol (n =10), MAPKAP 2/3 KO-chow (n =11) and MAPKAP 2/3 KO-cholesterol fed (n =12) animals. Results are group means ±SE. Two-way ANOVA.

Baseline Vascular Function

There were no significant differences for vascular function at study baseline between WT and KO mice for endothelium-dependent vasodilatation to iontophoresis of ACh (WT 333±7 AU VS. KO 331±7 AU, P>0.05) (**Figure 6.4A**) or maximal vasodilator dilator capacity to localised skin heating (WT 438±9 AU VS. KO 420±10 AU, P>0.05) (**Figure 6.4B**).

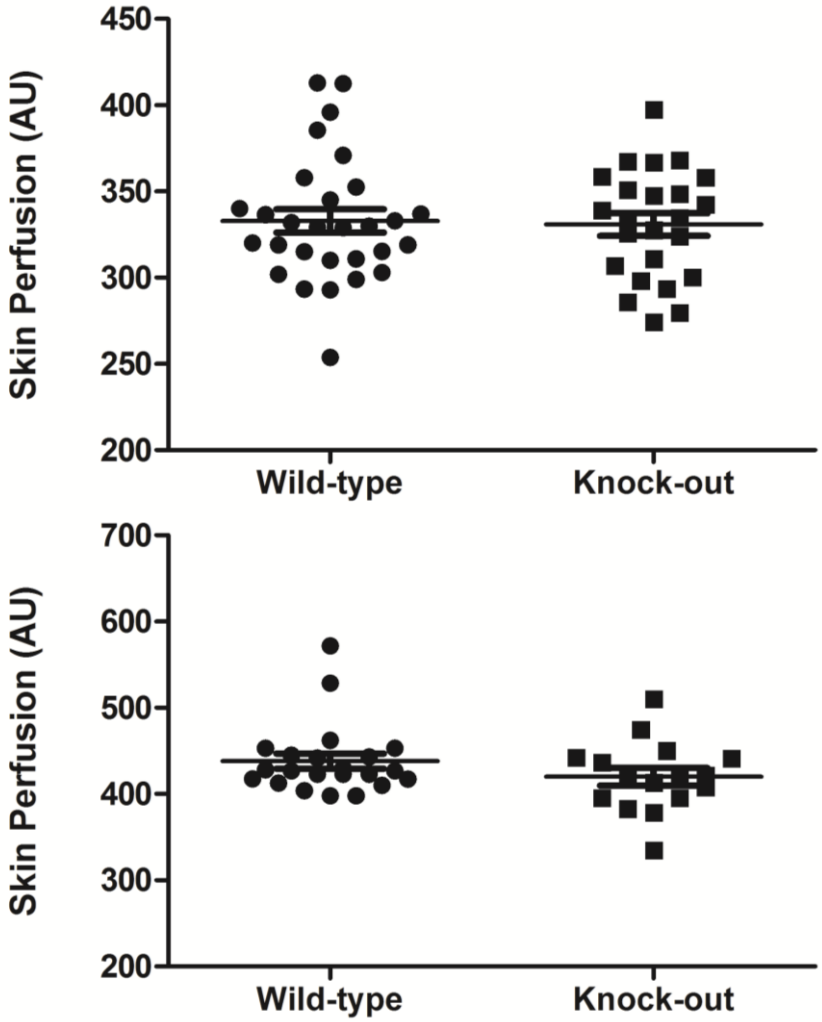

Figure 6.4. Baseline vascular function: Microvascular responses in arbitrary units (AU) at study baseline (week 0) to (A) endothelium-dependent ACh and (B) maximal dilator capacity in WT (n =24) and MAPKAP 2/3 KO (n =17) animals. Results are group means ±SE. Unpaired Student's t-test.

Plasma Cholesterol

LDL/vLDL

WT-cholesterol (10±1 mg/dl) and KO-cholesterol fed (10±1 mg/dl) mice had significantly greater LDL/vLDL in terminal measurements of plasma when compared to WT-chow fed mice (5±1 mg/dl) ($P<0.001$, $P<0.01$ respectively) (**Figure 6.5A**). KO-chow (5±1 mg/dl) fed animals had similar levels of LDL/vLDL in measurements of plasma when compared to WT-chow fed mice. KO-chow fed animals had statistically lower LDL/vLDL than KO-cholesterol ($P<0.001$) animal (**Figure 6.5A**).

HDL

There were no significant differences between the groups for measurements of HDL (WT-chow 19±1 mg/dl, WT-cholesterol 16±2 mg/dl, KO-chow 14±3 mg/dl and KO-cholesterol 17±2 mg/dl) (**Figure 6.5B**).

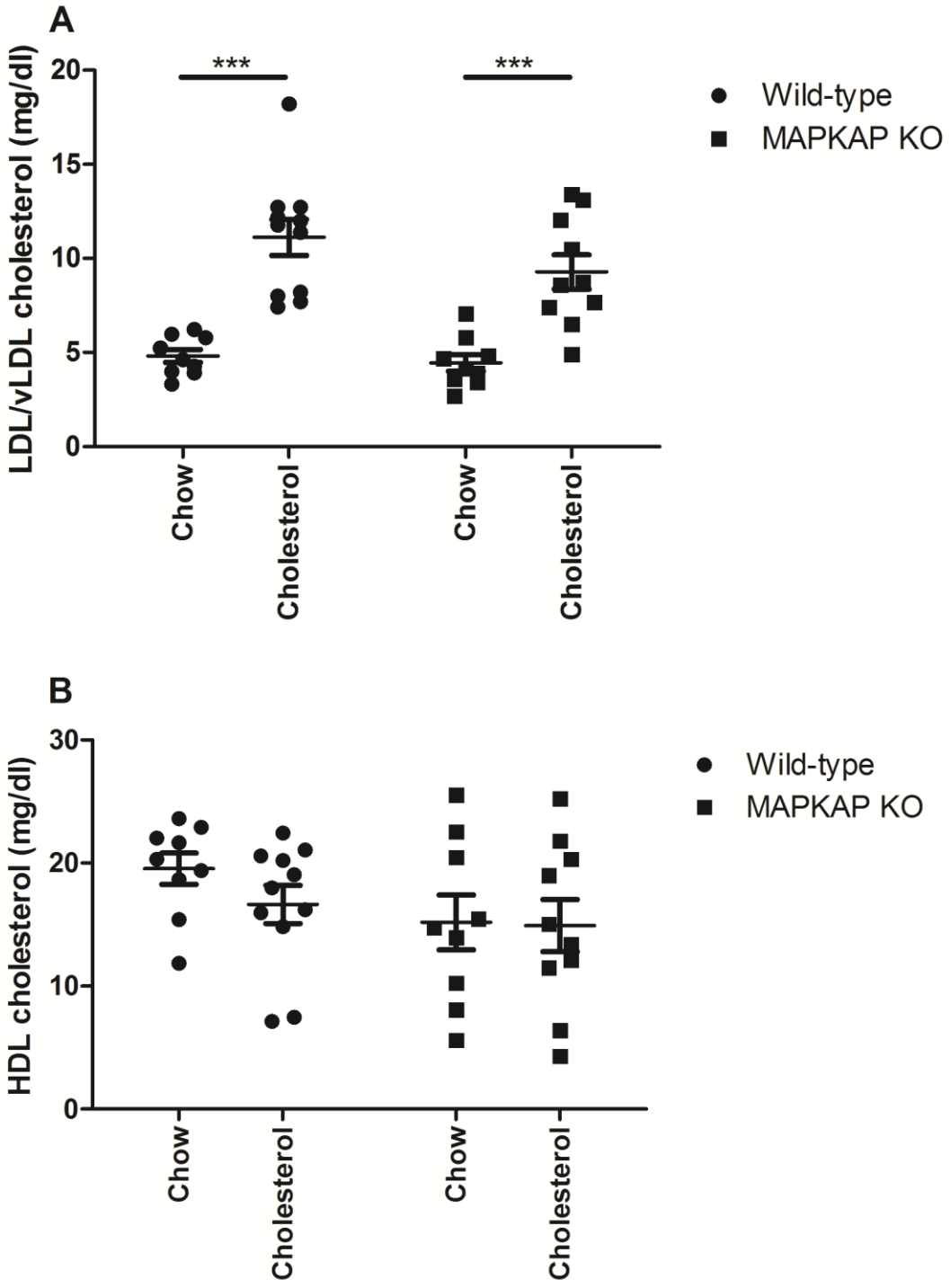

Figure 6.5. Plasma cholesterol: 20 week measurements of (A) low density lipoproteins and very low density lipoproteins (LDL/vLDL) and (B) High density lipoproteins (HDL) in the plasma of WT-chow (n =10), WT-cholesterol (n =9), MAPKAP KO-chow (n =9) and MAPKAP KO-cholesterol fed mice (n =10) (mg/dl). Results are group means ±SE. Two-way ANOVA. ***P<0.001.

Cardiac Hypertrophy

Cardiac mass was not significantly greater in WT-cholesterol fed mice (171±9 mg) when compared to WT-chow (151±4 mg) (**Figure 6.6A**). There were no significant differences between WT-chow and WT-cholesterol for tibia length (WT-chow 18.0±0.1 mm, WT-cholesterol 18.0±0.1 mm) ($P>0.05$) (**Figure 6.6B**). WT-cholesterol (9.0±0.4 ratio) fed mice had a significantly greater cardiovascular hypertrophy measurement compared to WT-chow fed mice (8.0±0.8 ratio) ($P<0.05$) (**Figure 6.6C**).

KO-chow fed animals had similar measurements of cardiac mass (149±4 mg) and cardiovascular hypertrophy (9.0±0.3 ratio) when compared to WT-chow fed animals (**Figure 6.6A/C**). KO-cholesterol fed mice had significantly lighter hearts (144±4mg) when compared to WT-cholesterol fed mice (171±9 mg) ($P<0.01$) but not a significantly lower cardiovascular hypertrophy measurement (KO-cholesterol 9.0±0.2 ratio) (**Figure 6.6C**). KO animals in both groups (KO-chow 17.0±0.2 mm and KO-cholesterol 16.0±1.0 mm) had significantly shorter tibias when compared to WT animals (WT-chow 18.0±0.1 mm and WT-cholesterol 18.0±0.1 mm) (**Figure 6.6B**).

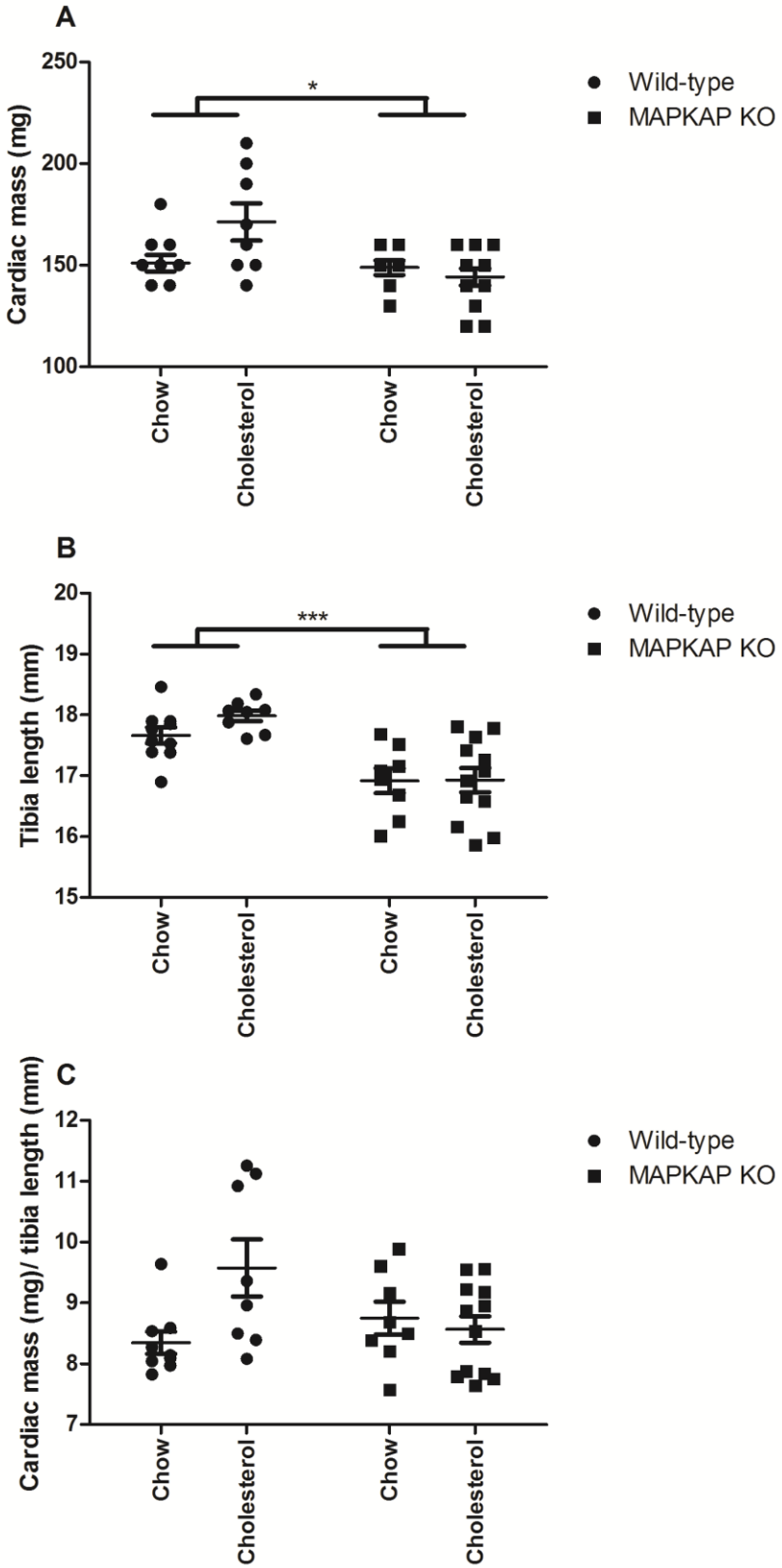

Figure 6.6. Cardiac hypertrophy: Cardiac mass (mg) (A), tibia Length (mm) (B) and cardiovascular hypertrophy (cardiac mass (mg)/average tibia length (mm)) (C) in WT-chow (n =10), WT-cholesterol (n =10), KO-chow (n =10) and KO-cholesterol (n =13) fed mice. Results are group means ±SE. Two-way ANOVA. *P<0.05, ***P<0.001.

Longitudinal Vascular Responses

Endothelium-dependent

There were no significant differences between the groups at study baseline for endothelium-dependent responses (WT-chow 332±7 AU, WT-cholesterol 334±13 AU, MAPKAP KO-chow 328±12 AU and MAPKAP KO-cholesterol 333±5 AU) (**Figure 6.7A**). MAPKAP KO-chow (331±15 AU) and MAPKAP KO-cholesterol (330±10 AU) fed mice had similar responses to WT-chow (339±8 AU) at study week 8. WT-cholesterol fed animals had significantly poorer responses to ACh at study week 8 when compared to WT-chow fed animals ($P<0.05$) (**Figure 6.7A**).

WT-cholesterol fed mice continued to have poorer microvascular responses to ACh at study week 12 when compared to WT-chow ($P<0.05$), KO-chow and KO-cholesterol fed animals, but these observations did not meet statistical significance ($P>0.05$) (**Figure 6.7A**). Week 20 measurements to ACh were significantly better in WT-chow and KO-chow fed mice when compared to WT-cholesterol fed mice ($P<0.01$, $P<0.05$ respectively). KO-cholesterol fed animals had greater endothelium-dependent vasodilation at 20 week measurements when compared to WT-cholesterol fed mice; however these observations did not meet statistical significance ($P>0.05$) (**Figure 6.7A**).

Endothelium-independent

There were no significant differences between vascular responses to endothelium-independent vasodilator SNP amongst the groups (WT-chow

354±20 AU, WT-cholesterol 334±10 AU, KO-chow 334±9 AU and KO-cholesterol 337±15 AU) ((**Figure 6.7B**)

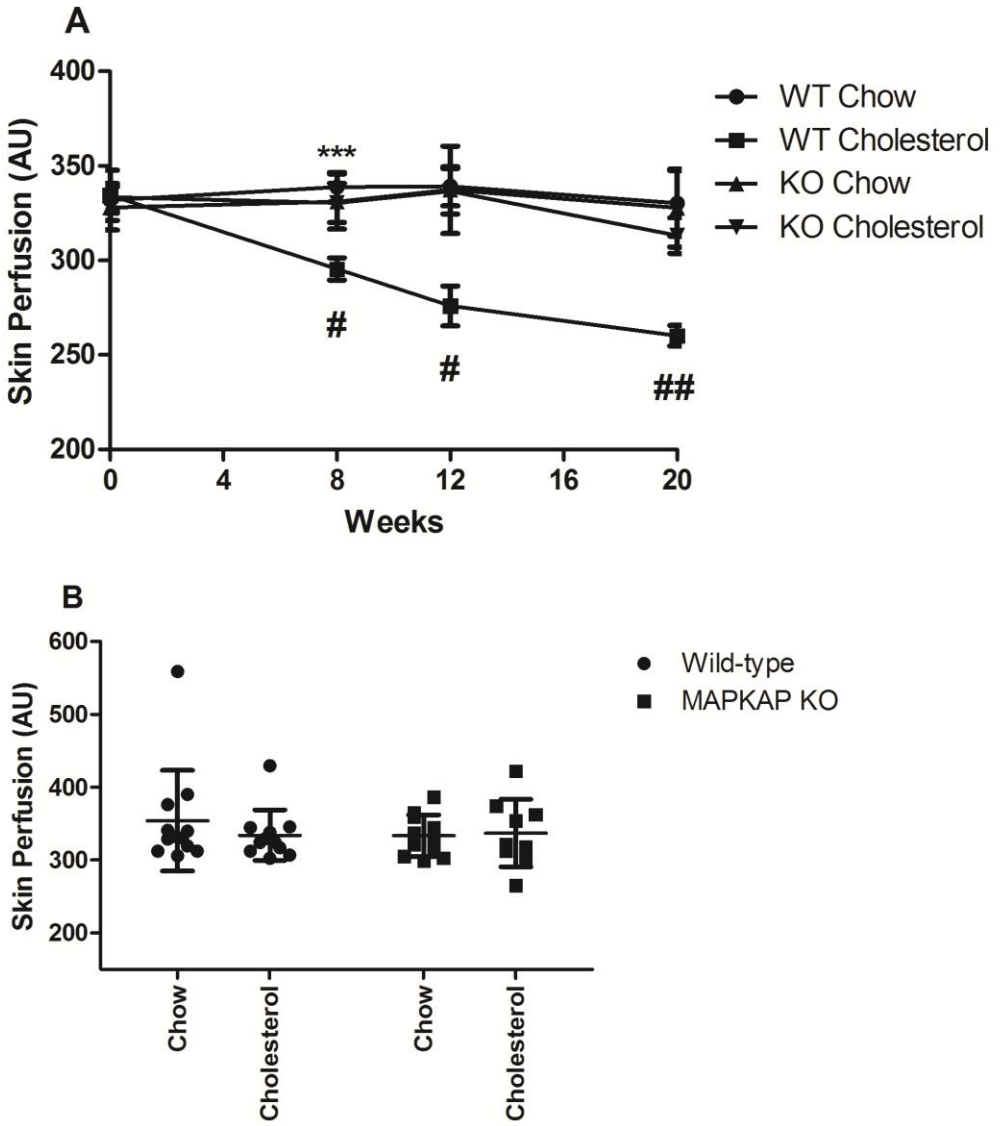

Figure 6.7. Longitudinal microvascular responses: (A) Microvascular responses in arbitrary units (AU) over 20 weeks to endothelium-dependent ACh and (B) week 20 responses to endothelium-independent SNP only in WT-chow (n =17), WT-cholesterol (n=12), MAPKAP 2/3 KO-chow (n =11) and MAPKAP 2/3 KO-cholesterol (n =13) fed animals. Results are group means ±SE. Changes were analysed by two-way ANOVA
**P<0.01 comparing genotypes

#P<0.05, ##P<0.01 comparing diet

Effect of NO Inhibition on Endothelium-dependent Responses

L-NAME administration to MAPKAP 2/3 KO-cholesterol fed mice at 20 weeks caused significant attenuation in the peak ACh response compared with the response without L-NAME (231±7 AU VS. 319±8 AU, P<0.001) and in WT-chow fed mice (242± 21 AU VS. 330±17 AU, P<0.05).

Baseline Cytokines

There were no significant differences between WT and KO mice for baseline inflammatory markers IL-1α (WT 885±76 pg/ml, KO 994±90 pg/ml), IL-6 (WT 1543±4 pg/ml, KO 1550±8 pg/ml), and IL-10 (WT 218±3 pg/ml, KO 218±3 pg/ml) (**Figure 5.8 A-C**).

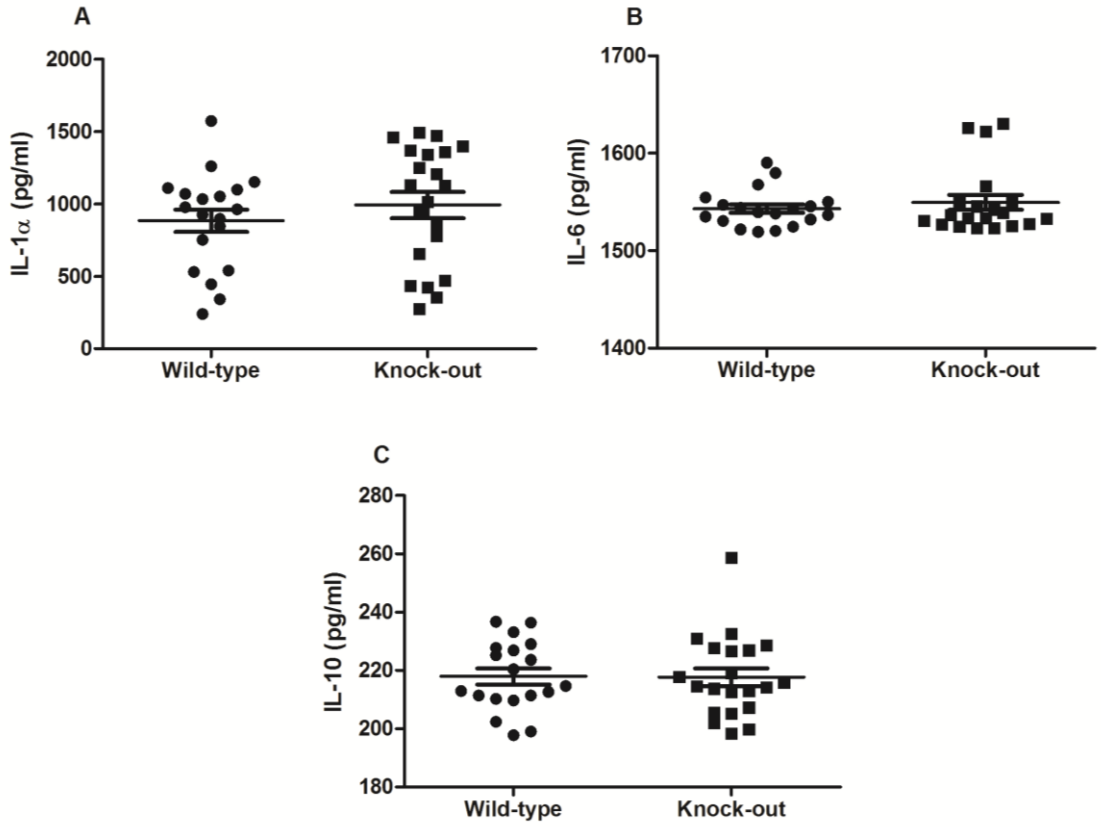

Figure 6.8. Baseline inflammatory marker: Study baseline plasma cytokines (pg/ml) (A) IL-1α, (B) IL-6 and (IL-10) in WT (n =20) and MAPKAP 2/3 KO (n =20) mice. Results are group means ±SE. Unpaired Student's t-test.

20 Week Measurement of Plasma Cytokines

Cholesterol feeding in WT mice significantly increased levels of inflammatory IL-1α (1707±12 pg/ml) and IL-6 (1994±10 pg/ml) when compared to WT-chow fed mice (IL-1α 1075±12 pg/ml ($P<0.001$), IL-6 1547±7 pg/ml ($P<0.001$).

Week 20 measurements of IL-1α levels were significantly greater in WT-cholesterol fed animals when compared to KO-chow and KO-cholesterol fed mice (**Figure 6.9A**). Levels of IL-6 were significantly higher in WT-cholesterol fed mice when compared to other groups (**Figure 6.9B**). Anti-inflammatory IL-10 in WT-chow fed mice as similar to KO-chow and KO-cholesterol fed mice however WT-cholesterol fed mice had lower 20 week measurements of IL-10 but this did not reach statistical significance (**Figure 6.9C**).

Correlations

Microvascular responses to ACh and localised heating at week 0 showed no significant correlations with cholesterol or any of the cytokines markers. In contrast, a number of significant correlations were observed at 20 weeks, IL-6 measurements negative correlated with ACh responses at 20 weeks ($r = -0.524$, $P<0.01$), cardiac mass ($r = 0.495$, $P<0.01$) and measurements of cardiac hypertrophy ($r = 0.675$, $P<0.001$). ACh response at week 20 also correlated with plasma levels of IL-10 ($r = 0.517$, $P<0.01$), IL-6 ($r = -0.524$, $P<0.01$), LDL/vLDL plasma cholesterol ($r = -0.22$, $P<0.01$) and measurements of cardiac hypertrophy ($r = -0.372$, $P<0.05$).

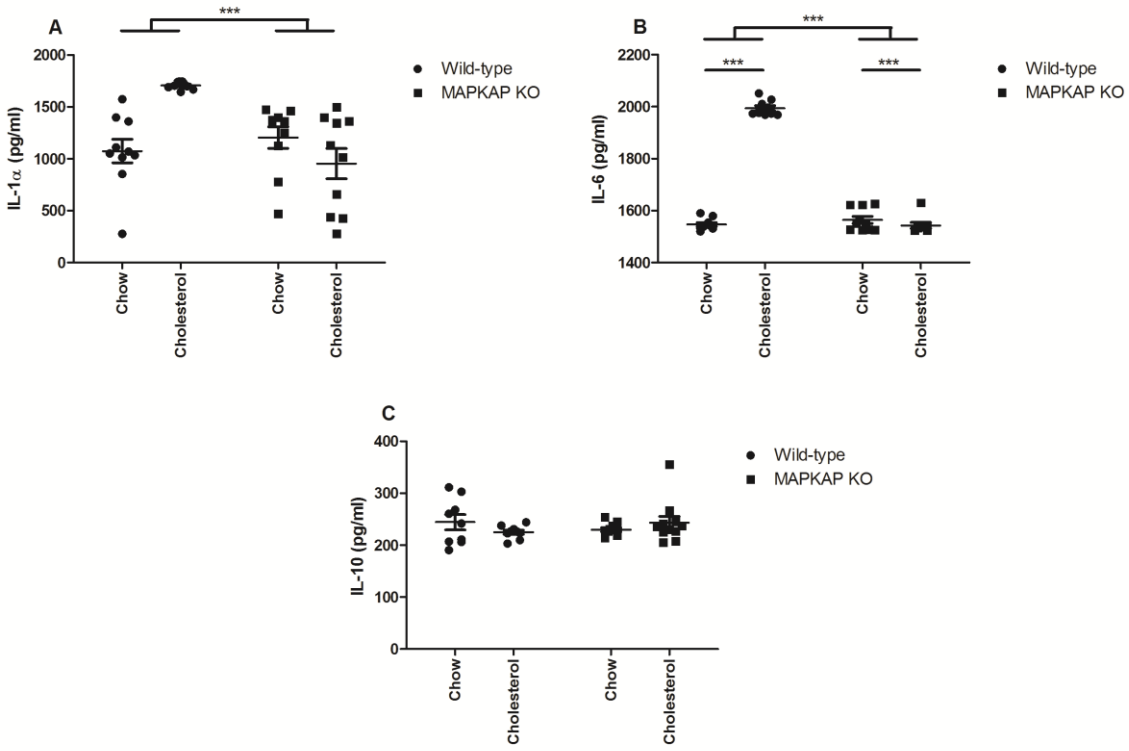

Figure 6.9. Week 20 measurements of inflammatory markers: Plasma cytokines (pg/ml) (A) IL-1α, (B) Il-6 and (C) IL-10 in WT-chow (n =10), WT-cholesterol (n =10), MAPKAP 2/3 KO-chow (n =10) and MAPKAP 2/3 KO-cholesterol fed (n =10) mice. Results are group means ±SE. Two-way ANOVA, ***P<0.001.

Discussion

The major findings from this study show that MAPKAP 2/3 KO-cholesterol fed mice displayed greater endothelium-dependent vasodilatation *in vivo* over 20 weeks. Importantly, although vascular responses to ACh were not statistically higher in MAPKAP 2/ 3 KO-cholesterol fed mice when compared to WT-cholesterol fed animals, MAPKAP 2/3-cholesterol fed mice had perseveration of NO, unlike WT-cholesterol fed mice as detailed in previous chapters.

WT-cholesterol fed mice displayed numerous dysfunctions when compared to other groups. In particular WT-cholesterol fed mice displayed significantly blunted endothelium-dependent responses to ACh; however VSMC reactivity

was unaffected as endothelium-independent responses to SNP were similar amongst the experimental groups, suggesting localised damaged to the endothelium. In previous chapters it has been shown that attenuated vasodilatation to ACh in WT-cholesterol fed mice is mediated via reduced NO (Belch *et al*., 2013). L-NAME administration MAPKAP KO-cholesterol fed mice significantly blunted ACh mediated vasodilatation, showing that NO was preserved in MAPKAP 2/3 KO-cholesterol fed mice after 20 weeks of cholesterol feeding. Furthermore L-NAME administration in WT-chow fed mice in this study also significantly blunted endothelium-dependent vasodilatation, confirming the preservation of NO in these mice over time (with age).

The activation of MAPKAP 2 has previously been described in the endothelium and in macrophage rich regions of aorta taken from LDLr KO mice (Jagavelu *et al*., 2007). Conversely an absence of MAKAP 2 has been reported in VSMCs, suggesting an intimate relationship between inflammation, the vascular endothelium and MAPKAPs. Double back crossing of MAPKAP 2 KO mice and LDLr KO mice has previously shown a significant reduction in lipid accumulation in the aorta and reduced macrophage infiltration (up to 50 and 60% respectively) (Jagavelu *et al*., 2007). MAPKAP 2 deficiency has further shown reduced foam cell formation *in vitro* and *in vivo*, in part this was due to reduced expression of scavenger receptor A, reduced aortic expression of VCAM-1 and chemokine MCP-1 (Jagavelu *et al*., 2007). Whereas Jagavelu *et al* reported that ICAM-1 staining does not significantly differ between LDLr KO and double MAPKAP 2/LDLr KO mice. MCP-1 is a chemoattractant protein important in macrophage accumulation in tissues (Oh *et al*., 2012), whereas VCAM-1 induces firm adhesion of monocytes to the endothelium and is significantly up regulated expressed in vascular tissue after cholesterol feeding (Li *et al*., 1993).

Thus an inability to express these molecules in MAPKAP 2/3 KO mice could have the potential to suppress vascular inflammation and preserve NO.

The protective role of MAPKAP 2/3 deficiency on NO in this study of vascular dysfunction is thought to be mediated in part by attenuated expression of IL-6 in the presence of dyslipidaemia, unlike WT-cholesterol fed animals. Circulating levels of IL-6 is a central mediator of the acute phase response and induces the production of CRP in hepatocytes, both molecules are established risk factors for CVD (Barnes et al., 2011, Hashizume and Mihara 2012, Fernandez-Real et al., 2001).

At 20 weeks MAPKAP 2/3 cholesterol fed mice had reduced plasma levels of IL-6 when compared to WT-cholesterol fed mice. Hung *et al* (2010) has previously reported the molecular consequences of IL-6 in the context of eNOS signalling. eNOS modulates basal vascular tone through the release of NO, inducing relaxation of VSMCs. IL-6 can specifically inhibit the release of NO, by increasing the potency (half-life) of calveolin-1. Increased caveolin-1 activity reduces eNOS activity by attenuating the eNOS activation pathway, though reduced phosphorylation at Ser1177, an established phosphorylation site implicated in endothelial dysfunction (Matsumoto *et al*., 2014)

There was a significant up regulation of IL-1α in WT-cholesterol fed mice, although levels were not significantly lower in MAPKAP 2/3 KO-cholesterol fed mice. IL-1α has been implicated as a marker of endothelial cell senescence (Mariotti *et al*., 2006), senescent endothelial cells have been observed on atherosclerotic plaques. IL-1α has been implicated in early atherosclerotic plaque formation through modulation of cell adhesion molecules. The IL-1ra has further shown inhibition of early atherosclerotic lesions in ApoE KO mice and

has important roles in the efflux of plasma cholesterol (Isoda and Ohsuzu, 2006, Isoda *et al*., 2004)

Previous reports have shown that MAPKAP 2/3 KO mice do not show generalised cardiovascular disease/dysfunction, when compared to WT control mice under basal, un-stimulated conditions, as evidenced by no significant changes in heart mass (standardised to body weight), no significant increases in cardio myocyte cell volume or length and no significant elevation in protein expression markers of pathological hypertrophy such as atrial natriuretic factor peptide (ANP) and brain natriuretic peptide (BNP) (Scharf *et al*., 2013, Kong *et al*., 2005). MAPKAP 2/3 KO-cholesterol fed mice displayed a near significant protection against cholesterol induced cardiac hypertrophy and lower cardiac mass, whereas WT-cholesterol fed mice had greater cardiac mass and a greater standardised measurements of cardiac hypertrophy. These results show that MAPKAP 2/3 promote cardiac hypertrophy potentially through the release of cytokines such as IL-6.

Dietary cholesterol induced significant dyslipidaemia in both WT and KO mice in this study. In agreement with previous reports there were no significant differences between HDL levels in MAPKAP 2/3 KO and WT mice on either diet (Jagavelu *et al*., 2007). However, previous reports have detailed significant increases in apoB lipoproteins, a sub class of LDL associated with CVD (Contois *et al*., 2009). Jagavelu *et al* described MAPKAP 2 deficient mice on an LDLr KO background in contrast to MAPKAP 2/ 3 KO (C57BL/6) mice used in this study. The current study did not find significant differences for LDL/vLDL plasma cholesterol between WT and KO mice fed cholesterol. The reason behind the differences observed between these two studies remains unknown;

it is possible that the double KO described by Jagavelu *et al* is more susceptible to lipid accumulation. One potential mechanism for this observed difference could be cholesterol efflux. LDLr KO mice display elevated LDL plasma cholesterol due to defective plasma clearance, whereas the MAPKAP 2/3 KO mice used in this study should have no endogenous depletion in this lipid receptor and thus dietary cholesterol is cleared by efflux, under normal homeostatic control

Previous reports have not found significant differences in body weights between WT and MAPKAP 2/3 KO mice, however in this study, MAPKAP 2/3 KO mice showed significantly lower baseline and terminal body weights (chow and cholesterol fed) when compared to WT mice. The reason behind these differences remains unknown. The significant differences in size between MAPKAP 2/3 and WT mice were further confirmed by measurement of tibia lengths. It is possible that the repeated inbred backcrossing of the MAPKAP 2/3 KO mice is one reason for the observed differences.

In conclusion MAPKAP 2/3 are important signalling molecules in cytokine synthesis and deficiency preserves NO in mice fed dietary cholesterol *in vivo*. Targeting the MAPKAP 2/3 pathway, with agents that block their action might provide a useful therapeutic option for inhibiting inflammation induced endothelial dysfunction and CVD.

Chapter 7

An Important Role for ABIN1 in Inflammation-Mediated Endothelial Dysfunction

Introduction

Previous chapters have detailed studies where the role of sub-clinical inflammation resulted in endothelial dysfunction through MAPK activation and explored how this can be abrogated through truncation of innate immune pathways. As discussed in the *Introduction (NF-κB Regulation in Inflammation),* TLR activation can also activate NF-κB, inducing nuclear translocation and gene expression. The A20-binding inhibitors of NF-κB (ABINs1-3) are suppressors of inflammation (**Figure 1.9**). Recent work suggests that ABIN1 restricts the activation of the canonical IKK complex and MAP kinases by binding to Lys63-linked and linear ubiquitin chains (Nanda *et al*., 2011). The ABIN1[D485N] knock-in mouse shows significant expansion of myeloid cells in various organs, but the role of this mutation in CVD has not been reported.

Aim

To determine the role of ABIN1 in the development of endothelial dysfunction through assessment of microvascular responses in ABIN1[D485N] mutant defective mice.

Methods

The methods description below is intended to provide an overview of experimental techniques used in this study. Further experimental details are described in *Materials and Methods Pages 62-92.*

Animals

The ABIN1[D485N] mice were originally described on a 129SvJxC57B/6 background (Nanda *et al*., 2011). Animals were subsequently backcrossed on a C57BL/6 background for at least 8 generations. Group allocations were randomly assigned as follows: WT control mice fed normal rodent chow, WT mice on a specifically tailored pro-atherogenic diet, ABIN1[D485N] mice on rodent chow and a pro-atherogenic diet.

Vascular Responses

Endothelium-dependent and endothelium-independent responses, maximum vasodilator response to localised skin heating were measured at study baseline (week 0) and 4 weeks later. Skin perfusion in the present study is expressed in AU ±SE and calculated using propriety software (MoorLDI software, version 5.2) as a percentage (%) change over baseline. ABIN1[D485N] mice displayed elevated skin perfusion compared to WT matched littermate controls, and it was necessary to normalise baseline perfusion to assess vascular differences between ABIN1[D485N] mice and WT mice.

Plasma Cholesterol

Plasma was used to quantify HDL and LDL/vLDL fractions at study week 4 only.

Cytokine Expression

Plasma was analysed at study baseline and 4 weeks.

Cardiac Hypertrophy

In cholesterol fed animals only, cardiac hypertrophy was assessed at study week 4.

Spleen Weight

In cholesterol fed animals only spleen mass was assessed at study week 4.

Results

Baseline Weight

WT animals were significantly heavier (24g±1) than ABIN1[D485N] mice (23g±1) at study week 0 (P<0.01) (12 weeks of age) (**Figure 7.1**). The mean group difference was 2g.

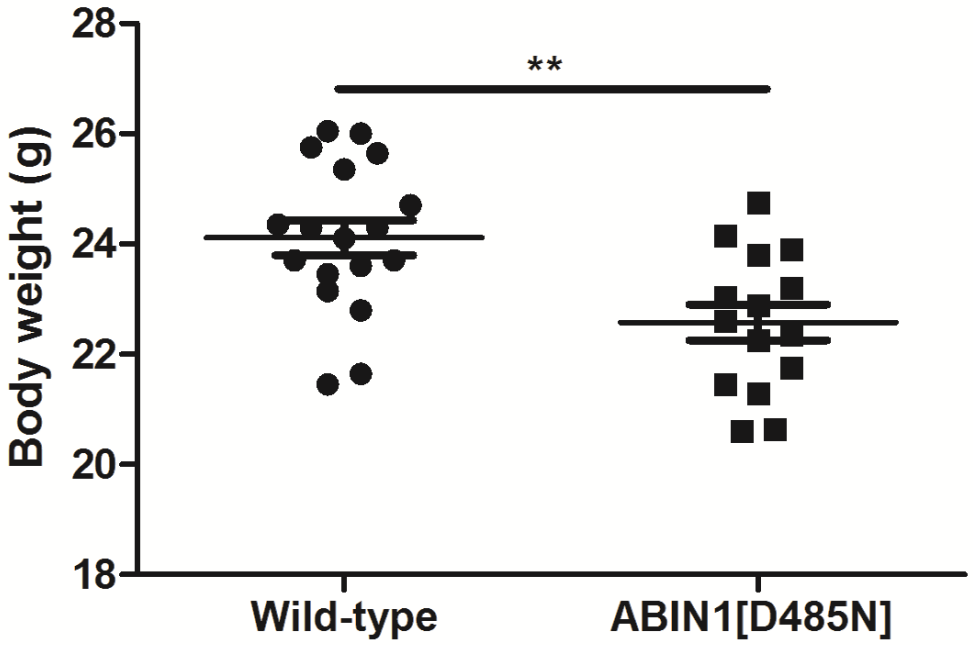

Figure 7.1. Baseline body weight: Body weights (12 weeks of age) in WT (n=18) and ABIN1[D485N] (n =15) mice. Differences between the groups were tested by unpaired Student's t-test. Results are group means in grams (g) ±SE. **P<0.01.

4 Week Measurements of Body Weight

WT animals significantly increased in weight during the study (4 weeks 26±1 g) ($P<0.001$) as did ABIN1[D485N] (4 weeks 25±1 g) ($P<0.001$) mice. Cholesterol feeding in WT mice (27±1 g) did not significantly alter terminal body weight compared with WT-chow fed mice (27±1g) (**Figure 7.2**). At the study end point (4 weeks) there were no significant differences in body weights for ABIN1[D485N]-chow (27±1 g) and ABIN1[D485N]-cholesterol fed mice (25±1 g) (**Figure 7.2**).

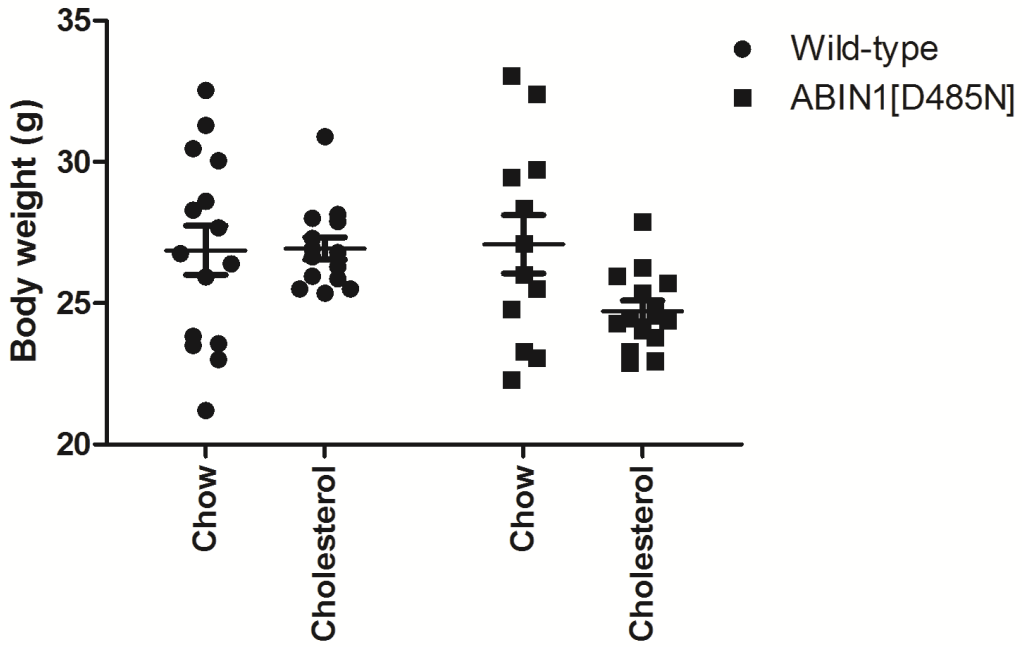

Figure 7.2. 4 Week measurements of body weight: Body weights (study week 4) in WT-chow (n =15), WT-cholesterol (n =14), ABIN1[D485N]-chow (n=12) and ABIN1[D485N]-cholesterol (n =14) fed mice. Two-way ANOVA. Results are group means in grams (g) ±SE.

Baseline Cytokines

Significant differences for baseline inflammatory markers were found between WT and ABIN1[D485N] animals. IL-1α was significantly greater in ABIN1[D485N] mice (WT 1376±42 pg/ml VS. ABIN1[D485N] 1658±66 pg/ml,

P<0.01) as was anti-inflammatory IL-10 (WT 213±10 pg/ml VS. ABIN1[D485N] 335±27 pg/ml, P<0.001) (**Figure 7.3 A/B** respectively). Whilst levels of IL-6 (WT 1325±74 pg/ml VS. ABIN1[D485N] 1684±267 pg/ml) were not significantly different (P>0.05) (**Figure 7.3 C**).

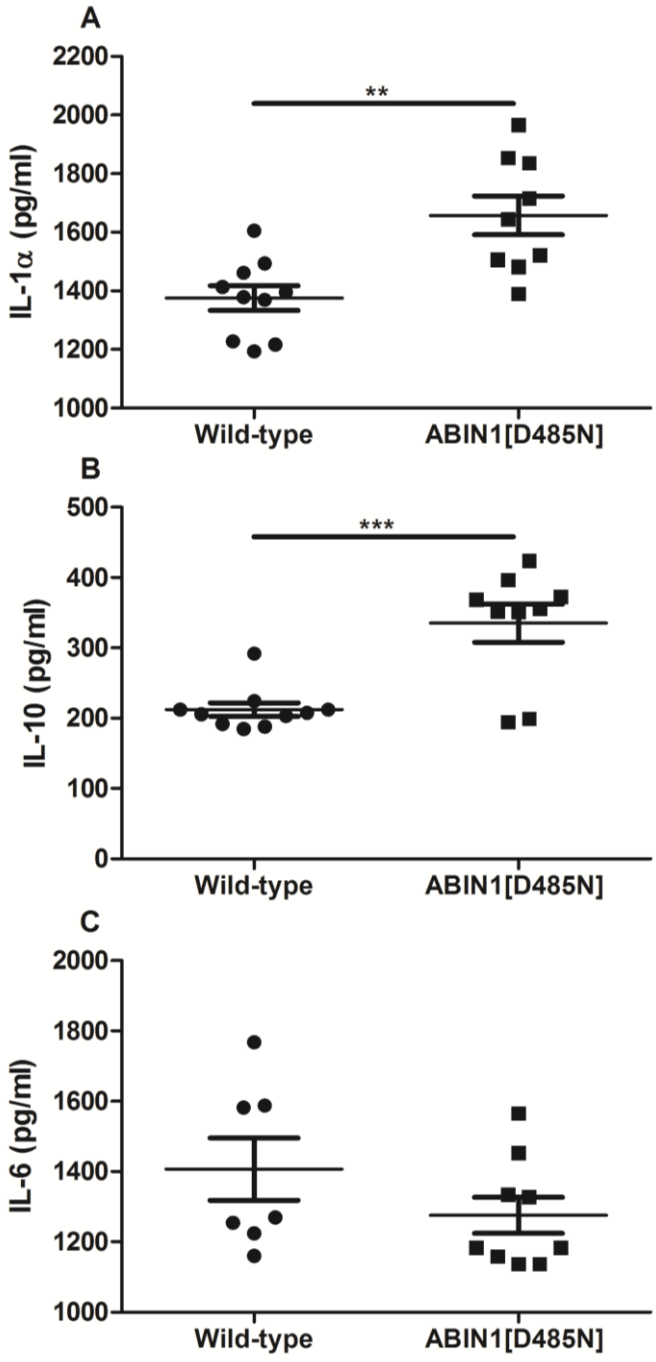

Figure 7.3. Baseline inflammatory markers: Baseline (12 weeks of age) plasma cytokines (pg/ml) for (A) IL-1α (B) IL-6 and (C) IL-10 in WT (n =10) and ABIN1[D485N] (n =9) mice. Differences were tested by unpaired Student's t-test. Results are group means ±SE. **P<0.01, ***P<0.01

Baseline Vascular Responses

Baseline (study week 0) vascular responses were not significantly different between WT and ABIN1[D485N] animals for endothelium-dependent responses or maximal dilator capacity (Ach: WT 21±3 % change ABIN1[D485N] 24±4 % change P>0.05; maximal dilator capacity: WT 86±7 % change ABIN1[D485N] 92±7 % change, P>0.05) (**Figure 8.3 A/B** respectively).

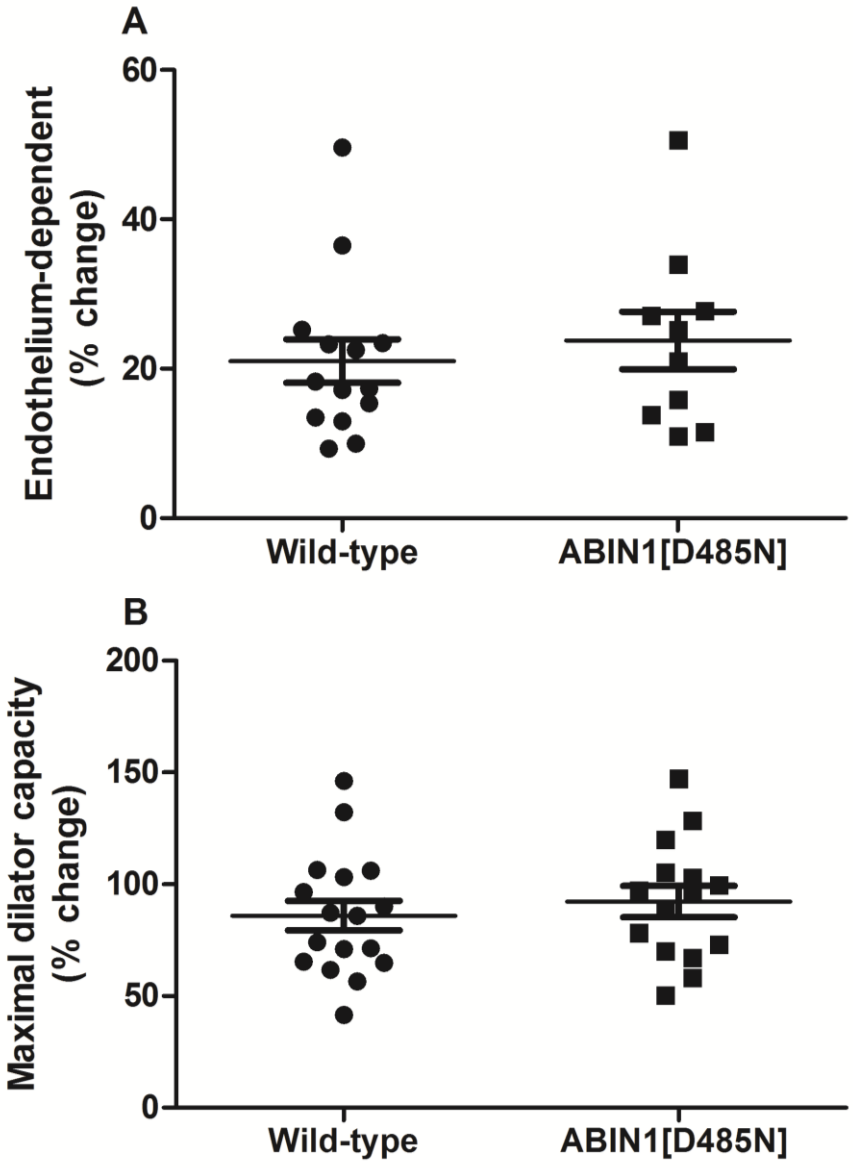

Figure 7.4. Baseline vascular function: Baseline microvascular responses in WT and ABIN1[D485N] animals: (A) endothelium-dependent responses (WT n =14, ABIN1[D485N] n =10) and (B) maximal dilator capacity (WT n =17, ABIN1[D485N] n =15). Unpaired Student's t-test. Results are group means ±SE (% change).

Plasma Cholesterol

LDL/vLDL

WT-cholesterol fed (9±1 mg/dl) mice had significantly greater LDL/vLDL at 4 week measurements when compared to WT-chow (5±1 mg/dl) ($P<0.05$). ABIN1[D485N]-chow fed animals had similar levels of LDL/vLDL when compared to WT-chow fed mice (5±1 mg/dl) (**Figure 7.5A**). There was no significant difference in LDL/vLDL in ABIN1[D485N]-cholesterol fed mice (5±1 mg/dl) when compared to WT-chow and ABIN1[D485N]-chow animals (**Figure 7.5A**). However levels of LDL/vLDL were higher in WT-cholesterol fed mice when compared to ABIN1[D485N]-chow ($P<0.01$) and ABIN1[D485N]-cholesterol ($P<0.01$).

HDL

WT-chow (21±2 mg/dl) fed animals had significantly greater HDL in 4 week measurements of plasma when compared to ABIN1[D485N]-chow (2±1 mg/dl, $P<0.001$) and ABIN1[D485N]-cholesterol (2±1 mg/dl, $P<0.001$) fed mice (**Figure 7.5B**). There were no significant differences between WT-cholesterol (16±1 mg/dl) mice for plasma HDL when compared to WT-chow fed animals (**Figure7.5B**).

Levels of HDL were not significantly different between ABIN1[D485N]-chow and ABIN1[D485N]-cholesterol fed mice. HDL levels were significantly greater in WT-cholesterol mice when compared to ABIN1[D485N]-chow ($P<0.001$) and ABIN1[D485N]-cholesterol ($P<0.001$) animals (**Figure 7.5B**).

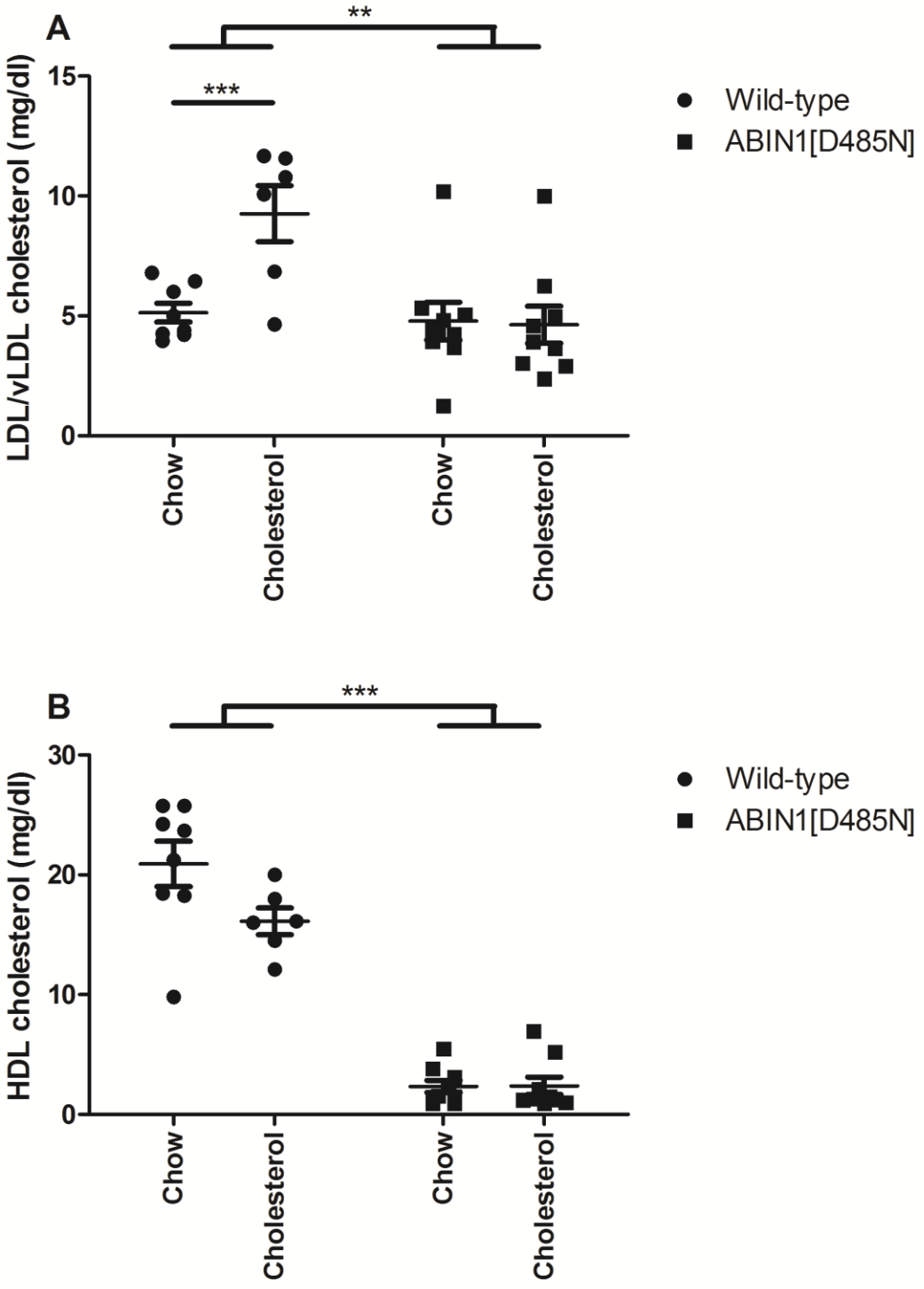

Figure 7.5. Plasma cholesterol: Study week 4, low density lipoproteins and very low density lipoproteins (LDL/vLDL) (A) and high density lipoproteins (HDL) (B) plasma WT-chow (n =8), WT-cholesterol (n =6), ABIN1[D485N]-chow (n =9) and ABIN1[D485N]-cholesterol fed mice (n =9). Results are group means (mg/dl ±SE). Two-way ANOVA, **P<0.01, **P<0.001

4 Weeks Measurements of Cytokines

Levels of IL-1α (4 weeks1457±49 pg/ml), IL-6 (4 weeks1533±10 pg/ml) and IL-10 (4 weeks 222±9 pg/ml) did not significantly change in WT-chow fed animal's over time, when compared to baseline values showing that WT-chow fed mice do not show age-related alterations, that would otherwise be associated with increased CVD risk.

Cholesterol feeding in WT mice caused adverse changes in inflammatory markers when compared to baseline values. There was a significant increase in IL-1α (4 weeks 16591±10, $P<0.001$) and IL-6 (4 weeks 1726±48, $P<0.01$). Cholesterol feeding in WT mice for 4 weeks did not significantly reduce levels of anti-inflammatory IL-10 (4 weeks 230±11, $P>0.05$) (**Figure 7.6A-C**).

Levels of IL-1α did not significantly increase further at 4 week measurements in ABIN1[D485N]-chow (1704±22 pg/ml) fed mice. However IL-1α remained significantly greater in ABIN1[D485N]-chow fed mice when compared to WT-chow fed animal ($P<0.001$) at study end point. Cholesterol feeding in ABIN1[D485N] mice did not result in a further significant increase in IL-1α (1672±8 pg/ml). Baseline and 4 week measurements of IL-1α in ABIN1[D485N] (on either diet) animals were similar to 4 weeks measurements obtained from WT-cholesterol fed mice (**Figure 7.6A**).

ABIN1[D485N]-chow fed animals displayed a significant increase in IL-6 (4 week 1739±21, $P<0.001$) in study end point measurements, a significant increase over time. This was similar to levels observed in WT-cholesterol fed animals. Levels of IL-6 significantly increased further in ABIN1[D485N]-cholesterol mice (1998±111 pg/ml), this was statistically greater than WT-chow

(P<0.001), ABIN1[D485N]-chow (P<0.01) and a near significant difference for WT-cholesterol fed mice (P>0.05) (**Figure 7.6B**).

4 weeks measurements of levels of IL-10 did not significantly change in ABIN1[D485N]-chow fed mice (414±57 pg/ml) when compared to baseline values. However IL-10 levels remained significantly greater in ABIN1[D485N]-chow animals when compared to WT-chow (P <0.01) and WT-cholesterol (P<0.05) fed (242±15 pg/ml) mice. (**Figure 7.6C**). Cholesterol feeding in ABIN1[D485N] mice (459±61 pg/ml) did not have significantly alter plasma IL-10 when compared to ABIN1[D485N]-chow animals (P>0.05). IL-10 levels in ABIN1[D485N]-cholesterol mice were significantly greater than WT-chow (P<0.01), WT-cholesterol (P<0.05) but not ABIN1[D485N]-chow (P>0.05).

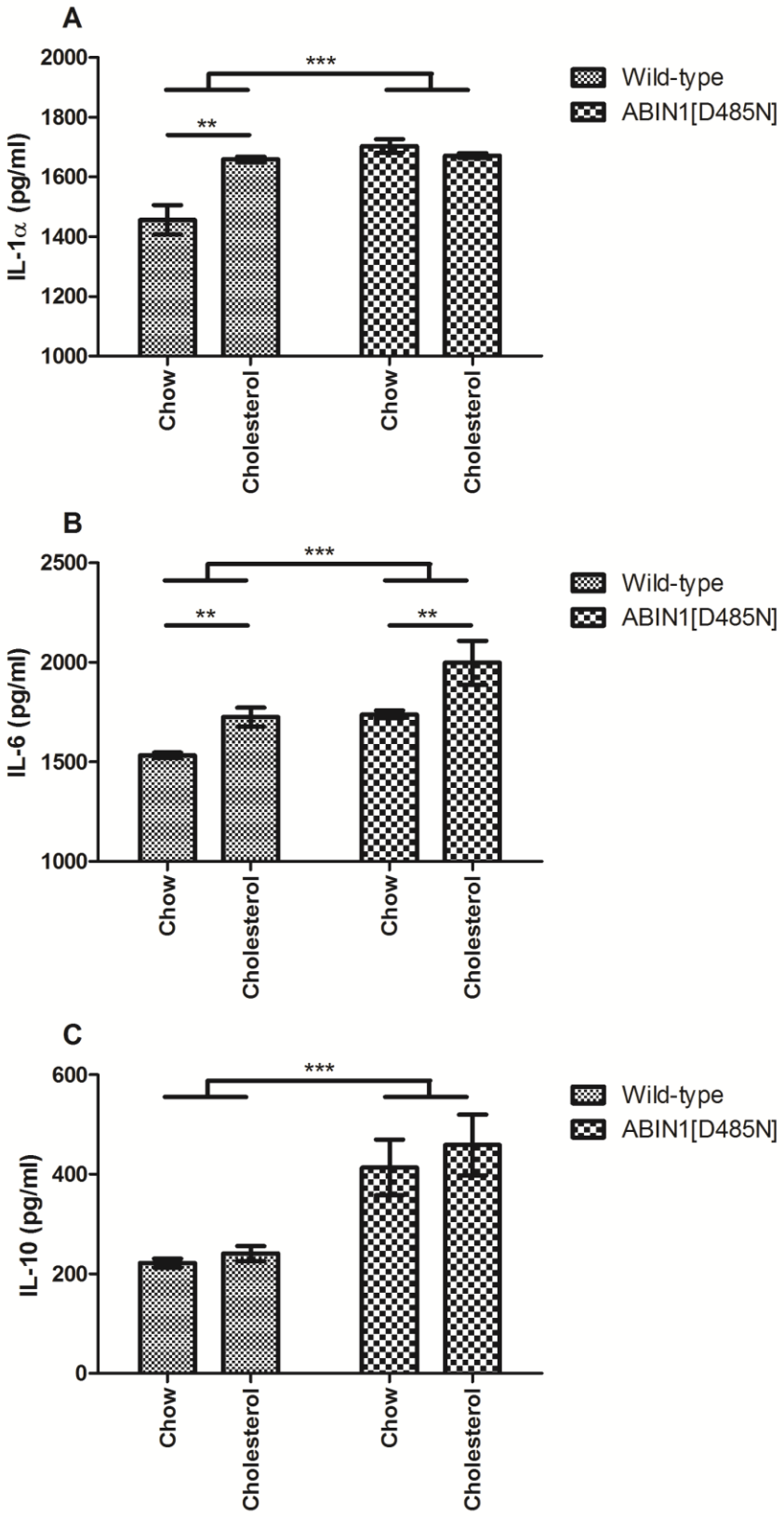

Figure 7.6. 4 week measurement of inflammatory markers: WT-chow (n =10), WT-cholesterol (n =7), ABIN1[D485N]-chow (n =10) and ABIN1[D485N]-cholesterol (n =10) fed animals for (A) IL-1α, (B) IL-6 and (C) IL-10. Results are group means (pg/ml ±SE). Two-way ANOVA. *P<0.05, **P<0.01, ***P<0.001.

Vascular Responses

Endothelium-dependent

WT animals on standard rodent chow diet did not show any significant changes in ACh mediated vasodilatation over the study duration (baseline 20±3 % change vs. 4 weeks 22±4 % change, $P>0.05$). WT mice fed cholesterol for four weeks have poorer ACh mediated microvascular responses when compared to baseline values (9±2 % change, $P<0.05$) and WT age matched mice on standard rodent chow ($P<0.01$).

Endothelium-dependent responses in ABIN1[D485N] animals fed chow (9±2 % change) were significantly attenuated when compared to values obtained at baseline (study week 0) ($P<0.01$). These were significantly lower than WT mice on the same diet ($P<0.05$) at 4 week measurements, but were similar in magnitude to those observed in WT cholesterol fed mice ($P>0.05$) (**Figure 8.7**).

Cholesterol feeding in ABIN1[D485N] mice further attenuated ACh microvascular vasodilatation (0.03±0.03% change) when compared to ABIN1[D485N]-chow fed animals ($P<0.001$). Responses to ACh were significantly poorer in ABIN1[D485N]-cholesterol fed animals when compared to WT chow ($P<0.001$) and WT-cholesterol ($P<0.001$) fed mice (**Figure 7.6**).

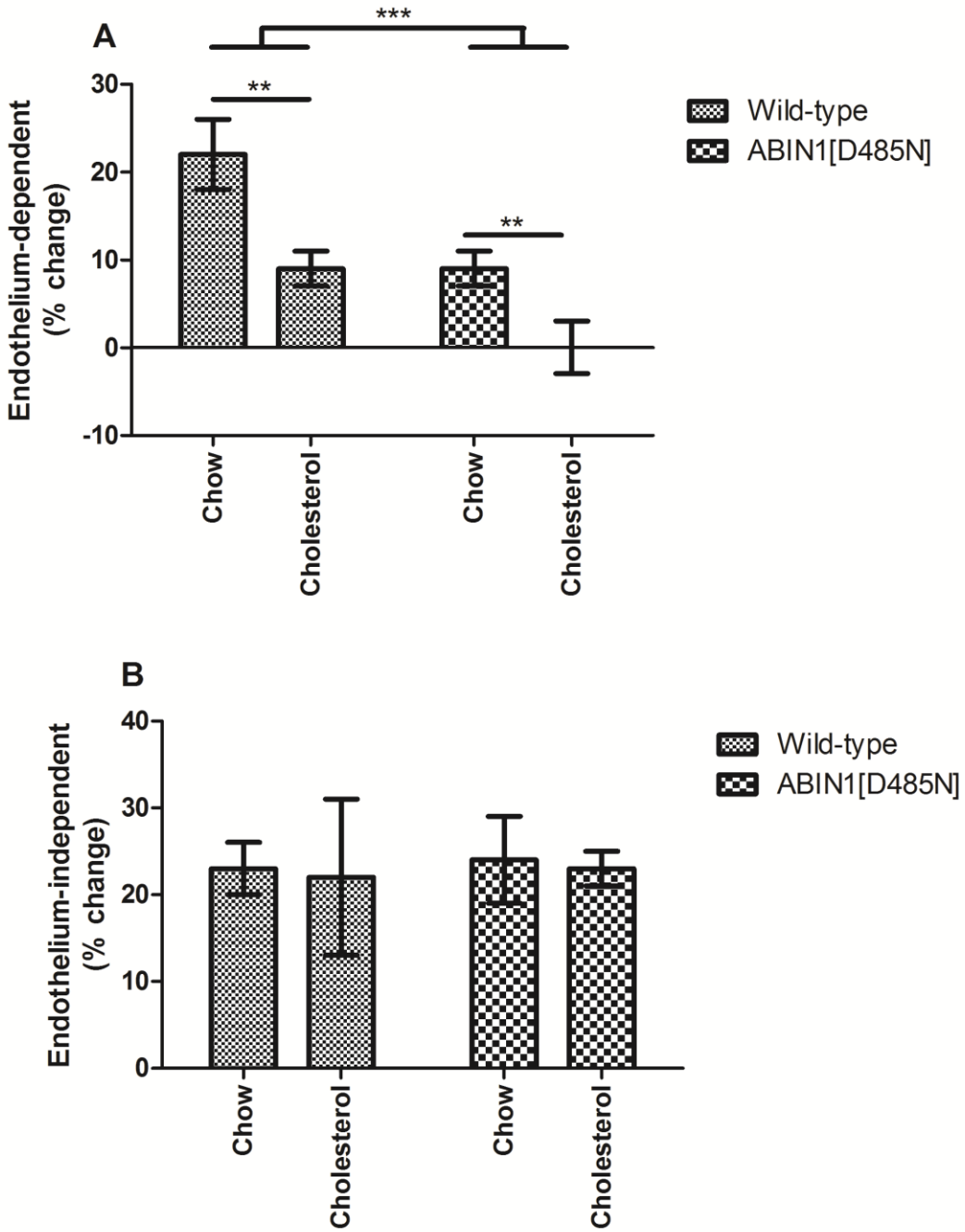

Figure 7.6. Study end point vascular function: Microvascular responses to (A) endothelium-dependent acetylcholine and (B) endothelium-independent sodium nitroprusside in WT chow (n =11), WT cholesterol (n =11), ABIN1[D485N]-chow (n =10) and ABIN1[D485N]-cholesterol (n =10) fed mice. Results are group means (% change ±SE). Two-way ANOVA. **P<0.01, ***P<0.001.

Endothelium-independent

Endothelium-independent responses were not significantly different between the groups (WT-chow 23±3 % change, WT-cholesterol 22±9 % change, ABIN1[D485N]-chow 24±5 % change, ABIN1[D485N]-cholesterol 23±2 % change, P>0.05 for all comparisons) (**Figure 7.6B**).

Cardiac hypertrophy

In cholesterol fed animals cardiac mass was not significantly different between the groups (WT 127±4 mg VS. ABIN1[D485N] 147±13 mg mice (P>0.05) **Figure 7.7A**.

There were no significant differences in the length of tibias between WT (18±1mm) and ABIN1[D485N] (18±2mm) mice (P>0.05) **Figure 7.7B**. ABIN1[D485N] mice had a significantly greater cardiac hypertrophy measurement when compared to WT mice (WT 7.1±0.2 VS. ABIN1[D485N] 8.2±0.7 P<0.05) (**Figure 7.7C**)

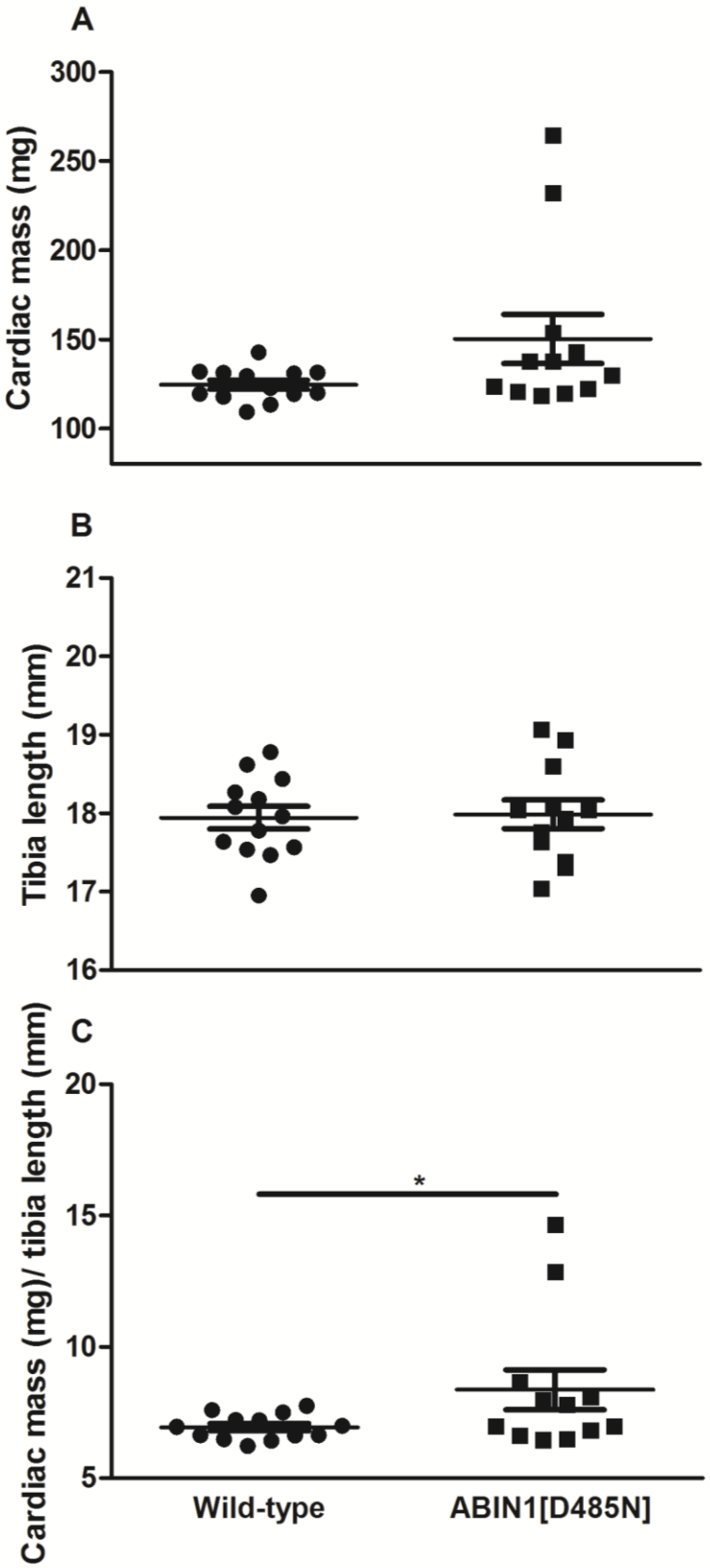

Figure 7.7. Cardiac hypertrophy: Cardiac hypertrophy measurement in WT (n =14) and ABIN1[D485N] mice (n =13) cholesterol fed mice: (A) cardiac mass (mg), (B) tibia length (mm) and (C) cardiac mass (mg)/tibia length (mm). Data are group means ±SE. Unpaired Student's t-test. *P<0.05

Spleen Weight

Splenic mass in cholesterol fed ABIN1[D485N] mice (460±20 mg) was greater when compared to WT-cholesterol fed animals (104±30 mg) (P<0.001) (**Figure 7.8**).

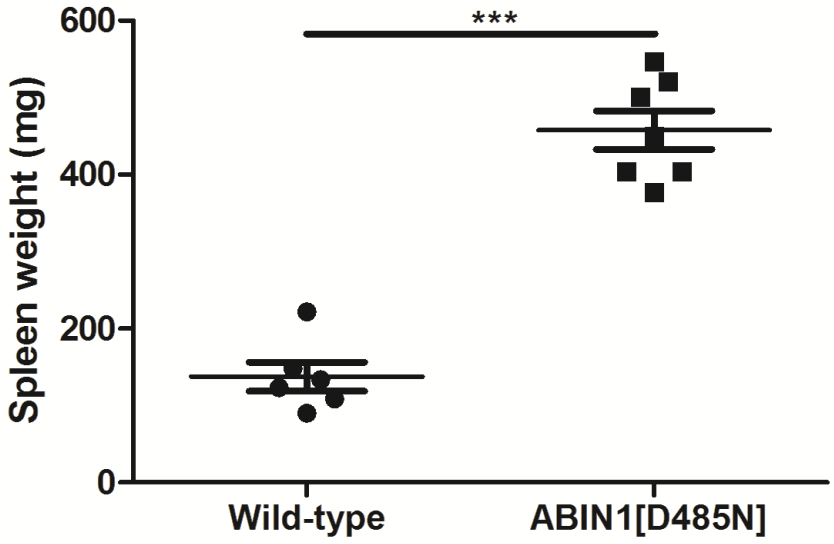

Figure 7.8. Spleen weight: WT (n =6) and ABIN1[D485N] (n =7) cholesterol fed animals. Results are group means Milligrams (mg ±SE). Student's t-test. ***P<0.0001

Correlations

Several significant associations were found at 4 week measurements to ACh responses, these negatively correlated with spleen mass (r= -0.722, P<0.05) and 4 week measurements of plasma cytokines for IL-1α (-.0764, P<0.01). HDL negatively correlated with IL-1α (r= -0.501, P<0.01) and IL-6 (r= -0.558, P<0.001).

Discussion

The main finding from this study is the onset of early CVD (endothelial dysfunction) in the polyubiquitin-binding-defective ABIN1[D485N] mice, a phenotype that is further exacerbated by cholesterol feeding. There were no significant differences in endothelium-independent responses, suggesting that VSMC activity was not compromised and indicates localised damage to the endothelium. Furthermore this study shows a significant reduction in plasma HDL of ABIN1[D485N] mice, an established risk factor for CVD.

It has previously been reported that ABIN1[D485N] mice have enhanced IKK and MAPK activity in B-cells, bone marrow derived macrophages and dendritic cells and display significant expansion of myeloid cells in spleen and lymph nodes (Nanda *et al*., 2011). Consequently, these mice bear a SLE-like phenotype as early as 3-4 months of age. Endothelial dysfunction is an early event in the development of CVD and this study shows it is present in ABIN1[D485N] mice at 4 months of age. Endothelial dysfunction was further exacerbated by dietary cholesterol showing elevated dysfunction when risk factors are combined (chronic inflammation and cholesterol).

Selective inhibition of NF-κB in endothelial cells has been shown to be protective against atherosclerotic lesion formation in CVD prone ApoE KO mice (Gareus *et al*., 2008). This data supports the notion that increase IKK activity, and hence increased NF-κB activation, has significant negative effects on the cardiovascular system. The activation of TLRs, in particular TLR-2 and TLR-4, is associated with atherogenesis whereas blockade of this signalling, achieved by amelioration of the MyD88, has shown atheroprotection (Bjorkbacka *et al*.,

2004). Similarly the SLE phenotype of the ABIN1[D485N] mice is abrogated when they are expressed on a MyD88-deficient background (Nanda *et al*., 2011), indicative of overlap in the signalling pathways involved in the development of SLE and CVD.

There was a significant increase in IL-1α in plasma of ABIN1[D485N] mice at the study baseline, although there was no apparent difference in vascular responses between the two groups, suggesting that the relative differences and duration of change was not sufficient to impact on vascular function at this time point. The differences in inflammatory markers between ABIN1[D485N] and WT mice are presumably mediated by the hyperactivation of NF-κB and MAPKs. Commensal gut flora can activate TLRs and stimulate NF-κB (Rakoff-Nahoum and Medzhitov, 2008, Rakoff-Nahoum *et al*., 2004) predisposing to chronic inflammation in ABIN1[D485N] mice.

The exact mechanism responsible for the onset of endothelial dysfunction in ABIN1[D485N] mice requires further investigation; however this may be mediated by IL-6. There was a significant increase in IL-6 over time in ABIN1[D485N] mice, and this was further exacerbated by cholesterol feeding in ABIN1[D485N] mice, which displayed the poorest endothelium-dependent responses. IL-6 is an established cardiovascular risk factor (Ridker *et al*., 2000b, Naya *et al*., 2007). Levels of IL-6 in WT-cholesterol mice at the end-point were similar to those observed in ABIN1[D485N]-chow mice, even though the latter group was not exposed to a major cardiovascular risk factor (cholesterol). A negative association between vascular responses and plasma levels of IL-6 has been described previously (Esteve *et al*., 2007). Taken

together these data suggest that the mutation in ABIN1[D485N] mice predisposes to CVD in part via increasing levels of IL-6.

As previously discussed IL-6 can inhibit activation of eNOS and attenuate vasodilation by increasing the half-life of caveolin-1, resulting in more eNOS binding and reducing NO. A loss in NO is associated with diseases such as hypertension (Moss *et al*., 2004) and is regarded as an early phase of atherosclerotic plaque formation (Hadi *et al*., 2005).

In previous chapters it has been established and reported in the literature that skin microvascular responses to ACh are mediated through the NO and that this is diminished by cholesterol feeding in WT mice (Belch *et al*., 2013). The loss of NO in the peripheral skin microcirculation increases total peripheral resistance. Reduced lumen diameter through attenuated vasodilatation (diminished NO) can lead to development of left ventricular hypertrophy, an adaptive response to increased cardiac load (greater force is needed to pulsate blood through narrow arteries). This adaptation is essential for survival, and inhibition of cardiac hypertrophy in mice shows increased mortality through pressure overload and heart failure (Dickhout and Austin, 2006). Thus cardiac hypertrophy in ABIN1[D485N]-cholesterol fed mice may be an adaptive response to diminished peripheral microvascular function.

It is important to note that under pathophysiological conditions cytokines are released from numerous cell types, including activated endothelial cells. Stimulated endothelial cells express IL-1α which is also associated with CVD (Isoda *et al*., 2003). This cytokine can contribute to atherosclerosis through the

expression of cell adhesion molecules (VCAM-1 and ICAM-1). Adhesion molecules are needed for the tethering of macrophages to the endothelial lining, for subsequent transmigration into the sub-endothelial space, an early phase in atherosclerotic plaque formation.

Surprisingly, plasma levels of the anti-inflammatory IL-10 were significantly greater in ABIN1[D485N] mice, an unreported finding. The exact mechanism and role of this remains unknown, however the higher levels of IL-10 may be a counter mechanism in ABIN1[D485N] mice in an attempt to attenuate pro-inflammatory responses in an autocrine loop. IL-10 can be synthesised by macrophages and attenuates pro-inflammatory cytokine expression through a JAK/STAT3 pathway (Pattison *et al*., 2012). Forsberg *et al* (Forsberg *et al*., 2007) have previously reported similar findings, showing increased levels of IL-10 in intra-epithelial lymphocytes in the context of coeliac disease. The ability to maintain these elevated levels of IL-10 are of particular interest and it needs to be established whether they can be sustained over a longer period of time (with greater age), and to establish whether ablation or sequestering of endogenous IL-10 in ABIN1[DN485] mice would further exacerbate the observed pathology in this and previous studies.

IL-10 levels are anti-atherogenic, facilitating the uptake and efflux of cholesterol, which in turn is associated with reduced cell death and progression of atherosclerotic lesions (Han *et al*., 2010). This may in part explain why ABIN1[D485N]-cholesterol fed mice, despite being fed dietary cholesterol for 4 weeks, did not display elevated LDL/vLDL unlike WT-cholesterol fed mice. Pinderski *et al* (Pinderski Oslund *et al*., 1999) have previously reported a lower

plasma cholesterol level in animals over expressing IL-10 compared with both C57BL/6 WT mice and homozygous IL-10 null animals fed cholesterol, although these observations were not statistically significant. In healthy individuals the efflux of cholesterol from the arterial intima is modulated by HDL and prevents lipid oxidation. Thus despite profound reductions in HDL ABIN1[D485N] mice may be able to efflux LDL/vLDL cholesterol through an IL-10-dependent mechanism to prevent significant accumulation in the blood stream. The mechanism behind the low plasma levels of HDL in ABIN1[D485N] remains unknown and requires further study.

This study aimed to establish a role for a mutation in ABIN1 in inflammatory-induced CVD development through assessment of endothelial function and measurement of systemic cytokine expression. Understanding the pathophysiological mechanisms and pathways responsible for early development of CVD in ABIN1[D485N] mice has potentially important clinical implications. The induction of chronic inflammation, endothelial dysfunction and cardiac hypertrophy by a single protein malformation highlights the need for selective therapeutic targets of inflammation to limit multi-organ disease, and the ABIN1 pathway might be one potential therapeutic target. Importantly, using a similar experimental approach in humans, previous studies have shown that RA patients have attenuated endothelium-dependent responses in the skin microcirculation, and that the degree of attenuation is related to the expression of systemic inflammatory cytokines(Galarraga *et al*., 2008), findings that are similar to those in the present study. Since endothelium-dependent responses in the microcirculation of the skin are indicative of defective coronary function (Khan *et al*., 2008) and future cardiovascular sequelae before clinical

presentation (Khan *et al*., 2005), data from the present study point to a potentially important role for ABIN1 in the development and progression of inflammation-induced CVD. The findings in this study are in agreement with irregularities in the NF-κB pathway that have previously been implicated for the onset of CVD.

In conclusion, this is the first *in vivo* observation to document the early development of CVD (endothelial dysfunction) as a result of a single protein mutation involved in NF-κB signalling, relevant to previously reported clinical genome wide association studies for SLE. The data suggest that ABIN1 dysfunction could be mechanistically involved in the early development of inflammation-induced CVD risk.

Chapter 8

Can Vitamin D Supplementation Reduce Inflammation and Improve Endothelial Function?

Introduction

There remains a need for better therapies targeted at reducing inflammatory mediated CVD burden. Synthetic molecules require vigorous pre-clinical and clinical testing as demonstrated by the MAPK p38 inhibitor SB-203580 to ensure safety (Lee *et al*., 2000). Therefore favourability is given to endogenous molecules that are present within physiological systems. Vitamin D is most often associated with bone metabolism; recent findings have shown vitamin D deficiency is associated with a number of chronic inflammatory disease conditions including RA (Kostoglou-Athanassiou *et al*., 2012) and atherosclerosis (Kassi *et al*., 2013). However, causality has been more difficult to prove. The role of vitamin D as an anti-inflammatory agent for the treatment of inflammatory disease conditions has previously been discussed in range of disease conditions including CVD (Holick and Chen, 2008, Ku *et al*., 2013, Lavie *et al*., 2011, Mangge *et al*., 2013). It is estimated that 25-50% of the world population are deficient in vitamin D.

Vitamin D is a biologically active steroid, and vitamin D receptors (VDRs) are widely expressed; importantly they are found on all cells associated with atherosclerotic lesions including endothelial cells, VSMCs and immune cells, extending the physiological roles of vitamin D beyond regulation of Ca^{2+} and phosphorus in the metabolism of bone.

Vitamin D broadly refers to a number of biologically active compounds. Vitamin D_3 is produced when light is absorbed through the skin (UV-B, 290-315nm) by the precursor 7-dehydrocholesterol (**Figure 8.1**). Ergocalciferol (vitamin D_2) is found in plants and is ingested through supplementation either as a tablet or in enriched dairy products. Both D_2 and D_3 are hydroxylated in the liver by the

enzyme 25-hydroxylase yielding the circulating form 25-hydroxy vitamin D (25(OH)D) (**Figure 8.1**). 25(OH)D is biologically inactive and requires further hydroxylation in the kidneys forming the compound 1,25-dihydroxy vitamin D (Calcitriol) through enzymatic action of 1-α-hydroxylase (**Figure 8.1**).

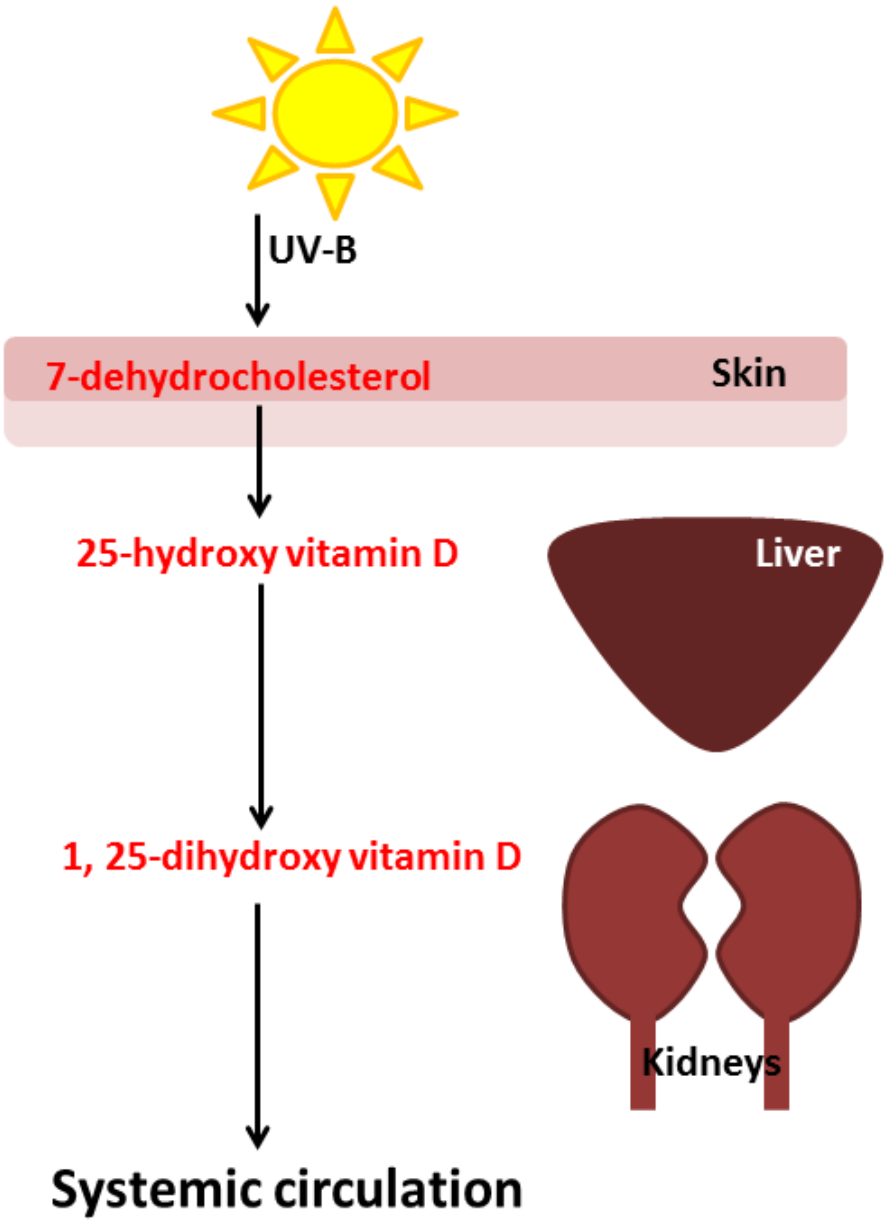

Figure 8.1. Vitamin D metabolism: Sun exposure of ultra violet (UV) B light produces 25-hydroxy vitamin D that undergoes hydroxylation in the liver and then in the kidneys, before being released into the systemic circulation as biologically active 1, 25hydroxy vitamin D (Calcitriol).

Although biologically potent, under clinical screens Calcitriol is not measured and levels of 25(OH)D are recorded, there is no general consensus on absolute levels of vitamin D in healthy individuals, but levels below 20-30 ng/ml are regarded as vitamin D deficient (VDD) (Ku *et al*., 2013). The major contribution to VDD is attributed to the lack of sun light exposure, UV-B light is readily absorbed by melanin in the skin, thus individuals of South Asian and African descent are commonly VDD (Darling *et al*., 2013). Vitamin D is highly fat soluble, therefore a deficiency of vitamin D is also associated with obesity and has been correlated with decreased insulin sensitivity, two existing risk factors for CVD (Grineva *et al*., 2013).

Vitamin D supplementation has shown to exert reduction in blood pressure through modulation of the renin angiotensin system, reinstating vitamin D as a therapeutic agent for CVD, suggesting vitamin D supplementation and potentially even treatment with systemic analogues of vitamin D maybe cardio-protective. Whereas VDD induces left ventricular hypertrophy and proliferation of VSMCs (Lavie *et al*., 2011), events proceeding endothelial dysfunction. Some clinical trials have shown favourable results with vitamin D treatment improving endothelial function in patients (Sugden *et al*., 2008, Borges *et al*., 1999).

Recent studies have conversely produced apparently conflicting results. The role of vitamin D in cardiac failure, myocardial infarction and stroke is showing either no association or only a weak beneficial effect dependent on age (Ford *et al*., 2014). Studies have also reported no clear relationship between vitamin D levels when comparing healthy volunteers to SLE patients for subclinical atherosclerotic burden (Jung *et al*., 2014) and in some cases studies have shown increased early atherosclerotic burden (greater intima-media thickness)

with elevated levels of plasma vitamin D (van Dijk *et al*., 2014). Furthermore there have been reports of no association between plasma levels of vitamin D and risk of thromboembolism (van Dijk *et al*., 2014, Folsom *et al*., 2014). Although limitations are widely discussed the underlying cause for these disparities remains unknown.

In the context of inflammation the exposure of sunlight in the treatment of microbial infections such as tuberculosis has shown favourable results by abrogating pathology, the likely mechanism is thought to be macrophage TLRs and increased expression of vitamin D 1-α-hydroxylase genes, increasing systemic levels of the biologically active Calcitriol (Liu *et al*., 2006).

Calcitriol can bind to VDRs and stimulate transcription to modulate gene expression of the antimicrobial agent cathelicidin (Yin and Agrawal, 2014). The VDR has a hormone and DNA-binding domain that can interact with the retinoid-X receptor forming a heterodimer, activating gene transcription. Studies have previously shown that macrophage TLR expression is reduced in the presence of VDD and this results in an inflammatory phenotype through the expression of pro-inflammatory cytokines TNF-α and IL-6 in healthy human patients (Ojaimi *et al*., 2013). Nonetheless conflicting data has been reported in an inflammatory disease cohort with the down regulation of mRNA for TLR2/4 after vitamin D dosing (Do *et al*., 2008). The reason for the apparent differences between these two studies remains unknown and further studies *in vivo* are needed to fully elucidate the potential benefits of vitamin D supplementation in health and in CVD.

Animal models of CVD and Calcitriol or paracalcitriol (synthetic VDR activator) supplementation have shown favourable results with improved cardiac function

(Artaza *et al*., 2011, Mancuso *et al*., 2008, Bodyak *et al*., 2007). However specific pathway studies have not been designed to explore the role of Calcitriol supplementation in an *in vivo* animal model relevant to inflammation. Vitamin D has shown to inhibit stress kinases p38, JNK and reduce TNF-α production in keratinocytes (Ravid *et al*., 2002). Such anti-inflammatory effects support a role for vitamin D in the treatment of dermatological disorders. As previously discussed in the *Introduction (Mitogen Activated Protein Kinases)* DUSP-1 can deactivate MAPK p38 attenuating pro-inflammatory responses. MSK 1/ 2 KO mice have an endogenous depletion in DUSP-1 giving one explanation for the hyper-inflammatory responses observed in MSK 1/ 2 KO mice and a potential mediator for the onset of microvascular dysfunction in these mice. Calcitriol has previously shown to increase the expression of DUSP-1 in bone marrow derived macrophages, thus attenuating MAPK p38 activation (Zhang *et al*., 2012). This study also showed an anti-inflammatory effect of Calcitriol treatment in the reduction and the release of pro-inflammatory cytokines TNF-α and IL-6. Evidencing the anti-inflammatory properties of Calcitriol on the innate immune system. Calcitriol has also shown to up regulate the production of anti-inflammatory molecule IL-10 (Heine *et al*., 2008) another deficiency in MSK 1/ 2 KO mice when compared to WT controls. The MSK 1/ 2 KO mouse model might therefore be suitable for the study of vitamin D in CVD, through assessment of endothelial function and systemic inflammation. MSK 1/ 2 KO mice display endogenous depletions in IL-10 and DUSP-1, described targets for Calcitriol. Furthermore MSK 1/ 2 KO mice display endothelial dysfunction and systemic inflammation, both which have been shown by others (Sugden *et al*., 2008, Borges *et al*., 1999) to be attenuated by vitamin D dosing.

Aim

To better understand the role of vitamin D supplementation in inflammatory prone MSK 1/ 2 KO-cholesterol fed mice in vascular function, blood pressure and systemic cytokine expression.

Methods

The methods description below is intended to provide an overview of experimental techniques used in this study. Further experimental details are described in *Materials and Methods Pages 62-92.*

Animals

Animals from the breeding strain MSK 1/ 2 were randomly allocated into two groups both were fed a pro-atherogenic diet.

Pharmacological Intervention

Standardised samples containing 200 ng Calcitriol (Cambridge Bioscience, UK) /250µL 0.5% carboxy meythcellulose were prepared and stored at -20^{o}C until used. This concentration has been used previously in an animal model of CVD (Takeda *et al*., 2010). Animals were gavaged twice weekly for the study duration (16 weeks) using a steel needle and a 1ml syringe. 0.5% carboxy meythcellulose was used as a vehicle control and administered to the control group.

Body Weight

Animals were weighed at study baseline and 16 weeks.

Longitudinal Assessment of Vascular Function

In vivo assessment of endothelium-dependent and endothelium-independent responses were assessed at study end point only (16 weeks) due to equipment availability.

Spleen Mass

Spleen mass was assessed at 16 weeks.

Cardiac Hypertrophy

Cardiac hypertrophy was assessed post mortem at 16 weeks.

Plasma Cholesterol

Measurements for LDL/vLDL and HDL were made at 16 weeks only.

Cytokine Expression

Measurements were made at study baseline and 16 weeks.

Blood Pressure

Blood pressure parameters (systolic, diastolic and mean arterial blood pressure and heart rate) were assessed *in vivo* at 16 weeks, due to equipment availability blood pressure was not assessed in previous studies and was only used for 16 week measurements in this study.

Results

Body Weights

MSK 1/ 2 KO mice in Calcitriol and vehicle treated groups had similar baseline (vehicle 27±1g VS. Calcitriol 28±1g, P>0.05) (**Figure 8.2A**) and 16 week measurements for body weights (**Figure 8.2B**) (vehicle 28±1g VS. Calcitriol 28±1g, P>0.05).

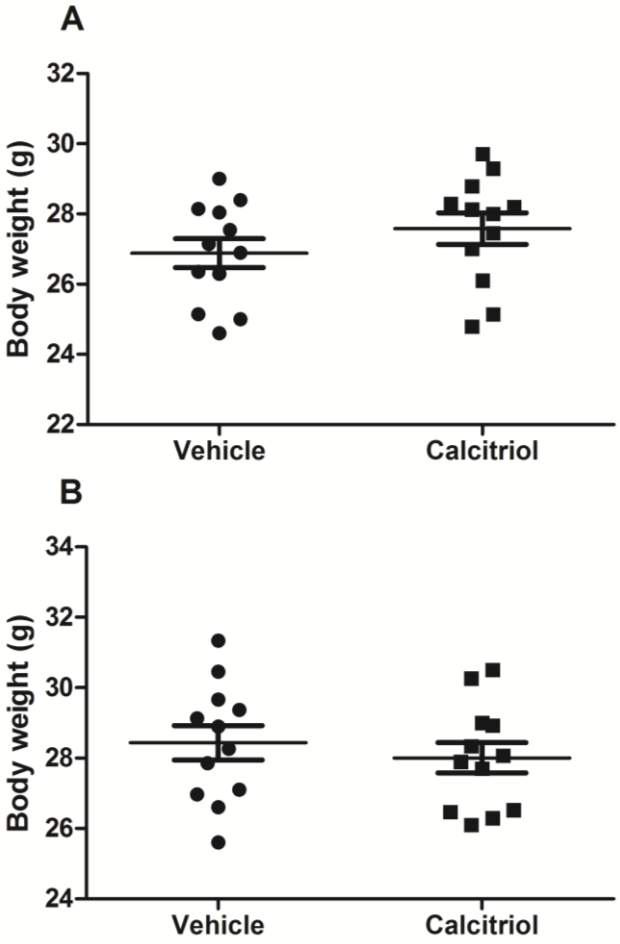

Figure 8.2. Body weights: Baseline (week 0) (A) and end point (16 weeks) (B) body weights in grams (g) in MSK 1/ 2 KO-cholesterol fed mice treated with vehicle (n =12) and Calcitriol (n =12). Results are group means ±SE. Unpaired Student's t-test.

Cardiac Hypertrophy

Calcitriol supplemented mice had significantly less cardiac mass (142±4 mg) when compared to vehicle treated animals (151±3 mg) (P<0.05) (**Figure 8.3A**). There were no significant differences between tibia lengths between the groups

(vehicle 18.0±0.2mm vs Calcitriol 18.0±0.1mm, P>0.05) (**Figure 8.3B**). Calcitriol treated mice had a significantly lower cardiovascular hypertrophy measurement (7.8±0.2) when compared to vehicle treated mice (8.9±0.1, P<0.05) (**Figure 8.3C**).

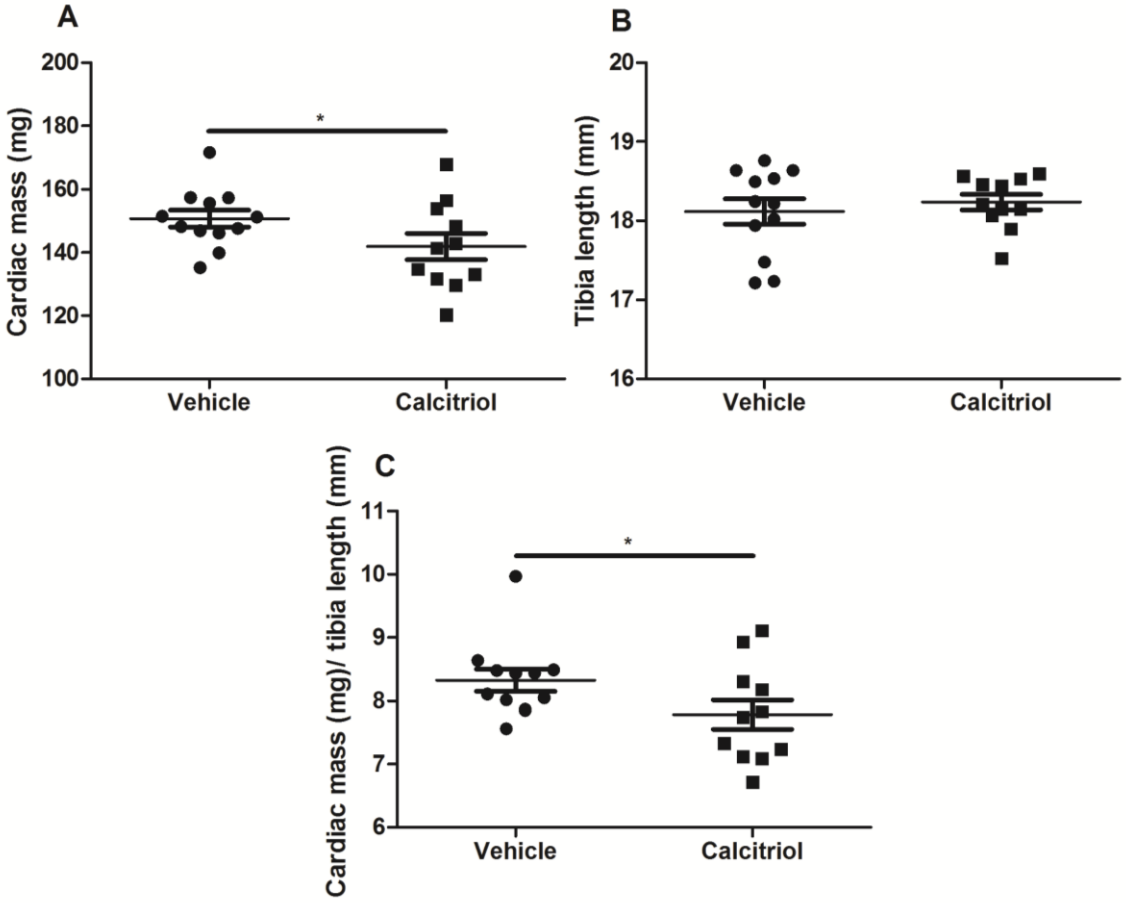

Figure 8.3. Cardiac hypertrophy: (A) cardiac mass (mg) (B) average tibia length (mm) and (C) cardiac hypertrophy (cardiac mass (mg)/ average tibia length (mm) in MSK 1/ 2 KO-cholesterol fed mice treated with vehicle (n =12) or Calcitriol (n =11). Results are group means ±SE. Unpaired Student's t-test

Spleen mass

Calcitriol treated mice had lighter spleens (117±8 mg) when compared to vehicle treated animals (133±8 mg) however these observations did not meet statistical significance (P >0.05) (**Figure 8.4**).

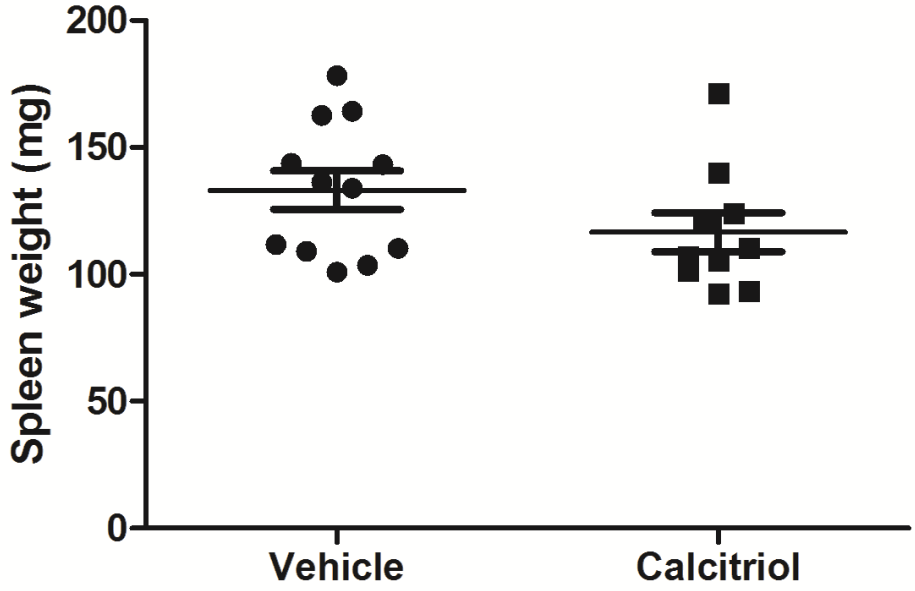

Figure 8.4. Spleen mass: Spleen weight (mg) at 16 weeks in MSK 1/ 2 KO-cholesterol fed mice treated with vehicle (n =12) or Calcitriol (n =10). Results are group means ±SE. Unpaired Student's t-test.

Blood Pressure

Systolic Blood Pressure

Terminal systolic blood pressure was lower in Calcitriol treated animals (117±4 mmHg) when compared to vehicle treated mice (127±5 mmHg) however this did not reach statistical significance (P >0.05) (**Figure 8.5A**).

Diastolic Blood Pressure

Terminal diastolic blood pressure was significantly lower in Calcitriol treated animals (82±4 mmHg) when compared to vehicle treated mice (93±4 mmHg) (P <0.05) (**Figure 8.5B**).

Mean arterial pressure (MAP)

Terminal MAP was significantly lower in Calcitriol treated animals (82±4 mmHg) when compared to vehicle treated mice (93±4 mmHg) (P<0.05) (**Figure 8.5C**).

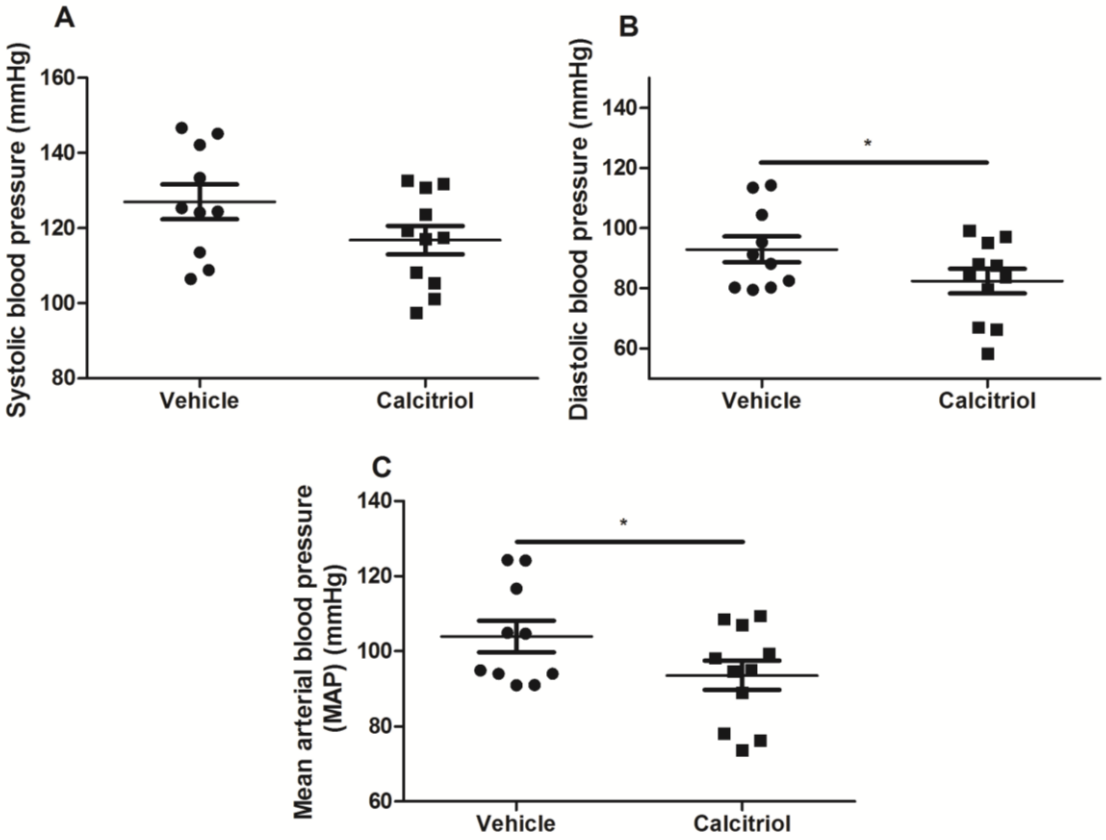

Figure 8.5. Blood Pressure: 16 week measurement of (A) diastolic blood pressure, (B) systolic blood pressure and (C) mean arterial pressure (MAP) (mmHg ±SE) in MSK1/ 2 KO-cholesterol fed mice supplemented with vehicle (n =10) and Calcitriol (n =11). Results are group means ±SE. Unpaired Student's t-test. *P<0.05.

Vascular Function

Endothelium-dependent

Endothelium-dependent vasodilatation to ACh was significantly greater in Calcitriol treated mice (296±6 AU) when compared to vehicle treated animals (272±6 AU) (P<0.01) (**Figure 8.6**).

Endothelium-Independent

There were no significant differences for endothelium-independent responses between the groups (vehicle 326±9 AU VS. Calcitriol 339±15 AU, P>0.05) (**Figure 8.6B**).

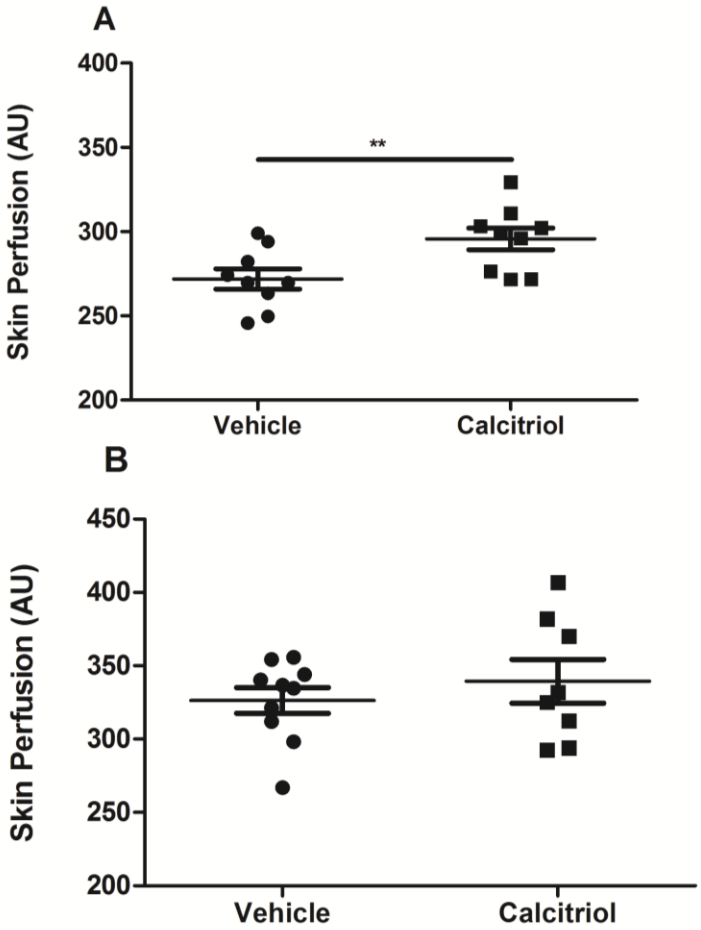

Figure 8.6. Vascular function: 16 week measurement of (A) endothelium-dependent and (B) independent responses (AU) in MSK 1/ 2 KO-cholesterol fed supplemented with vehicle (n =10) and Calcitriol (n =11). Results are group means ±SE Unpaired Student's t-test. **P<0.01

Plasma Cholesterol

HDL

There were no significant differences for HDL between the groups (vehicle 15±2 mg/dl vs Calcitriol 16±3 mg/dl, P>0.05) (**Figure 8.7A**).

LDL/vLDL

There were no significant differences for LDL/vLDL between the groups (vehicle 10±1 mg/dl vs Calcitriol 13±2 mg/dl, P>0.05) (**Figure 8.7B**).

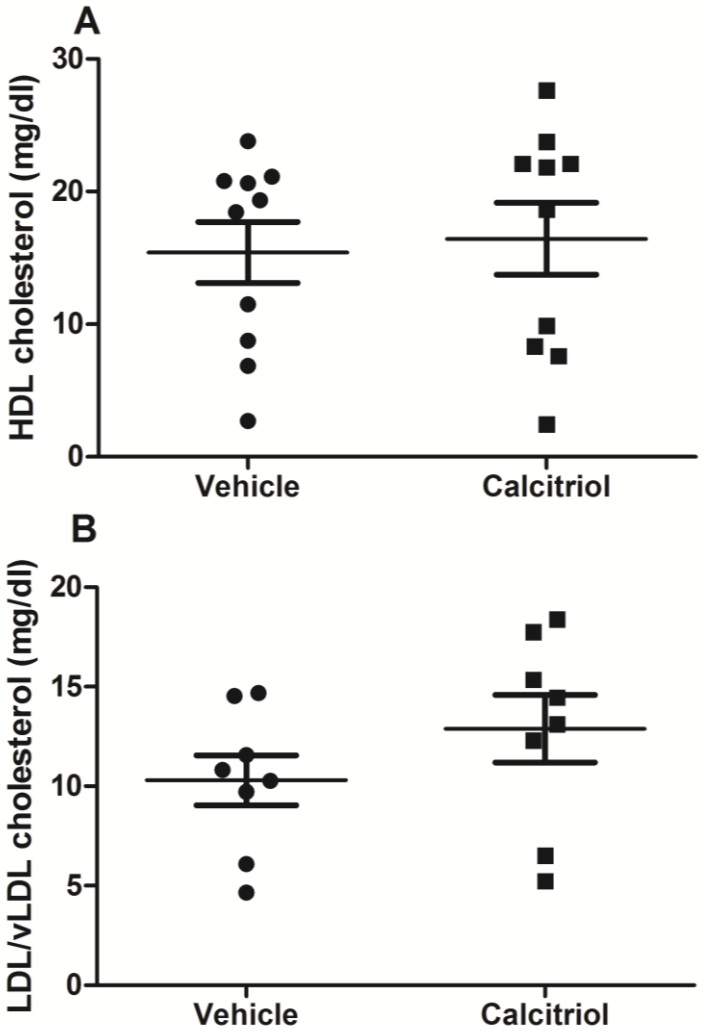

Figure 8.7. Plasma cholesterol: 16 weeks measurements of plasma (A) high density lipoprotein (HDL) and (B) low density lipoprotein and very low density lipoproteins (LDL/vLDL) in MSK 1/ 2 KO-cholesterol fed vehicle(n =10) and Calcitriol (n =10) supplemented mice. Results are group means ±SE. Student's t-test

Baseline Cytokines

There were no significant difference for baseline cytokines between the groups for IL-6 (vehicle 1344±18 pg/ml VS. Calcitriol 1408±37 pg/ml, P>0.05) and IL-10 (vehicle 175±6 pg/ml VS. Calcitriol 198±19 pg/ml, P>0.05), however there was

a significant differences for IL-1α (vehicle 1170±8 pg/ml vs Calcitriol 1211±17 pg/ml, P<0.05) between the groups (**Figures 8.8 A-C** respectively).

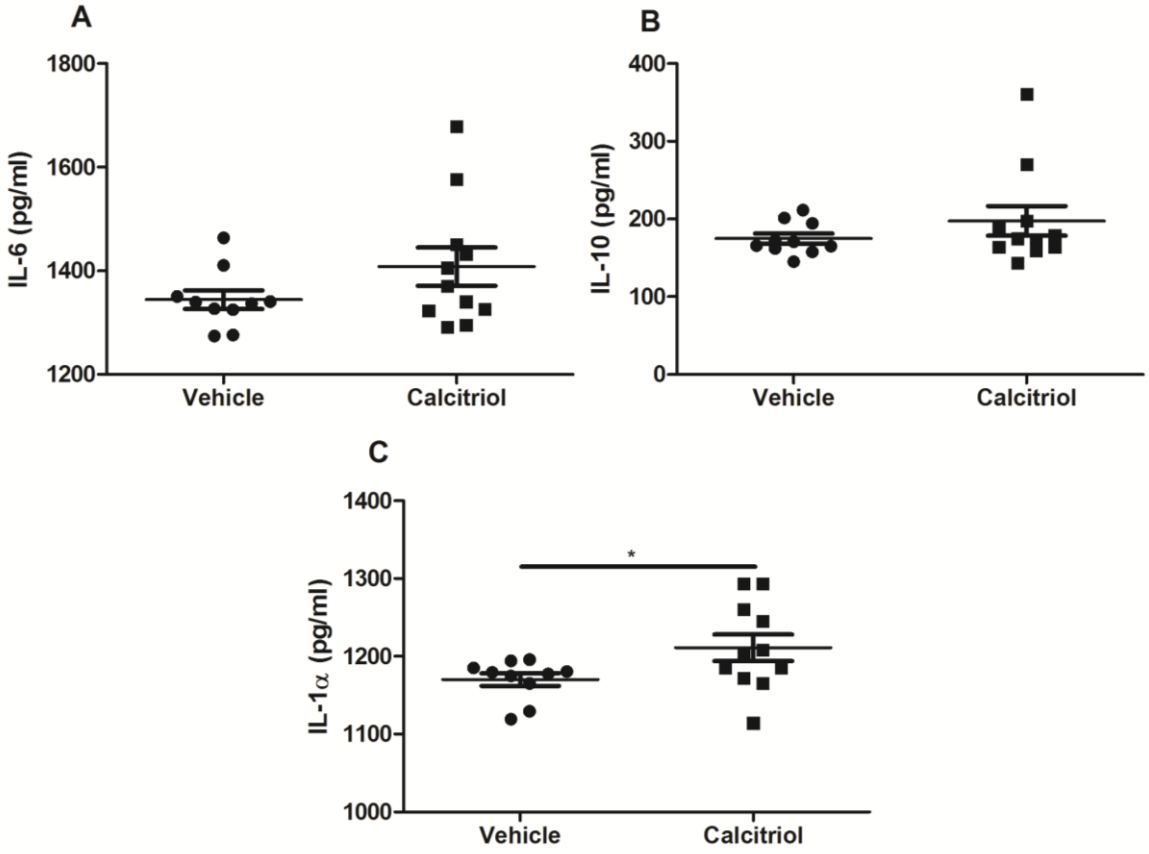

Figure 8.8. Study baseline inflammatory markers: Baseline plasma inflammatory markers (A) IL-1α, (B) IL-10 and (C) IL-6 (pg/ml) in MSK 1/ 2 KO-cholesterol fed, vehicle (n =10) and Calcitriol (n =11) treated mice. Results are group means ±SE. Unpaired Student's t-test. *P<0.05

16 Week Measurement of Cytokines

There were no significant differences in cytokine expression between vehicle and Calcitriol treated mice for IL-1α and IL-10, (**Figure 7.7A/B** respectively). However IL-6 (vehicle 1285±9 pg/ml VS. Calcitriol 1356±32 pg/ml, P<0.05) was significantly greater in the Calcitriol supplemented group (**Figure 7.7-C**).

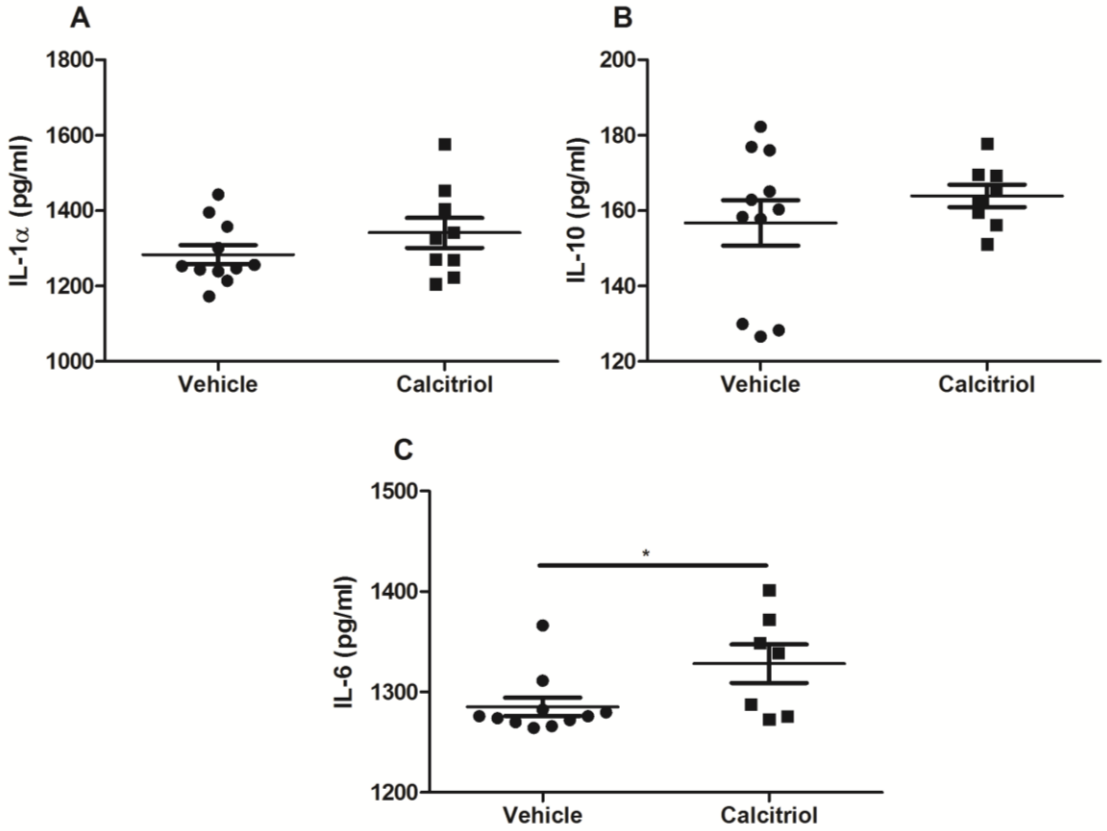

Figure 8.9. Week 20 plasma measures of cytokines: Week 16 measurement of (A) IL-1α, (B) IL-6 and (C) IL-10 (pg/ml) in MSK 1/ 2 KO-cholesterol fed, vehicle (n =11) and Calcitriol (n =8) treated mice. Results are group means ±SE. Unpaired Student's t-test. *P<0.05

Correlations

At study endpoint several significant correlations for spleen weight VS.: cardiac mass (r= 0.480, P<0.05), cardiac hypertrophy measurement (r= 0.464, P<.05) and plasma HDL (r= -0.499, P<0.05) were found. ACh responses correlated with 16 week measurements of IL-10 (r= -0.604, P<0.05).

Discussion

The main findings from this study show that MSK 1/ 2 KO-cholesterol fed mice supplemented with Calcitriol have better endothelium-dependent vasodilatation *in vivo* as evidenced by measurements of skin microvascular responses to ACh. Maximal dilatory capacity to localised skin heating was not significantly different

between groups, suggesting modulation at the level of the endothelium. Calcitriol supplemented animals had lower systemic blood pressure, lower cardiac mass and lower cardiovascular hypertrophy. These data suggest a possible protective role for vitamin D in the development and progression of inflammation induced CVD.

Takeda *et al* (Takeda *et al*., 2010) have previously shown reduced atherosclerosis in ApoE KO mice when supplemented with Calcitriol orally (200ng). In agreement with the current study, showing preserved endothelial function, an early event in atherosclerotic plaque formation. The frequency of administration and dose were similar in this and the previous study by Takeda *et al*. However, Takeda *et al* also found reduced levels of tissue macrophages and increased levels of IL-10, findings that are not consistent with the present study. Zhang *et al* (2012) reported that vitamin D was able to specifically up regulate DUSP-1 and attenuate the expression of TNF-α and IL-6 in peripheral blood monocytes from humans and in mouse bone marrow derived macrophages. MSK 1/ 2 KO mice display reduced levels of DUSP-1 and this in part is thought to mediate their hyper-inflammatory predisposition to endotoxin shock when challenged with a bolus injection of LPS (Ananieva *et al*., 2008, Zhang *et al*., 2012).

The present study sought to establish the role of vitamin D in inflammatory cytokine expression; there were no significant differences between plasma levels of IL-1α and IL-10 between the experimental groups in this study. However plasma levels of IL-6 were significantly greater in Calcitriol supplemented mice, an unexplained finding. Previous studies have shown reduced mRNA expression of TNF-α, IL-6 and IFN-gamma in Calcitriol

supplemented cells, an effect that can be blocked with the addition of the vitamin D receptor antagonist TEI-9647 (Diaz *et al*., 2009). Previous studies have also shown that anti-inflammatory levels of IL-10 are associated with increased plaque formation (Mallat *et al*., 1999) in mice. Barrera *et al* (2012) showed that Calcitriol supplementation to trophoblasts (the outer layer of cells in a blastocyst that provides nutrients to the growing embryo) reduced IL-10 expression. This is in contrast to the hypothesis that the anti-inflammatory effects of Calcitriol supplementation in the context of CVD are mediated by the resolution of inflammation, through increased expression of negative regulators of inflammation such as IL-10 and DUSP-1. The reduced effects of IL-10 expression in a study by Barrera *et al* were also associated with reduced TNF-α production. It is believed Calcitriol contains a DNA binding domain and it is hypothesised that Calcitriol can negatively regulate inflammatory responses through the vitamin D receptor (Barrera *et al*., 2012, Takeda *et al*., 2010). These findings however are not consistent with the present *in vivo* study, where there were no significant differences in plasma cytokines for IL-1α, IL-10 but a significant increase in plasma IL-6.

One possible explanation for the unaltered levels of IL-10 in this study may be in part mediated by the MSK 1/ 2 KO phenotype. These mice display significantly reduced levels of IL-10 when compared to WT mice (Ananieva *et al*., 2008) and the Calcitriol supplementation may not have been sufficient to restore the genetic defect mediated through a loss of MSK 1/ 2. Importantly the study end point measurements for IL-10 between this and the study (plasma IL-10) conducted by Takeda *et al* (IL-10 mRNA) were different and it is possible that vitamin D dosing in MSK 1/ 2 KO mice may have induced differences in mRNA levels but not translated in to plasma protein levels. Furthermore the

previous studies detailing the anti-inflammatory Calcitriol may not be applicable in this model (MSK 1/ 2 KO mice). The predisposition to hyper-inflammation may be greater in MSK 1 2 KO mice such that they may mask the anti-inflammatory effects mediated by Calcitriol.

The immune modulator effects of the vitamin D receptor, a super family of vitamin A receptors is through gene regulation. The biologically active hormone, Calcitriol binds to the VDR and associates with specific sequences called vitamin D responsive elements (VDRE) that are found in the promoter region of genes and thus functions as an inducible transcription factor. Binding to the ligand-binding domain (LBD) of the VDR induces dimerization with retinoid X receptors. Resulting heterodimers bind DNA to VDRE and up regulate gene expression. The VDR-LBD interaction is this essential for ligand dependent transcription (Ito *et al*., 2013). Humans and animals aberrant in vitamin D display a higher risk of infection (Thornton *et al*., 2013, Thornton *et al*., 2014) (Cantorna *et al*., 2004) and this is thought to be mediated by deficient macrophage function. Therefore the protective effects of Calcitriol as noted by previous studies on the regulation of gene expression may be more applicable to subclinical acute inflammation. The MSK 1/ 2 KO mouse model is indicative of low grade, sub clinical inflammation when challenged with a cholesterol diet, however this phenotype as characterised in a previous chapter is inherently chronic, resulting in the progressive deterioration of microvascular function and the current dose and dosing period of Calcitriol may not have been sufficient to significantly affect protein levels of pro-inflammatory cytokines. Previous studies have shown dose dependent inhibition of TNF-α production in peripheral blood monocytes from patients (Panichi *et al*., 1998), a similar experimental approach

using mouse bone marrow derived macrophages may yield better mechanistic insight the role of vitamin D in inflammatory gene expression.

In contrast to these reports Sun and Zemel (2008) shows pro-inflammatory effects of Calcitriol supplementation in adipocytes and macrophages. Using the mouse macrophage cell line RAW 264.7 Sun and Zemel (2008) shows that Calcitriol can up regulate TNF, IL-6 and MCP-1 in a Ca^{2+} dependent manner, through attenuated expression after using the calcium channel inhibitor Nifedipine (Sun and Zemel, 2008). It is however important to note that this study was conducted in an isolated, *in vitro* setting that is devoid of humoral factors in the blood and tissue, and may not be representative of *in vivo* effects of vitamin D as observed in the present study.

TLR activation also induces the activation of NF-kB. Previous studies have reported reduced chemokine expression after Calcitriol supplementation *in vitro*, an effect mediated by inhibition of IkB phosphorylation and NF-kB activation (Kavandi *et al*., 2012). Although not addressed in the current study, it is possible that the apparent protective vascular and cardiovascular phenotype observed in Calcitriol treated mice is in part through the modulation of other transcription factors such as NF-kB (De Filippo *et al*., 2013), therefore it is important to note that the results from this *in vivo* study may be multi-modal.

Vitamin D has been described to have pleiotropic effects , in particular vitamin D supplementation has shown protection from hydrogen peroxide (H_2O_2) formation in endothelial cells *in vitro* (Polidoro *et al*., 2013) (Kallay *et al*., 2002, Wu *et al*., 2011), a contributor to endothelial dysfunction. The protective blood pressure effects observed in this study through Calcitriol supplementation may be mediated through preserved endothelial function in the peripheral circulation.

Peripheral resistance increases as the small blood vessels (such as the skin microcirculation) become dysfunctional; a loss of NO would result in an altered, more constricted vascular lumen. Great force is needed to pulsate blood to distal tissues through narrow arteries and thus cardiac hypertrophy is one mechanism by which this achieved. Specific cardiac myocyte deletion of the VDR results in cardiac hypertrophy in the hearts of mice through potential suppression the pro-hypertrophic pathways and increased expression of arterial natriuretic peptide (Chen *et al*., 2011).

In conclusion, this study shows that Calcitriol supplementation to inflammatory prone MSK 1/ 2 KO-cholesterol fed mice resulted in a degree of CVD-protection. Measured by endothelium function, cardiac mass, blood pressure and cardiac hypertrophy. The protection observed is not supported by the resolution of plasma inflammatory molecules and thus further work is required to better understand the role of Calcitriol in vascular dysfunction relevant to the MSK 1/ 2 pathway. Targeting specific components of the Calcitriol pathways may offer a novel therapeutic option for inflammatory mediated pathologies such as CVD. These data are in line with conflicting data previously published.

Chapter 9

Discussion and Future work

Aim of Thesis

The aim of this thesis was to develop the understanding of the inflammatory pathways involved in early CVD development through assessment of vascular function *in vivo*.

Key Findings

The studies in this thesis show that the changes in skin microvascular function are representative of underlying pathophysiology and therefore the novel experimental set-up can provide a useful tool for exploring specific pathways and mechanisms underlying the development and progression of CVD in animal models. Importantly attenuated responses in the skin microcirculation to ACh are indicative of the changing systemic inflammatory burden through the release of pro-inflammatory cytokines into the systemic circulation, as evidenced by cholesterol feeding in WT mice and assessment of vascular function and cytokine levels in the plasma of MSK 1/ 2 KO and ABIN1(DN485) mice. The key findings are summarised in **Figure 9.1**.

The novel finding that deletion of MSK 1/2 produced a marked inflammatory state with consequent early endothelial dysfunction and reduced NO, without overt clinical disease offers an innovative avenue for therapeutic intervention to limit CVD in humans. Activators of MSK 1/ 2 may be used to address a wide range of inflammatory mediated pathologies relevant to CVD including MI and stroke. Furthermore, studies interrogating irregularities in the MSK 1/ 2 pathway may in part contribute to the knowledge of why there is significant disease heterogeneity in human CVD, and may in part explain the onset of CVD in otherwise healthy individuals that do not display traditional risk factors such as

high plasma cholesterol or obesity. This hypothesis is supported by the onset of microvascular dysfunction in MSK 1/ 2 KO-chow fed mice that were not exposed to a CVD risk factor, dietary cholesterol.

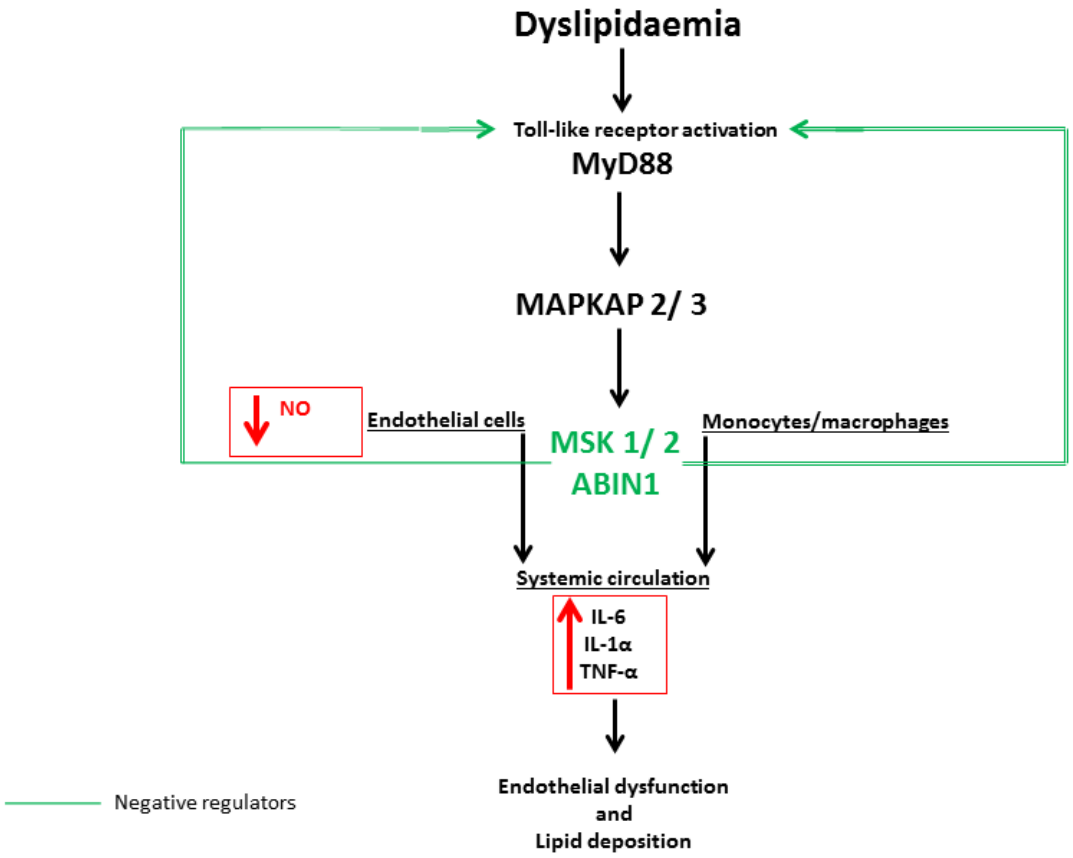

Figure 9.1. Summary of key findings: Myeloid differentiation primary responses 88 (MyD88), mitogen-activated-protein kinase activated proteins 2/ 3 (MAPKAP 2/ 3), mitogen and stress activated kinases 1 /2 (MSK 1/ 2), A20-binding inhibitor of NF-κB-1 (ABIN1).

An inability to negatively regulate pro-inflammatory signals after TLR stimulation can therefore be associated as a CVD risk factor as evidenced by the second unique finding in this thesis that polyubiquitin-binding-defective ABIN1[D485N] mice are prone to CVD. The phenotype in ABIN1(DN485) mice was further exacerbated by cholesterol feeding, a conclusion that offers additional

therapeutic promise to limit inflammation induced CVD relevant to patient cohorts (SLE and RA) that displays enhanced CVD risk, a currently unexplained phenomenon. A cessation or strict regulation of saturated fats and dietary cholesterol that is associated with an increased risk of CVD in rheumatoid patients may help reduce the significant CVD burden. Data in this thesis support the notion that increased NF-κB activation has significant negative effects on the cardiovascular system. TLR2 and TLR4 activation is regarded as a key event in the pathophysiology of CVD (Bjorkbacka *et al*., 2004, Cole *et al*., 2013, Falck-Hansen *et al*., 2013, Mullick *et al*., 2005, Tobias and Curtiss, 2007) and is associated with atherogenesis, whereas blockade of this signalling pathway, achieved by amelioration of the MyD88, has shown atheroprotection previously (Bjorkbacka *et al*., 2004). Similarly the SLE phenotype of the ABIN1[D485N] mice is abrogated when they are expressed on a MyD88-deficient background (Nanda *et al*., 2011), indicative of overlap in the signalling pathways involved in the development of SLE and CVD.

More broadly applicable to the onset of CVD, truncation of cytokine signalling through knock-down of innate immune signalling in this thesis (MyD88 and MAPKAP 2/3 KO) show preserved endothelial function through abrogated systemic cytokine expression and preserved NO . Conferring with the notion that blockade of innate immune signalling relevant to reduced atherosclerotic plaque formation in previous studies also protects against endothelial dysfunction *in vivo* through diminished systemic cytokine production and preservation of NO (Bjorkbacka *et al*., 2004, Jagavelu *et al*., 2007).

Numerous studies have focused their investigation on inflammatory stimuli that can initiate the activation of innate immune responses and the release of pro-

inflammatory mediators, such that there is now a broad literature base showing the activation of specific TLRs (Kawai and Akira, 2009). The studies in this thesis support with the notion that that TLR activation in excess is detrimental to vascular function as evidenced by the onset of early CVD in MSK 1/ 2 KO and ABIN1(DN485) mutant defective mice.

The physiological importance of endogenous negative feedback mechanisms after the activation of TLR in MSK 1/ 2 KO and ABIN-1 mutant defective mice demonstrates the essential need for successive deactivation of effector pathways after receptor stimulation. This notion, that cytokine expression is detrimental to vascular function is supported by the MyD88 and MAPKAP 2/ 3 KO mouse studies; an inability to stimulate cytokine expression confers vascular protection in the face of an established risk factor, dietary cholesterol.

Selectively targeting these pathways may provide a novel tool to limit inflammatory mediated CVD. The ability to manipulate these intrinsic mechanisms holds great therapeutic potential, allowing selective activation of mediators that suppress inflammation without blocking inflammatory pathways of host defence to pathological organisms. In particular TLRs are important in host defence for the detection of bacterial products for clearance, blockade of these signals would compromises host immunity such that it would resemble the clinical scenario of a patient on immunosuppression therapy or individuals suffering from the human immunodeficiency virus. The work detailed in the previous chapters highlights the lack of therapeutic targets in clinical medicine that selectively target endogenous pathways and sequentially promote the resolution of inflammation, however these studies offer a unique therapeutic approach that will be broadly be applicable to numerous inflammatory mediated

pathologies including MI and stroke. In particular it will be of key importance to establish the role of MSK 1/ 2 in MI. The bi-phasic monocyte response observed after the myocardium becomes ischaemic is a key contributor to myocardial damage and a contributor to heart failure after infarction. The cell polarity of MSK 1/ 2 KO macrophages must be established in CVD as selective activators may promote healing (through the resolution of inflammation) of the myocardium after an acute event, similar reports have been shown through the use of angiotensin inhibitors (Leuschner *et al*., 2010a).

Similar approaches in CVD testing in humans have previously shown that RA patients have attenuated endothelium-dependent responses in the skin microcirculation. In addition, the degree of attenuation is related to the expression of systemic inflammatory cytokines (Galarraga *et al*., 2008), these findings are similar to those presented in this thesis. Since endothelium-dependent responses in the microcirculation of the skin are indicative of defective coronary function (Khan *et al*., 2008b) and future cardiovascular sequelae before clinical presentation (Khan *et al*., 2005), the findings from this thesis highlight the important role for innate immunity in the development and progression of inflammation-induced CVD. The technique described in this thesis offers a mode of research translation, allowing CVD in patients to be studied further with the use of animal models, answering key questions in the pathophysiological complexity of human CVD.

The studies in this thesis aimed to establish a role for candidate kinases in inflammatory-induced CVD development through assessment of endothelial function and measurement of systemic cytokine expression. In conclusion, these are the first *in vivo* observations to document the early development of

CVD (endothelial dysfunction) as a result of a single protein mutation involved in NF-κB signalling. Similarly MSK 1/ 2 are mediators of vascular dysfunction and targeting the MAPKAP 2/3 pathway and/or selective inhibition of TLRS through MyD88 inhibition, with agents that block their action might provide a useful therapeutic option for inhibiting inflammation induced endothelial dysfunction and CVD.

Limitations

Rodent models of LDI

Genetically altered mice were used in these investigations to better understand the role of innate immune signalling cascades in the pathogenesis of endothelial dysfunction. It is important to note that rodent skin varies considerably to that of humans and responses to the iontophoresis of vasoactive chemicals may be significantly different when compared to similar experimental approaches in clinical cohorts. For example mice have a densely packed fur coat, which they maintain through grooming. The density of hair follicles in rodent skin is greater than that of human skin, an important limitation to note as ion movement during iontophoresis is facilitated through hair follicles and therefore the rodents used in studies detailed in this thesis may have shown a greater vasodilator capacity when compared to humans, through a greater net movement of ions through hair follicles. Nonetheless ion movement during iontophoresis is largely dependent on the duration of current (the length of the iontophoresis protocol) and it is important to note that the studies in this thesis used a protocol that was similar to those used in humans clinical studies and that animals of the same genetic background were used to reduce variability in drug iontophoresis

responses. Importantly values obtained from rodent studies in this thesis are comparable to attenuated responses obtained in human studies. Thus reduced responses as observed by attenuated vasodilator responses to endothelium-dependent agonist ACh in the skin microcirculation in mice are comparable to the human clinical scenario, however a direct comparable study is needed for validation. A study by Schuler *et al* (2014) has previously compared endothelium-dependent responses in the mouse using Doppler flow-mediated vasodilatation and concludes that the physiology observed in the mouse is similar to that in humans, re-instating the high suitability of non-invasive techniques for the measurements of endothelial function in both humans and mice.

Murine model systems have grown in popularity due to a greater operator control of pathophysiology through combined genetic alterations and diet interventions, similar to the studies in this thesis where genes of interest can be deleted, mutated and animals can be fed specifically tailored diets. The sequencing of the human and mouse genome has revealed 300 genes that are uniquely expressed in both humans and mice, Mestas and Hughes (2004) have previously discussed the major differences between the two species in relation to the immune system and the short comings of using rodent models for modelling human clinical disease. The major differences between the mouse and the human physiology have previously been widely reported, such that there are numerous studies that have shown effective therapies in mice but limited efficacy in humans. Human circulating blood is neutrophil rich and this is contrary to murine blood that is lymphocyte dense. The studies in this thesis have focused on the ability of the vascular endothelium to respond to stimuli

and induce endothelial cell activation, a pre-requisite for the tethering of monocytes for subsequent transmigration. Monocytes respond to environmental stimuli through numerous receptor mediated pathways and the TLRs are the predominately studied system for pro-inflammatory responses. There are a number of differences between mouse and human TLR expression, firstly the number of discovered TLRs in the human and mouse vary, as previously discussed in the '*Introduction – Toll like receptors and inflammation' and illustrated in Figure 1.4 (extracellular and intracellular expression of TLRs)* humans have 10 TLRs and the mouse 13. Nonetheless the ability to purify proteins from rodents is easier and has facilitated research in solving the structure of the TLRs, importantly murine TLRs provide a framework for understanding the biochemical basis for receptor function in the absence of human evidence. Although the mouse may be a suitable model for some pathological disease processes such as atherosclerotic plaque formation and MI, murine studies investigating hypersensitivity have been limited. The ectodomain of TLR4 an important ligand in inflammation mediated CVD in humans and in mice does not respond to nickel sensitisation in mice, unlike humans who can develop contact dermatitis upon exposure. In humans, nickel atoms can chelate histidines residues found in the ectodomain of TLR4 and induce activation of the receptor, these histidines are absent in the mouse and rodent models of human pathology must therefore carefully selected. Schuler *et al* (2014) demonstrated the fundamental similarity in endothelium-dependent vasodilatation in humans and mice and confirmed the dependency of the response on eNOS and NO. Furthermore genetic alteration and knock-down of innate immune protein has allows researchers to precisely map the function of immune proteins (Bryant and Monie, 2012). Thus the use of the mouse in

scientific investigation can be both useful and limiting. Subsequent investigations modelling human clinical disease should be carefully monitored for physiological and biochemical similarity.

Barrier Breeding Facility VS. Conventional Unit.

Animals were initially bred and maintained in a barrier breeding facility and subsequently transferred to a conventional unit for vascular function testing. It is possible that the acute stress induced from transferring the animals from the barrier breeding facility to another site for vascular testing, coupled with their hyper-inflammatory phenotype is responsible for the initial differences in body weights and plasma cytokines in the various studies. Animals were allowed a minimum of 7 days to acclimate before commencement of vascular studies and it is possible that animals like the ABIN1(DN485) and the MSK 1/ 2 KO mice may need a longer habitualisation period than their WT counter parts. Rudd *et al* (2013) has previously reported a loss in appetite in mice subjected to inflammation both acutely and chronically. The immune induced anorexia response is dependent on MyD88 in myeloid cells. It has previously been shown that ABIN-1 (D485N) mice crossed on to an MyD88 deficient background are rescued from the SLE phenotype and work within this thesis shows that MyD88 KO mice had significantly higher body weights than their WT counter parts at study baseline, unlike MSK 1/ 2 and ABIN1(DN485) mice. Further studies examining the role of inflammation on appetite regulation in response to acute stress may therefore be favourable.

Cholesterol Challenge

C57BL/6 WT mice have endogenously high levels of HDL. Dietary cholesterol does not significantly impair (reduce) HDL plasma in C57BL/6 WT mice, a reduction otherwise associated with an increased risk for CVD. Diets that are routinely used in metabolic studies are higher in fat (>40% fat) and may therefore be tested in this model of vascular pathophysiology, to assess whether a similar pattern of dysfunction is observed.

Mouse Model Generation

Animal models used in this thesis were specifically generated from embryonic stem cell lines from 129S2/SvPasCrl animals and subsequently backcrossed to C57BL/6 mice. A documented passenger gene locus effect has previously been described (Lusis *et al*., 2007). Genes that contain significant polymorphisms from the embryonic mouse to the backcross mouse strain may affect the overall phenotype, allowing conclusions to be drawn that at not inherently based on a KO or induction of a transgene, with the possible introduction of numerous 'sister' genes and/ or deletions. In order to better understand the effect of passenger genes on the described phenotypes, animals may therefore be backcrossed onto other mouse lines and retested for the onset of endothelial dysfunction.

Future work

Technique Development

Development of Iontophoresis

Future work could establish additional iontophoresis protocols for bradykinin, methacholine and histamine, vascular agonists that are used routinely in *ex vivo* research. These molecules have shown specificity for vascular pathways of vasodilatation, however their *in vivo* effects remain poorly defined in animal models of inflammation. In conjunction with the development of other agonist based protocols and the use of inhibitors such as indomethacin would allow further interrogation of the skin microvascular network. Mechanisms such as prostaglandins, an eicosanoids derived from cyclooxygenase produced by mammalian cells with a role in local tissue homeostasis. Importantly prostaglandins can modulate vascular tone under basal conditions and platelet aggregation, therefore the role of the described inflammatory pathways in relation to prostaglandin induced vasodilatation may offer further insights in to the multimodal nature of endothelial dysfunction *in vivo*.

Imaging

LDI in the context of small animal vascular research could further be developed for the application of full field laser perfusion imaging (FLPI), known as laser speckle contrast imaging. FLPI uses video frame rate acquisition, where 25 images per second can be recorded for transient changes in flow, something not possible by standard LDI. This may permit the use of a shorter vascular (iontophoresis protocol) reducing the length of time that an animal is under general anaesthetic and allow faster more transient changes in flow to be monitored.

Future Studies

Sex Dependent Studies

All studies described in this thesis were specifically carried out on C57BL/6 male mice. The use of LDI and iontophoresis in humans has shown impairment of the skin microcirculation in the context of preeclampsia, animal models of the hypertensive disorder have been described previously (Davisson *et al*., 2002), however the *in vivo* effects on endothelial function in this model have not been addressed. Furthermore research reveals that women are more likely to suffer an adverse cardiovascular event than males and diseases such as SLE are more prevalent in females. Thus application of this technique into sex specific pathologies would therefore be favourable.

Backcrossing

The animal models used in this thesis were specifically maintained on a C57BL/6 background for the study of endothelial dysfunction, however the MSK 1/ 2 and ABIN1 models could provide further insight into the atherosclerotic process. The hyper-inflammatory phenotype observed in these models would suggest exacerbated atherosclerotic plaque formation. However the mechanisms by which this may manifest would be highly valuable and could be achieved through backcrossing with the ApoE / LDLr KO models of dyslipidaemia, in combination with therapeutics agents such as vitamin D to limit the progression of the disease.

Conclusion

LDI and the iontophoresis of vasoactive chemicals may provide a useful physiological technique for the non-invasive assessment of CVD in animal

models. MSK 1/ 2 and ABIN1 are novel kinase targets that may help limit CVD in the human population, further study is required to address the involvement of these pathways in CVD in patients and individual who are regarded as at risk of CVD.

References

ADACHI, O., KAWAI, T., TAKEDA, K., MATSUMOTO, M., TSUTSUI, H., SAKAGAMI, M., NAKANISHI, K. & AKIRA, S. 1998. Targeted disruption of the MyD88 gene results in loss of IL-1- and IL-18-mediated function. *Immunity,* 9, 143-50.

ADRIANTO, I., WANG, S., WILEY, G. B., LESSARD, C. J., KELLY, J. A., ADLER, A. J., GLENN, S. B., WILLIAMS, A. H., ZIEGLER, J. T., COMEAU, M. E., MARION, M. C., WAKELAND, B. E., LIANG, C., KAUFMAN, K. M., GUTHRIDGE, J. M., ALARCON-RIQUELME, M. E., ALARCON, G. S., ANAYA, J. M., BAE, S. C., KIM, J. H., JOO, Y. B., BOACKLE, S. A., BROWN, E. E., PETRI, M. A., RAMSEY-GOLDMAN, R., REVEILLE, J. D., VILA, L. M., CRISWELL, L. A., EDBERG, J. C., FREEDMAN, B. I., GILKESON, G. S., JACOB, C. O., JAMES, J. A., KAMEN, D. L., KIMBERLY, R. P., MARTIN, J., MERRILL, J. T., NIEWOLD, T. B., PONS-ESTEL, B. A., SCOFIELD, R. H., STEVENS, A. M., TSAO, B. P., VYSE, T. J., LANGEFELD, C. D., HARLEY, J. B., WAKELAND, E. K., MOSER, K. L., MONTGOMERY, C. G. & GAFFNEY, P. M. 2012. Association of two independent functional risk haplotypes in TNIP1 with systemic lupus erythematosus. *Arthritis and Rheumatism,* 64, 3695-705.

AIT-OUFELLA, H., TALEB, S., MALLAT, Z. & TEDGUI, A. 2011. Recent advances on the role of cytokines in atherosclerosis. *Arteriosclerosis, Thrombosis, And Vascular Biology,* 31, 969-79.

AKBAR, N., MOHAMED, T., WHITEHEAD, D. & AZZAWI, M. 2011. Biocompatibility of amorphous silica nanoparticles: Size and charge

effect on vascular function, in vitro. *Biotechnology and Applied Biochemistry,* 58, 353-62.

ALLEN, M., SVENSSON, L., ROACH, M., HAMBOR, J., MCNEISH, J. & GABEL, C. A. 2000. Deficiency of the stress kinase p38alpha results in embryonic lethality: characterization of the kinase dependence of stress responses of enzyme-deficient embryonic stem cells. *The Journal of Experimental Medicine,* 191, 859-70.

ALP, N. J. & CHANNON, K. M. 2004. Regulation of endothelial nitric oxide synthase by tetrahydrobiopterin in vascular disease. *Arteriosclerosis, Thrombosis, and Vascular Biology,* 24, 413-20.

ANANIEVA, O., DARRAGH, J., JOHANSEN, C., CARR, J. M., MCILRATH, J., PARK, J. M., WINGATE, A., MONK, C. E., TOTH, R., SANTOS, S. G., IVERSEN, L. & ARTHUR, J. S. 2008. The kinases MSK1 and MSK2 act as negative regulators of Toll-like receptor signaling. *Nature Immunology,* 9, 1028-36.

ARSLAN, F., HOUTGRAAF, J. H., KEOGH, B., KAZEMI, K., DE JONG, R., MCCORMACK, W. J., O'NEILL, L. A., MCGUIRK, P., TIMMERS, L., SMEETS, M. B., AKEROYD, L., REILLY, M., PASTERKAMP, G. & DE KLEIJN, D. P. 2012. Treatment with OPN-305, a humanized anti-Toll-Like receptor-2 antibody, reduces myocardial ischemia/reperfusion injury in pigs. *Circulation. Cardiovascular Interventions,* 5, 279-87.

ARTAZA, J. N., CONTRERAS, S., GARCIA, L. A., MEHROTRA, R., GIBBONS, G., SHOHET, R., MARTINS, D. & NORRIS, K. C. 2011. Vitamin D and cardiovascular disease: potential role in health disparities. *Journal of Health Care for the Poor and Underserved,* 22, 23-38.

ARTHUR, J. S. 2008. MSK activation and physiological roles. *Frontiers in Bioscience : a Journal and Virtual Library,* 13, 5866-79.

ARTHUR, J. S. & LEY, S. C. 2013. Mitogen-activated protein kinases in innate immunity. *Nature Reviews. Immunology,* 13, 679-92.

ASIFA, G. Z., LIAQUAT, A., MURTAZA, I., KAZMI, S. A. & JAVED, Q. 2013. Tumor necrosis factor-alpha gene promoter region polymorphism and the risk of coronary heart disease. *The Scientific World Journal,* 2013, 203492.

B©*LANGER, A. 2009. *Therapeutic electrophysical agents : evidence behind practice,* Philadelphia, Pa. ; London, Lippincott Williams & Wilkins.

BABOS, L., JARAI, Z. & NEMCSIK, J. 2013. Evaluation of microvascular reactivity with laser Doppler flowmetry in chronic kidney disease. *World Journal of Nephrology,* 2, 77-83.

BARAC, A., CAMPIA, U. & PANZA, J. A. 2007. Methods for evaluating endothelial function in humans. *Hypertension,* 49, 748-60.

BARBULESCU, A. L., VREJU, F., COJOCARU-GOFITA, I. R., MUSETESCU, A. E. & CIUREA, P. L. 2012. Impaired arterial stiffness in systemic lupus ertythematosus - correlations with inflammation markers. *Current Health Sciences Journal,* 38, 61-5.

BARNES, T. C., ANDERSON, M. E. & MOOTS, R. J. 2011. The many faces of interleukin-6: the role of IL-6 in inflammation, vasculopathy, and fibrosis in systemic sclerosis. *International Journal of Rheumatology*, 2011, 721608.

BARNES, T. C., SPILLER, D. G., ANDERSON, M. E., EDWARDS, S. W. & MOOTS, R. J. 2011. Endothelial activation and apoptosis mediated by

neutrophil-dependent interleukin 6 trans-signalling: a novel target for systemic sclerosis? *Annals Of The Rheumatic Diseases,* 70, 366-72.

BARRERA, D., NOYOLA-MARTINEZ, N., AVILA, E., HALHALI, A., LARREA, F. & DIAZ, L. 2012. Calcitriol inhibits interleukin-10 expression in cultured human trophoblasts under normal and inflammatory conditions. *Cytokine,* 57, 316-21.

BELCH, J. J., AKBAR, N., ALAPATI, V., PETRIE, J., ARTHUR, S. & KHAN, F. 2013. Longitudinal assessment of endothelial function in the microvasculature of mice in-vivo. *Microvascular Research,* 85, 86-92.

BJORKBACKA, H., KUNJATHOOR, V. V., MOORE, K. J., KOEHN, S., ORDIJA, C. M., LEE, M. A., MEANS, T., HALMEN, K., LUSTER, A. D., GOLENBOCK, D. T. & FREEMAN, M. W. 2004. Reduced atherosclerosis in MyD88-null mice links elevated serum cholesterol levels to activation of innate immunity signaling pathways. *Nature Medicine,* 10, 416-21.

BODYAK, N., AYUS, J. C., ACHINGER, S., SHIVALINGAPPA, V., KE, Q., CHEN, Y. S., RIGOR, D. L., STILLMAN, I., TAMEZ, H., KROEGER, P. E., WU-WONG, R. R., KARUMANCHI, S. A., THADHANI, R. & KANG, P. M. 2007. Activated vitamin D attenuates left ventricular abnormalities induced by dietary sodium in Dahl salt-sensitive animals. *Proceedings of The National Academy of Sciences of the United States Of America,* 104, 16810-5.

BOESTEN, L. S., ZADELAAR, A. S., VAN NIEUWKOOP, A., GIJBELS, M. J., DE WINTHER, M. P., HAVEKES, L. M. & VAN VLIJMEN, B. J. 2005. Tumor necrosis factor-alpha promotes atherosclerotic lesion progression in APOE*3-Leiden transgenic mice. *Cardiovascular Research,* 66, 179-85.

BONETTI, P. O., LERMAN, L. O. & LERMAN, A. 2003. Endothelial dysfunction: a marker of atherosclerotic risk. Arteriosclerosis, Thrombosis, and Vascular Biology*,* 23, 168-75.

BOONYASRISAWAT, W., EBERLE, D., BACCI, S., ZHANG, Y. Y., NOLAN, D., GERVINO, E. V., JOHNSTONE, M. T., TRISCHITTA, V., SHOELSON, S. E. & DORIA, A. 2007. Tag polymorphisms at the A20 (TNFAIP3) locus are associated with lower gene expression and increased risk of coronary artery disease in type 2 diabetes. *Diabetes,* 56, 499-505.

BOREL, J. C., ROUX-LOMBARD, P., TAMISIER, R., ARNAUD, C., MONNERET, D., ARNOL, N., BAGUET, J. P., LEVY, P. & PEPIN, J. L. 2009. Endothelial dysfunction and specific inflammation in obesity hypoventilation syndrome. *PLoS One,* 4, e6733.

BORGES, A. C., FERES, T., VIANNA, L. M. & PAIVA, T. B. 1999. Effect of cholecalciferol treatment on the relaxant responses of spontaneously hypertensive rat arteries to acetylcholine. *Hypertension,* 34, 897-901.

BRANEN, L., HOVGAARD, L., NITULESCU, M., BENGTSSON, E., NILSSON, J. & JOVINGE, S. 2004. Inhibition of tumor necrosis factor-alpha reduces atherosclerosis in apolipoprotein E knockout mice. Arteriosclerosis, Thrombosis, and Vascular Biology*,* 24, 2137-42.

BRITTON, K. A., MASSARO, J. M., MURABITO, J. M., KREGER, B. E., HOFFMANN, U. & FOX, C. S. 2013. Body fat distribution, incident cardiovascular disease, cancer, and all-cause mortality. *Journal of The American College of Cardiology,* 62, 921-5.

Bryant, C. E., Monie, T. P., 2012. Mice, men and the relatives: cross-species studies underpin innate immunity. Open Biology, 2(4), 1-10.

CALLIGARIS, S. D., LECANDA, M., SOLIS, F., EZQUER, M., GUTIERREZ, J., BRANDAN, E., LEIVA, A., SOBREVIA, L. & CONGET, P. 2013. Mice long-term high-fat diet feeding recapitulates human cardiovascular alterations: an animal model to study the early phases of diabetic cardiomyopathy. *PLoS One,* 8, e60931.

CANTORNA, M. T., ZHU, Y., FROICU, M. & WITTKE, A. 2004. Vitamin D status, 1,25-dihydroxyvitamin D3, and the immune system. *The American Journal of Clinical Nutrition,* 80, 1717S-20S.

CASTER, D. J., KORTE, E. A., NANDA, S. K., MCLEISH, K. R., OLIVER, R. K., G'SELL R, T., SHEEHAN, R. M., FREEMAN, D. W., COVENTRY, S. C., KELLY, J. A., GUTHRIDGE, J. M., JAMES, J. A., SIVILS, K. L., ALARCON-RIQUELME, M. E., SCOFIELD, R. H., ADRIANTO, I., GAFFNEY, P. M., STEVENS, A. M., FREEDMAN, B. I., LANGEFELD, C. D., TSAO, B. P., PONS-ESTEL, B. A., JACOB, C. O., KAMEN, D. L., GILKESON, G. S., BROWN, E. E., ALARCON, G. S., EDBERG, J. C., KIMBERLY, R. P., MARTIN, J., MERRILL, J. T., HARLEY, J. B., KAUFMAN, K. M., REVEILLE, J. D., ANAYA, J. M., CRISWELL, L. A., VILA, L. M., PETRI, M., RAMSEY-GOLDMAN, R., BAE, S. C., BOACKLE, S. A., VYSE, T. J., NIEWOLD, T. B., COHEN, P. & POWELL, D. W. 2013. ABIN1 dysfunction as a genetic basis for lupus nephritis. *Journal of The American Society of Nephrology,* 24, 1743-54.

CHAMBERLAIN, J., EVANS, D., KING, A., DEWBERRY, R., DOWER, S., CROSSMAN, D. & FRANCIS, S. 2006. Interleukin-1beta and signaling of interleukin-1 in vascular wall and circulating cells modulates the extent of neointima formation in mice. The American Journal of Pathology*,* 168, 1396-403.

CHEN, S., LAW, C. S., GRIGSBY, C. L., OLSEN, K., HONG, T. T., ZHANG, Y., YEGHIAZARIANS, Y. & GARDNER, D. G. 2011. Cardiomyocyte-specific deletion of the vitamin D receptor gene results in cardiac hypertrophy. *Circulation,* 124, 1838-47.

CHERRY, P. D., FURCHGOTT, R. F., ZAWADZKI, J. V. & JOTHIANANDAN, D. 1982. Role of endothelial cells in relaxation of isolated arteries by bradykinin. *Proceedings of The National Academy of Sciences of The United States of America,* 79, 2106-10.

CHI, H., MESSAS, E., LEVINE, R. A., GRAVES, D. T. & AMAR, S. 2004. Interleukin-1 receptor signaling mediates atherosclerosis associated with bacterial exposure and/or a high-fat diet in a murine apolipoprotein E heterozygote model: pharmacotherapeutic implications. *Circulation,* 110, 1678-85.

CHO, H. C., YU, G., LEE, M. Y., KIM, H. S., SHIN, D. H. & KIM, Y. N. 2013. TNF-alpha polymorphisms and coronary artery disease: association study in the Korean population. *Cytokine,* 62, 104-9.

CINES, D. B., POLLAK, E. S., BUCK, C. A., LOSCALZO, J., ZIMMERMAN, G. A., MCEVER, R. P., POBER, J. S., WICK, T. M., KONKLE, B. A., SCHWARTZ, B. S., BARNATHAN, E. S., MCCRAE, K. R., HUG, B. A., SCHMIDT, A. M. & STERN, D. M. 1998. Endothelial cells in physiology and in the pathophysiology of vascular disorders. *Blood,* 91, 3527-61.

CLAPP, B. R., HINGORANI, A. D., KHARBANDA, R. K., MOHAMED-ALI, V., STEPHENS, J. W., VALLANCE, P. & MACALLISTER, R. J. 2004. Inflammation-induced endothelial dysfunction involves reduced nitric oxide bioavailability and increased oxidant stress. *Cardiovascular Research,* 64, 172-8.

CLAPP, B. R., HIRSCHFIELD, G. M., STORRY, C., GALLIMORE, J. R., STIDWILL, R. P., SINGER, M., DEANFIELD, J. E., MACALLISTER, R. J., PEPYS, M. B., VALLANCE, P. & HINGORANI, A. D. 2005. Inflammation and endothelial function: direct vascular effects of human C-reactive protein on nitric oxide bioavailability. *Circulation,* 111, 1530-6.

COLE, J. E., KASSITERIDI, C. & MONACO, C. 2013. Toll-like receptors in atherosclerosis: a 'Pandora's box' of advances and controversies. *Trends in Pharmacological Sciences,* 34, 629-36.

CONTOIS, J. H., MCCONNELL, J. P., SETHI, A. A., CSAKO, G., DEVARAJ, S., HOEFNER, D. M. & WARNICK, G. R. 2009. Apolipoprotein B and cardiovascular disease risk: position statement from the AACC Lipoproteins and Vascular Diseases Division Working Group on Best Practices. *Clinical Chemistry,* 55, 407-19.

CORSON, M. A., JAMES, N. L., LATTA, S. E., NEREM, R. M., BERK, B. C. & HARRISON, D. G. 1996. Phosphorylation of endothelial nitric oxide synthase in response to fluid shear stress. *Circulation Research,* 79, 984-91.

D'AGOSTINO, R. B., SR., PENCINA, M. J., MASSARO, J. M. & COADY, S. 2013. Cardiovascular Disease Risk Assessment: Insights from Framingham. *Global Heart,* 8, 11-23.

DARLING, A. L., HART, K. H., MACDONALD, H. M., HORTON, K., KANG'OMBE, A. R., BERRY, J. L. & LANHAM-NEW, S. A. 2013. Vitamin D deficiency in UK South Asian Women of childbearing age: a comparative longitudinal investigation with UK Caucasian women. *Osteoporosis International,* 24, 477-88.

DARRAGH, J., ANANIEVA, O., COURTNEY, A., ELCOMBE, S. & ARTHUR, J. S. 2010. MSK1 regulates the transcription of IL-1ra in response to TLR activation in macrophages. *The Biochemical Journal,* 425, 595-602.

DAVIGNON, J. 2004. Beneficial cardiovascular pleiotropic effects of statins. *Circulation,* 109, III39-43.

DAVISSON, R. L., HOFFMANN, D. S., BUTZ, G. M., ALDAPE, G., SCHLAGER, G., MERRILL, D. C., SETHI, S., WEISS, R. M. & BATES, J. N. 2002. Discovery of a spontaneous genetic mouse model of preeclampsia. *Hypertension,* 39, 337-42.

DAWBER, T. R., MEADORS, G. F. & MOORE, F. E., JR. 1951. Epidemiological approaches to heart disease: the Framingham Study. *American Journal Of Public Health And The Nation's Health,* 41, 279-81.

DE ANDRADE, C. R., LEITE, P. F., MONTEZANO, A. C., CASOLARI, D. A., YOGI, A., TOSTES, R. C., HADDAD, R., EBERLIN, M. N., LAURINDO, F. R., DE SOUZA, H. P., CORREA, F. M. & DE OLIVEIRA, A. M. 2009. Increased endothelin-1 reactivity and endothelial dysfunction in carotid arteries from rats with hyperhomocysteinemia. *British Journal of Pharmacology,* 157, 568-80.

DE FILIPPO, K., DUDECK, A., HASENBERG, M., NYE, E., VAN ROOIJEN, N., HARTMANN, K., GUNZER, M., ROERS, A. & HOGG, N. 2013. Mast cell and macrophage chemokines CXCL1/CXCL2 control the early stage of neutrophil recruitment during tissue inflammation. *Blood,* 121, 4930-7.

DEBBABI, H., BONNIN, P., DUCLUZEAU, P. H., LEFTHERIOTIS, G. & LEVY, B. I. 2010. Noninvasive assessment of endothelial function in the skin microcirculation. *American Journal of Hypertension,* 23, 541-6.

DIAZ, L., NOYOLA-MARTINEZ, N., BARRERA, D., HERNANDEZ, G., AVILA, E., HALHALI, A. & LARREA, F. 2009. Calcitriol inhibits TNF-alpha-induced inflammatory cytokines in human trophoblasts. *Journal of Reproductive Immunology,* 81, 17-24.

DICKHOUT, J. G. & AUSTIN, R. C. 2006. Proteasomal regulation of cardiac hypertrophy: is demolition necessary for building? *Circulation,* 114, 1796-8.

DO, J. E., KWON, S. Y., PARK, S. & LEE, E. S. 2008. Effects of vitamin D on expression of Toll-like receptors of monocytes from patients with Behcet's disease. *Rheumatology,* 47, 840-8.

DUNZENDORFER, S., LEE, H. K. & TOBIAS, P. S. 2004. Flow-dependent regulation of endothelial Toll-like receptor 2 expression through inhibition of SP1 activity. *Circulation Research,* 95, 684-91.

DURAN, W. N., BRESLIN, J. W. & SANCHEZ, F. A. 2010. The NO cascade, eNOS location, and microvascular permeability. *Cardiovascular Research,* 87, 254-61.

EICHNER, J. E., DUNN, S. T., PERVEEN, G., THOMPSON, D. M., STEWART, K. E. & STROEHLA, B. C. 2002. Apolipoprotein E polymorphism and cardiovascular disease: a HuGE review. *American Journal of Epidemiology,* 155, 487-95.

ESDAILE, J. M., ABRAHAMOWICZ, M., GRODZICKY, T., LI, Y., PANARITIS, C., DU BERGER, R., COTE, R., GROVER, S. A., FORTIN, P. R., CLARKE, A. E. & SENECAL, J. L. 2001. Traditional Framingham risk factors fail to fully account for accelerated atherosclerosis in systemic lupus erythematosus. *Arthritis and Rheumatism,* 44, 2331-7.

ESPER, R. J., NORDABY, R. A., VILARINO, J. O., PARAGANO, A., CACHARRON, J. L. & MACHADO, R. A. 2006. Endothelial dysfunction: a comprehensive appraisal. *Cardiovascular Diabetology,* 5, 4.

ESTEVE, E., CASTRO, A., LOPEZ-BERMEJO, A., VENDRELL, J., RICART, W. & FERNANDEZ-REAL, J. M. 2007. Serum interleukin-6 correlates with endothelial dysfunction in healthy men independently of insulin sensitivity. *Diabetes Care,* 30, 939-45.

ESTEVE, E., VILLUENDAS, G., MALLOLAS, J., VENDRELL, J., LOPEZ-BERMEJO, A., RODRIGUEZ, M., RECASENS, M., RICART, W., SAN MILLAN, J. L., ESCOBAR-MORREALE, H., RICHART, C. & FERNANDEZ-REAL, J. M. 2006. Polymorphisms in the interleukin-6 receptor gene are associated with body mass index and with characteristics of the metabolic syndrome. *Clinical Endocrinology,* 65, 88-91.

EVORA, P. R., NATHER, J., TUBINO, P. V., ALBUQUERQUE, A. A., CELOTTO, A. C. & RODRIGUES, A. J. 2013. Curbing inflammation in the ischemic heart disease. *InternationalJournal of Inflammation,* 2013, 183061.

FALCK-HANSEN, M., KASSITERIDI, C. & MONACO, C. 2013. Toll-like receptors in atherosclerosis. *International Journal of Molecular Sciences,* 14, 14008-23.

FENG, M., WHITESALL, S., ZHANG, Y., BEIBEL, M., D'ALECY, L. & DIPETRILLO, K. 2008a. Validation of volume-pressure recording tail-cuff blood pressure measurements. *American Journal of Hypertension,* 21, 1288-91.

FENG, Y., ZHAO, H., XU, X., BUYS, E. S., RAHER, M. J., BOPASSA, J. C., THIBAULT, H., SCHERRER-CROSBIE, M., SCHMIDT, U. & CHAO, W. 2008b. Innate immune adaptor MyD88 mediates neutrophil recruitment and myocardial injury after ischemia-reperfusion in mice. *American journal of physiology. Heart and Circulatory Physiology,* 295, H1311-H1318.

FERNANDEZ-REAL, J. M., BROCH, M., VENDRELL, J., RICHART, C. & RICART, W. 2000. Interleukin-6 gene polymorphism and lipid abnormalities in healthy subjects. *The Journal of Clinical Endocrinology and Metabolism,* 85, 1334-9.

FERNANDEZ-REAL, J. M., VAYREDA, M., RICHART, C., GUTIERREZ, C., BROCH, M., VENDRELL, J. & RICART, W. 2001. Circulating interleukin 6 levels, blood pressure, and insulin sensitivity in apparently healthy men and women. *The Journal of Clinical Endocrinology and Metabolism,* 86, 1154-9.

FICHTLSCHERER, S., BREUER, S., HEESCHEN, C., DIMMELER, S. & ZEIHER, A. M. 2004. Interleukin-10 serum levels and systemic endothelial vasoreactivity in patients with coronary artery disease. *Journal of The American College of Cardiology,* 44, 44-9.

FOLSOM, A. R., ROETKER, N. S., ROSAMOND, W. D., HECKBERT, S. R., BASU, S., CUSHMAN, M. & LUTSEY, P. L. 2014. Serum 25-hydroxyvitamin D and risk of venous thromboembolism: The Atherosclerosis Risk in Communities (ARIC) Study. *Journal of Thrombosis and Haemostasis,* doi: 10.1111/jth.12665 (ahead of print).

FORD, J. A., MACLENNAN, G. S., AVENELL, A., BOLLAND, M., GREY, A. & WITHAM, M. 2014. Cardiovascular disease and vitamin D

supplementation: trial analysis, systematic review, and meta-analysis. *The American Journal of Clinical Nutrition*, doi: 10.3945/ajcn.113.082602.

FORSBERG, G., HERNELL, O., HAMMARSTROM, S. & HAMMARSTROM, M. L. 2007. Concomitant increase of IL-10 and pro-inflammatory cytokines in intraepithelial lymphocyte subsets in celiac disease. *International Immunology,* 19, 993-1001.

FRANCIS, S. E., CAMP, N. J., BURTON, A. J., DEWBERRY, R. M., GUNN, J., STEPHENS-LLOYD, A., CUMBERLAND, D. C., GERSHLICK, A. & CROSSMAN, D. C. 2001. Interleukin 1 receptor antagonist gene polymorphism and restenosis after coronary angioplasty. *Heart,* 86, 336-40.

FURCHGOTT, R. F. 1983. Role of endothelium in responses of vascular smooth muscle. *Circulation Research,* 53, 557-73.

FURCHGOTT, R. F. 1984. The role of endothelium in the responses of vascular smooth muscle to drugs. *Annual Review of Pharmacology and Toxicology,* 24, 175-97.

FURCHGOTT, R. F. & ZAWADZKI, J. V. 1980. The obligatory role of endothelial cells in the relaxation of arterial smooth muscle by acetylcholine. *Nature,* 288, 373-6.

GALARRAGA, B., KHAN, F., KUMAR, P., PULLAR, T. & BELCH, J. J. 2008. C-reactive protein: the underlying cause of microvascular dysfunction in rheumatoid arthritis. *Rheumatology (Oxford),* 47, 1780-4.

GALLIS, B., CORTHALS, G. L., GOODLETT, D. R., UEBA, H., KIM, F., PRESNELL, S. R., FIGEYS, D., HARRISON, D. G., BERK, B. C., AEBERSOLD, R. & CORSON, M. A. 1999. Identification of flow-dependent endothelial nitric-oxide synthase phosphorylation sites by

mass spectrometry and regulation of phosphorylation and nitric oxide production by the phosphatidylinositol 3-kinase inhibitor LY294002. *The Journal of Biological Chemistry,* 274, 30101-8.

GAREUS, R., KOTSAKI, E., XANTHOULEA, S., VAN DER MADE, I., GIJBELS, M. J., KARDAKARIS, R., POLYKRATIS, A., KOLLIAS, G., DE WINTHER, M. P. & PASPARAKIS, M. 2008. Endothelial cell-specific NF-kappaB inhibition protects mice from atherosclerosis. *Cell Metabolism,* 8, 372-83.

GEORGE, J., CARR, E., DAVIES, J., BELCH, J. J. & STRUTHERS, A. 2006. High-dose allopurinol improves endothelial function by profoundly reducing vascular oxidative stress and not by lowering uric acid. *Circulation,* 114, 2508-16.

GORSKA, M. M., LIANG, Q., STAFFORD, S. J., GOPLEN, N., DHARAJIYA, N., GUO, L., SUR, S., GAESTEL, M. & ALAM, R. 2007. MK2 controls the level of negative feedback in the NF-kappaB pathway and is essential for vascular permeability and airway inflammation. *The Journal of Experimental Medicine,* 204, 1637-52.

GRINEVA, E. N., KARONOVA, T., MICHEEVA, E., BELYAEVA, O. & NIKITINA, I. L. 2013. Vitamin D deficiency is a risk factor for obesity and diabetes type 2 in women at late reproductive age. *Aging,* 5, 575-81.

GRUNDY, S. M., BENJAMIN, I. J., BURKE, G. L., CHAIT, A., ECKEL, R. H., HOWARD, B. V., MITCH, W., SMITH, S. C., JR. & SOWERS, J. R. 1999. Diabetes and cardiovascular disease: a statement for healthcare professionals from the American Heart Association. *Circulation,* 100, 1134-46.

GUMA, M., HAMMAKER, D., TOPOLEWSKI, K., CORR, M., BOYLE, D. L., KARIN, M. & FIRESTEIN, G. S. 2012. Antiinflammatory functions of p38 in mouse models of rheumatoid arthritis: advantages of targeting upstream kinases MKK-3 or MKK-6. *Arthritis and Rheumatism,* 64, 2887-95.

HADI, H. A., CARR, C. S. & AL SUWAIDI, J. 2005. Endothelial dysfunction: cardiovascular risk factors, therapy, and outcome. *Vascular Health and Risk Management,* 1, 183-98.

HAN, J. 2006. MyD88 beyond Toll. *Nature Immunology,* 7, 370-1.

HAN, X., KITAMOTO, S., WANG, H. & BOISVERT, W. A. 2010. Interleukin-10 overexpression in macrophages suppresses atherosclerosis in hyperlipidemic mice. *FASEB Journal : official publication of the Federation of American Societies for Experimental Biology,* 24, 2869-80.

HASHIZUME, M. & MIHARA, M. 2012. Blockade of IL-6 and TNF-alpha inhibited oxLDL-induced production of MCP-1 via scavenger receptor induction. *The European Journal of Pharmacology,* 689, 249-54.

HE, C. F., LIU, Y. S., CHENG, Y. L., GAO, J. P., PAN, T. M., HAN, J. W., QUAN, C., SUN, L. D., ZHENG, H. F., ZUO, X. B., XU, S. X., SHENG, Y. J., YAO, S., HU, W. L., LI, Y., YU, Z. Y., YIN, X. Y., ZHANG, X. J., CUI, Y. & YANG, S. 2010. TNIP1, SLC15A4, ETS1, RasGRP3 and IKZF1 are associated with clinical features of systemic lupus erythematosus in a Chinese Han population. *Lupus,* 19, 1181-6.

HEGEN, M., GAESTEL, M., NICKERSON-NUTTER, C. L., LIN, L. L. & TELLIEZ, J. B. 2006. MAPKAP kinase 2-deficient mice are resistant to collagen-induced arthritis. *Journal of Immunology,* 177, 1913-7.

HEINE, G., NIESNER, U., CHANG, H. D., STEINMEYER, A., ZUGEL, U., ZUBERBIER, T., RADBRUCH, A. & WORM, M. 2008. 1,25-dihydroxyvitamin D(3) promotes IL-10 production in human B cells. *European Journal of Immunology,* 38, 2210-8.

HERRERA, M. D., MINGORANCE, C., RODRIGUEZ-RODRIGUEZ, R. & ALVAREZ DE SOTOMAYOR, M. 2010. Endothelial dysfunction and aging: an update. *Ageing Research Reviews,* 9, 142-52.

HOGE, M. & AMAR, S. 2007. Role of interleukin-1 in bacterial atherogenesis. *Timely Topics in Medicine. Cardiovascular Diseases,* 11, E5.

HOLICK, M. F. & CHEN, T. C. 2008. Vitamin D deficiency: a worldwide problem with health consequences. *The American Journal of Clinical Nutrition,* 87, 1080S-6S.

HOSOI, T., YOKOYAMA, S., MATSUO, S., AKIRA, S. & OZAWA, K. 2010. Myeloid differentiation factor 88 (MyD88)-deficiency increases risk of diabetes in mice. *PLoS One,* 5(9):e12537.

HUBER, S. A., SAKKINEN, P., CONZE, D., HARDIN, N. & TRACY, R. 1999. Interleukin-6 exacerbates early atherosclerosis in mice. *Arteriosclerosis, Thrombosis, and Vascular Biology,* 19, 2364-7.

HUNG, M. J., CHERNG, W. J., HUNG, M. Y., WU, H. T. & PANG, J. H. 2010.liu Interleukin-6 inhibits endothelial nitric oxide synthase activation and increases endothelial nitric oxide synthase binding to stabilized caveolin-1 in human vascular endothelial cells. *Journal of Hypertension,* 28, 940-51.

HUSSAIN, S. M., OLDENBURG, B., WANG, Y., ZOUNGAS, S. & TONKIN, A. M. 2013. Assessment of cardiovascular disease risk in South asian populations. *International Journal of Vascular Medicine,* 2013, 786801.

INGLESSIS, I., SHIN, J. T., LEPORE, J. J., PALACIOS, I. F., ZAPOL, W. M., BLOCH, K. D. & SEMIGRAN, M. J. 2004. Hemodynamic effects of inhaled nitric oxide in right ventricular myocardial infarction and cardiogenic shock. *Journal of The American College of Cardiology,* 44, 793-8.

ISHIBASHI, S., BROWN, M. S., GOLDSTEIN, J. L., GERARD, R. D., HAMMER, R. E. & HERZ, J. 1993. Hypercholesterolemia in low density lipoprotein receptor knockout mice and its reversal by adenovirus-mediated gene delivery.*The Journal of Clinical Investigation,* 92, 883-93.

ISHIBASHI, S., GOLDSTEIN, J. L., BROWN, M. S., HERZ, J. & BURNS, D. K. 1994a. Massive xanthomatosis and atherosclerosis in cholesterol-fed low density lipoprotein receptor-negative mice. *The Journal of clinical Investigation,* 93, 1885-93.

ISHIBASHI, S., HERZ, J., MAEDA, N., GOLDSTEIN, J. L. & BROWN, M. S. 1994b. The two-receptor model of lipoprotein clearance: tests of the hypothesis in "knockout" mice lacking the low density lipoprotein receptor, apolipoprotein E, or both proteins. *Proceedings of the National Academy of Sciences of the United States of America,* 91, 4431-5.

ISODA, K. & OHSUZU, F. 2006. The effect of interleukin-1 receptor antagonist on arteries and cholesterol metabolism. *Journal of Atherosclerosis and Thrombosis,* 13, 21-30.

ISODA, K., SAWADA, S., ISHIGAMI, N., MATSUKI, T., MIYAZAKI, K., KUSUHARA, M., IWAKURA, Y. & OHSUZU, F. 2004. Lack of interleukin-1 receptor antagonist modulates plaque composition in apolipoprotein E-deficient mice. *Arteriosclerosis, Thrombosis, and Vascular Biology,* 24, 1068-73.

ISODA, K., SHIIGAI, M., ISHIGAMI, N., MATSUKI, T., HORAI, R., NISHIKAWA, K., KUSUHARA, M., NISHIDA, Y., IWAKURA, Y. & OHSUZU, F. 2003. Deficiency of interleukin-1 receptor antagonist promotes neointimal formation after injury. *Circulation,* 108, 516-8.

ITO, I., WAKU, T., AOKI, M., ABE, R., NAGAI, Y., WATANABE, T., NAKAJIMA, Y., OHKIDO, I., YOKOYAMA, K., MIYACHI, H., SHIMIZU, T., MURAYAMA, A., KISHIMOTO, H., NAGASAWA, K. & YANAGISAWA, J. 2013. A nonclassical vitamin D receptor pathway suppresses renal fibrosis. *The Journal of Clinical Investigation,* 123, 4579-94.

JAGAVELU, K., TIETGE, U. J., GAESTEL, M., DREXLER, H., SCHIEFFER, B. & BAVENDIEK, U. 2007. Systemic deficiency of the MAP kinase-activated protein kinase 2 reduces atherosclerosis in hypercholesterolemic mice. *Circulation Research,* 101, 1104-12.

JONES, K. L. & DEWAN, A. K. 2003. Type 2 diabetes mellitus in adolescence: lipid and cardiovascular risk factors. *Current Diabetes Reports,* 3, 255-62.

JUNG, J. Y., KOH, B. R., BAE, C. B., KIM, H. A. & SUH, C. H. 2014. Carotid subclinical atherosclerosis is associated with disease activity but not vitamin D in Korean systemic lupus erythematosus. *Lupus*.

KALLAY, E., BAREIS, P., BAJNA, E., KRIWANEK, S., BONNER, E., TOYOKUNI, S. & CROSS, H. S. 2002. Vitamin D receptor activity and prevention of colonic hyperproliferation and oxidative stress. *Food and Chemical Toxicology : an international journal published for the British Industrial Biological Research Association,* 40, 1191-6.

KAMADA, Y., NAGARETANI, H., TAMURA, S., OHAMA, T., MARUYAMA, T., HIRAOKA, H., YAMASHITA, S., YAMADA, A., KISO, S., INUI, Y., ITO,

N., KAYANOKI, Y., KAWATA, S. & MATSUZAWA, Y. 2001. Vascular endothelial dysfunction resulting from L-arginine deficiency in a patient with lysinuric protein intolerance. *The Journal of Clinical Investigation,* 108, 717-24.

KASSI, E., ADAMOPOULOS, C., BASDRA, E. K. & PAPAVASSILIOU, A. G. 2013. Role of vitamin D in atherosclerosis. *Circulation,* 128, 2517-31.

KATHIRESAN, S., GONA, P., LARSON, M. G., VITA, J. A., MITCHELL, G. F., TOFLER, G. H., LEVY, D., NEWTON-CHEH, C., WANG, T. J., BENJAMIN, E. J. & VASAN, R. S. 2006. Cross-sectional relations of multiple biomarkers from distinct biological pathways to brachial artery endothelial function. *Circulation,* 113, 938-45.

KAVANDI, L., COLLIER, M. A., NGUYEN, H. & SYED, V. 2012. Progesterone and calcitriol attenuate inflammatory cytokines CXCL1 and CXCL2 in ovarian and endometrial cancer cells. *Journal of Cellular Biochemistry,* 113, 3143-52.

KAWAI, T., ADACHI, O., OGAWA, T., TAKEDA, K. & AKIRA, S. 1999. Unresponsiveness of MyD88-deficient mice to endotoxin. *Immunity,* 11, 115-22.

KAWAI, T. & AKIRA, S. 2009. The roles of TLRs, RLRs and NLRs in pathogen recognition. *International Immunology,* 21, 317-37.

KESO, T., PEROLA, M., LAIPPALA, P., ILVESKOSKI, E., KUNNAS, T. A., MIKKELSSON, J., PENTTILA, A., HURME, M. & KARHUNEN, P. J. 2001. Polymorphisms within the tumor necrosis factor locus and prevalence of coronary artery disease in middle-aged men. *Atherosclerosis,* 154, 691-7.

KHAN, F., BELCH, J. J., MACLEOD, M. & MIRES, G. 2005. Changes in endothelial function precede the clinical disease in women in whom preeclampsia develops. *Hypertension,* 46, 1123-8.

KHAN, F., ELHADD, T. A., GREENE, S. A. & BELCH, J. J. 2000. Impaired skin microvascular function in children, adolescents, and young adults with type 1 diabetes. *Diabetes Care,* 23, 215-20.

KHAN, F., LITCHFIELD, S. J., STONEBRIDGE, P. A. & BELCH, J. J. 1999. Lipid-lowering and skin vascular responses in patients with hypercholesterolaemia and peripheral arterial obstructive disease. *Vascular Medicine,* 4, 233-8.

KHAN, F., PATTERSON, D., BELCH, J. J., HIRATA, K. & LANG, C. C. 2008. Relationship between peripheral and coronary function using laser Doppler imaging and transthoracic echocardiography. *Clinical Science,* 115, 295-300.

KHAN, F., SPENCE, V. A., WILSON, S. B. & ABBOT, N. C. 1991. Quantification of sympathetic vascular responses in skin by laser Doppler flowmetry. *International Journal of Microcirculation, Clinical and Experimental / sponsored by the European Society for Microcirculation,* 10, 145-53.

KHANNA, V., JAIN, M., SINGH, V., KANSHANA, J. S., PRAKASH, P., BARTHWAL, M. K., MURTHY, P. S. & DIKSHIT, M. 2013. Cholesterol diet withdrawal leads to an initial plaque instability and subsequent regression of accelerated iliac artery atherosclerosis in rabbits. *PLoS One,* 8, e77037.

KIM, C., SANO, Y., TODOROVA, K., CARLSON, B. A., ARPA, L., CELADA, A., LAWRENCE, T., OTSU, K., BRISSETTE, J. L., ARTHUR, J. S. & PARK,

J. M. 2008. The kinase p38 alpha serves cell type-specific inflammatory functions in skin injury and coordinates pro- and anti-inflammatory gene expression. *Nature Immunology,* 9, 1019-27.

KONG, S. W., BODYAK, N., YUE, P., LIU, Z., BROWN, J., IZUMO, S. & KANG, P. M. 2005. Genetic expression profiles during physiological and pathological cardiac hypertrophy and heart failure in rats. *Physiological Genomics,* 21, 34-42.

KOSTOGLOU-ATHANASSIOU, I., ATHANASSIOU, P., LYRAKI, A., RAFTAKIS, I. & ANTONIADIS, C. 2012. Vitamin D and rheumatoid arthritis. *Therapeutic Advances in Endocrinology and Metabolism,* 3, 181-7.

KOTLYAROV, A., NEININGER, A., SCHUBERT, C., ECKERT, R., BIRCHMEIER, C., VOLK, H. D. & GAESTEL, M. 1999. MAPKAP kinase 2 is essential for LPS-induced TNF-alpha biosynthesis. *Nature Cell Biology,* 1, 94-7.

KRUGER, A., STEWART, J., SAHITYANI, R., O'RIORDAN, E., THOMPSON, C., ADLER, S., GARRICK, R., VALLANCE, P. & GOLIGORSKY, M. S. 2006. Laser Doppler flowmetry detection of endothelial dysfunction in end-stage renal disease patients: correlation with cardiovascular risk. *Kidney International,* 70, 157-64.

KU, Y. C., LIU, M. E., KU, C. S., LIU, T. Y. & LIN, S. L. 2013. Relationship between vitamin D deficiency and cardiovascular disease. *World Journal of Cardiology,* 5, 337-46.

KYOI, S., OTANI, H., MATSUHISA, S., AKITA, Y., TATSUMI, K., ENOKI, C., FUJIWARA, H., IMAMURA, H., KAMIHATA, H. & IWASAKA, T. 2006. Opposing effect of p38 MAP kinase and JNK inhibitors on the

development of heart failure in the cardiomyopathic hamster. *Cardiovascular Research,* 69, 888-98.

LAMALICE, L., LE BOEUF, F. & HUOT, J. 2007. Endothelial cell migration during angiogenesis. *Circulation Research,* 100, 782-94.

LAMATTINA, L., GARCIA-MATA, C., GRAZIANO, M. & PAGNUSSAT, G. 2003. Nitric oxide: the versatility of an extensive signal molecule. *Annual Review of Plant Biology,* 54, 109-36.

LAVIE, C. J., LEE, J. H. & MILANI, R. V. 2011. Vitamin D and cardiovascular disease will it live up to its hype? *Journal of the American College of Cardiology,* 58, 1547-56.

LEACH, L., EATON, B. M., WESTCOTT, E. D. & FIRTH, J. A. 1995. Effect of histamine on endothelial permeability and structure and adhesion molecules of the paracellular junctions of perfused human placental microvessels. *Microvascular Research,* 50, 323-37.

LEE, J. C., KUMAR, S., GRISWOLD, D. E., UNDERWOOD, D. C., VOTTA, B. J. & ADAMS, J. L. 2000. Inhibition of p38 MAP kinase as a therapeutic strategy. *Immunopharmacology,* 47, 185-201.

LESNIEWSKI, L. A., CONNELL, M. L., DURRANT, J. R., FOLIAN, B. J., ANDERSON, M. C., DONATO, A. J. & SEALS, D. R. 2009. B6D2F1 Mice are a suitable model of oxidative stress-mediated impaired endothelium-dependent dilation with aging. *The Journals of Gerontology. Series A, Biological Sciences and Medical Sciences,* 64, 9-20.

LEUSCHNER, F., PANIZZI, P., CHICO-CALERO, I., LEE, W. W., UENO, T., CORTEZ-RETAMOZO, V., WATERMAN, P., GORBATOV, R., MARINELLI, B., IWAMOTO, Y., CHUDNOVSKIY, A., FIGUEIREDO, J. L., SOSNOVIK, D. E., PITTET, M. J., SWIRSKI, F. K., WEISSLEDER, R.

& NAHRENDORF, M. 2010a. Angiotensin-converting enzyme inhibition prevents the release of monocytes from their splenic reservoir in mice with myocardial infarction. *Circulations Research,* 107, 1364-73.

LEUSCHNER, F., PANIZZI, P., CHICO-CALERO, I., LEE, W. W., UENO, T., CORTEZ-RETAMOZO, V., WATERMAN, P., GORBATOV, R., MARINELLI, B., IWAMOTO, Y., CHUDNOVSKIY, A., FIGUEIREDO, J. L., SOSNOVIK, D. E., PITTET, M. J., SWIRSKI, F. K., WEISSLEDER, R. & NAHRENDORF, M. 2010b. Angiotensin-converting enzyme inhibition prevents the release of monocytes from their splenic reservoir in mice with myocardial infarction. *Circulation Research,* 107, 1364-73.

LEY, K., LAUDANNA, C., CYBULSKY, M. I. & NOURSHARGH, S. 2007. Getting to the site of inflammation: the leukocyte adhesion cascade updated. *Nature reviews. Immunology,* 7, 678-89.

LI, H., CYBULSKY, M. I., GIMBRONE, M. A., JR. & LIBBY, P. 1993. An atherogenic diet rapidly induces VCAM-1, a cytokine-regulatable mononuclear leukocyte adhesion molecule, in rabbit aortic endothelium. *Arteriosclerosis and Thrombosis : a Journal of Vascular Biology / American Heart Association,* 13, 197-204.

LIBBY, P., RIDKER, P. M. & HANSSON, G. K. 2009. Inflammation in atherosclerosis: from pathophysiology to practice. *Journal of the American College* of *Cardiology,* 54, 2129-38.

LIBBY, P., RIDKER, P. M. & HANSSON, G. K. 2011. Progress and challenges in translating the biology of atherosclerosis. *Nature,* 473, 317-25.

LIU, H. H., ZHAO, D., MA, C. S., LIU, X. H., LV, Q., QI, Y., LI, Y., REN, J. & LIU, J. 2012. C-reactive protein predicts the severity of coronary artery

disease beyond low-density lipoprotein cholesterol. *Angiology,* 63, 218-22.

LIU, P. T., STENGER, S., LI, H., WENZEL, L., TAN, B. H., KRUTZIK, S. R., OCHOA, M. T., SCHAUBER, J., WU, K., MEINKEN, C., KAMEN, D. L., WAGNER, M., BALS, R., STEINMEYER, A., ZUGEL, U., GALLO, R. L., EISENBERG, D., HEWISON, M., HOLLIS, B. W., ADAMS, J. S., BLOOM, B. R. & MODLIN, R. L. 2006. Toll-like receptor triggering of a vitamin D-mediated human antimicrobial response. *Science,* 311, 1770-3.

LONDON, G. M., GUERIN, A. P., MARCHAIS, S. J., METIVIER, F., PANNIER, B. & ADDA, H. 2003. Arterial media calcification in end-stage renal disease: impact on all-cause and cardiovascular mortality. *Nephrology, dialysis, transplantation : official publication of the European Dialysis and Transplant Association - European Renal Association,* 18, 1731-40.

LU, L., PU, L. J., XU, X. W., ZHANG, Q., ZHANG, R. Y., ZHANG, J. S., HU, J., YANG, Z. K., LU, A. K., DING, F. H., SHEN, J., CHEN, Q. J., LOU, S., FANG, D. H. & SHEN, W. F. 2007. Association of serum levels of glycated albumin, C-reactive protein and tumor necrosis factor-alpha with the severity of coronary artery disease and renal impairment in patients with type 2 diabetes mellitus. *Clinical Biochemistry,* 40, 810-6.

LUENGO-FERNANDEZ, R., LEAL, J., GRAY, A., PETERSEN, S. & RAYNER, M. 2006. Cost of cardiovascular diseases in the United Kingdom. *Heart,* 92, 1384-1389.

LUSIS, A. J., YU, J. & WANG, S. S. 2007. The problem of passenger genes in transgenic mice. *Arteriosclerosis, Thrombosis, and Vascular Biology,* 27, 2100-3.

MALLAT, Z., BESNARD, S., DURIEZ, M., DELEUZE, V., EMMANUEL, F., BUREAU, M. F., SOUBRIER, F., ESPOSITO, B., DUEZ, H., FIEVET, C., STAELS, B., DUVERGER, N., SCHERMAN, D. & TEDGUI, A. 1999. Protective role of interleukin-10 in atherosclerosis. *Circulation Research,* 85, e17-24.

MALLAT, Z. & TEDGUI, A. 2007. Cytokines as regulators of atherosclerosis in murine models. *Current Drug Targets,* 8, 1264-72.

MANCUSO, P., RAHMAN, A., HERSHEY, S. D., DANDU, L., NIBBELINK, K. A. & SIMPSON, R. U. 2008. 1,25-Dihydroxyvitamin-D3 treatment reduces cardiac hypertrophy and left ventricular diameter in spontaneously hypertensive heart failure-prone (cp/+) rats independent of changes in serum leptin. *Journal of Cardiovascular Pharmacology,* 51, 559-64.

MANGGE, H., WEGHUBER, D., PRASSL, R., HAARA, A., SCHNEDL, W., POSTOLACHE, T. T. & FUCHS, D. 2013. The Role of Vitamin D in Atherosclerosis Inflammation Revisited: More a Bystander than a Player? *Current Vascular Pharmacology*. (ahead of print)

MARIOTTI, M., CASTIGLIONI, S., BERNARDINI, D. & MAIER, J. A. 2006. Interleukin 1 alpha is a marker of endothelial cellular senescent. *Immunity & Ageing : I & A,* 3, 4.

MATSUMOTO, S., SHIMABUKURO, M., FUKUDA, D., SOEKI, T., YAMAKAWA, K., MASUZAKI, H. & SATA, M. 2014. Azilsartan, an angiotensin II type 1 receptor blocker, restores endothelial function by reducing vascular inflammation and by increasing the phosphorylation ratio Ser(1177)/Thr(497) of endothelial nitric oxide synthase in diabetic mice. *Cardiovascular Diabetology,* 13, 30.

MEI, S., GU, H., WARD, A., YANG, X., GUO, H., HE, K., LIU, Z. & CAO, W. 2012. p38 mitogen-activated protein kinase (MAPK) promotes cholesterol ester accumulation in macrophages through inhibition of macroautophagy. *The Journal of Biological Chemistry,* 287, 11761-8.

Mestas, J., Hughes, C. C., 2004. Of mice and not men: differences between mouse and human immunology. Journal of Immunology, 172 (5), 2731-2738.

MEYRELLES, S. S., PEOTTA, V. A., PEREIRA, T. M. & VASQUEZ, E. C. 2011. Endothelial dysfunction in the apolipoprotein E-deficient mouse: insights into the influence of diet, gender and aging. *Lipids in Health and Disease,* 10, 211.

MIHARA, M., HASHIZUME, M., YOSHIDA, H., SUZUKI, M. & SHIINA, M. 2012. IL-6/IL-6 receptor system and its role in physiological and pathological conditions.*Clinical Science (Journal),* 122, 143-59.

MINET, C., VIVODTZEV, I., TAMISIER, R., ARBIB, F., WUYAM, B., TIMSIT, J. F., MONNERET, D., BOREL, J. C., BAGUET, J. P., LEVY, P. & PEPIN, J. L. 2012. Reduced six-minute walking distance, high fat-free-mass index and hypercapnia are associated with endothelial dysfunction in COPD. *Respiratory Physiology and Neurobiology,* 183, 128-34.

MOSS, M. B., BRUNINI, T. M., SOARES DE MOURA, R., NOVAES MALAGRIS, L. E., ROBERTS, N. B., ELLORY, J. C., MANN, G. E. & MENDES RIBEIRO, A. C. 2004. Diminished L-arginine bioavailability in hypertension. *Clinical Science,* 107, 391-7.

MOSSER, D. M. 2003. The many faces of macrophage activation. *Journal of Leukocyte Biology,* 73, 209-12.

MULLICK, A. E., TOBIAS, P. S. & CURTISS, L. K. 2005. Modulation of atherosclerosis in mice by Toll-like receptor 2. *The Journal of Clinical Investigation,* 115, 3149-56.

Muslin, A., 2008. MAPK signalling in cardiovascular health and disease: Molecular Mechansims and Therauetic Targets. Clinical Sciences (Lond), 115(7), 203-218.

NAHRENDORF, M. & SWIRSKI, F. K. 2013. Monocyte and macrophage heterogeneity in the heart. *Circulation Research,* 112, 1624-33.

NAHRENDORF, M., SWIRSKI, F. K., AIKAWA, E., STANGENBERG, L., WURDINGER, T., FIGUEIREDO, J. L., LIBBY, P., WEISSLEDER, R. & PITTET, M. J. 2007. The healing myocardium sequentially mobilizes two monocyte subsets with divergent and complementary functions. *The Journal of Experimental Medicine,* 204, 3037-47.

NAKASHIMA, Y., PLUMP, A. S., RAINES, E. W., BRESLOW, J. L. & ROSS, R. 1994. ApoE-deficient mice develop lesions of all phases of atherosclerosis throughout the arterial tree. *Arteriosclerosis and Thrombosis : a Journal of Vascular Biology / American Heart Association,* 14, 133-40.

NANDA, S. K., VENIGALLA, R. K., ORDUREAU, A., PATTERSON-KANE, J. C., POWELL, D. W., TOTH, R., ARTHUR, J. S. & COHEN, P. 2011. Polyubiquitin binding to ABIN1 is required to prevent autoimmunity. *The Journal of Experimental Medicine,* 208, 1215-28.

NASEEM, K. M. 2005. The role of nitric oxide in cardiovascular diseases. *Molecular Aspects* of *Medicine*, 26, 33-65.

NAYA, M., TSUKAMOTO, T., MORITA, K., KATOH, C., FURUMOTO, T., FUJII, S., TAMAKI, N. & TSUTSUI, H. 2007. Plasma interleukin-6 and tumor

necrosis factor-alpha can predict coronary endothelial dysfunction in hypertensive patients. *Hypertension Research,* 30, 541-8.

OH, D. Y., MORINAGA, H., TALUKDAR, S., BAE, E. J. & OLEFSKY, J. M. 2012. Increased macrophage migration into adipose tissue in obese mice. *Diabetes,* 61, 346-54.

OJAIMI, S., SKINNER, N. A., STRAUSS, B. J., SUNDARARAJAN, V., WOOLLEY, I. & VISVANATHAN, K. 2013. Vitamin D deficiency impacts on expression of toll-like receptor-2 and cytokine profile: a pilot study. *Journal of Translational Medicine,* 11, 176.

OZAKI, K., OHNISHI, Y., IIDA, A., SEKINE, A., YAMADA, R., TSUNODA, T., SATO, H., HORI, M., NAKAMURA, Y. & TANAKA, T. 2002. Functional SNPs in the lymphotoxin-alpha gene that are associated with susceptibility to myocardial infarction. *Nature Genetics,* 32, 650-4.

OZAKI, K. & TANAKA, T. 2005. Genome-wide association study to identify SNPs conferring risk of myocardial infarction and their functional analyses. *Cellular and Molecular Life Sciences,* 62, 1804-13.

PALMER, R. M., ASHTON, D. S. & MONCADA, S. 1988. Vascular endothelial cells synthesize nitric oxide from L-arginine. *Nature,* 333, 664-6.

PANICHI, V., DE PIETRO, S., ANDREINI, B., BIANCHI, A. M., MIGLIORI, M., TACCOLA, D., GIOVANNINI, L., TETTA, C. & PALLA, R. 1998. Calcitriol modulates in vivo and in vitro cytokine production: a role for intracellular calcium. *Kidney International,* 54, 1463-9.

PARK, D. W., LEE, H. K., JEONG, T. W., KIM, J. S., BAE, Y. S., CHIN, B. R. & BAEK, S. H. 2012. The JAK2-Akt-glycogen synthase kinase-3beta signaling pathway is involved in toll-like receptor 2-induced monocyte

chemoattractant protein-1 regulation. *Molecular Medicine Reports,* 5, 1063-7.

PARK, S. Y., CHO, Y. R., KIM, H. J., HIGASHIMORI, T., DANTON, C., LEE, M. K., DEY, A., ROTHERMEL, B., KIM, Y. B., KALINOWSKI, A., RUSSELL, K. S. & KIM, J. K. 2005. Unraveling the temporal pattern of diet-induced insulin resistance in individual organs and cardiac dysfunction in C57BL/6 mice. *Diabetes,* 54, 3530-40.

PATTISON, M. J., MACKENZIE, K. F. & ARTHUR, J. S. 2012. Inhibition of JAKs in macrophages increases lipopolysaccharide-induced cytokine production by blocking IL-10-mediated feedback. *Journal of Immunology,* 189, 2784-92.

PEARSON, T. A., MENSAH, G. A., ALEXANDER, R. W., ANDERSON, J. L., CANNON, R. O., 3RD, CRIQUI, M., FADL, Y. Y., FORTMANN, S. P., HONG, Y., MYERS, G. L., RIFAI, N., SMITH, S. C., JR., TAUBERT, K., TRACY, R. P. & VINICOR, F. 2003. Markers of inflammation and cardiovascular disease: application to clinical and public health practice: A statement for healthcare professionals from the Centers for Disease Control and Prevention and the American Heart Association. *Circulation,* 107, 499-511.

PEOTTA, V. A., BHANDARY, P., OGU, U., VOLK, K. A. & ROGHAIR, R. D. 2014. Reduced blood pressure of CFTR-F508del carriers correlates with diminished arterial reactivity rather than circulating blood volume in mice. *PloS One,* 9, e96756.

PICONI, S., TRABATTONI, D., LURAGHI, C., PERILLI, E., BORELLI, M., PACEI, M., RIZZARDINI, G., LATTUADA, A., BRAY, D. H., CATALANO, M., SPARACO, A. & CLERICI, M. 2009. Treatment of periodontal

disease results in improvements in endothelial dysfunction and reduction of the carotid intima-media thickness. *FASEB Journal : official publication of the Federation of American Societies for Experimental Biology,* 23, 1196-204.

PINDERSKI OSLUND, L. J., HEDRICK, C. C., OLVERA, T., HAGENBAUGH, A., TERRITO, M., BERLINER, J. A. & FYFE, A. I. 1999. Interleukin-10 blocks atherosclerotic events in vitro and in vivo. *Arteriosclerosis, Thrombosis, and Vascular Biology,* 19, 2847-53.

PLUMP, A. S., SMITH, J. D., HAYEK, T., AALTO-SETALA, K., WALSH, A., VERSTUYFT, J. G., RUBIN, E. M. & BRESLOW, J. L. 1992. Severe hypercholesterolemia and atherosclerosis in apolipoprotein E-deficient mice created by homologous recombination in ES cells. *Cell,* 71, 343-53.

POLIDORO, L., PROPERZI, G., MARAMPON, F., GRAVINA, G. L., FESTUCCIA, C., DI CESARE, E., SCARSELLA, L., CICCARELLI, C., ZANI, B. M. & FERRI, C. 2013. Vitamin D protects human endothelial cells from H(2)O(2) oxidant injury through the Mek/Erk-Sirt1 axis activation. *Journal of Cardiovascular Translational Research,* 6, 221-31.

POPA, C., NETEA, M. G., VAN RIEL, P. L., VAN DER MEER, J. W. & STALENHOEF, A. F. 2007. The role of TNF-alpha in chronic inflammatory conditions, intermediary metabolism, and cardiovascular risk. *Journal of Lipid Research,* 48, 751-62.

PRADHAN, A. D., MANSON, J. E., RIFAI, N., BURING, J. E. & RIDKER, P. M. 2001. C-reactive protein, interleukin 6, and risk of developing type 2 diabetes mellitus. *Journal of the American Medical Association,* 286, 327-34.

PRADO, C. M., RAMOS, S. G., ELIAS, J., JR. & ROSSI, M. A. 2008. Turbulent blood flow plays an essential localizing role in the development of atherosclerotic lesions in experimentally induced hypercholesterolaemia in rats. *International Journal of Experimental Pathology,* 89, 72-80.

RAKOFF-NAHOUM, S. & MEDZHITOV, R. 2008. Innate immune recognition of the indigenous microbial flora. *Mucosal Immunology,* 1 Suppl 1, S10-4.

RAKOFF-NAHOUM, S., PAGLINO, J., ESLAMI-VARZANEH, F., EDBERG, S. & MEDZHITOV, R. 2004. Recognition of commensal microflora by toll-like receptors is required for intestinal homeostasis. *Cell,* 118, 229-41.

RAVID, A., RUBINSTEIN, E., GAMADY, A., ROTEM, C., LIBERMAN, U. A. & KOREN, R. 2002. Vitamin D inhibits the activation of stress-activated protein kinases by physiological and environmental stresses in keratinocytes. *The Journal of Endocrinology,* 173, 525-32.

RIAD, A., BIEN, S., GRATZ, M., ESCHER, F., WESTERMANN, D., HEIMESAAT, M. M., BERESWILL, S., KRIEG, T., FELIX, S. B., SCHULTHEISS, H. P., KROEMER, H. K. & TSCHOPE, C. 2008a. Toll-like receptor-4 deficiency attenuates doxorubicin-induced cardiomyopathy in mice. *European Journal of Heart Failure,* 10, 233-43.

RIAD, A., JAGER, S., SOBIREY, M., ESCHER, F., YAULEMA-RISS, A., WESTERMANN, D., KARATAS, A., HEIMESAAT, M. M., BERESWILL, S., DRAGUN, D., PAUSCHINGER, M., SCHULTHEISS, H. P. & TSCHOPE, C. 2008b. Toll-like receptor-4 modulates survival by induction of left ventricular remodeling after myocardial infarction in mice. *Journal of Immunology,* 180, 6954-61.

RIAD, A., MEYER ZU SCHWABEDISSEN, H., WEITMANN, K., HERDA, L. R., DORR, M., EMPEN, K., KIEBACK, A., HUMMEL, A., REINTHALER, M.,

GRUBE, M., KLINGEL, K., NAUCK, M., KANDOLF, R., HOFFMANN, W., KROEMER, H. K. & FELIX, S. B. 2012. Variants of Toll-like receptor 4 predict cardiac recovery in patients with dilated cardiomyopathy. *The Journal of biological Chemistry,* 287, 27236-43.

RIDDELL, D. R. & OWEN, J. S. 1999. Nitric oxide and platelet aggregation. *Vitamins and Hormones,* 57, 25-48.

RIDKER, P. M., RIFAI, N., STAMPFER, M. J. & HENNEKENS, C. H. 2000a. Plasma concentration of interleukin-6 and the risk of future myocardial infarction among apparently healthy men. *Circulation,* 101, 1767-72.

RIDKER, P. M., RIFAI, N., STAMPFER, M. J. & HENNEKENS, C. H. 2000b. Plasma Concentration of Interleukin-6 and the Risk of Future Myocardial Infarction Among Apparently Healthy Men. *Circulation,* 101, 1767-1772.

ROIFMAN, I., BECK, P. L., ANDERSON, T. J., EISENBERG, M. J. & GENEST, J. 2011. Chronic inflammatory diseases and cardiovascular risk: a systematic review. *The Canadian Journal of Cardiology,* 27, 174-82.

RONKINA, N., KOTLYAROV, A., DITTRICH-BREIHOLZ, O., KRACHT, M., HITTI, E., MILARSKI, K., ASKEW, R., MARUSIC, S., LIN, L. L., GAESTEL, M. & TELLIEZ, J. B. 2007. The mitogen-activated protein kinase (MAPK)-activated protein kinases MK2 and MK3 cooperate in stimulation of tumor necrosis factor biosynthesis and stabilization of p38 MAPK. *Molecular and Cellular Biology,* 27, 170-81.

RUEDA-CLAUSEN, C. F., LOPEZ-JARAMILLO, P., LUENGAS, C., DEL PILAR OUBINA, M., CACHOFEIRO, V. & LAHERA, V. 2009. Inflammation but not endothelial dysfunction is associated with the severity of coronary artery disease in dyslipidemic subjects. *Mediators of Inflammation,* 2009, 469169.

RUSSELL, J. C. 2003. Of mice and men, rats and atherosclerosis. *Cardiovascular Research,* 59, 810-1.

SCHARF, M., NEEF, S., FREUND, R., GEERS-KNORR, C., FRANZ-WACHTEL, M., BRANDIS, A., KRONE, D., SCHNEIDER, H., GROOS, S., MENON, M. B., CHANG, K. C., KRAFT, T., MEISSNER, J. D., BOHELER, K. R., MAIER, L. S., GAESTEL, M. & SCHEIBE, R. J. 2013. Mitogen-activated protein kinase-activated protein kinases 2 and 3 regulate SERCA2a expression and fiber type composition to modulate skeletal muscle and cardiomyocyte function. *Molecular and Cellular Biology,* 33, 2586-602.

Schuler, D., Sansone, R., Freudenberger T., Mateos, R. A., Weber, G., Momma, T., Goy C., Altschmeid, J., Haendeler, J., Fischer, J., Kelm, M., Heiss, C. 2014. Measuremenst of Endothelium-dependent Vasodilatation in Mice. Arteriosclerosis, Thrombosis and Vascular Biology, DOI: 10.1161/ATVBAHA.114.304699.

SEEGER, F. H., SEDDING, D., LANGHEINRICH, A. C., HAENDELER, J., ZEIHER, A. M. & DIMMELER, S. 2010. Inhibition of the p38 MAP kinase in vivo improves number and functional activity of vasculogenic cells and reduces atherosclerotic disease progression. *Basic Research in Cardiology,* 105, 389-97.

SEMIGRAN, M. J., COCKRILL, B. A., KACMAREK, R., THOMPSON, B. T., ZAPOL, W. M., DEC, G. W. & FIFER, M. A. 1994. Hemodynamic effects of inhaled nitric oxide in heart failure. *Journal of the American College of Cardiology,* 24, 982-8.

SHREENIWAS, R., KOGA, S., KARAKURUM, M., PINSKY, D., KAISER, E., BRETT, J., WOLITZKY, B. A., NORTON, C., PLOCINSKI, J.,

BENJAMIN, W. & *ET AL*. 1992. Hypoxia-mediated induction of endothelial cell interleukin-1 alpha. An autocrine mechanism promoting expression of leukocyte adhesion molecules on the vessel surface. *The Journal of Clinical Investigation,* 90, 2333-9.

SIGAUDO-ROUSSEL, D., DEMIOT, C., FROMY, B., KOITKA, A., LEFTHERIOTIS, G., ABRAHAM, P. & SAUMET, J. L. 2004. Early endothelial dysfunction severely impairs skin blood flow response to local pressure application in streptozotocin-induced diabetic mice. *Diabetes,* 53, 1564-9.

SINGER, W. D., OSIMIRI, L. C. & FRIEDBERG, E. C. 2013. Increased dietary cholesterol promotes enhanced mutagenesis in DNA polymerase kappa-deficient mice. *DNA repair,* 12, 817-23.

SINGHAL, A. 2005. Endothelial dysfunction: role in obesity-related disorders and the early origins of CVD. *Proceedings of the Nutrition Society,* 64, 15-22.

SUGDEN, J. A., DAVIES, J. I., WITHAM, M. D., MORRIS, A. D. & STRUTHERS, A. D. 2008. Vitamin D improves endothelial function in patients with Type 2 diabetes mellitus and low vitamin D levels. *Diabetic Medicine : Journal of the British Diabetic Association,* 25, 320-5.

SUMARA, G., BELWAL, M. & RICCI, R. 2005. "Jnking" atherosclerosis. *Cellular and Molecular Life Sciences,* 62, 2487-94.

SUN, X. & ZEMEL, M. B. 2008. Calcitriol and calcium regulate cytokine production and adipocyte-macrophage cross-talk. *The Journal of Nutritional Biochemistry,* 19, 392-9.

SURWIT, R. S., KUHN, C. M., COCHRANE, C., MCCUBBIN, J. A. & FEINGLOS, M. N. 1988. Diet-induced type II diabetes in C57BL/6J mice. *Diabetes,* 37, 1163-7.

SWIRSKI, F. K., NAHRENDORF, M., ETZRODT, M., WILDGRUBER, M., CORTEZ-RETAMOZO, V., PANIZZI, P., FIGUEIREDO, J. L., KOHLER, R. H., CHUDNOVSKIY, A., WATERMAN, P., AIKAWA, E., MEMPEL, T. R., LIBBY, P., WEISSLEDER, R. & PITTET, M. J. 2009. Identification of splenic reservoir monocytes and their deployment to inflammatory sites. *Science,* 325, 612-6.

TAKEDA, M., YAMASHITA, T., SASAKI, N., NAKAJIMA, K., KITA, T., SHINOHARA, M., ISHIDA, T. & HIRATA, K. 2010. Oral administration of an active form of vitamin D3 (calcitriol) decreases atherosclerosis in mice by inducing regulatory T cells and immature dendritic cells with tolerogenic functions. *Arteriosclerosis, Thrombosis, and Vascular Biology,* 30, 2495-503.

TALUKDER, M. A., JOHNSON, W. M., VARADHARAJ, S., LIAN, J., KEARNS, P. N., EL-MAHDY, M. A., LIU, X. & ZWEIER, J. L. 2011. Chronic cigarette smoking causes hypertension, increased oxidative stress, impaired NO bioavailability, endothelial dysfunction, and cardiac remodeling in mice. *American journal of physiology. Heart and Circulatory Physiology,* 300, H388-96.

TEDGUI, A. & MALLAT, Z. 2006. Cytokines in atherosclerosis: pathogenic and regulatory pathways. *Physiological Reviews,* 86, 515-81.

THOMAS, T., TIMMER, M., CESNULEVICIUS, K., HITTI, E., KOTLYAROV, A. & GAESTEL, M. 2008. MAPKAP kinase 2-deficiency prevents neurons

from cell death by reducing neuroinflammation--relevance in a mouse model of Parkinson's disease. *Journal of Neurochemistry,* 105, 2039-52.

THORNTON, K. A., MARIN, C., MORA-PLAZAS, M. & VILLAMOR, E. 2013. Vitamin D deficiency associated with increased incidence of gastrointestinal and ear infections in school-age children. *The Pediatric Infectious Disease Journal,* 32, 585-93.

THORNTON, K. A., MORA-PLAZAS, M., MARIN, C. & VILLAMOR, E. 2014. Vitamin a deficiency is associated with gastrointestinal and respiratory morbidity in school-age children. *The Journal of Nutrition,* 144, 496-503.

TOBIAS, P. S. & CURTISS, L. K. 2007. Toll-like receptors in atherosclerosis. *Biochemical Society Transactions,* 35, 1453-5.

TSUDA, M., KITAZAKI, T. & IMAI, Y. 1983. Changes in the profiles of rodent plasma lipoproteins and apolipoproteins after cholesterol feeding. *Journal of Biochemistry,* 93, 1071-7.

TURESSON, C., JACOBSSON, L. T. & MATTESON, E. L. 2008. Cardiovascular co-morbidity in rheumatic diseases. *Vascular Health and Risk Management,* 4, 605-14.

TURESSON, C. & MATTESON, E. L. 2013. Malignancy as a comorbidity in rheumatic diseases. *Rheumatology,* 52, 5-14.

TURNER, J., BELCH, J. J. & KHAN, F. 2008. Current concepts in assessment of microvascular endothelial function using laser Doppler imaging and iontophoresis. *Trends in Cardiovascular Medicine,* 18, 109-16.

VAN DER HEIDEN, K., CUHLMANN, S., LUONG LE, A., ZAKKAR, M. & EVANS, P. C. 2010. Role of nuclear factor kappaB in cardiovascular health and disease. *Clinical Science,* 118, 593-605.

VAN DIJK, S. C., SOHL, E., OUDSHOORN, C., ENNEMAN, A. W., HAM, A. C., SWART, K. M., VAN WIJNGAARDEN, J. P., BROUWER-BROLSMA, E. M., VAN DER ZWALUW, N. L., UITTERLINDEN, A. G., DE GROOT, L. C., DHONUKSHE-RUTTEN, R. A., LIPS, P., VAN SCHOOR, N. M., BLOM, H. J., GELEIJNSE, J. M., FESKENS, E. J., SMULDERS, Y. M., ZILLIKENS, M. C., DE JONGH, R. T., VAN DEN MEIRACKER, A. H., MATTACE RASO, F. U. & VAN DER VELDE, N. 2014. Non-linear associations between serum 25-OH vitamin D and indices of arterial stiffness and arteriosclerosis in an older population. *Age and Ageing*. doi: 10.1093/ageing/afu095 (ahead of print).

VAN KUIJK, J. P., FLU, W. J., WELTEN, G. M., HOEKS, S. E., CHONCHOL, M., VIDAKOVIC, R., VERHAGEN, H. J., BAX, J. J. & POLDERMANS, D. 2010. Long-term prognosis of patients with peripheral arterial disease with or without polyvascular atherosclerotic disease. *European Heart Journal,* 31, 992-9.

VAUGHN, S. E., KOTTYAN, L. C., MUNROE, M. E. & HARLEY, J. B. 2012. Genetic susceptibility to lupus: the biological basis of genetic risk found in B cell signaling pathways. *Journal of Leukocyte Biology,* 92, 577-91.

VERMA, S., BUCHANAN, M. R. & ANDERSON, T. J. 2003. Endothelial function testing as a biomarker of vascular disease. *Circulation,* 108, 2054-9.

WALKER, A. E., SEIBERT, S. M., DONATO, A. J., PIERCE, G. L. & SEALS, D. R. 2010. Vascular endothelial function is related to white blood cell count and myeloperoxidase among healthy middle-aged and older adults. *Hypertension,* 55, 363-9.

WANG, X. & LIU, Y. 2007. Regulation of innate immune response by MAP kinase phosphatase-1. *Cellular Signalling,* 19, 1372-82.

WEIDNER, G. & CAIN, V. S. 2003. The gender gap in heart disease: lessons from Eastern Europe. *American Journal of Public Health,* 93, 768-70.

WIGGIN, G. R., SOLOAGA, A., FOSTER, J. M., MURRAY-TAIT, V., COHEN, P. & ARTHUR, J. S. 2002. MSK1 and MSK2 are required for the mitogen- and stress-induced phosphorylation of CREB and ATF1 in fibroblasts. *Molecular and Cellular Biology,* 22, 2871-81.

WILSON, S. B., JENNINGS, P. E. & BELCH, J. J. 1992. Detection of microvascular impairment in type I diabetics by laser Doppler flowmetry. *Clinical Physiology,* 12, 195-208.

WINN, R. K. & HARLAN, J. M. 2005. The role of endothelial cell apoptosis in inflammatory and immune diseases. *Journal of Thrombosis and Haemostasis : JTH,* 3, 1815-24.

WOLFRUM, S., TEUPSER, D., TAN, M., CHEN, K. Y. & BRESLOW, J. L. 2007. The protective effect of A20 on atherosclerosis in apolipoprotein E-deficient mice is associated with reduced expression of NF-kappaB target genes. *Proceedings of the National Academy of Sciences of the United States of America,* 104, 18601-6.

WU, C. C., CHANG, J. H., CHEN, C. C., SU, S. B., YANG, L. K., MA, W. Y., ZHENG, C. M., DIANG, L. K. & LU, K. C. 2011. Calcitriol treatment attenuates inflammation and oxidative stress in hemodialysis patients with secondary hyperparathyroidism. *The Tohoku Journal of Experimental Medicine,* 223, 153-9.

YANG, Y., KIM, S. C., YU, T., YI, Y. S., RHEE, M. H., SUNG, G. H., YOO, B. C. & CHO, J. Y. 2014. Functional roles of p38 mitogen-activated protein kinase in macrophage-mediated inflammatory responses. *Mediators of Inflammation,* 2014, 352371.

YIN, K. & AGRAWAL, D. K. 2014. Vitamin D and inflammatory diseases. *Journal of Inflammation Research,* 7, 69-87.

YU, M., ZHOU, H., ZHAO, J., XIAO, N., ROYCHOWDHURY, S., SCHMITT, D., HU, B., HARDING, C. V., HISE, A. G., HAZEN, S. L., DEFRANCO, A. L., FOX, P. L., MORTON, R. E., DICORLETO, P. E., FEBBRAIO, M., NAGY, L. E., SMITH, J. D., WANG, J. A. & LI, X. 2014. MyD88-dependent interplay between myeloid and endothelial cells in the initiation and progression of obesity-associated inflammatory diseases. *The Journal of Experimental Medicine,* 211, 887-907.

ZAWADA, A. M., ROGACEV, K. S., SCHIRMER, S. H., SESTER, M., BOHM, M., FLISER, D. & HEINE, G. H. 2012. Monocyte heterogeneity in human cardiovascular disease. *Immunobiology,* 217, 1273-84.

ZEMSE, S. M., CHIAO, C. W., HILGERS, R. H. & WEBB, R. C. 2010. Interleukin-10 inhibits the in vivo and in vitro adverse effects of TNF-alpha on the endothelium of murine aorta. *American Journal of Physiology - Heart* and Circulatory *Physiology,* 299, H1160-7.

ZHANG, W., ELIMBAN, V., NIJJAR, M. S., GUPTA, S. K. & DHALLA, N. S. 2003. Role of mitogen-activated protein kinase in cardiac hypertrophy and heart failure. *Experimental and Clinical Cardiology,* 8, 173-83.

ZHANG, Y., LEUNG, D. Y., RICHERS, B. N., LIU, Y., REMIGIO, L. K., RICHES, D. W. & GOLEVA, E. 2012. Vitamin D inhibits monocyte/macrophage proinflammatory cytokine production by targeting MAPK phosphatase-1. *Journal of Immunology,* 188, 2127-35.

ZHAO, X. M. & QIN, S. C. 2011. Oxidative stress of platelet and atherosclerosis. *Sheng li ke xue jin zhan. Progress in Physiology,* 42, 33-8.

ZHOU, J., WU, R., HIGH, A. A., SLAUGHTER, C. A., FINKELSTEIN, D., REHG, J. E., REDECKE, V. & HACKER, H. 2011. A20-binding inhibitor of NF-kappaB (ABIN1) controls Toll-like receptor-mediated CCAAT/enhancer-binding protein beta activation and protects from inflammatory disease. *Proceedings of the National Academy of Sciences of the United States of America,* 108, E998-1006.

ZIMMERMAN, M. A., REZNIKOV, L. L., RAEBURN, C. D. & SELZMAN, C. H. 2004. Interleukin-10 attenuates the response to vascular injury. *Journal* of *Surgical Research,* 121, 206-13.

Microvascular Research 85 (2013) 86–92

Contents lists available at SciVerse ScienceDirect

Microvascular Research

journal homepage: www.elsevier.com/locate/ymvre

Longitudinal assessment of endothelial function in the microvasculature of mice *in-vivo*

Jill J.F. Belch [a], Naveed Akbar [a], Venkateswara Alapati [b], John Petrie [b], Simon Arthur [c], Faisel Khan [a,*]

[a] Vascular & Inflammatory Diseases Research Unit, Dundee, DD1 9SY, Scotland
[b] Diabetes Centre, Ninewells Hospital and Medical School, Dundee, DD1 9SY, Scotland
[c] MRC Protein Phosphorylation Unit, University of Dundee, Dundee, DD1 5EH, Scotland

ARTICLE INFO

Article history:
Accepted 10 October 2012
Available online 31 October 2012

ABSTRACT

Endothelial dysfunction is associated with early development of cardiovascular disease, making longitudinal measurements desirable. We devised a protocol using laser Doppler imaging (LDI) and iontophoresis of acetylcholine (ACh) and sodium nitroprusside (SNP) to assess the skin microcirculation longitudinally in mice every 4 weeks for 24 weeks in two groups of C57BL/6 mice, chow versus high-cholesterol diet(known to induce endothelial dysfunction). LDI measurements were compared with vascular function (isometric tension) measured using wire myography in the tail artery in response to ACh and SNP. Microvascular responses to ACh were significantly reduced in cholesterol-fed versus chow-fed mice from week 4 onwards ($P<0.005$, ANOVA). Pre-treatment with N(G)-nitro-L-arginine methyl-ester-hydrochloride (L-NAME) showed a significant reduction in ACh response compared with vehicle-treated animals ($P<0.05$) at baseline and at 12 weeks. In cholesterol-fed mice, ACh responses were 226 ± 21 and 180 ± 21 AU ($P=0.03$) before and after L-NAME, respectively. A reduction in ex-vivo ACh response was detected in the tail artery in cholesterol-fed mice, and a significant correlation found between peak microvascular ACh response and maximum ACh response in the tail artery ($r=0.699$, $P=0.017$). No changes were found in SNP responses in the microvasculature or tail artery. Using this protocol, we have shown longitudinal decreases in microvascular endothelial function to cholesterol feeding. L-NAME studies confirm that the reduced vasodilatation to ACh in cholesterol-fed mice was mediated partly through reduced NO bioavailability. Wire myography of tail arteries confirmed that *in-vivo* measurements of microvascular function reflect ex-vivo vascular function in other beds. Longitudinal assessments of skin microvascular function in mice could provide a useful translatable model for assessing early endothelial dysfunction.

Introduction

Endothelial dysfunction is an early event in the development of atherosclerosis and is closely associated with cardiovascular disease (CVD), thus making it a key measurement in CVD studies (Bonetti et al., 2003; Esper et al., 2006). The endothelium consists of the innermost layer of cells in blood vessels and is involved in many areas of vascular biology including thrombosis, angiogenesis, inflammation and also plays a vital role in controlling vascular tone (Sumpio et al., 2002). An established method for assessing endothelial function is to measure endothelium-dependent changes in vascular tone in response to vasoactive drugs such as acetylcholine (ACh) (Khan et al., 2008; Ludmer et al., 1986; Morris et al., 1995; Panza et al., 1990; Turner et al., 2008). In animal studies, this is carried out by intra-vital microscopy, or more commonly by *ex-vivo* wire myography, which allows investigators to examine functional responses and vascular reactivity of isolated resistance arteries (Shafaroudi et al., 2005). This technique has been utilized successfully in vessels from various species (Argyle and McGrath, 2000; Arribas et al., 1997; Docherty et al., 2001; Jones et al., 2003; Symons et al., 2001), including transgenic models (Eichhorn et al., 2009; Sainsbury et al., 2004), and in pathological disease states (Sharifi et al., 1998). A major limitation of using such methodology is that animals need to be culled in order to harvest the required vascular tissue. Thus, only a 'snapshot' of vascular function at a set time can be obtained in a given animal and limits longitudinal study involving multiple sample points. It can also limit the ability to examine early changes in vascular function and monitor disease progression over

Abbreviations: ACh, Acetylcholine; CVD, Cardiovascular disease; LDI, Laser Doppler imaging; L-NAME, N (G)-nitro-L-arginine methyl ester hydrochloride; NO, Nitric oxide; PE, Phenylephrine; SNP, Sodium nitroprusside; WT, Wild-type.

* Corresponding author at: Vascular & Inflammatory Diseases Research Unit, Centre for Cardiovascular & Lung Biology, Mail Box 1, Ninewells Hospital and Medical School, Dundee, DD1 9SY, Scotland. Fax: +44 1382 632333.
E-mail addresses: J.J.F.Belch@dundee.ac.uk (J.J.F. Belch), N.Akbar@dundee.ac.uk (N. Akbar), alapativ@googlemail.com (V. Alapati), John.Petrie@glasgow.ac.uk (J. Petrie), J.S.C.Arthur@Dundee.ac.uk (S. Arthur), f.khan@dundee.ac.uk (F. Khan).

0026-2862/$ – see front matter © 2012 Elsevier Inc. All rights reserved.
http://dx.doi.org/10.1016/j.mvr.2012.10.008

time. As with all *in-vitro* techniques, it also suffers from the limitation that the tissue is kept in a controlled environment outside normal physiological conditions and therefore may not always be translatable to *in-vivo* conditions.

Some clinical studies relating to endothelial function testing have utilized the cutaneous microvasculature. It has been established that there are implications for microvascular function in a range of diseases including diabetes (Khan et al., 2000; Morris et al., 1995), rheumatoid arthritis (Galarraga et al., 2008) and in patients with cardiovascular risk factors (Huang et al., 2007; Ijzerman et al., 2003; Khan et al., 2003). Therefore, it may prove to be potentially very useful to be able to measure early microvascular dysfunction in animal studies of these diseases, and also in mouse models in which the genotype has been altered. However, there is a relative lack of studies longitudinally measuring early changes in endothelial function in animals *in-vivo*. We therefore aimed to devise a method for using laser Doppler imaging and iontophoresis of vasoactive chemicals to measure endothelial function longitudinally over time in the skin microvasculature of mice. The laser Doppler imager (LDI) allows measurement of changes in cutaneous perfusion in response to vasoactive drugs that work through the endothelium (e.g. ACh) and which can be delivered locally to an area of skin by iontophoresis. The primary aim of this study was to use LDI and iontophoresis of vasoactive drugs to measure early changes in endothelial function in two groups of 'wild-type' (WT) mice, one fed a regular mouse 'chow' diet and the other fed a high-cholesterol 'atherogenic' diet, which is known to induce endothelial dysfunction. This was a longitudinal study with skin microvascular function measured monthly in the same animals over a period of 24 weeks. One of the secondary aims was to compare our *in-vivo* measurements of microvascular function using the LDI methodology with the established wire myography technique for assessing vascular function in the mouse tail artery, a resistance vessel which is representative of the skin circulation given its role in thermoregulation. Since previous studies in humans have shown that microvascular responses in the skin might be representative of generalised vascular function in other vascular beds (Cracowski et al., 2006), this would allow us to assess whether our *in-vivo* measurement of skin microvascular function in mice was representative of *ex-vivo* vascular function in another vascular bed. Hypercholesterolemia is known to produce a reduction in nitric oxide (NO) bioavailability, and therefore a further secondary aim was to confirm that in our *in vivo* experimental method ACh-mediated vasodilatation reflected NO-mediated changes in normal chow-fed animals and that a reduced vasodilator response to ACh in hypercholesterolemic animals reflected reduced NO bioavailability.

Methods

All work was carried out under a valid U.K. Home Office project licence by a U.K. Home Office Personal Licence holder, and after approval from the institutional animal ethics committee. All animals in the study were an inbred C57BL/6 strain; male, aged between 16 and 28 weeks, housed in groups of up to five. Following baseline measurements of skin microvascular function, animals were randomly separated into groups according to their diet regime and followed-up for 24 weeks. A group of 19 mice remained on the 'normal' rodent chow while the remaining 19 were given a specially designed 'atherogenic' diet (TD.01383 diet, Harlan-Teklad), which consisted of a standardized 18% protein rodent chow with added cholesterol (2% by weight cholesterol). Group numbers were based on previous studies conducted by Sigaudo-Roussel et al. (2004). However, given the longitudinal nature of our study we anticipated the possibility of a small risk of animal death by repeated anaesthesia. Thus to account for any loss we increased our numbers as a safe guard. However we reported no loss of animals due to the experimental design.

Laser Doppler Imaging and Iontophoresis

Iontophoresis of vasoactive compounds requires clean contact with the epidermis; similarly, LDI measurements are most accurate on hair-free, unblemished skin. Therefore, 24–36 hours prior to measurements of microvascular perfusion, the animals' skin was prepared by first shaving the hair from both flanks using an electric shaver. Remaining hair was removed using a depilatory cream (Veet®, Reckitt-Benckiser).

General anesthesia of animals was required to prevent body movements creating artefacts during skin perfusion measurements. Induction of anesthesia was achieved using a 5% combination of Isoflurane (Abbott Laboratories) in oxygen (2 L/minute) delivered via standard Boyle's Apparatus into a small Perspex (induction) chamber. Anesthesia was maintained using a 1.5%–2% concentration of Isoflurane in oxygen (1.5 L/minute) delivered via a nose cone. The level of anesthesia was determined by testing of rear foot reflexes. During all procedures the animal's body temperature was maintained at 37 °C using a heat mat with core body temperature monitored using an electric temperature probe inserted into the animal's rectum.

Animals were housed and experiments conducted in a laboratory with a room temperature set at 22 ± 2 °C. A LDI (moorLDI, Moor Instruments, Axminster, UK) was used to measure microvascular perfusion. LDI utilizes a stable helium neon (HeNe) laser source (633 nm) (2 mW nominal power). The region of interest (ROI) was determined by the size of the iontophoresis chamber. A scan area of 4 cm^2 was used for all measurements. Scan resolution was set at 10 ms/pixel, equating to an average scan time of 49 seconds, with an upper cut off frequency of 15 kHz and direct current (DC) for normalization. Anesthetised animals were laid on their side with the left side flank facing upwards. An iontophoresis chamber (ION6 probe, Moor Instruments Ltd, Devon, UK), consisting of a 20 mm internal diameter ring with a wire electrode running round the inner surface, was attached to a 3.2 cm^2 area of the lower flank (between the ribs and legs) using double-sided adhesive tape, forming a watertight seal with the skin. A second 'reference' electrode pad was attached to the underside of the animal in order to complete the iontophoresis circuit. The 2 electrodes were attached to an iontophoresis controller (MIC2 Iontophoresis Controller, Moor Instruments Ltd, Devon, UK). This study involved measuring cutaneous microvascular responses repeatedly in the same animals at 4-week intervals over 24 weeks and therefore effort was made to ensure repeated measures were taken from the same flank and at a similar site. Due to the area (3.2 cm^2) required for placement of the iontophoresis chamber, and the relatively small size of the animal, the iontophoresis chamber could only be positioned realistically in one area and so we are confident that the measurement site was similar on repeated testing.

The laser scanner was placed over the mouse at a distance of 30 cm and set to scan continuously. Perfusion was expressed as a function of the number of red blood cells multiplied by their mean velocity and an output in relative perfusion in arbitrary units (AU) was obtained using the proprietary software (moorLDI software, version 5.2). The iontophoresis chamber was initially filled with ~2 ml of a 1% concentration of the α_1-adrenergic receptor agonist, phenylephrine (PE) and sealed with a clear Perspex cap. Three initial baseline scans were taken (without current applied), with each scan taking approximately 1 minute. To standardize baseline perfusion, skin blood vessels were pre-constricted by iontophoresis of PE for 6 minutes using an anodal current strength of 100 μA. Following normalized baseline measurements of pre-constricted skin microvessels, a 2% solution of ACh was iontophoresed continuously for approximately 10 minutes (using an anodal current strength of 100 μA) to provide a cumulative dose–response. Iontophoretic dose is defined as current multiplied by time of application Dose (μA/second) = current (μA) x time (seconds), and the amount of drug delivered is directly proportional to the iontophoretic dose applied (Turner et al., 2008).

At a different site on the opposite flank of the animal, sodium nitroprusside (SNP) was used as an endothelium-independent control to assess the function of the vascular smooth muscle. As with ACh, initial baseline measurements were taken before the blood vessels of the skin were pre-constricted using iontophoresis (100 μA) of PE for 6 minutes. Further normalized baseline measurements were taken for 3 minutes followed by the continual iontophoresis of a 2% solution of SNP using a cathodal current strength of 100 μA for 10 minutes. To reduce the amount of time that each animal was under general anesthetic, and to limit the amount of drug exposure, endothelium-independent responses to SNP were only measured at the end point of the study (24 weeks).

Role of nitric oxide in the response to acetylcholine

In order to determine the contribution of endothelium-derived NO to ACh-mediated vasodilatation, 8 additional animals fed normal rodent chow were studied at baseline (week 0) and were pre-treated with the non-selective inhibitor of nitric oxide synthase (NOS), L-NAME (Sigma Chemicals) before iontophoresis of ACh. L-NAME was delivered according to a previous protocol (Jones et al., 2003) whereby a dose of 20 mg/kg was given via an intraperitoneal (i.p.) injection 30 minutes prior to laser Doppler measurement (iontophoresis protocol as above). The drug vehicle (de-ionised, sterile water) was administered via i.p. injection to a further separate group of 7 and served as controls. Following baseline measurements, mice were randomly assigned to receive normal chow ($n=4$) or the atherogenic diet ($n=4$) for 12 weeks after which the experiments (ACh-mediated vasodilatation in L-NAME-treated mice) were repeated.

Assessment of tail artery function using wire myography

At the end point of the study; ex vivo functional vascular studies were performed in 11 chow-fed mice and 11 cholesterol-fed mice on a Mulvany–Halpern four-channel wire myograph (Danish MyoTech). Group numbers were determined by previously published protocols for small resistance vessels (Chotani et al., 2000; Faraci et al., 1998; Sainsbury et al., 2004). Animals were culled by CO_2 exposure delivered in an increasing concentration within a perspex chamber. Tails were immediately removed and arteries dissected under a dissecting microscope and transferred immediately to ice-cold PSS (physiological saline solution: 119 mM NaCl, 4.7 mM KCl, 1.2 mM $MgSO_4$, 1.2 mM KH_2PO_4. 24.8 mM Na HCO_3, 2.5 mM $CaCl_2$, 11.0 mM glucose). Approximately 2 mm length (200–300 μm in diameter) segments were isolated from the tips and stored in PSS overnight at 4 °C. Arterial segments were mounted on two 40 μm diameter stainless steel wires attached to a force transducer and micrometer, respectively. The temperature was raised to 37 °C, and a gas mixture (5% CO2/95% O2) was bubbled in for the duration of the experiment. After 30 min of equilibration, each vessel was set to an optimal normalized internal diameter. Arteries were then preconstricted with 10^{-7} M U-46619 (a thromboxane A_2 mimetic) and then relaxed with 1 μM of ACh. Vessel segments that showed at least 70% relaxation were deemed viable and considered for further experiment. Isometric tension was measured and concentration–response curves were plotted for the endothelium-dependent dilator agonist ACh (10^{-9} to 10^{-4} M) and the endothelium-independent dilator agonist SNP (10^{-9} to 10^{-4} M).

Measurement of total plasma cholesterol levels

A colorimetric assay [Biovision, Catalog #K603-100] was used to measure total cholesterol in the plasma of mice. Blood samples of up to 200 μl were taken via the tail vein at each measurement time-point from which approximately 100 μl of plasma was obtained. Plasma levels of total cholesterol were measured at baseline (Week 0), mid-point (Week 12) and endpoint (Week 24).

Post-mortem lipid staining of aorta

En-face staining of animals' aorta with Oil Red O was carried out to assess the atherogenic response of the animals to their respective diets. Oil Red O is a stain used to determine lipid deposition on the vessel wall. The entire aortic tree was dissected, with fat and connective tissue carefully removed. The aorta was cut longitudinally, pinned onto a paraffin block, stained with oil red O and digitally scanned. Atherosclerotic lesion area was assessed using Adobe Photoshop software and expressed as a percent of the total surface area encompassed by the aortic arch, thoracic aorta, abdominal aorta, or total aorta as indicated.

Data analysis

Longitudinal changes in skin perfusion over 24 weeks and dose–response curves were analyzed using ANOVA for repeated measures, followed by post-hoc Bonferroni tests. Results for skin microcirculation responses were analysed using SPSS version 15.0. Statistical analysis for myography data was carried out using GraphPad Prism (Version 5). Non-linear regression was utilized to produce dose–response graphs and EC_{50} values. The association between LDI skin microvascular responses and myography measurements and lipid deposition was tested using Pearson correlation coefficients. The null hypothesis was rejected at $P=<0.05$.

Results

Plasma levels of total cholesterol and body weight

Fig. 1 shows that total cholesterol levels remained constant for the duration of the study in the normal chow-fed animals. In the atherogenic diet-fed mice, there was a significant increase in total cholesterol from baseline to 12 and 24 weeks ($P<0.01$, respectively for both). There was no significant difference in body weights between the groups at baseline (26.72 ± 2.40 g vs. 25.67 ± 2.22 g; chow and atherogenic fed, respectively, $P>0.05$) or at the end of study (33.22 ± 2.16 g vs. 34.28 ± 4.47 g; chow and atherogenic fed, respectively, $P>0.05$).

Baseline skin microvascular responses to acetylcholine

Basal skin perfusion was not significantly different in mice assigned to receive chow (251.4 ± 24.0 AU) or the atherogenic diet (240.3 ± 27.2 AU). In both groups there was a reduction in skin perfusion in response to iontophoresis of 2% PE, giving a stable corrected baseline

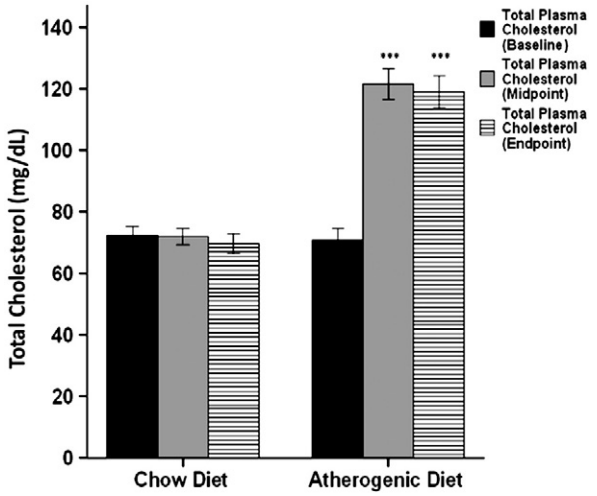

Fig. 1. Total plasma cholesterol levels in chow- and atherogenic diet-fed mice ($n=19$ for each group). Samples were analyzed at baseline (Week 0), study mid-point (Week 12), study end-point (Week 24).

(234.4 ± 17.7 AU versus 210.0 ± 19.7 AU, respectively, $P > 0.05$). This corrected baseline was sustained until 2% ACh was administered. Pilot work showed that the PE-induced preconstriction persists for at least 30 minutes and therefore covers the duration of the ACh protocol. Fig. 2 shows that skin microvascular response to iontophoresis of ACh were not significantly different in the both groups of mice at baseline (week 0).

Longitudinal changes in microvascular responses to ACh in mice fed an atherogenic vs. normal chow diet over 24 weeks

Fig. 3 shows that in comparison to baseline responses at week 0, there were no significant changes in the response to ACh in mice fed a chow diet over 24 weeks. A significant reduction ($P < 0.005$, ANOVA) in ACh responses was seen in the atherogenic diet-fed mice compared with chow-fed mice group. The ACh response was reduced in atherogenic diet-fed mice at week 4 ($P < 0.01$ post-hoc analysis comparing chow vs atherogenic diet) then a further reduction at week 8 ($P < 0.001$ post-hoc analysis comparing chow vs atherogenic diet). ACh responses in the atherogenic diet mice remained significantly lower than in the chow-fed mice from week 8 to 24 ($P < 0.001$ post-hoc analysis comparing chow vs atherogenic diet for all time points).

Microvascular responses to SNP in mice fed an atherogenic diet vs. normal chow diet

The microvascular response to SNP in chow-fed mice at week 24 was 368 ± 32 AU versus the atherogenic group response of 371 ± 21 AU, which was not significantly different.

Role of nitric oxide in hyperaemic response to acetylcholine

Fig. 4 shows the effect of blocking NOS by pre-treatment with L-NAME (20 mg/kg, i.p) on ACh-mediated vasodilatation in mice given normal chow at baseline (week 0). There was a significant reduction in ACh response in L-NAME treated animals compared with vehicle treated animals ($P < 0.05$). At 12 weeks, mice fed normal chow showed a similar reduction in peak ACh response following L-NAME (310 ± 33 AU vs 248 ± 26 AU before versus after L-NAME, respectively, $P = 0.02$). In animals fed an atherogenic diet for 12 weeks, ACh-mediated vasodilatation before L-NAME was 226 ± 21 AU, and this response was reduced to 180 ± 21 AU ($P = 0.03$) following L-NAME. The degree of change in ACh response at 12 weeks following L-NAME was significantly greater in animals fed normal chow compared with animals fed an atherogenic diet (62 AU vs 46 AU, $P < 0.05$).

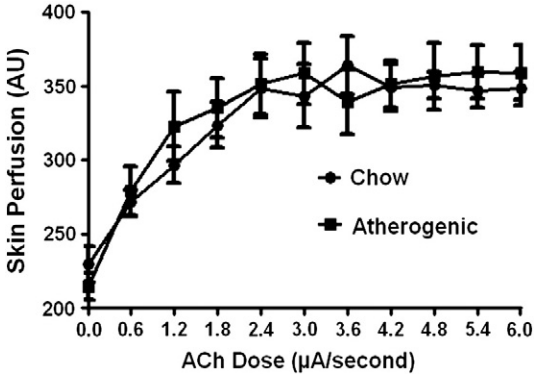

Fig. 2. Skin perfusion response to ACh iontophoresis at the start of study (Week 0) showing no significant difference in vascular response between animals assigned to receive normal rodent chow ($n = 19$) or an atherogenic diet ($n = 19$). Cutaneous microvasculature was preconstricted with phenylephrine as described in Methods. Skin perfusion was measured in arbitrary units (AU). Error bars are SEM.

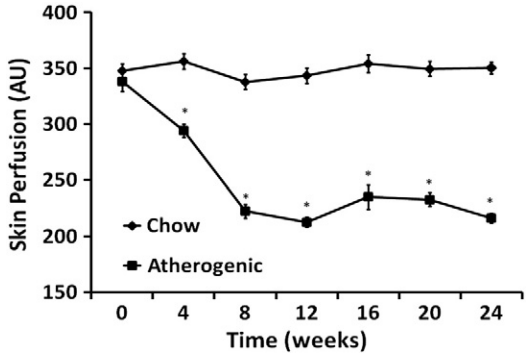

Fig. 3. Longitudinal assessment of microcirculation response to ACh in mice fed an atherogenic diet ($n = 19$) vs. normal chow diet ($n = 19$) over 24 weeks. Skin microvascular responses to ACh (AU) were significantly reduced ($P < 0.05$) from week 4 in animals fed an atherogenic diet compared with the chow-fed animals. $^{*}P < 0.01$, $^{**}P < 0.001$ (post-hoc analysis). Error bars are SEM.

Relaxation in the tail artery to ACh and SNP measured by wire myography ex-vivo

The tail artery response to ACh was calculated as a measure of endothelial function in mice fed an atherogenic diet versus a normal chow diet. The sensitivity of ACh response did not change as there was no significant change in EC_{50} across groups (chow; −log[6.6 ± 0.1]M vs atherogenic; -log[6.1 ± 0.1]M, $P > 0.05$) as shown in Fig. 5. However, the extent of relaxation was reduced in the atherogenic diet group (chow-fed, 75.7 ± 4.8% vs atherogenic, 54.3 ± 3.9%, $P < 0.05$).

There was no significant difference in tail artery response to SNP in the atherogenic diet group compared with the chow-fed group (Fig. 6). There was also no change in the sensitivity of SNP response indicated by lack of significant change in EC_{50} across groups (chow; −log [6.7 ± 0.1]M vs atherogenic; −log[6.9 ± 0.1]M, $P > 0.05$).

Correlations between microvascular response to ACh and tail artery vascular function

We found a significant correlation when plotting the peak microvascular response to ACh against the maximum ACh-mediated relaxation in the tail artery at week 24 ($r = 0.699$, $P = 0.017$). There was a positive correlation between the microvascular response to SNP and tail artery response at week 24 but this did not quite reach statistical significance ($r = 0.347$, $P = 0.173$).

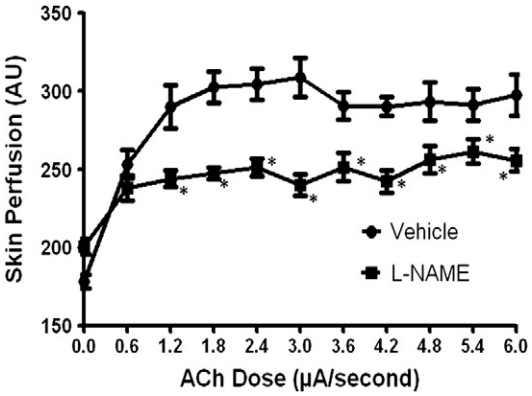

Fig. 4. Effect of L-NAME (20 mg/kg, i.p., $n = 7$) and vehicle (De-ionized water, i.p. $n = 7$) on microvascular response to ACh in chow-fed at baseline (week 0). Skin perfusion was measured in arbitrary units (AU). Error bars are SEM.

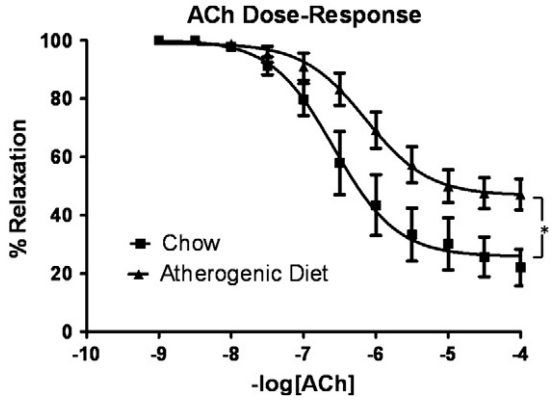

Fig. 5. Ex-vivo measurement of tail artery relaxation to ACh, measured by wire myography, in chow-fed mice ($n=11$) versus atherogenic diet mice ($n=11$). *$P<0.05$.

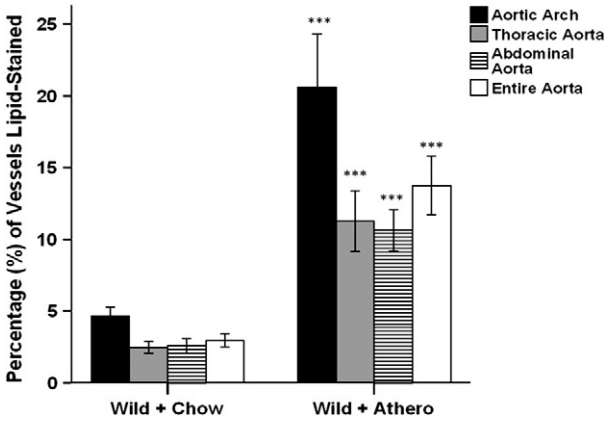

Fig. 7. Percentage of aortic vessel stained for lipid with Oil Red O stain in chow- and atherogenic diet-fed mice ($n=19$ for each group).

Post-mortem analysis of aorta–lipid deposition

Fig. 7 shows the level of lipid deposition on the arterial wall through en-face staining of the excised aorta with Oil Red O stain. Lipid deposition was significantly ($P<0.01$) greater in all areas of the aorta of atherogenic diet-fed mice compared with chow-fed mice.

There were significant negative correlations between the percentage of entire aorta covered in lipid and iontophoretic responses to ACh at 8 weeks ($r=-0.751$, $P<0.001$) and at 24 weeks ($r=-0.826$, $P<0.001$).

Discussion

In this study, we have used LDI combined with iontophoresis of vasoactive chemicals to measure *in-vivo* skin microvascular function longitudinally over 24 weeks in response to an intervention (high cholesterol diet) known to produce endothelial dysfunction and atherosclerosis. Measurements of total plasma cholesterol confirm that the atherogenic diet used in this study was successful in increasing plasma cholesterol levels. The subsequent atherogenic response was measured post-mortem and showed significant lipid deposition in the aorta vessel wall. The main findings from our study are that, using this technique, early development and progression of endothelial dysfunction can be detected in the skin microcirculation of mice. The significant correlation between impairment in ACh-mediated vascular responses at 8 weeks and the percentage of lipid deposition in the aorta at 24 weeks provides supportive evidence that early measurements of endothelial dysfunction in the skin microcirculation reflect atherosclerosis burden using this mouse model.

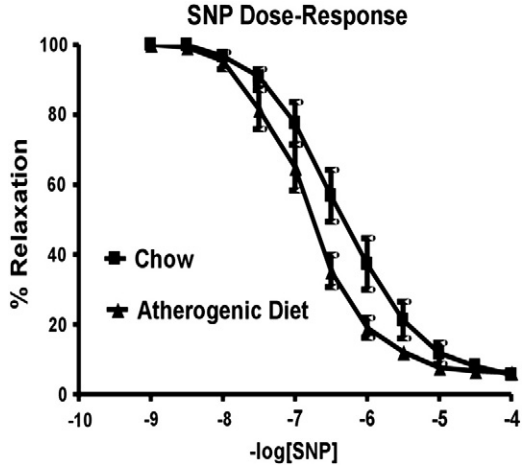

Fig. 6. Ex-vivo measurement of tail artery relaxation response to SNP, measured by wire myography, in chow-fed mice ($n=11$) versus atherogenic diet mice ($n=11$).

We found that in contrast to mice fed a standard chow diet, who maintained ACh-mediated vasodilatation over 24 weeks, mice fed a high-cholesterol, atherogenic diet showed significantly attenuated skin microvascular responses to ACh after 4 weeks and continued to remain so for the remainder of the 24-week duration of the study. The finding that microvascular responses to SNP, which provide a measure of endothelium-independent smooth muscle cell function, remained relatively intact in high cholesterol-fed mice throughout the 24-week period supports the concept that the impairment in microvascular function was specifically at the level of the endothelium and not due to a generalized reduction in vasodilator capacity.

ACh mediates endothelium-dependent vasodilatation via muscarinic receptors on the endothelial cell surface. This leads to an increase in intracellular calcium concentration, activation of endothelial NO synthase and a subsequent increase in NO production. In our model, the contribution of endothelium-derived NO to the baseline ACh response at week 0 and at 12 weeks following normal chow feeding was confirmed as shown by the significant reduction in the ACh following pre-treatment with L-NAME, a non-selective inhibitor of NOS. In cholesterol-fed mice, the microvascular response to iontophoresis of ACh at 12 weeks was significantly reduced and pre-treatment with L-NAME produced a smaller reduction in ACh-mediated vasodilatation than that observed at baseline suggesting that NO bioavailability had been partly compromised by the high cholesterol diet. However, since a significant vasodilator response was still evident in L-NAME treated mice, this suggests that additional mechanisms for ACh-mediated vasodilatation, independent of NO, must be in operation. In addition to the contribution of NO to ACh-mediated vasodilatation, prostaglandins and endothelium-derived hyperpolarizing factor are also thought to make a contribution (Gaubert et al., 2007). We did not carry out experiments to examine other possible pathways as the primary purpose of this study was to use the LDI and iontophoresis technique assess longitudinal changes in endothelial function to an intervention known to induce atherosclerosis, rather than to tease out the specific underlying mechanisms affected by the high cholesterol diet.

To further examine whether evidence for the presence of endothelial dysfunction measured *in-vivo* in the skin microvasculature using this technique was representative of changes in endothelial function in other vessels of the animal, we performed functional studies of the mouse tail arteries *ex-vivo* using wire myography. The sensitivity of ACh response in tail arteries did not change (indicated by no significant change in EC_{50} across groups). However, the extent of relaxation was

reduced in the high cholesterol diet group after 24 weeks, indicative of endothelial dysfunction. These results significantly correlated with measurements in the microcirculation at 24 weeks, indicating that the endothelial dysfunction was present in vascular beds other than the skin within the high cholesterol diet group and that measurements made in the skin were reflective of changes in vascular function in other vascular beds. There was no difference in the extent of relaxation or sensitivity of SNP response in the tail-artery response between the diet groups, confirming the observation seen *in-vivo* in the microvasculature. There was a borderline significant correlation between the peak SNP response in the skin microcirculation and tail artery response. It is possible that this lack of correlation was due to the fact that the values were at the top end of the dose–response curves where there was little variability across groups meaning that our ability to pick up significant relationships might not have been sensitive enough, especially with the relatively small number of mice in this study.

A limitation of this *ex-vivo* work was the use of U-46619 (a synthetic analogue of prostaglandin PGH2) as a preconstrictor agent for the myography experiments. This was in contrast to the *in-vivo* laser Doppler methodology which used the α_1-adrenergic receptor agonist, PE to establish a pre-constricted baseline. This was due to an incompatibility of the separate methodologies; there was no way of delivering U-46619 iontophoretically *in-vivo* and similarly, the myography protocol was not optimised to use PE. Future studies could endeavour to synchronise the methodologies. A further limitation is that more detailed exploration of the nature of endothelial dysfunction could have been evaluated in the isolated vessels preparation *ex vivo,* however as stated above, the primary objective of the current study was to test the ability to measure changes in endothelial function longitudinally *in-vivo* over time.

The use of LDI to measure skin microcirculation response to iontophoresis of vasoactive test drugs has been developed over a number of years and used in a variety of patient populations including the elderly, diabetes, CVD and rheumatoid arthritis patients. However there is still some disagreement about the most reliable protocol (Cracowski et al., 2006; Turner et al., 2008). The use of the iontophoresis and LDI procedures in mice meant that a number of physiological, technical and operational issues had to be resolved and developed. Technical considerations included the iontophoresis protocol (drug concentration and iontophoresis current/duration), current-induced vasodilatation and the location of the iontophoresis and scanning area. Previous studies in humans have shown that current-induced hyperemia can be an issue with iontophoresis drug delivery, especially at higher currents (Åsberg et al., 1999; Durand et al., 2002a,2002b; Grossmann et al., 1995), and at the cathode (Abou-Elenin et al., 2002; Berliner, 1997; Morris et al., 1995; Morris and Shore, 1996). In our pilot work, we did not observe any current-induced vasodilatation during iontophoresis of deionized water with anodal and cathodal currents of 100 μA (unpublished results); therefore all measured increases in skin perfusion were drug-specific. We also found that moving the iontophoresis and scanning site from one flank of the animal to the other made no significant difference to the perfusion response. Indeed, one of the advantages of using laser-Doppler imaging is that it eliminates the spatial heterogeneity seen in single-point flowmetry studies (Fagrell and Nilsson, 1995; Morris et al., 1995; Turner et al., 2008). This was particularly important in this study where repeated measures over time were required.

Previous work carried out in mice using laser Doppler technology utilized a multi-fiber, single point laser Doppler probe in diabetic mice Sigaudo-Roussel et al. (2004). In that study the authors found that ACh delivered via iontophoresis produced an increase of 81 ± 25% in skin perfusion while SNP produced a 54 ± 15% increase. They have subsequently used this technique successfully in further studies using mice (Demiot et al., 2006a,b; Garry et al., 2007; Gaubert et al., 2007). Our results are comparable although by using LDI as opposed to flowmetry, we appear to have reduced the variability of the results with a typical increase of 88.4 ± 5.2% and 83.9 ± 9.2% for ACh and SNP respectively, further emphasizing the advantage of LDI over classical Doppler flowmetry.

There are a number of methods currently used in animal studies for measuring endothelial cell function in large arteries/blood vessels including wire-myography, pressure-myography and organ-bath experiments. Although these methods are reliable and fully established, they require the culling of animals making longitudinal studies difficult. Additionally, they remove tissue from normal physiological conditions and do not necessarily reflect the status of the microcirculation. Anesthetics have the potential to induce changes in blood flow. The use of isoflurane as an anesthetic in this study allowed the induction of adequate immobilization with quick recovery. It has previously been reported that gaseous anesthesia produces less interference with the microcirculation as opposed to other agonists such as ketamine and benzodiazepine, which require injection into the peritoneal cavity. Furthermore, it has been shown that isoflurane causes no significant change in tissue perfusion or oxygenation and maintains normal cardiac output (Baudelet et al., 2004). In our own pilot work, we observed no significant change in baseline perfusion before and after isoflurane.

In conclusion, we have used LDI in combination with iontophoresis of vasoactive chemicals to measure longitudinal changes in microvascular endothelial cell function *in-vivo* and have shown that early changes in skin microvascular function are representative of atherosclerotic burden. In this regard, the skin microcirculation might provide a useful platform to better understand the relationship between early endothelial dysfunction and development and progression of atherosclerosis in mice. The advantage of measuring endothelial function *in-vivo* is that by definition animals are kept alive during the procedure meaning that multiple measurements can be made on the same animal over time, thereby increasing the amount of data captured from each animal and importantly limiting the number of animals culled. The observation that early endothelial dysfunction measured in the skin microvasculature may reflect endothelial dysfunction in other vascular beds is a potentially important finding. This mirrors what has been observed in humans (Bonetti et al., 2003), confirming the *in-vivo* measurement of endothelial dysfunction using LDI as a translatable biomarker. However, further studies will be required to confirm this observation. We believe that this methodology could allow tracking of development of early endothelial dysfunction in the microvasculature in various animal models of CVD, especially in transgenic mice models to allow a better understanding of specific pathways and mechanisms underlying development and progression CVD.

Conflict of interest statement

None

Acknowledgments and sponsorship

This work was carried out as part of a Medical Research Council-funded PhD studentship. Venkateswara Alapati's work was supported by Diabetes U.K. The Laser Doppler imager was purchased with a grant from Tenovus Scotland. We would additionally like to acknowledge Jamie Turner for technical assistance with experiments. Funding bodies did not contribute to the study design, data collection, analysis and interpretation of results or in the report writing.

References

Abou-Elenin, K., Xydakis, A., Hamdy, O., Economides, P.A., Horton, E.S., Veves, A., 2002. The effect of aspirin and various iontophoresis solution vehicles on skin microvascular reactivity. Microvasc. Res. 63, 91–95.

Argyle, S.A., McGrath, J.C., 2000. An α(1A)/α(1L)-adrenoceptor mediates contraction of canine subcutaneous resistance arteries. J. Pharmacol. Exp. Ther. 295, 627–633.

Arribas, S.M., Vila, E., McGrath, J.C., 1997. Impairment of vasodilator function in basilar arteries from aged rats. Stroke 28, 1812–1820.
Åsberg, A., Holm, T., Vassbotn, T., Andreassen, A.K., Hartmann, A., 1999. Nonspecific microvascular vasodilation during iontophoresis is attenuated by application of hyperosmolar saline. Microvasc. Res. 58, 41–48.
Baudelet, C., Ansiaux, R., Jordan, B.F., Havaux, X., Macq, B., Gallez, B., 2004. Physiological noise in murine solid tumours using T2*-weighted gradient-echo imaging: a marker of tumour acute hypoxia? Phys. Med. Biol. 49, 3389–3411.
Berliner, M.N., 1997. Skin microcirculation during tapwater iontophoresis in humans: cathode stimulates more than anode. Microvasc. Res. 54, 74–80.
Bonetti, P.O., Lerman, L.O., Lerman, A., 2003. Endothelial dysfunction: a marker of atherosclerotic risk. Arterioscler. Thromb. Vasc. Biol. 23, 168–175.
Chotani, M.A., Flavahan, S., Mitra, S., Daunt, D., Flavahan, N.A., 2000. Silent alpha(2C)-adrenergic receptors enable cold-induced vasoconstriction in cutaneous arteries. Am. J. Physiol. Heart Circ. Physiol. 4, 1075–1083.
Cracowski, J.L., Minson, C.T., Salvat-Melis, M., Halliwill, J.R., 2006. Methodological issues in the assessment of skin microvascular endothelial function in humans. Trends Pharmacol. Sci. 27, 503–508.
Demiot, C., Fromy, B., Saumet, J.L., Sigaudo-Roussel, D., 2006a. Preservation of pressure-induced cutaneous vasodilation by limiting oxidative stress in short-term diabetic mice. Cardiovasc. Res. 69, 245–252.
Demiot, C., Tartas, M., Fromy, B., Abraham, P., Saumet, J.L., Sigaudo-Roussel, D., 2006b. Aldose reductase pathway inhibition improved vascular and C-fiber functions, allowing for pressure-induced vasodilation restoration during severe diabetic neuropathy. Diabetes 55, 1478–1483.
Docherty, C.C., Kalmar-Nagy, J., Engelen, M., Nathanielsz, P.W., 2001. Development of fetal vascular responses to endothelin-1 and acetylcholine in the sheep. Am. J. Physiol. Regul. Integr. Comp. Physiol. 280, R554–R562.
Durand, S., Fromy, B., Bouye, P., Saumet, J.L., Abraham, P., 2002a. Current-induced vasodilation during water iontophoresis (5 min, 0.10 mA) is delayed from current onset and involves aspirin sensitive mechanisms. J. Vasc. Res. 39, 59–71.
Durand, S., Fromy, B., Bouye, P., Saumet, J.L., Abraham, P., 2002b. Vasodilatation in response to repeated anodal current application in the human skin relies on aspirin-sensitive mechanisms. J. Physiol. (Lond.) 540, 261–269.
Eichhorn, B., Muller, G., Leuner, A., Sawamura, T., Ravens, U., Morawietz, H., 2009. Impaired vascular function in small resistance arteries of LOX-1 overexpressing mice on high-fat diet. Cardiovasc. Res. 82, 493–502.
Esper, R.J., Nordaby, R.A., Vilariño, J.O., Paragano, A., Cacharrón, J.L., Machado, R.A., 2006. Endothelial dysfunction: a comprehensive appraisal. Cardiovasc. Diabetol. 5, 4.
Fagrell, B., Nilsson, G., 1995. Advantages and limitations of one-point laser Doppler perfusion monitoring in clinical practice. Vasc. Med. Rev. 6, 97–101.
Faraci, F.M., Sigmund, C.D., Shesely, E.G., Maeda, N., Heistad, D.D., 1998. Responses of carotid artery in mice deficient in expression of the gene for endothelial NO synthase. Am. J. Physiol. 274, 564–570.
Galarraga, B., Khan, F., Kumar, P., Pullar, T., Belch, J.J.F., 2008. C-reactive protein: the underlying cause of microvascular dysfunction in rheumatoid arthritis. Rheumatology (Oxford) 47, 1780–1784.
Garry, A., Fromy, B., Blondeau, N., Henrion, D., Brau, F., Gounon, P., Guy, N., Heurteaux, C., Lazdunski, M., Saumet, J.L., 2007. Altered acetylcholine, bradykinin and cutaneous pressure-induced vasodilation in mice lacking the TREK1 potassium channel: the endothelial link. EMBO Rep. 8, 354–359.
Gaubert, M.L., Sigaudo-Roussel, D., Tartas, M., Berrut, G., Saumet, J.L., Fromy, B., 2007. Endothelium-derived hyperpolarizing factor as an in-vivo back-up mechanism in the cutaneous microcirculation in old mice. J. Physiol. (Lond.) 585, 617–626.
Grossmann, M., Jamieson, M.J., Kellogg Jr., D.L., Kosiba, W.A., Pergola, P.E., Crandall, C.G., Shepherd, A.M.M., 1995. The effect of iontophoresis on the cutaneous vasculature: evidence for current-induced hyperemia. Microvasc. Res. 50, 444–452.
Huang, A.L., Silver, A.E., Shvenke, E., Schopfer, D.W., Jahangir, E., Titas, M.A., Shpilman, A., Menzoian, J.O., Watkins, M.T., Raffetto, J.D., Gibbons, G., Woodson, J., Shaw, P.M., Dhadly, M., Eberhardt, R.T., Keaney Jr., J.F., Gokce, N., Vita, J.A., 2007. Predictive value of reactive hyperemia for cardiovascular events in patients with peripheral arterial disease undergoing vascular surgery. Arterioscler. Thromb. Vasc. Biol. 27, 2113–2119.
Ijzerman, R.G., De Jongh, R.T., Beijk, M.A.M., Van Weissenbruch, M.M., Delemarre-van De Waal, H.A., Serne, E.H., Stehouwer, C.D.A., 2003. Individuals at increased coronary heart disease risk are characterized by an impaired microvascular function in skin. Eur. J. Clin. Invest. 33, 536–542.
Jones, R.D., Pugh, P.J., Hall, J., Channer, K.S., Jones, T.H., 2003. Altered circulating hormone levels, endothelial function and vascular reactivity in the testicular feminised mouse. Eur. J. Endocrinol. 148, 111–120.
Khan, F., Elhadd, T.A., Greene, S.A., Belch, J.J.F., 2000. Impaired skin microvascular function in children, adolescents, and young adults with type I diabetes. Diabetes Care 23, 215–220.
Khan, F., Green, F.C., Forsyth, J.S., Greene, S.A., Morris, A.D., Belch, J.J.F., 2003. Impaired microvascular function in normal children: effects of adiposity and poor glucose handling. J. Physiol. (Lond.) 551, 705–711.
Khan, F., Patterson, D., Belch, J.J., Hirata, K., Lang, C.C., 2008. Relationship between peripheral and coronary function using laser Doppler imaging and transthoracic echocardiography (2008). Clin. Sci. (Lond.) 115 (9), 295–300.
Ludmer, P.L., Selwyn, A.P., Shook, T.L., 1986. Paradoxical vasoconstriction induced by acetylcholine in atherosclerotic coronary arteries. N. Engl. J. Med. 31, 1046–1051.
Morris, S.J., Shore, A.C., 1996. Skin blood flow responses to the iontophoresis of acetylcholine and sodium nitroprusside in man: possible mechanisms. J. Physiol. (Lond.) 496, 531–542.
Morris, S.J., Shore, A.C., Tooke, J.E., 1995. Responses of the skin microcirculation to acetylcholine and sodium nitroprusside in patients with NIDDM. Diabetologia 38, 1337–1344.
Panza, J.A., Quyyumi, A.A., Brush Jr., J.E., Epstein, S.E., 1990. Abnormal endothelium-dependent vascular relaxation in patients with essential hypertension. N. Engl. J. Med. 323, 22–27.
Sainsbury, C.A., Sattar, N., Connell, J.M., Hillier, C., Petrie, J.R., 2004. Non-esterified fatty acids impair endothelium-dependent vasodilation in rat mesenteric resistance vessels. Clin. Sci. (Lond.) 107, 625–629.
Shafaroudi, M.M., McBride, M., Deighan, C., Wokoma, A., Macmillan, J., Daly, C.J., McGrath, J.C., 2005. Two "knockout" mouse models demonstrate that aortic vasodilatation is mediated via α_{2A}-adrenoceptors located on the endothelium. J. Pharmacol. Exp. Ther. 314, 804–810.
Sharifi, A.M., Li, J.S., Endemann, D., Schiffrin, E.L., 1998. Effects of enalapril and amlodipine on small-artery structure and composition, and on endothelial dysfunction in spontaneously hypertensive rats. J. Hypertens. 16, 457–466.
Sigaudo-Roussel, D., Demiot, C., Fromy, B., Koïtka, A., Lefthériotis, G., Abraham, P., Saumet, J.L., 2004. Early endothelial dysfunction severely impairs skin blood flow response to local pressure application in streptozotocin-induced diabetic mice. Diabetes 53, 1564–1569.
Sumpio, B.E., Timothy Riley, J., Dardik, A., 2002. Cells in focus: endothelial cell. Int. J. Biochem. Cell Biol. 34, 1508–1512.
Symons, J.D., Gunawardena, S., Kappagoda, C.T., Dhond, M.R., 2001. Volume overload left ventricular hypertrophy: effects on coronary microvascular reactivity in rabbits. Exp. Physiol. 86, 725–732.
Turner, J., Belch, J.J.F., Khan, F., 2008. Current concepts in assessment of microvascular endothelial function using laser Doppler imaging and iontophoresis. Trends Cardiovasc. Med. 18, 109–116.